

Hanford Tank 241-C-106: Impact of Cement Reactions on Release of Contaminants from Residual Waste



August 2006



Prepared for CH2M HILL Hanford Group, Inc.
and the U.S. Department of Energy
under Contract DE-AC05-76RL01830 by

Pacific Northwest National Laboratory

Operated by Battelle for the U.S. Department of Energy

DISCLAIMER

This report was prepared as an account of work sponsored by an agency of the United States Government. Neither the United States Government nor any agency thereof, nor Battelle Memorial Institute, nor any of their employees, makes **any warranty, express or implied, or assumes any legal liability or responsibility for the accuracy, completeness, or usefulness of any information, apparatus, product, or process disclosed, or represents that its use would not infringe privately owned rights.** Reference herein to any specific commercial product, process, or service by trade name, trademark, manufacturer, or otherwise does not necessarily constitute or imply its endorsement, recommendation, or favoring by the United States Government or any agency thereof, or Battelle Memorial Institute. The views and opinions of authors expressed herein do not necessarily state or reflect those of the United States Government or any agency thereof.

PACIFIC NORTHWEST NATIONAL LABORATORY

operated by

BATTELLE

for the

UNITED STATES DEPARTMENT OF ENERGY

under Contract DE-AC05-76RL01830

Printed in the United States of America

**Available to DOE and DOE contractors from the
Office of Scientific and Technical Information,**

P.O. Box 62, Oak Ridge, TN 37831-0062;

ph: (865) 576-8401

fax: (865) 576-5728

email: reports@adonis.osti.gov

**Available to the public from the National Technical Information Service,
U.S. Department of Commerce, 5285 Port Royal Rd., Springfield, VA 22161**

ph: (800) 553-6847

fax: (703) 605-6900

email: orders@ntis.fedworld.gov

online ordering: <http://www.ntis.gov/ordering.htm>

The cover image shows an SEM micrograph of particles present in tank C-106 residual waste after leaching of the material with a $\text{Ca}(\text{OH})_2$ solution. EDS analysis indicates that the major elements in most of these phases are Ca, Al, Mn, O, and C.
Cover design is by S.B. Neely, Pacific Northwest National Laboratory, Richland, Washington.



This document was printed on recycled paper.

Hanford Tank 241-C-106: Impact of Cement Reactions on Release of Contaminants from Residual Waste

W. J. Deutsch K. J. Cantrell
K. M. Krupka C. F. Brown
M. J. Lindberg H. T. Schaefer

August 2006

Prepared for
CH2M HILL Hanford Group, Inc. and
the U.S. Department of Energy
under Contract DE-AC05-76RL01830

Pacific Northwest National Laboratory
Richland, Washington 99352

Summary

The CH2M HILL Hanford Group, Inc. (CH2M HILL) is producing risk/performance assessments to support the closure of single-shell tanks at the U.S. Department of Energy's Hanford Site. As part of this effort, staff at Pacific Northwest National Laboratory were asked to develop release models for contaminants of concern that are present in residual sludge remaining in tank 241-C-106 (C-106) after final retrieval of waste from the tank. Initial work to produce release models was conducted on residual tank sludge using pure water as the leaching agent. The results were reported in Deutsch et al. (2005a). One of the options under consideration for closure after waste retrieval is to fill the tanks with a cementitious grout to minimize infiltration and maintain the physical integrity of the tanks. The presence of a cementitious grout above the residual waste may impact contaminant leaching. This report describes testing of the residual waste with a leaching solution that simulates the composition of water passing through a grout and contacting the residual waste at the bottom of the tank.

The primary contaminants of concern in the sludge are ^{99}Tc , ^{238}U , ^{129}I , and Cr because of their potential mobility in the environment and the long half-lives of the radionuclides. A key result from this work is that high percentages ($\geq 90\%$) of these primary contaminants are not readily leachable from the residual waste in contact with pure water or with the cementitious grout simulants. This minimizes their future release to the environment, and is similar to results found in related studies of sludges from tanks AY-102, C-203, and C-204.

The simulants selected to represent the solutions that will contact the residual sludge consisted of a 0.01 M $\text{Ca}(\text{OH})_2$ solution and a solution in equilibrium with calcite (CaCO_3). The $\text{Ca}(\text{OH})_2$ solution represented fresh grout and the CaCO_3 solution represented aged grout in which calcite had precipitated on the surfaces of the grout and this mineral controlled the major ion composition of the solution in contact with the grout. Laboratory tests were conducted to evaluate the leachability of sludge constituents and to characterize the sludge solid phases before and after leaching. The leaching tests consisted of single-contact batch tests and six stages of sequential batch leaching tests. Solid phase analyses consisted of x-ray diffraction (XRD) and scanning electron microscopy/energy dispersive spectrometry (SEM/EDS) analyses to identify reactive phases and estimate their composition.

The results of the leaching tests with the grout simulants were compared to the results for the pure water tests. ^{99}Tc was approximately 4 times more leachable in the $\text{Ca}(\text{OH})_2$ leachant than in water, but the increase in leachability was still only $\sim 10\%$ of the total ^{99}Tc in the sludge. The leachability of ^{238}U was approximately equal for the cementitious conditions and the pure water conditions. In each case, only a few percent of the total ^{238}U in the sludge was leachable. The other primary contaminants of interest (^{129}I and Cr) were not detected in the leachates and, thus, also appear to be in a stable form in the residual sludge. Other components of the sludge that were less leachable in the cementitious simulants were Fe, Mn, and oxalate. Components that were more leachable were Al, ^{90}Sr , and ^{137}Cs . Al is probably more mobile because it forms a strong solution complex $[\text{Al}(\text{OH})_4^-]$ under the high pH (12) conditions of the simulants and ^{90}Sr and ^{137}Cs are more mobile because the Ca in the simulant competes with these cations for ion exchange sites on the sludge.

Interactions of the cement simulants with the residual sludge produced a change in some of the mineralogy of the sludge. It appears that the Mn minerals rhodochrosite (MnCO_3) and lindbergitte

($\text{MnC}_2\text{O}_4 \cdot 2\text{H}_2\text{O}$) were converted to calcite (CaCO_3), whewellite ($\text{CaC}_2\text{O}_4 \cdot \text{H}_2\text{O}$) and a poorly defined amorphous Mn oxyhydroxide phase. Dawsonite ($\text{NaAl}(\text{OH})_2\text{CO}_3$) was converted to calcite and released Na and Al to solution. These phase transformations account for some of the changes in leachability between the cement simulant and pure water systems.

Because a correlation could not be established between the contaminants of interest and the identified solid phases, mechanistic release models for these contaminants could not be developed. In their place, empirical release models were developed based on initial sludge concentrations and dissolved contaminant concentrations in the leaching solutions. These empirical models provide the source terms for the release of contaminants from residual sludge in tank C-106 filled with cementitious grout.

Acknowledgments

The authors wish to acknowledge M. Connelly, F.J. Anderson, and F.M. Mann at CH2M HILL Hanford Group, Inc. (Richland, Washington) for providing project funding and technical guidance. We greatly appreciate the technical reviews provided by T.E. Jones (CH2M HILL), M.I. Wood (Fluor Hanford, Inc., Richland, Washington), R.J. Serne, and W. Um (both of PNNL). The authors would also like to thank B.W. Arey (PNNL) for conducting the SEM/EDS analyses of the sludge samples and S.R. Baum, K.M. Geiszler, I.V. Kutnyakov, and R.D. Orr (all of PNNL) for completing the chemical and radiochemical analyses of the solution samples from our studies. We are also particularly grateful to L.F. Morasch (PNNL) for completing the editorial review and K.R. Neiderhiser (PNNL) for final formatting of this technical report.

Acronyms and Abbreviations

ASTM	American Society for Testing and Materials
BSE	backscattered electron
C-106	241-C-106 tank
CH2M HILL	CH2M HILL Hanford Group, Inc.
CSH	calcium silicate hydrogel
DDI	double deionized (water)
DOE	U.S. Department of Energy
EDS	energy dispersive spectrometry
EPA	U.S. Environmental Protection Agency
EQL	estimated quantitation limit
GEA	gamma energy analysis
HASQARD	Hanford Analytical Services Quality Assurance Requirements Document
HF	hydrofluoric
ICP-MS	inductively coupled plasma-mass spectroscopy (spectrometer)
ICP-OES	inductively coupled plasma-optical emission spectroscopy (same as ICP-AES)
ICDD	International Center for Diffraction Data, Newtown Square, Pennsylvania
JCPDS	Joint Committee on Powder Diffraction Standards
LEPS	Low Energy Photon System
LSC	liquid scintillation counting
NIST	National Institute of Standards and Technology
PDF TM	powder diffraction file
PNNL	Pacific Northwest National Laboratory
QA	quality assurance
RPL	Radiochemical Processing Laboratory
SE	secondary electron
SEM	scanning electron microscopy (or microscope)
SRM	Standard Reference Material
TEM	transmission electron microscopy (or microscope)
XRD	x-ray powder diffractometry analysis (commonly called x-ray diffraction)

Units of Measure

Å	angstrom
θ	angle of incidence (Bragg angle)
$\Delta_f G_{298}^\circ$	Gibbs energy of formation from the elements in their reference states at 298.15 K
°C	temperature in degrees Celsius [$T(^{\circ}\text{C}) = T(\text{K}) - 273.15$]
Ci	curie
cps	counts per second
ft	foot
g	gram
gal	gallon
in.	inch
K	temperature in degrees (without degree symbol) Kelvin [$T(\text{K}) = T(^{\circ}\text{C}) + 273.15$]
K_{298}°	equilibrium constant at 298.15 K
kcal	kilocalorie, one calorie equals 4.1840 joules
keV	kilo-electron volt
kJ	kilojoule, one joule equals 4.1840 thermochemical calories
L	liter
μ	micro (prefix, 10^{-6})
μCi	microcurie
μg	microgram
μm	micrometer
M	molarity, mol/L
mA	milliAmpere
mg	milligram
mL	milliliter
mM	millimolar
rpm	revolution per minute
λ	wavelength
wt%	weight percent

Contents

Summary	iii
Acknowledgments.....	v
Acronyms and Abbreviations	vii
Units of Measure.....	ix
1.0 Introduction	1.1
1.1 Scope.....	1.1
1.2 C-106 Tank Description.....	1.2
2.0 Background.....	2.1
3.0 Materials and Laboratory Test Methods.....	3.1
3.1 Tank C-106 Samples	3.1
3.2 Cement Simulation Tests	3.3
3.2.1 Moisture Content.....	3.4
3.2.2 Single Contact Batch Leaching Test	3.4
3.2.3 Sequential Contact Leaching Test.....	3.5
3.2.4 pH.....	3.5
3.2.5 Anion Analysis.....	3.5
3.2.6 Cations and Trace Metals.....	3.5
3.2.7 Alkalinity.....	3.6
3.2.8 Radioanalysis	3.6
3.3 XRD Analysis	3.7
3.4 SEM/EDS Analysis.....	3.9
4.0 Analytical Results.....	4.1
4.1 Leaching Tests	4.1
4.1.1 Single Contact Batch Leaching	4.1
4.1.2 Sequential Contact Leaching Test.....	4.3
4.2 XRD Results.....	4.16
4.3 SEM/EDS Results	4.19
5.0 Contaminant Release Model.....	5.1
5.1 Modification of the Conceptual Model of Chemical Transformations of Tank C-106 Sludge Resulting from a Cementitious Tank Filler.....	5.2
5.2 Release Models for Technetium, Uranium, Iodine, and Chromium in a Tank Filled with Cementitious Grout	5.3
6.0 Conclusions	6.1
7.0 References	7.1
Appendix A – X-Ray Diffraction Patterns for Ca(OH) ₂ - and Ca(OH) ₂ /CaCO ₃ -Leached Tank C-106 Residual Waste	A.1

Appendix B – SEM Micrographs and EDS Results for 1-Month Ca(OH) ₂ -Leached Tank C-106 Residual Waste	B.1
Appendix C – SEM Micrographs and EDS Results for Stage 6 Sequential Ca(OH) ₂ -Leached Tank C-106 Residual Waste.....	C.1
Appendix D – SEM Micrographs and EDS Results for 1-Month Ca(OH) ₂ /CaCO ₃ -Leached Tank C-106 Residual Waste.....	D.1
Appendix E – SEM Micrographs and EDS Results for Stage 6 Sequential Ca(OH) ₂ /CaCO ₃ -Leached Tank C-106 Residual Waste	E.1
Appendix F – Solution Concentrations of Tank C-106 Solution Contact Tests with Residual Sludge	F.1

Figures

1.1 Location Map of Hanford Waste Management Area C Containing Tank C-106.....	1.2
1.2 Tank C-106 Configuration	1.3
1.3 Tank C-106 Sludge at 222-S Laboratory	1.4
3.1 Tank C-106 Field Primary Solid Composite Sludge Sample 404	3.2
3.2 Tank C-106 Field Duplicate Solid Composite Sludge Sample 405	3.2
3.3 Leach Test Flowpath.....	3.3
3.4 Exploded Schematic View of the XRD Sample Holder.....	3.7
3.5 XRD Pattern for Collodion Film Measured in the Absence of any Sludge Material.....	3.8
4.1 Background-Subtracted XRD Patterns for 1-Month and Stage 6 Sequential Ca(OH) ₂ -Leached and for Unleached C-106 Residual Waste Compared to the Matching PDF Database Patterns	4.17
4.2 Background-Subtracted XRD Patterns for 1-Month and Stage 6 Sequential CaCO ₃ -Leached and for Unleached C-106 Residual Waste Compared to the Matching PDF Database Patterns.....	4.18
4.3 Comparison of Background-Subtracted XRD Patterns for 1-Month Ca(OH) ₂ - and 1-Month CaCO ₃ - Leached Samples of Unleached C-106 Residual Waste	4.19
4.4 Low Magnification SEM Micrographs of Particles Present in 1-Month and Stage 6 Sequential Ca(OH) ₂ -Leached and 1-Month and Stage 6 Sequential CaCO ₃ -Leached C-106 Residual Waste	4.23
4.5 Low Magnification SEM Micrographs of Particles Present in the Unleached, 1-Month Water-Leached, and HF Stage 1 Extract of Oxalic Acid-Treated Residual Waste from Tank C-106.....	4.24
4.6 SEM Micrograph of Typical Particle Aggregates Present in 1-Month Ca(OH) ₂ -Leached C-106 Residual Waste and Spectra for Areas Analyzed by EDS	4.25
4.7 SEM Micrograph of Typical Particles Present in Stage 6 Sequential Ca(OH) ₂ -Leached C-106 Residual Waste and Spectra for Areas Analyzed by EDS	4.26
4.8 SEM Micrograph of Typical Particles Present in Stage 6 Sequential Ca(OH) ₂ -Leached C-106 Residual Waste and Spectra for Areas Analyzed by EDS	4.27

4.9	SEM Micrograph of Typical Particles Present in 1-Month CaCO ₃ -Leached C-106 Residual Waste and Spectra for Areas Analyzed by EDS	4.28
4.10	SEM Micrograph of Typical Particles Present in Stage 6 Sequential CaCO ₃ -Leached C-106 Residual Waste and Spectra for Areas Analyzed by EDS	4.29
4.11	SEM Micrograph of Typical Particles Present in Stage 6 Sequential CaCO ₃ -Leached C-106 Residual Waste and Spectra for Areas Analyzed by EDS	4.30
4.12	Backscatter-Electron SEM Image and Colorized Element Maps for a Particle Aggregate from the 1-Month Ca(OH) ₂ -Leached C-106 Residual Waste	4.33
4.13	Backscatter-Electron SEM Micrograph and Element Distribution Maps for Particles in 1-Month Ca(OH) ₂ -Leached C-106 Residual Waste	4.34
4.14	Backscatter-Electron SEM Image and Colorized Element Maps for a Particle Aggregate from the Stage 6 Sequential Ca(OH) ₂ -Leached C-106 Residual Waste.....	4.35
4.15	Backscatter-Electron SEM Micrograph and Element Distribution Maps for Particles in Stage 6 Sequential Ca(OH) ₂ -Leached C-106 Residual Waste	4.36
4.16	Backscatter-Electron SEM Micrograph and Element Distribution Maps for Particles in Stage 6 Sequential Ca(OH) ₂ -Leached C-106 Residual Waste	4.37
4.17	Backscatter-Electron SEM Image and Colorized Element Maps for a Particle Aggregate from the 1-Month CaCO ₃ -Leached C-106 Residual Waste	4.38
4.18	Backscatter-Electron SEM Micrograph and Element Distribution Maps for Particles in 1-Month CaCO ₃ -Leached C-106 Residual Waste.....	4.39
4.19	Backscatter-Electron SEM Image and a Colorized Element Map for a Particle Aggregate from the Stage 6 Sequential CaCO ₃ -Leached C-106 Residual Waste.....	4.40
4.20	Backscatter-Electron SEM Micrograph and Element Distribution Maps for Particles in Stage 6 Sequential CaCO ₃ -Leached C-106 Residual Waste	4.41
5.1	Source Release Model Development for Long-Term Risk/Performance Assessments	5.1
5.2	Chemical Transformations of Tank C-106 Residual Sludge Resulting from Contact with Cementitious Grout Leachate	5.2

Tables

2.1	Sample 403 – Tank C-106 Liquid Sample Composition.....	2.2
3.1	Tank C-106 Samples Provided by 222-S Laboratory to PNNL.....	3.1
4.1	Water Extract pH and Alkalinity Values Corrected to Grams of Dry Sludge.....	4.2
4.2	⁹⁹ Tc, ²³⁸ U, and ¹²⁹ I Concentrations Leached During Single-Contact Batch Tests	4.2
4.3	Leachable Percentages of ⁹⁹ Tc, ²³⁸ U, and ¹²⁹ I in C-106 Sludge Samples Compared with Fusion Results	4.2
4.4	Leachable Metal Concentrations in Single Contact Batch Test	4.4
4.5	Average Anion Concentrations Leached During Single Contact Batch Test.....	4.4
4.6	¹³⁷ Cs Leached During Single Contact Batch Test	4.5

4.7	⁹⁰ Sr and Actinides Leached During Single Contact Batch Test	4.5
4.8	Contact Times, pH Range, and Alkalinities for Sequential Contact Leaching Test on Tank C-106 Sludge Samples	4.5
4.9	⁹⁹ Tc and ²³⁸ U Concentrations Leached During Sequential Contact Test.....	4.7
4.10	Water-Leachable Percentages of ⁹⁹ Tc, ²³⁸ U, and ¹²⁹ I in Tank C-106 Sludge Sequential Contact Leaching Test Relative to Fusion Results.....	4.8
4.11	Metals Concentrations Leached During Sequential Contact Tests	4.9
4.12	Anion Concentrations Leached During Sequential Contact Tests	4.12
4.13	¹³⁷ Cs Concentrations Leached During Sequential Contact Tests	4.13
4.14	⁹⁰ Sr and Actinide Concentrations Leached During Sequential Contact Tests.....	4.14
4.15	Comparison of XRD and SEM/EDS Results for the Unleached Samples of Residual Waste from Tank C-106 to the Results for the Ca(OH) ₂ - and CaCO ₃ -Leached Samples	4.20
5.1	Summary of Contaminant Release Model Data for Tank C-106, Fresh Cement Scenario	5.4
5.2	Summary of Contaminant Release Model Data for Tank C-106, Aged Cement Scenario	5.4
5.3	Summary of Contaminant Release Model Data for C-106, Fresh Water Scenario	5.5

1.0 Introduction

One of the closure methods under consideration for the Hanford tanks after waste retrieval is to fill them with a cement grout to maintain the structural integrity of the tank. The grout would be poured on top of any residual waste left in the tank, and little mixing between the materials is expected. Recharge water entering the tank in the future would pass through the cementitious material before contacting residual waste at the bottom of the tank. This water would take on the chemical characteristics of the cement. Leaching studies of residual tank waste are being conducted to develop long-term contaminant release rates for use in performance assessments. In the past, the leaching studies were conducted with deionized water. Now that filling the tanks with cementitious material is being considered as a possible component of the closure process, leaching studies with simulants of fresh and aged cement will also be conducted as part of the closure assessment process.

This report describes the development of release models for contaminants of concern that may be present in residual sludge in Hanford tank 241-C-106 (C-106) after closure. These release models are necessary components of the risk assessments being conducted as part of the closure process. From the perspective of long-term risk to the environment, the primary contaminants of concern are ^{99}Tc , ^{238}U , ^{129}I , and Cr because of their mobility in the environment and long half-lives for the radionuclides. Sludge samples and a sample of the liquid from tank C-106 were collected after final sludge retrieval to characterize the geochemistry of the reactive phases and to quantify the release of primary contaminants into water that may contact residual sludge after tank closure.

The remainder of this section describes the scope of work for laboratory testing and release model development as well as background information on this tank. The samples and laboratory testing procedures for this project are described in Section 2 of this report, and the results are provided in Section 3. Release models are discussed in Section 4 and general conclusions in Section 5. Cited references are listed in Section 6, and supporting material is included in the appendices.

1.1 Scope

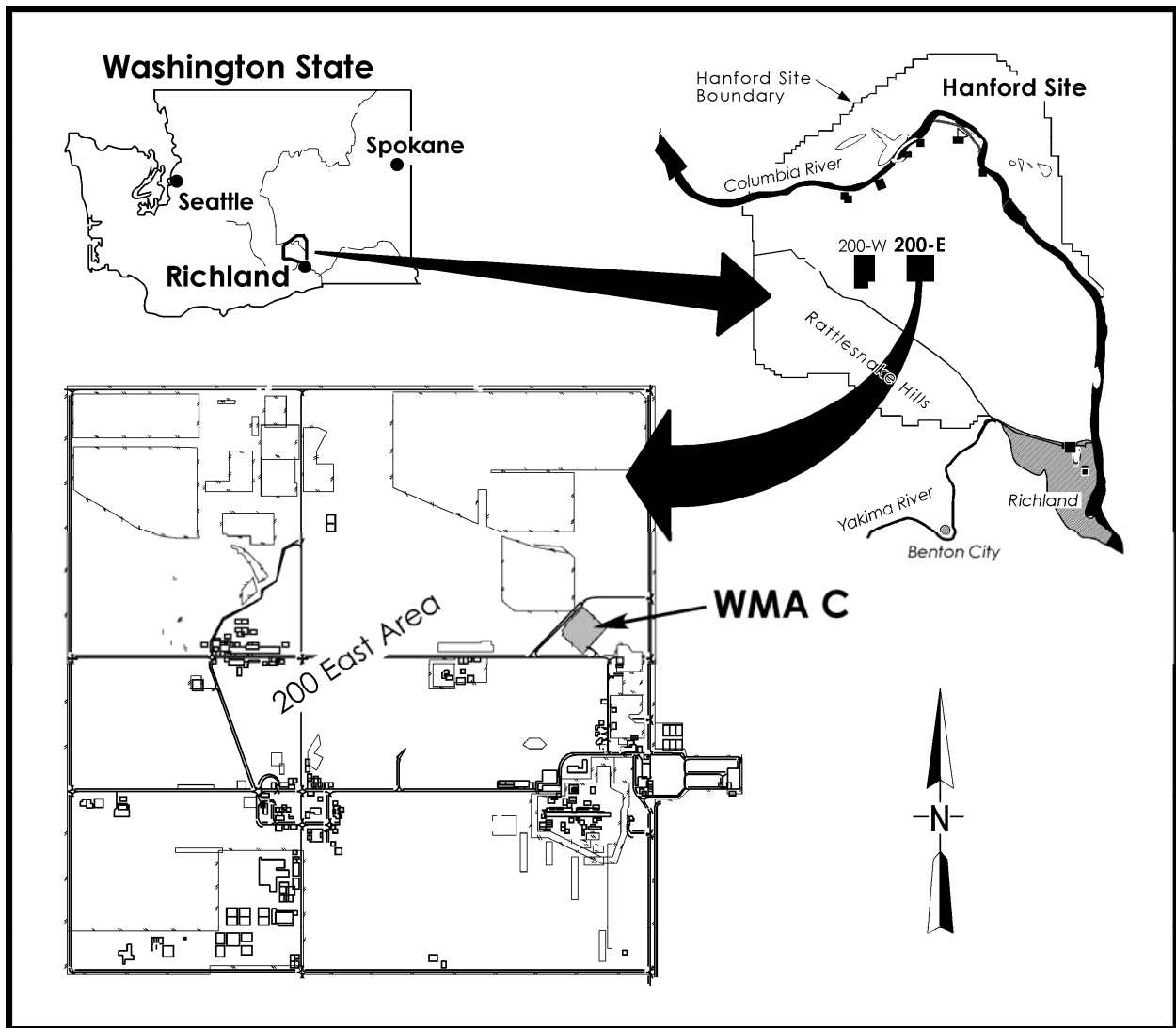
Initial (Tier 1) laboratory tests were conducted to characterize the sludge and identify water-leachable constituents. The Tier 1 tests consisted primarily of fusion and acid digestions (which measured element concentrations in the solid) and water leaching of contaminants from the sludge to evaluate their mobility in infiltrating water. Based on the results of Tier 1 tests, additional analyses were performed to augment the characterization of the material and determine the controlling mechanism(s) for release of contaminants. Tier 2 tests consisted of analyses of the solids using x-ray diffraction (XRD) and scanning electron microscopy/energy dispersive spectrometry (SEM/EDS) to identify reactive phases, and selective extractions in order to quantify the release of contaminants from particular solid phases. The results of these initial tests were documented in Deutsch et al. (2005a). Subsequent Tier 1 and 2 tests on tank C-106 residual waste were conducted using cement simulants to leach the waste. The results of these tests are the subject of this report.

The laboratory results of residual sludge and liquid testing were used to develop source term models that describe the release of contaminants as infiltrating water contacts the solids in the future. These models simulate the geochemical system in the tank sludge and take into account interactions between the

solution phase and the contaminant-containing solids. The release models are simplifications of the complex geochemical interactions occurring between the phases; however, they adequately represent the release of the key contaminants ^{99}Tc , ^{238}U , ^{129}I , and Cr from the sludge as measured in laboratory tests.

1.2 C-106 Tank Description

Tank C-106 is a single-shell underground waste tank located in the C Tank Farm in the 200 East Area of the Hanford Site (Figure 1.1). It was constructed between 1943 and 1944 and put into service during September 1947. This tank is 22.8 m (75 ft) in diameter and has a capacity of 2,006,268 L (530,000 gal) when filled to a depth of 5.2 m (17 ft). Figure 1.2 is a diagram showing the configuration of tank C-106.



2005/DCL/C/009 (11/17)

Figure 1.1. Location Map of Hanford Waste Management Area C Containing Tank C-106

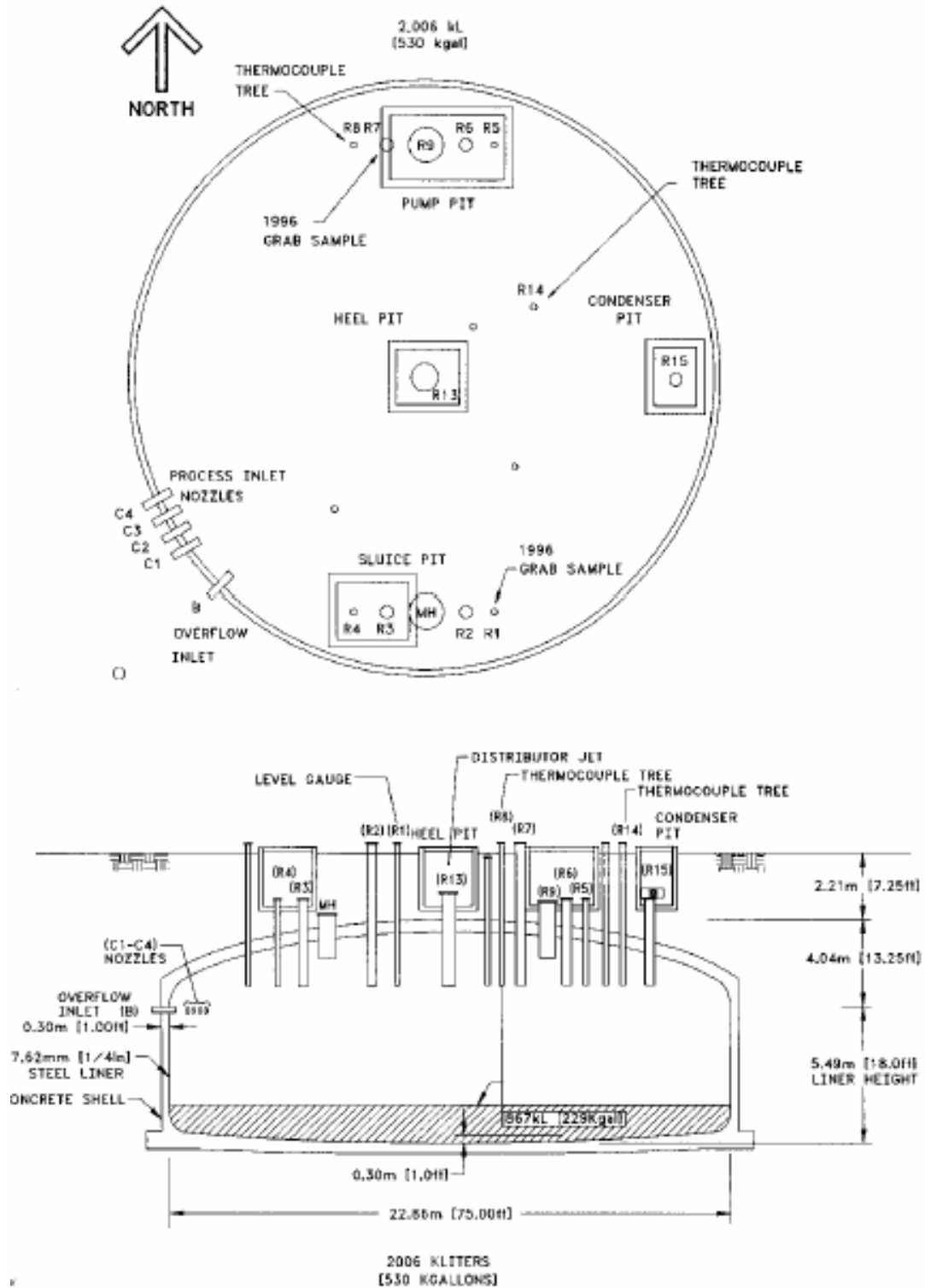


Figure 1.2. Tank C-106 Configuration (Conner 1996)

In late 2003, sludge from tank C-106 was further removed using a 0.9 M oxalic acid solution to dissolve and suspend the solids and pump out as much as possible. The goal was to lower the sludge volume from about 68,137 to 10,599 L (18,000 to 2,800 gal [360 ft³]). This goal was achieved by several additions and removals of the oxalic acid solution. After the final removal, the sludge was rinsed with water to remove as much of the acid solution as possible. Approximately 151,416 L (40,000 gal) or 35.5 cm (14 in.) of water was added to measure the sludge volume, and then as much liquid as possible was removed. A 0.5-M NaOH solution was added to neutralize the residual waste, and then removed. The residual liquid in the tank was sampled for analysis through Riser 14 (Figure 1.2), and multiple sludge samples were acquired using a clamshell device by CH2M HILL Hanford Group, Inc. (CH2M HILL) in January 2004. All samples were delivered to the Hanford 222-S Laboratory for processing and characterization. Figure 1.3 is a picture of the sludge at the 222-S Laboratory. Subsamples were sent to Pacific Northwest National Laboratory (PNNL) for testing and release model development.



Figure 1.3. Tank C-106 Sludge at 222-S Laboratory

2.0 Background

Fresh cement/grout will contain pore fluids that have high pH values (>12) and high concentrations of soluble salts. Infiltration will enter the cement/grout initially through pores and then through cracks as the grout ages. At the outset, the most readily soluble salts will leach out, lowering the dissolved concentrations of these salts and the pH within the cement grout pore fluids. In addition, carbon dioxide will enter the cement as air moves into the pores/fractures and as water with dissolved CO₂ migrates through the grout. Carbon dioxide is an acidic gas that forms carbonic acid when it dissolves in water. It will also react with Ca(OH)₂ (portlandite) in the cement grout to precipitate calcite (CaCO₃) and lower the pH.



Carbonation and calcite precipitation are considered the most common chemical reactions influencing the performance of cement based materials in natural systems. In addition to the formation of calcite from Ca(OH)₂, this mineral also forms from decalcification of calcium silicate hydrogel (CSH), which typically constitutes 40% to 50% of cement. During this stage of cement weathering, CO₂(aq) decomposes the remaining CSH gel into CaCO₃(s), acid-soluble silica gel, and water.



Eventually, the solutions in contact with aged cement grout come into equilibrium with calcite as the surfaces of the solid become coated with this mineral.

In order to evaluate the impact of a cement-based leaching solution on residual tank sludge, experiments were conducted in which post-retrieval sludge from tank C-106 was leached with a saturated Ca(OH)₂ solution followed by a saturated CaCO₃ solution. The Ca(OH)₂ (pH ~ 12.4) solution represented the early stages of the cement system in which the grout is relatively fresh, and the CaCO₃ solution (pH ~ 8.3) represented the weathered grout system. The compositions of the resulting leachates from the Ca(OH)₂/sludge and CaCO₃/sludge systems have been compared to the previous deionized water leaches to evaluate the relative impact of the various leachants on contaminant mobility.

Several oxalic acid additions were made to tank C-106 during final retrieval of sludge to dissolve and remove as much solids as possible. After the final acid wash, a 0.5-M NaOH solution was added to the tank to neutralize the system. As much of the solution as possible was then pumped from the tank. The residual tank liquid was sampled as well as the sludge. The results of the PNNL analysis of the residual liquid are shown in Table 2.1. The solution pH is 12.9 because of the added NaOH. The major cations in solution are Na (10,200 mg/L average) and Al (121 mg/L average), while the major anions are carbonate (9,930 mg/L average) and oxalate (1,345 mg/L average). The MINTEQ calculated total OH⁻ concentration is 2,200 mg/L. Because the pH of the Ca(OH)₂-saturated solution is expected to be similar to that of the pore water in the post-retrieval C-106 sludge, it is likely that pH will not be a strong driver for reactions with the early cement-dominated system. However, the high calcium concentration in the cement grout leaching solution will likely enhance calcite and, perhaps, calcium oxalate precipitation in the sludge.

Table 2.1. Sample 403 – Tank C-106 Liquid Sample Composition

Analyte	Concentration (mg/L*)	
	Primary	Duplicate
pH	12.9	
Metals		
Al	126.0	116.
Ba	3.5	(0.09)
Ca	21.9	(4.1)
Cr	(0.28)	(0.34)
Fe	(1.9)	(0.6)
K	(14.)	(12.)
Mg	(0.9)	(0.24)
Mn	(0.16)	(0.1)
Na	10,300.	10,100.
Ni	3.9	3.0
Si	(158.)	(141.)
Radionuclides		
⁹⁹ Tc	0.0003	(0.00012)
²³⁸ U	1.24	1.03
¹³⁷ Cs (μCi/L)	505	442
Total Alpha (μCi/L)	30.3	30.2
Total Beta (μCi/L)	470	469
Anions		
Oxalate	1,340.	1,350.
CO ₃ ²⁻	10,020.	9,840.
Cl ⁻	20.5	20.5
NO ₃ ⁻	9.43	9.41
F ⁻	1.38	<1.17
SO ₄ ²⁻	27.6	27.6
PO ₄ ³⁻	75.1	74.6
* mg/L unless otherwise noted.		

XRD analysis of the C-106 sludge samples showed detectable quantities of the following crystalline phases:

- lindbergite [MnC₂O₄·2H₂O]
- gibbsite [Al(OH)₃]
- dawsonite [NaAlCO₃(OH)₂]
- hematite (Fe₂O₃)
- böhmite [AlO(OH)]
- rhodochrosite (MnCO₃)
- whewellite (Ca oxalate monohydrate, CaC₂O₄·H₂O)

Except for lindbergite, these minerals were also present in the 1-month water-leached, 82-day water-leached, and hydrofluoric (HF)-extracted sludge samples. The $\text{Ca}(\text{OH})_2$ -saturated system will likely stabilize the carbonate minerals (dawsonite and rhodochrosite) and have little effect on the solubility of the metal oxide/hydroxide phases (gibbsite, hematite, and böhmite) because the pH should not change appreciably. The Mn oxalate solid should dissolve in this system, while the solubility of the Ca oxalate will depend on the final Ca and oxalate concentrations in the mixture of grout leachate and residual pore water.

For the CaCO_3 -saturated system, it is expected that the carbonate minerals (dawsonite and rhodochrosite) will partially dissolved in the lower pH environment, and the oxalate minerals (lindbergite and whewellite) will also be soluble because of the lack of oxalate in the leaching solution. The metal oxide and hydroxide minerals (gibbsite, hematite, and böhmite) are not expected to dissolve appreciably in this system because they are relatively insoluble at a pH of 8.

Deionized water leaches were conducted on C-106 sludges for time periods of 1 day, 2 weeks, and 1 month (Deutsch et al. 2005a). In addition to these single step leaches, sequential water leaches were conducted. In the sequential leaches, the same sludge sample was extracted for periods of 1 to 4 days repeatedly with fresh deionized water for 5 periods in sequence. These same samples were then sequentially leached for periods of 43 and 82 days. All of these leach experiments were conducted using 0.3 g of sludge and 30 mL of water. The resulting pH values of the final solutions from the water leaching tests were in the range of 6.7 to 7.7. The major leachable metals were Na and Mn. The major leachable anions were oxalate and carbonate. During the planned leaching experiments with $\text{Ca}(\text{OH})_2$ -saturated and CaCO_3 -saturated solutions, it was expected that Na and Mn would again be the most leachable metals and oxalate would be a major leachable anion. Carbonate is not expected to be very leachable from the $\text{Ca}(\text{OH})_2$ -saturated solution, but may be leachable at the lower pH of the CaCO_3 system if soluble carbonate minerals are present.

The primary contaminants of concern in the C-106 sludge are ^{99}Tc , ^{238}U , ^{129}I , and Cr because of their potential mobility in the environment and the long half-lives of the radionuclides. In the deionized water leaches, it was found that only low percentages (<10%) of these primary contaminants were readily leachable from the residual waste, probably because of the previous in-tank mobilization and solids removal with oxalic acid during retrieval.

3.0 Materials and Laboratory Test Methods

Sludge and liquid samples from tank C-106 were collected by CH2M HILL during post retrieval activities in January 2004. This section provides a description of the samples and the various tests used to characterize the material, measure contaminant release, and identify controlling solids.

All laboratory activities were conducted in accordance with the requirements of Title 10, Code of Federal Regulations, Part 830.120 "Quality Assurance" and the *Hanford Analytical Services Quality Assurance Requirements Document* (HASQARD, DOE 1998). These requirements were implemented using PNNL's internal quality assurance (QA) plan.^(a) PNNL's QA Plan is based on the requirements of U.S. Department of Energy (DOE) Order 414.1A, the HASQARD, relevant elements of NQA-1-1989 (ASME 1989), as well as recognized industry standards (e.g., U.S. Environmental Protection Agency [EPA], ASTM, American National Standards Institute).

3.1 Tank C-106 Samples

On January 26, 2004, after neutralization of tank waste with NaOH and during pumping of residual fluid from tank C-106, a sample of the liquid was collected and transported to the Hanford 222-S Laboratory for storage and analysis. On January 29, 2004, nine clamshell samples of residual sludge were collected from the tank and sent to the 222-S Laboratory. On January 30 the sludge samples were extruded in the 11A Hot Cell. Part of the extruded samples was combined to produce the Field Primary Solid Composite. The remaining sludge was combined to produce the Field Duplicate Solid Composite. On April 13, 2004, samples of the sludge and liquid were shipped to the PNNL Radiochemical Processing Laboratory (RPL). Table 3.1 lists the samples received by PNNL.

Testing of sludge samples to develop contaminant release models was conducted on Field Primary Solid Composite S04T000404 (primary 404, Figure 3.1) and Field Duplicate Solid Composite S04T000405 (duplicate 405, Figure 3.2). Liquid sample S04T000403 (403) was also analyzed to determine the pore water concentrations of contaminants in the sludge.

Table 3.1. Tank C-106 Samples Provided by 222-S Laboratory to PNNL

Sample	Jar Size (mL)	Labcore Number	Net Weight/Volume of Material (g)
Field Primary Solid Composite	60	S04T000109	20.4
Field Primary Solid Composite	60	S04T000404	20.6
Field Duplicate Solid Composite	60	S04T000405	20.1
6C-03-11 (Liquid)	60	S04T000403	61.6

(a) PNNL. 2001. *Conducting Analytical Work in Support of Regulatory Programs*. Internal unpublished procedure, Pacific Northwest National Laboratory, Richland, Washington.



Figure 3.1. Tank C-106 Field Primary Solid Composite Sludge Sample 404



Figure 3.2. Tank C-106 Field Duplicate Solid Composite Sludge Sample 405

3.2 Cement Simulation Tests

Batch and sequential contact leach tests were conducted on C-106 residual sludge samples using Ca(OH)_2 -saturated and CaCO_3 -saturated solutions. Figure 3.3 shows the flowpaths of the experiments, which are described in detail in this section.

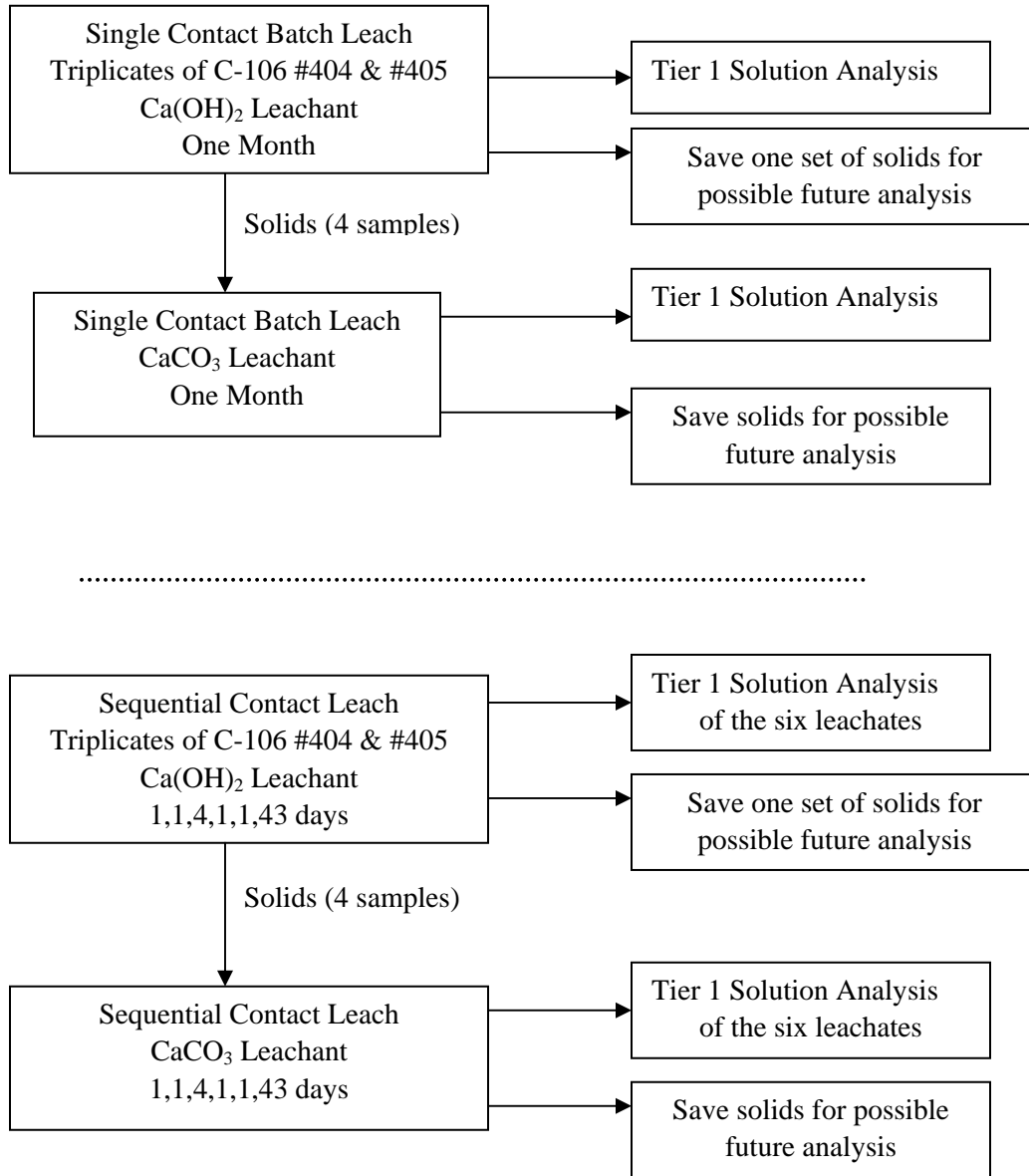


Figure 3.3. Leach Test Flowpath

Ca(OH)_2 -Saturated Leaching Solution

A sufficient quantity of fresh Ca(OH)_2 (~1.4 g/L @ 25°C) was added to deionized water to just saturate the solution. Excess solid Ca(OH)_2 is undesirable because it will buffer the pH at a higher than expected value. Because CO_2 in air is very soluble in water at high pH and the resulting dissolved

carbonate will precipitate as calcite in the $\text{Ca}(\text{OH})_2$ -saturated solution, care was taken to minimize contact of the solution with atmospheric air. When possible, Teflon containers were used because they have low air diffusion coefficients. Air space in the containers was also minimized and the vessel was tightly sealed to limit leakage of air into the vessel. The pH of an aliquot of the $\text{Ca}(\text{OH})_2$ solution was measured as well as the dissolved calcium concentration.

Calcite-Saturated Leaching Solution

The calcite-saturated solution was prepared by adding excess powdered calcite to deionized water and stirring or shaking the mixture for 24 hours. The temperature during equilibration was a few degrees above room temperature. By preparing the solution at a slightly elevated temperature the possibility of calcite precipitation during the test at room temperature was minimized. (Calcite undergoes retrograde solubility.) There was no need to minimize contact of this solution with the atmosphere. After the solution was prepared, the pH value and calcium and carbonate concentrations were measured and compared to expected equilibrium values and concentrations [pH = 8.3, Ca^{2+} = 20 mg/L, TIC = 58 mg/L, P_{CO_2} = 0.0003 atm (fixed)].

3.2.1 Moisture Content

The moisture contents of the tank waste samples were measured to calculate dry weight concentrations for constituents in the waste. Dry weight concentrations provide a consistent measurement unit for comparison purposes that eliminates the effect of variable water content on sample concentrations.

Gravimetric water content of the waste material was determined using ASTM procedure D2216-98, *Standard Test Method for Laboratory Determination of Water (Moisture) Content of Soil and Rock by Mass* (ASTM 1998) with the following minor exceptions: (1) the volume of sample recommended was decreased due to radiological concerns and (2) the sample was dried at a lower oven temperature, 105°C, for a longer period of time to prevent dehydration of the solids.

Sludge samples were placed in tarred containers, weighed, and dried in an oven until a constant weight was achieved, usually requiring 24 to 48 hours. The container was then removed from the oven, sealed, cooled, and weighed. All weighings were performed using a calibrated balance. The gravimetric water content is computed as the percentage change in soil weight before and after oven drying (i.e., $\{[\text{wet weight} - \text{dry weight}]/\text{dry weight}\}$).

3.2.2 Single Contact Batch Leaching Test

In this test, 0.3 g of C-106 sludge were added to 30 mL of a $\text{Ca}(\text{OH})_2$ -saturated solution and leached in the same fashion as was done in the Tier 1 water leaches (Deutsch et al. 2005a). Triplicate samples of C-106 sludges #404 and #405 were tested. Because there were not significant differences in the 1 day, two week, and 1 month water leaches, this test was only conducted for a time period of one month. The leachates from these experiments were analyzed for the same parameters that were measured in the Tier 1 water-leaching experiments. After leaching, two of the samples of remaining solid materials were saved for the single contact batch-leaching tests using the CaCO_3 leaching solution described in the following paragraph. The third sample was saved for possible future XRD/SEM/EDS analysis. None of these solids were used for the sequential leaches described in the following section. This will allow a

comparison to be made of the results of the 1-month single contact test and the first day of the sequential leach to confirm that contact time does not affect the results.

Two of the final solids from the single contact $\text{Ca}(\text{OH})_2$ leaching tests were added to 30 mL of the CaCO_3 -saturated solution and leached in the same fashion as was done for the other single contact tests. Duplicate samples of C-106 sludge #404 and #405 were tested. The contact time was 1 month. The leachates from these experiments were analyzed for the same parameters that were measured in the Tier 1 water-leaching experiments. After leaching, the remaining solid materials were saved for possible future XRD and SEM analysis.

3.2.3 Sequential Contact Leaching Test

Because there were significant differences in the early stages of the sequential water leaches (primarily depletion of Na, Mn, and oxalate), the sequential leach tests mimicked the deionized water tests and were conducted for time periods of 1, 1, 4, 1, 1, and 43 days (Figure 3.3). (The long-term 82-day leach was not necessary because the results of the deionized water leach test were not that different than observed in the 43-day test.) In the sequential contact leaching tests, 0.3 g of triplicate fresh samples of #404 and #405 C-106 sludge were added to 30 mL of a $\text{Ca}(\text{OH})_2$ -saturated solution and leached for the stated periods of time. The leachates from these experiments were analyzed for the same parameters that were measured in the Tier 1 water-leaching experiments. After leaching, two of the three remaining solid materials were saved for the second phase of these leach tests using the CaCO_3 leachant. The third sample was saved for possible future XRD/SEM/EDS analysis.

The final solids from the sequential $\text{Ca}(\text{OH})_2$ leach tests were used for the CaCO_3 leach tests. These tests were also conducted using 30 mL of the CaCO_3 -saturated solution as the leachant for time periods of 1, 1, 4, 1, 1, and 43 days. The leachates from these experiments were analyzed for the same parameters that were measured in the Tier 1 water-leaching experiments. After leaching, the remaining solid materials were saved for possible future XRD and SEM analysis.

3.2.4 pH

The pH values of the solutions were measured using a solid-state pH electrode and a pH meter calibrated with buffers bracketing the expected range. This measurement is similar to EPA Method 9040B (EPA 1995).

3.2.5 Anion Analysis

Anion analysis was performed using an ion chromatograph. Fluoride, acetate, formate, chloride, nitrite, bromide, nitrate, carbonate, sulfate, oxalate, and phosphate were separated on a Dionex AS17 column with a gradient elution technique from 1 mM to 35 mM NaOH and measured using a conductivity detector. This methodology is similar to EPA Method 9056A (EPA 1994b) with the exception of using gradient elution with NaOH.

3.2.6 Cations and Trace Metals

Major cation analysis (including Al, Ca, Fe, K, Mg, Mn, Na, and Si) was performed by inductively coupled plasma-optical emission spectroscopy (ICP-OES) EPA Method 6010B (EPA 1996).

Radiochemical analysis for ^{99}Tc , ^{238}U , ^{239}Pu , ^{241}Am , ^{237}Np and ^{129}I was performed by inductively coupled plasma-mass spectroscopy (ICP-MS). This method is similar to EPA Method 6020 (EPA 1994a). For both ICP-OES and ICP-MS, high-purity calibration standards were used to generate calibration curves and to verify continuing calibration during the analysis. Multiple dilutions of selected samples (ranging from 3x to 100x) were made and analyzed to investigate and correct for matrix interferences.

3.2.7 Alkalinity

The sample alkalinity was measured by standard titration. A volume of standardized sulfuric acid (H_2SO_4) was added to the sample to an endpoint of pH 4.5. The volume of H_2SO_4 needed to achieve the endpoint is used to calculate the total ($\text{OH}^- + \text{HCO}_3^- + \text{CO}_3^{2-}$) alkalinity as calcium carbonate (CaCO_3). The alkalinity procedure is similar to Standard Method 2320 B (Clesceri et al. 1998).

3.2.8 Radioanalysis

In addition to the radionuclides listed in Section 3.2.6 that were analyzed in solution by ICP-MS, short-lived radionuclides were analyzed by conventional counting methods as described in the following sections.

3.2.8.1 Gamma Energy Analysis

All samples for gamma energy analysis (GEA) were analyzed using 60% efficient intrinsic-germanium gamma detectors. All germanium counters were efficiency calibrated for distinct geometries using mixed gamma standards traceable to the National Institute of Standards and Technology (NIST). Direct solids, acid extracts, and water extracts were analyzed for gamma energy. Spectral analysis was conducted using libraries containing most mixed-fission products, activation products, and natural decay products. Control samples were run throughout the analysis to ensure correct operation of the detectors. The controls contained isotopes with photo peaks spanning the full detector range and were monitored for peak position, counting rate, and full-width half-maximum. Details are found in PNNL internal procedure AGG-RRL-001.^(a)

3.2.8.2 ^{90}Sr Analyses

Aliquots of filtered acid extracts, fusions, and water extracts were diluted in 8 M HNO_3 and submitted for strontium separation and analysis by internal PNNL procedure AGG-RRL-003.2.^(b) A 0.1 to 5 mL aliquot of sample was spiked with ^{85}Sr tracer and passed through a SrSpec[®] column (Eichrom Technologies, Chicago) to capture Sr. The columns were washed with 10 column volumes (20 mL) of 8 M HNO_3 . The strontium was eluted from the SrSpec column into glass liquid scintillation vials using 15 mL of deionized water. The vials were placed under a heat lamp overnight to evaporate the water to dryness. A 15 mL Optifluor[®] scintillation cocktail was added to each vial. Gamma spectroscopy was used to determine the chemical yield from the added ^{85}Sr tracer. The samples were then analyzed by liquid scintillation counting (LSC) to determine the amount of ^{90}Sr originally present in the sludge

(a) AGG-RRL-001, 2004 *Gamma Energy Analysis, Operation, and Instrument Verification using Genie2000 Support Software*, Technical Procedure, Pacific Northwest National Laboratory, Richland, Washington.

(b) AGG-RRL-003.2. 2000. *Tc99 and Sr90 Analysis using Eichrom TEVA-spec and Sr-spec Resin*. Technical Procedure, Pacific Northwest National Laboratory, Richland, Washington.

sample. A matrix spike, a blank spike, a duplicate, and blanks were run with each sample set to determine the efficiency of the separation procedure as well as the purity of reagents.

3.3 XRD Analysis

Crystalline phases present in the 1-month and Stage 6 sequential samples of residual waste from tank C-106 leached with $\text{Ca}(\text{OH})_2$ and $\text{Ca}(\text{OH})_2/\text{CaCO}_3$ were characterized by standard powder XRD techniques. Because the sludge materials were highly radioactive, dispersible powders, it was necessary to prepare the XRD mounts of these samples inside a fumehood regulated for handling radioactive materials. Sludge samples were prepared for XRD analysis by placing a milligram quantity of each sample and a trace quantity of reference-material corundum powder ($\alpha\text{-Al}_2\text{O}_3$, alumina) (NIST Standard Reference Material [NIST SRM] 676) into a mixture of water and collodion solution. The collodion solution consists of 2% nitrocellulose dissolved in amyl acetate, and is an x-ray amorphous, viscous binder commonly used to make random powder mounts for XRD when only a limited amount of sample is available. The addition of trace quantities of reference-material corundum powder to each slurry provided an internal 2θ standard for each XRD pattern. Using a pipette, each slurry was transferred onto a circular-shaped platform (1-cm diameter) and placed on top of the post located on the base inside a disposable XRD specimen holder (Figure 3.4). This specimen holder was designed specifically for safe handling of dispersible powders containing highly radioactive or hazardous materials (Strachan et al. 2003). After allowing samples to air dry overnight, the holder was assembled and a piece of Kapton[®] film was placed between the cap and the retainer. The holder was sealed with wicking glue and removed from the fumehood.

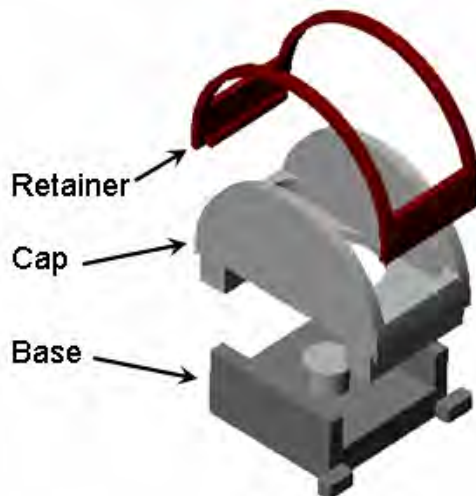


Figure 3.4. Exploded Schematic View of the XRD Sample Holder (Kapton[®] film not shown)

Each sample was analyzed using a Scintag XRD unit equipped with a Peltier thermoelectrically-cooled detector and a copper x-ray tube. The diffractometer was operated at 45 kV and 40 mA. Individual scans were obtained from 2 to $65^\circ 2\theta$ with a dwell time of 4 and 14 seconds. Scans were collected electronically and processed using the JADE[®] XRD pattern-processing software.

Krupka et al. (2004) prepared and analyzed by XRD a sample consisting of only a dry film of the collodion solution so that its contribution relative to the background signals of the XRD patterns for the sludge samples could be quantified. The resulting XRD pattern for the collodion solution film is shown in Figure 3.5. The most obvious feature of this diffraction pattern is the broad peak positioned between 10° and $30^\circ 2\theta$. The symmetry of this peak is characteristic of those resulting from the XRD of amorphous (noncrystalline) material. Although subtracting the collodion background from sludge XRD patterns allows for better phase matching, this process may eliminate minor reflections and inconspicuous features of a pattern. Therefore, each as-measured XRD pattern was examined before and after background subtraction to ensure that the integrity of the pattern was maintained. For background subtraction, the JADE[®] software provides the user with control over the selection of background-subtraction points. This process allows a better fit to 2θ regions under broad reflections, such as those resulting from amorphous materials. On average, 30 to 40 background points were selected from each XRD pattern, and a cubic-spline curve was then fit through each set of points. Adjustments to this curve were made by selecting additional background points in regions of a pattern that were difficult to fit. Once a well-matched curve was fitted to a pattern, the background was subtracted from each as-measured XRD pattern, resulting in a smooth tracing.

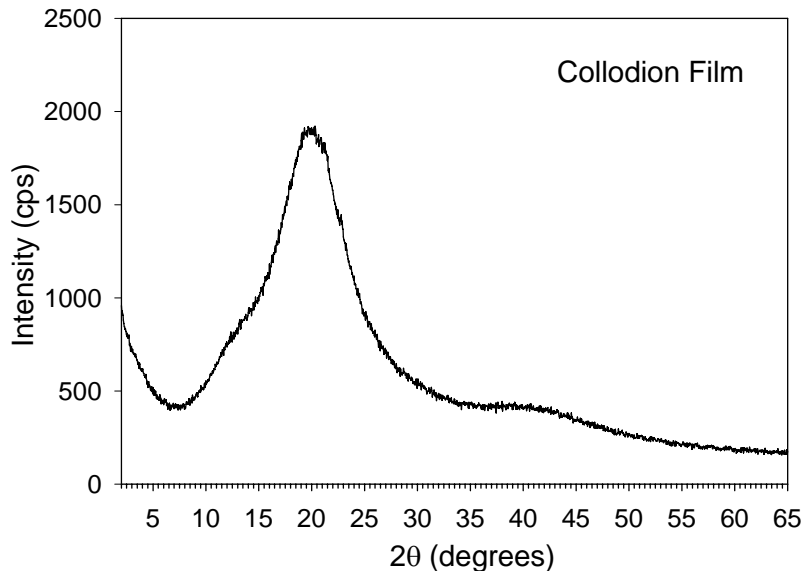


Figure 3.5. XRD Pattern for Collodion Film Measured in the Absence of any Sludge Material (from Krupka et al. 2004)

Identification of the mineral phases in the background-subtracted patterns was based on a comparison of the XRD patterns measured for the sludge samples with the mineral powder diffraction files (PDFTM) published by the Joint Committee on Powder Diffraction Standards (JCPDS) International Center for Diffraction Data (ICDD). As a rule of thumb, a crystalline phase must be present at greater than 5 wt% of the total sample mass (greater than 1 wt% under optimum conditions) to be readily detected by XRD. In general, the measured peak intensities depend on several factors, including the combined mass of each crystalline phase in the sample. Due to the physical characteristics of these tank sludge samples such as high radioactivity, high dispersibility, and variable moisture content, the mass of tank sludge combined with the collodion solution for each XRD mount could not be controlled or easily determined. Dissimilarities in mineral segregation (settling) resulting from the different densities of minerals mixed with the

collodion solution and associated effects on relative peak intensities also influence the overall pattern intensity. The combined effect of these factors could have some effect on the characteristic mineral peak intensities, which precluded quantitative comparisons of peak intensities for equivalent reflections in background-subtracted XRD patterns for different sludge samples.

3.4 SEM/EDS Analysis

The morphologies, sizes, surface textures, and compositions of phases present in the 1-month and Stage 6 sequential samples of residual waste from tank C-106 leached with $\text{Ca}(\text{OH})_2$ and $\text{Ca}(\text{OH})_2/\text{CaCO}_3$ were studied by SEM/EDS and EDS element mapping. Two or three mounts were prepared of each sample to compensate for the possibility that one or more less-than-optimum mounts of a sample might occur, thus improving the likelihood of obtaining representative SEM images of each sample. The mounts used for SEM/EDS consisted of double-sided carbon tape attached to standard aluminum mounting stubs. For each mount, small aliquots of each sludge sample were placed on the exposed upper surface of the carbon tape using a micro spatula. Each mount was then coated with carbon using a vacuum sputter-coater to improve the conductivity of the samples and thus the quality of the SEM images and EDS signals.

A JEOL JSM-840 SEM was used for high-resolution imaging of micrometer/submicrometer-size particles from the sludge samples. The SEM system is equipped with an Oxford^(a) INCA EDS software system that was used for semi-qualitative element analysis. As noted in Deutsch et al. (2005b), the JEOL JSM-840 SEM was upgraded in late calendar year 2005 to the Oxford INCA software to automate the collection of EDS spectra over multi-micrometer-size areas of an SEM-imaged sample. This upgrade permits the mapping of the spatial distributions over user-selected areas and/or lines of the relative concentrations of any user-specified element detectable by EDS. Operating conditions for the SEM/EDS analyses consisted of 10 to 20 keV for SEM imaging, and 20-30 keV, 100 live seconds^(b) for the EDS analyses.

The EDS analyses of particles are limited to elements with atomic weights heavier than boron. Photomicrographs of high-resolution secondary electron (SE) images and backscattered electron (BSE) images were obtained as digital images and stored in electronic format. To help identify particles that contain elements with large atomic numbers, such as uranium, the SEM was typically operated in the BSE mode. Secondary electrons are low-energy electrons ejected from the probed specimen as a result of inelastic collisions with beam electrons, whereas backscattered electrons are primary electrons emitted as a result of elastic collisions. Backscattered electron emission intensity is a function of the element's atomic number — the larger the atomic number, the brighter the signal. Backscattered electron images are obtained in exactly the same way as secondary electron images.

The SEM micrographs included in the main body of this report (Section 4.3) were selected because they show typical morphologies, sizes, and surface textures of particles in the sludge subsample mounts. All of the SEM micrographs and EDS spectra determined for samples of 1-month and Stage 6 sequential

(a) Oxford Instruments, Concord, Massachusetts.

(b) Live time is when (real time less dead time) the EDS system is available to detect incoming x-ray photons. Dead time is the portion of the total analyzing time that is actually spent processing or measuring x-rays. While each x-ray pulse is being measured, the system cannot measure another x-ray that may enter the detector and is, therefore, said to be “dead.”

samples of residual waste from tank C-106 leached with $\text{Ca}(\text{OH})_2$ - and $\text{Ca}(\text{OH})_2/\text{CaCO}_3$ are shown in Appendices B through D at the end of this report. The entire area of each SEM mount was examined by SEM at low magnification (typically 50 to 100x) to identify those particles and surface features that were typical or unusual for the sample. During this examination, SEM micrographs were recorded at low magnification (e.g., 100x) for typically one or two areas of the mount to show a general perspective of the sizes, types, and distributions of particles that make up the SEM mount. Within these imaged regions, additional SEM micrographs were recorded of several particles at greater magnifications to provide a more detailed representation of the particles' characteristics, and selected points on these particles then analyzed by EDS. Depending on the perceived importance of such particles, regions on these particles were sometimes analyzed by SEM and EDS at even greater magnifications. Compositions determined by EDS are qualitative and have large uncertainties resulting from alignment artifacts caused by the variable sample and detector configurations that exist when different particles are imaged by SEM.

4.0 Analytical Results

This section provides the results of the cement simulant leach tests conducted on sludge samples from tank C-106. These results are compared to the double deionized (DDI) water leach data as well as the fusion data presented in Deutsch et al. (2005a). The discussion begins with the results of the single contact batch leaching tests in Section 4.1.1 followed by the results of the sequential contact leach test (Section 4.1.2), x-ray diffraction analyses (Section 4.2) and SEM/EDS analyses (Section 4.3).

4.1 Leaching Tests

The results of the leaching tests of sludge samples are discussed in this section. These include results from the single contact batch leaching and sequential contact leaching tests. Concentration values in this section are given in terms of μg or μCi per gram of dry sludge. The data are presented in tabular form with a comparison of results from the DDI water leach to the $\text{Ca}(\text{OH})_2$ and the CaCO_3 leaches.

4.1.1 Single Contact Batch Leaching

4.1.1.1 Digestion Factors and Moisture Contents

The digestion factors for the tank C-106 404 and 405 sludge samples used for the DDI water extract varied from 7 to 13.5 g/L. The digestion factors for the same sludges used for the $\text{Ca}(\text{OH})_2$ and the CaCO_3 leaches varied from 8.8 to 11.8. These digestion factors are the ratios of wet weight of sludge to 30 mL of the leachate used to dissolve the soluble portion of the solid. The digestion factors were then multiplied by the percent solids, as determined from moisture content analysis, to convert to a dry weight basis. The variability is a function of the mass of sludge used, which ranged from approximately 0.2 to 0.4 g. The moisture contents averaged about 50.5% for the C-106 samples used in the DDI water extraction and 12.1% for the samples used in the $\text{Ca}(\text{OH})_2$ and the CaCO_3 leaches.

4.1.1.2 pH and Alkalinity – Single Contact Batch Leaching

The range of pH and alkalinity values for the sludge sample extracts is listed in Table 4.1. The pH values for the 1-month single contact water leach test were in the range of 7.00 to 7.42. pH values for the 1-month single contact leaching tests using $\text{Ca}(\text{OH})_2$ and CaCO_3 are not available; however, the values for Stage 6 (43-day contact) of the sequential contact leach tests using $\text{Ca}(\text{OH})_2$ and CaCO_3 were 11.98 to 12.23 and 11.54 to 11.75, respectively. These high pH values represent the highly alkaline condition of the $\text{Ca}(\text{OH})_2$ leaching solution. Apparently the high alkalinity is not significantly reduced by six stages of leaching with the CaCO_3 solution.

The total alkalinities of the extracts reported in units of mg CaCO_3/g sludge are also shown in Table 4.1. The range of the DDI water extract was 14.8 to 23.9 compared to 406 to 740 for the $\text{Ca}(\text{OH})_2$ tests and 337 to 418 for the CaCO_3 tests. The higher value for the $\text{Ca}(\text{OH})_2$ and the CaCO_3 leaches are attributable to the composition of the leaching solutions and not to material released from the sludge.

Table 4.1. Water Extract pH and Alkalinity Values Corrected to Grams of Dry Sludge

Sample Number	pH	Total Alkalinity as CaCO ₃ at pH 4.5 Endpoint (mg/g)
C-106 Water Leach Range, 1 month	7.00 to 7.42	14.8 to 23.9
C-106 Ca(OH) ₂ Range, 1 month	11.98 to 12.23*	406 to 740
C-106 CaCO ₃ Range, 1 month	11.54 to 11.75*	337 to 418
*pH values measured for Stage 6 of the selective extractions.		

4.1.1.3 ⁹⁹Tc, ²³⁸U, and ¹²⁹I – Single Contact Batch Leaching

⁹⁹Tc, ²³⁸U, and ¹²⁹I are important potential long-term risk constituents in tank sludge because of their long half-lives and high mobility once dissolved in water. Table 4.2 lists the concentrations of these radionuclides in units of µg leached/g solid and µCi leached/g solid for the single-contact extracts. Table 4.3 lists the percentage of the total ⁹⁹Tc, ²³⁸U, and ¹²⁹I leached from the sludge by each leach test versus the total available concentration given by the fusion analysis reported in Deutsch et al. (2005a). The water-leachable amount of ⁹⁹Tc ranges from 0.034 to 0.0322 µg/g, which is 2.4 to 3.2% of the total ⁹⁹Tc. For the simulated cement leachate sample the soluble ⁹⁹Tc ranged from 0.112 to 0.131 µg/g (8.6 to 11.8% of the available ⁹⁹Tc) for the Ca(OH)₂ leachate and was not detectable in the CaCO₃ leachate.

Table 4.2. ⁹⁹Tc, ²³⁸U, and ¹²⁹I Concentrations Leached During Single-Contact Batch Tests

	⁹⁹ Tc (µCi/g)	⁹⁹ Tc (µg/g)	²³⁸ U (µCi/g)	²³⁸ U (µg/g)	¹²⁹ I (µCi/g)	¹²⁹ I (µg/g)
C-106 Water Leach Range, 1 month	5.17E-04 to 5.80E-04	3.04E-02 to 3.22E-02	1.04E-06 to 1.26E-06	3.04E+00 to 3.70E+00	<7.70E-06	<4.36E-02
C-106 Ca(OH) ₂ Range, 1 month	1.91E-03 to 2.22E-03	1.12E-01 to 1.31E-01	8.44E-07 to 2.56E-06	2.48E+00 to 7.53E+00	<2.18E-05	<1.23E-01
C-106 CaCO ₃ Range, 1 month	<1.04E-03	<6.12E-02	1.79E-06 to 2.96E-06	5.26E+00 to 8.72E+00	NA	NA

Table 4.3. Leachable Percentages of ⁹⁹Tc, ²³⁸U, and ¹²⁹I in C-106 Sludge Samples Compared with Fusion Results

	⁹⁹ Tc	²³⁸ U	¹²⁹ I
	(% Leachable)		
C-106 Water Leach Range, 1 month	2.4 to 3.2	1.3 to 1.4	< 1.1
C-106 Ca(OH) ₂ Range, 1 month	8.6 to 11.8	1.8 to 2.9	< 3.1
C-106 CaCO ₃ Range, 1 month	< 6.0	2.2 to 3.4	NA

The water-leachable amount of ²³⁸U ranged from 3.04 to 3.70 µg/g, which is 1.3 to 1.4% of the total ²³⁸U. For the simulated cement leachate sample, the soluble ²³⁸U ranged from 2.48 to 7.53 µg/g (1.8 to 2.9% of the available ²³⁸U) for the Ca(OH)₂ leachate and 5.26 to 8.72 µg/g (2.2 to 3.4% of the available ²³⁸U) for the CaCO₃ leachate. There was no detectable ¹²⁹I in DDI water or simulated cement leaches.

4.1.1.4 Selected Metal Concentrations – Single Contact Batch Test

Metals detected at measurable concentrations in one or more samples are listed in Table 4.4. The water extracts show that Na and Mn are the primary water-soluble constituents with much smaller amounts of Ba, Ca, Mg, and Ni, also being leachable. Very little Al or Fe were water leachable from the sludge. The primary soluble metals in the $\text{Ca}(\text{OH})_2$ leach tests were Al and Na with no detectable Mn. The only soluble metal seen in the CaCO_3 tests was Na. (Note that the concentrations measured in the water leachates are the sums of the water-leachable amounts and the initial dissolved pore water concentrations.)

4.1.1.5 Anion Concentrations – Single Contact Batch Test

The anion concentrations in single contact batch test from the tank C-106 sludge samples are listed in Table 4.5. The primary leachable anion for the water leach test was oxalate, with much smaller quantities of leachable chloride. There were no detectable anions in the $\text{Ca}(\text{OH})_2$ or the CaCO_3 leached samples; however, the detection limit for carbonate was high at 61,200 $\mu\text{g/g}$. The presence of high concentrations of oxalate (33,900 to 41,600 $\mu\text{g/g}$) in the water extracts shows that the sludge has the capacity to act as a reductant for more oxidized species. However, its presence in the sludge in contact with air suggests the oxalate is not readily oxidized in this environment.

4.1.1.6 Radioanalytical Results – Single Contact Batch Test

The results of the GEA analysis for ^{137}Cs in the single contact batch test are listed in Table 4.6. For the tank C-106 sludge samples, ^{137}Cs was not analyzed in the 1-month water leachates, but was measured at values of 2.03 and 2.65 $\mu\text{g/g}$ in the 1-day water leach. The leachable concentrations of ^{137}Cs were measured in the range of 0.095 to 0.138 $\mu\text{g/g}$ for the $\text{Ca}(\text{OH})_2$ and the CaCO_3 leaches.

Table 4.7 lists the leachable concentrations of ^{90}Sr , ^{239}Pu , ^{237}Np , and ^{241}Am in terms of the original sludge compositions. The ^{90}Sr concentration was not measured in the 1-month water extract but ranged from 0.310 to 0.697 $\mu\text{g/g}$ in the 1-day water leach. The amounts measured in the simulated cement leach ranged from 0.049 to 0.146 $\mu\text{g/g}$ for the $\text{Ca}(\text{OH})_2$ leachates and 0.022 to 0.517 $\mu\text{g/g}$ for the CaCO_3 leachates. Leachable quantities of ^{237}Np (0.651 to 0.985 $\mu\text{g/g}$) and ^{241}Am (0.0016 to 0.0029 $\mu\text{g/g}$) were measured in the water leach samples, but no detectable ^{239}Pu was found. ^{237}Np , ^{239}Pu , and ^{241}Am were not detected in any of the $\text{Ca}(\text{OH})_2$ and CaCO_3 leachates.

4.1.2 Sequential Contact Leaching Test

The sequential contact leaching tests were conducted by contacting each sludge sample with sequential 30-mL quantities of fresh leach solutions consisting of DDI water, $\text{Ca}(\text{OH})_2$ and CaCO_3 . As shown in Table 4.8, the sludge was contacted six times with each solution. The first five contacts were of short duration (1 or 4 days each), which was assumed sufficient for leaching contaminants of concern from the sludge. To test this assumption, an extended period of leaching was conducted in which the sludge, after the first five stages of leaching, was contacted for 43 days (Stage 6). The objective of this state was to evaluate the long-term leaching characteristics of contaminants from the sludge. Very little of the primary contaminants of concern, ^{99}Tc , ^{238}U , and ^{129}I was leachable during these tests. Over 90% of the ^{99}Tc , ^{238}U , and ^{129}I remained in the sludge and was not leachable during the six stages of leaching with the three solutions.

Table 4.4. Leachable Metal Concentrations in Single Contact Batch Test

Sample Number	Al (µg/g)	Ba (µg/g)	Ca (µg/g)	Cr (µg/g)	Fe (µg/g)	K (µg/g)	Mg (µg/g)	Mn (µg/g)	Ni (µg/g)	Na (µg/g)
C-106 Water Leach Range, 1 month	<2.61E+01	1.26E+01 to 2.64E+01	5.98E+01 to 1.26E+02	2.28E+00 to 3.90E+00	<1.05E+01	<2.61E+02	1.62E+02 to 2.32E+02	7.66E+03 to 1.39E+04	8.90E+01 to 1.33E+02	9.23E+03 to 1.06E+04
C-106 Ca(OH) ₂ Range, 1 month	8.67E+03 to 1.48E+04	<3.06E+02	(2.14E+02) to 3.88E+02	<1.54E+02	<3.06E+02	<7.65E+04	<6.12E+02	<3.06E+02	<6.12E+02	1.99E+04 to 2.65E+04
C-106 CaCO ₃ Range, 1 month	<1.53E+03	<3.06E+02	8.26E+02 to 1.45E+04	<1.54E+02	<3.06E+02	<7.65E+04	<6.12E+02	<3.06E+02	<6.12E+02	4.73E+03 to 6.29E+03

Table 4.5. Average Anion Concentrations Leached During Single Contact Batch Test

	Fluoride (µg/g)	Chloride (µg/g)	Nitrite (µg/g)	Bromide (µg/g)	Nitrate (µg/g)	Carbonate (µg/g)	Sulfate (µg/g)	Oxalate* (µg/g)	Phosphate (µg/g)
C-106 Water Leach Range, 1 month	<2.14E+02	2.60E+2 to 7.77E+02	<7.86E+02	<8.38E+02	<7.53E+02	<8.71E+04	<7.13E+02	3.39E+04 to 4.16E+04	<1.06E+00
C-106 Ca(OH) ₂ Range, 1 month	<1.43E+02	<2.89E+02	<5.52E+02	<5.88E+02	<5.30E+02	<6.12E+04	<5.00E+02	<2.18E+03	<6.18E+02
C-106 CaCO ₃ Range, 1 month	<1.43E+02	<2.88E+02	<5.52E+02	<5.88E+02	<5.30E+02	<6.12E+04	<5.01E+02	<4.22E+02	<6.18E+02
*Oxalate continuing calibration verification was not within the procedural +/- 10 %. All other quality control was in control.									

Table 4.6. ¹³⁷Cs Leached During Single Contact Batch Test

	¹³⁷ Cs (μCi/g)	¹³⁷ Cs (μg/g)
C-106 Water Leach Range, 1 day	1.76E+02 to 2.31E+02	2.03 to 2.65
C-106 Ca(OH) ₂ Range, 1 month	8.50E+00 to 1.20E+01	9.77E-02 to 1.38E-01
C-106 CaCO ₃ Range, 1 month	8.25E+00 to 1.11E+01	9.48E-02 to 1.28E-01

Table 4.7. ⁹⁰Sr and Actinides Leached During Single Contact Batch Test

	⁹⁰ Sr (μCi/g)	⁹⁰ Th (μg/g)	²³⁹ Pu (μCi/g)	²³⁹ Pu (μg/g)	²³⁷ Np (μCi/g)	²³⁷ Np (μg/g)	²⁴¹ Am (μCi/g)	²⁴¹ Am (μg/g)
C-106 Water Leach Range, 1 month	NA	NA	<9.73E-04	<1.57E-02	4.62E-04 to 6.99E-04	6.51E-01 to 9.85E-01	4.85E-04 to 8.61E-04	1.65E-03 to 2.93E-03
C-106 Ca(OH) ₂ Range, 1 month	6.81E+00 to 2.05E+01	4.86E-02 to 1.46E-01	<7.58E-03	<1.22E-01	<8.69E-05	<1.22E-01	<2.08E+00	<6.12E-01
C-106 CaCO ₃ Range, 1 month	3.01E+00 to 7.99E+01	2.15E-02 to 5.71E-01	<7.56E-03	<1.22E-01	<8.66E-05	<1.22E-01	<2.08E+00	<6.12E-01

Table 4.8. Contact Times, pH Range, and Alkalinities for Sequential Contact Leaching Test on Tank C-106 Sludge Samples

Contact Stage	Contact Duration (Days)	Extractants	pH	Alkalinity as CaCO ₃ (mg/g)
1	1	C-106 Water	6.72 to 7.06	37.6 to 64.7
		C-106 Ca(OH) ₂	11.43 to 12.30	388 to 844
		C-106 CaCO ₃	11.45 to 11.54	377 to 442
2	1	C-106 Water	6.80 to 6.94	<55
		C-106 Ca(OH) ₂	12.24 to 12.49	280 to 804
		C-106 CaCO ₃	11.30 to 11.51	377 to 529
3	4	C-106 Water	6.77 to 7.02	<55
		C-106 Ca(OH) ₂	12.38 to 12.62	331 to 719
		C-106 CaCO ₃	11.38 to 11.55	388 to 681
4	1	C-106 Water	6.67 to 6.77	<55
		C-106 Ca(OH) ₂	12.14 to 12.50	377 to 641
		C-106 CaCO ₃	11.39 to 11.45	396 to 445
5	1	C-106 Water	6.68 to 6.74	<55
		C-106 Ca(OH) ₂	12.44 to 12.58	321 to 685
		C-106 CaCO ₃	11.14 to 11.40	331 to 442
6	43	C-106 Water	7.47	13.7
		C-106 Ca(OH) ₂	11.98 to 12.23	388 to 709
		C-106 CaCO ₃	11.54 to 11.75	396 to 520

4.1.2.1 Digestion Factors and Moisture Contents – Sequential Contact Leaching Test

The digestion factors for the C-106 sludge samples used for the sequential contact leaching tests varied from 4.5 g/L to 10.7 g/L. These digestion factors are the ratios of wet weight of sludge to the amount of extractant (30 mL) used to dissolve the soluble portion of the solid. The digestion factors were then multiplied by the percent solids, as determined from moisture content analysis, to convert concentrations to a dry weight basis. The variability in digestion factors is a function of the mass of sludge used, which ranged from approximately 0.2 to 0.35 g.

The moisture contents [(wet wt – dry wt)/dry wt] averaged about 50.5% for the C-106 samples used in the DDI water extraction and 12.1% for the samples used in the Ca(OH)₂ and the CaCO₃ leaches.

4.1.2.2 pH and Alkalinity – Sequential Contact Leaching Test

Table 4.8 lists the pH values and alkalinities for the leachates from the sequential contact leaching tests. The water leachate pH values for the first five stages were in the range 6.87 to 7.03 and then increased to an average of 7.5 in Stage 6. The increase in pH at Stage 6 may reflect equilibration with a carbonate mineral. The average pH value of 12.3 for the Ca(OH)₂ leachates corresponds to the pH of the Ca(OH)₂-saturated solution used as the leachant. This suggests that the pH is controlled by the solution with no noticeable effect from the sludge. The average pH of 11.5 for the CaCO₃ solution was higher than the expected pH of 8.3, which suggests that the sludge and its pore water controls the pH during this portion of the leaching tests. There were measurable alkalinity values only in the first stage of the water extract (37.6 to 64.7 mg CaCO₃ per gram) and the sixth stage (average value of 13.2 mg CaCO₃ per gram). The average alkalinity values for the simulated cement leaches were 524 mg CaCO₃ per gram sludge for the Ca(OH)₂ leaches and 449 mg CaCO₃ per gram sludge for the CaCO₃ leaches.

4.1.2.3 ⁹⁹Tc, ²³⁸U, and ¹²⁹I – Sequential Contact Leaching Test

Table 4.9 lists the amount of ⁹⁹Tc, ²³⁸U, and ¹²⁹I leached from the sludge samples during the sequential contact leaching tests, and Table 4.10 lists the percentages of the available radionuclides that were leached. As was found in the single-contact water leach tests (Table 4.3), very little of the ⁹⁹Tc, ²³⁸U, or ¹²⁹I was leachable. Only 1.3% to 2.0% of the ⁹⁹Tc was water leachable, whereas 5.2% to 6.3% was leachable with the Ca(OH)₂ solution. Approximately 4% of the ²³⁸U was water leachable throughout the six contact stages and <1.0 % was leached by the Ca(OH)₂ and CaCO₃ solutions. There was no detectable ¹²⁹I in any of the leaching solutions. These results show the recalcitrant nature of the residual ⁹⁹Tc, ²³⁸U, and ¹²⁹I in the sludge in tank C-106 after the oxalic acid sluicing campaign.

4.1.2.4 Selected Metals Concentrations – Sequential Contact Leaching Test

Table 4.11 lists the concentration of metals leached during the sequential contact leaching tests. Al is leachable in the sludge samples during the majority of the water-leach and CaCO₃-leach stages, whereas it is not leachable (at a detection limit of 1.37E+03 µg/g) in most of the Ca(OH)₂ leach stages. Na is leachable during all of the water-leach and Ca(OH)₂-leach stages, but is not apparently leachable (at a detection limit of 2.46E+03 µg/g) during the CaCO₃-leach stages. Because the CaCO₃ leaches were conducted after the Ca(OH)₂ leaches on the same sludge samples, this may be due to removal of the majority of the leachable Na during the Ca(OH)₂ leaches rather than a change in geochemical conditions that made the Na less mobile.

Table 4.9. ^{99}Tc and ^{238}U Concentrations Leached During Sequential Contact Test

	^{99}Tc ($\mu\text{Ci/g}$)	^{99}Tc ($\mu\text{g/g}$)	^{238}U ($\mu\text{Ci/g}$)	^{238}U ($\mu\text{g/g}$)	^{129}I ($\mu\text{Ci/g}$)	^{129}I ($\mu\text{g/g}$)
Stage 1						
C-106 Water Leach	2.20E-04 to 3.47E-04	1.29E-02 to 2.04E-02	2.25E-06 to 2.70E-06	6.62E+00 to 7.95E+00	<9.76E-06	<5.53E-02
C-106 Ca(OH) ₂	1.09E-03 to 1.39E-03	6.41E-2 to 8.16E-02	<2.19E-08	<6.45E-02	<2.28E-05	<1.29E-01
C-106 CaCO ₃	<9.33E-02	<5.49E+00	1.67E-08 to 3.34E-08	7.33E-02 to 9.83E-02	<9.67E-05	<5.47E-01
Stage 2						
C-106 Water Leach	<9.98E-05	<5.87E-03	4.40E-07 to 5.76E-07	1.30E+00 to 1.69E+00	NA	NA
C-106 Ca(OH) ₂	<1.10E-03	<6.45E-02	3.98E-8 to 8.21E-08	1.17E-01 to 2.41E-01	<2.28E-05	<1.29E-01
C-106 CaCO ₃	<9.33E-02	<5.49E+00	2.80E-08 to 3.12E-08	6.24E-02 to 9.17E-02	<9.67E-05	<5.47E-01
Stage 3						
C-106 Water Leach	<1.13E-04	<6.63E-03	1.87E-07 to 2.33E-07	5.51E-01 to 6.85E-01	NA	NA
C-106 Ca(OH) ₂	<1.10E-03	<6.45E-02	3.75E-08 to 7.11E-08	1.10E-01 to 2.09E-01	<2.28E-05	<1.29E-01
C-106 CaCO ₃	<9.33E-02	<5.49E+00	1.67E-08 to 3.87E-08	9.47E-2 to 1.14E-01	<9.67E-05	<5.47E-01
Stage 4						
C-106 Water Leach	<1.13E-04	<6.63E-03	6.07E-08 to 9.12E-08	1.78E-01 to 2.68E-01	NA	NA
C-106 Ca(OH) ₂	<1.10E-03	<6.45E-02	3.12E-08 to 5.84E-08	1.13E-01 to 1.81E-01	<2.28E-05	<1.29E-01
C-106 CaCO ₃	<9.33E-02	<5.49E+00	3.47E-08 to 4.24E-08	9.42E-02 to 1.25E-04	<9.67E-05	<5.47E-01
Stage 5						
C-106 Water Leach	<1.13E-04	<6.63E-03	2.87E-08 to 3.41E-08	8.45E-02 to 1.00E-01	NA	NA
C-106 Ca(OH) ₂	<1.10E-03	<6.45E-02	2.72E-08 to 7.58E-08	8.01E-02 to 2.23E-01	<2.28E-05	<1.29E-01
C-106 CaCO ₃	<9.33E-02	<5.49E+00	1.87E-08 to 4.35E-08	8.45E-02 to 1.28E-01	<9.67E-05	<5.47E-01
Stage 6						
C-106 Water Leach	6.15E-04	3.62E-02	7.63E-08	2.25E-01	<8.65E-06	<4.89E-02
C-106 Ca(OH) ₂	1.28E-03 to 2.39E-03	7.55E-02 to 1.41E-01	1.90E-08 to 3.02E-08	5.59E-02 to 8.89E-02	<2.28E-05	<1.29E-01
C-106 CaCO ₃	<9.33E-02	<5.49E+00	3.21E-08 to 3.87E-08	9.43E-02 to 1.14E-01	<9.67E-05	<5.47E-01

Table 4.10. Water-Leachable Percentages of ⁹⁹Tc, ²³⁸U, and ¹²⁹I in Tank C-106 Sludge Sequential Contact Leaching Test Relative to Fusion Results

	⁹⁹ Tc	²³⁸ U	¹²⁹ I
	(% Leachable)		
Stage 1			
C-106 Water Leach	1.3 to 2.0	2.8 to 3.4	<1.4
C-106 Ca(OH) ₂	5.2 to 6.3	0.3	<3.2
C-106 CaCO ₃	ND	0.02 to 0.04	<13.6
Stage 2			
C-106 Water Leach	<0.58	0.5 to 0.7	NA
C-106 Ca(OH) ₂	<6.4	0.02 to 0.1	<3.2
C-106 CaCO ₃	ND	0.03 to 0.04	<13.6
Stage 3			
C-106 Water Leach	<0.58	0.2 to 0.3	NA
C-106 Ca(OH) ₂	<6.4	0.06 to 0.09	<3.2
C-106 CaCO ₃	ND	0.02 to 0.05	<13.6
Stage 4			
C-106 Water Leach	<0.58	0.08 to 0.11	NA
C-106 Ca(OH) ₂	<6.4	0.05 to 0.09	<3.2
C-106 CaCO ₃	ND	0.04 to 0.05	<13.6
Stage 5			
C-106 Water Leach	<0.58	0.03 to 0.04	NA
C-106 Ca(OH) ₂	<6.4	0.02 to 0.08	<3.2
C-106 CaCO ₃	ND	0.02 to 0.05	<13.6
Stage 6			
C-106 Water Leach	<0.58	0.09 to 0.10	NA
C-106 Ca(OH) ₂	<6.4	0.02 to 0.04	<3.2
C-106 CaCO ₃	ND	0.04 to 0.05	<13.6
ND= Detection limit for the leached value is higher than the totals measured.			
NA = Not analyzed.			

Ba, Mg, Mn, and Ni only had detectable leachable concentrations during the water-leach stages. This may partially be due to the higher detection limits for Ba, Mg, and Ni during the Ca(OH)₂ and CaCO₃ leaches. The Mn detection limit for the Ca(OH)₂ and CaCO₃ leaches was lower than the water leaches; therefore, it appears that Mn was less leachable in the Ca(OH)₂ and CaCO₃ solutions. This may be due to the formation of Mn hydroxide or carbonate solids under the high pH conditions of these solutions. Ca was water leachable during all stages of the sequential extractions. The Ca concentrations for the Ca(OH)₂ and CaCO₃ leach tests reflect the Ca in the leaching solutions. Cr, Fe, and K were not leachable with any of the leaching solutions.

Table 4.11. Metals Concentrations Leached During Sequential Contact Tests

	Al (µg/g)	Ba (µg/g)	Ca (µg/g)	Cr (µg/g)	Fe (µg/g)	K (µg/g)	Mg (µg/g)	Mn (µg/g)	Ni (µg/g)	Na (µg/g)
Stage 1										
C-106 Water Leach	81.9E+01 to 1.38E+02	3.83E+01 to 1.02E+02	2.91E+02 to 9.73E+02	<6.12E+01	<1.11E+02	<1.39E+03	1.61E+02 to 2.91E+02	9.65E+03 to 1.64E+04	1.91E+02 to 3.29E+02	9.50E+03 to 1.30E+04
C-106 Ca(OH) ₂	2.30E+03 to 4.98E+03	<2.74E+02	1.32E+03 to 2.91E+04	<1.23E+02	<2.74E+02	<8.07E+04	<5.47E+02	<3.23E+02	<5.47E+02	5.26E+03 to 1.39E+04
C-106 CaCO ₃	1.84E+03 to 3.58E+03	<2.74E+02	7.22E+03 to 1.11E+04	<1.37E+02	<2.74E+02	<6.84E+04	<5.49E+02	<2.74E+02	<5.49E+02	<2.46E+03
Stage 2										
C-106 Water Leach	6.25E+01 to 1.22E+02	3.03E+01 to 5.49E+01	3.46E+02 to 7.06E+02	<6.91E+01	<1.11E+02	<1.39E+03	1.45E+02 to 2.08E+02	9.08E+03 to 1.20E+04	1.66E+02 to 4.05E+02	1.79E+03 to 2.45E+03
C-106 Ca(OH) ₂	<1.37E+03	<2.74E+02	1.88E+04 to 5.83E+04	<1.37E+02	<2.74E+02	<8.07E+04	<5.47E+02	<3.23E+02	<5.47E+02	6.34E+03 to 1.20E+04
C-106 CaCO ₃	2.49E+3 to 4.48E+03	<2.74E+02	1.10E+04 to 1.31E+04	<1.37E+02	<2.74E+02	<6.84E+04	<5.49E+02	<2.74E+02	<5.49E+02	<2.46E+03
Stage 3										
C-106 Water Leach	6.66E+01 to 1.23E+02	4.11E+01 to 6.72E+01	3.60E+02 to 6.18E+02	<6.91E+01	<1.11E+02	<1.39E+03	1.24E+02 to 1.51E+02	5.99E+03 to 7.89E+03	1.75E+02 to 3.80E+02	1.35E+03 to 1.99E+03
C-106 Ca(OH) ₂	<1.37E+03	<2.74E+02	3.94E+04 to 1.40E+05	<1.17E+02	<2.74E+02	<8.07E+04	<5.47E+02	<3.23E+02	<5.47E+02	2.99E+03 to 6.12E+03
C-106 CaCO ₃	2.59E+03 to 5.50E+03	<2.74E+02	6.81E+03 to 1.46E+04	<1.37E+02	<2.74E+02	<6.84E+04	<5.49E+02	<2.74E+02	<5.49E+02	<2.46E+03

Table 4.11. (contd)

	Al (µg/g)	Ba (µg/g)	Ca (µg/g)	Cr (µg/g)	Fe (µg/g)	K (µg/g)	Mg (µg/g)	Mn (µg/g)	Ni (µg/g)	Na (µg/g)
Stage 4										
C-106 Water Leach	6.31E+01 to 1.16E+02	3.85E+01 to 9.57E+01	3.40E+02 to 8.31E+02	<6.91E+01	<1.11E+02	<1.39E+03	(6.34E+01)	2.68E+3 to 3.67E+03	2.17E+02 to 3.18E+02	9.11E+02 to 1.45E+03
C-106 Ca(OH) ₂	<1.37E+03	<2.74E+02	1.67E+04 to 6.63E+04	<1.17E+02	<2.74E+02	<8.07E+04	<5.47E+02	<3.23E+02	<5.47E+02	4.93E+03 to 9.74E+03
C-106 CaCO ₃	4.09E+03 to 4.91E+03	<2.74E+02	9.81E+03 to 1.23E+04	<1.37E+02	<2.74E+02	<6.84E+04	<5.49E+02	<2.74E+02	<5.49E+02	<2.46E+03
Stage 5										
C-106 Water Leach	6.64E+01 to 1.30E+02	(2.04E+01) to 2.32E+02	4.30E+02 to 8.72E+02	<1.37E+02	<1.11E+02	<1.39E+03	(6.79E+01)	1.32E+03 to 2.03E+03	1.85E+02 to 2.29E+02	8.84E+02 to 1.30E+02
C-106 Ca(OH) ₂	<1.61E+03	<2.74E+02	4.78E+04 to 6.98E+04	<1.37E+02	<2.74E+02	<8.07E+04	<5.47E+02	<3.23E+02	<5.47E+02	1.76E+03 to 2.93E+03
C-106 CaCO ₃	2.06E+3 to 4.53E+03	<2.74E+02	4.75E+02 to 9.14E+03	<1.37E+02	<2.74E+02	<6.84E+04	<5.49E+02	<2.74E+02	<5.49E+02	<2.46E+03
Stage 6										
C-106 Water Leach	<2.76E+01	1.76E+01	2.72E+02	<6.91E+01	<1.11E+01	<2.76E+02	3.74E+01	1.23E+03	5.92E+01	4.06E+03
C-106 Ca(OH) ₂	1.61E+03 to 1.97E+03	<2.74E+02	1.18E+04 to 3.12E+04	<1.37E+02	<2.74E+02	<8.07E+04	<5.47E+02	<3.23E+02	<5.47E+02	4.26E+3 to 1.15E+04
C-106 CaCO ₃	3.99E+03 to 4.84E+03	<2.74E+02	9.12E+03 to 1.23E+04	<1.37E+02	<2.74E+02	<6.84E+04	<5.49E+02	<2.74E+02	<5.49E+02	(3.00E+02) to 6.05E+02

4.1.2.5 Anion Concentrations – Sequential Contact Leaching Test

The leachable anion concentrations at the six stages of the sequential contact leaching test are listed in Table 4.12. The primary water leachable anions at Stage 1 were oxalate and carbonate, with much less leachable quantities of chloride and fluoride. Oxalate continues to leach from the sludge samples in measurable quantities at all stages of the test; however, the amount of carbonate leached is below the detection limit after stage 1. (The detection limit for carbonate is high at a level of about 10,000 $\mu\text{g/g}$ in water leached samples.) The amount of oxalate leaching from the sludge decreases fairly uniformly throughout the six stages of leaching.

The uniform release of oxalate does not occur in the simulated cement leach. Oxalate was measurable only in Stage 1 of the $\text{Ca}(\text{OH})_2$ leach. No other anions appear to be leachable in any of the other stages of the $\text{Ca}(\text{OH})_2$ or the CaCO_3 extracts. It is difficult to compare the anion leaching data due to the elevated detection limits for the simulated cement leaching. The elevated detection limits are due to the higher hydroxide and carbonate concentrations in the prepared extraction solutions.

4.1.2.6 Radioanalytical Results – Sequential Contact Leaching Test

The results of the GEA analysis of the sequential contact leaching test for ^{137}Cs are listed in Table 4.13. The water leachable concentrations of ^{137}Cs for the first contacts were in the range of 1.83 to 2.88 $\mu\text{Ci/g}$ for the C-106 sludge samples. The subsequent concentrations in each water leachate decrease by over a factor of ten compared to the initial level. This shows that a small amount of the ^{137}Cs is very leachable, but the remaining majority is relatively recalcitrant to water leaching. ^{137}Cs appears to be more mobile in the simulated cement leaches. ^{137}Cs was released in the $\text{Ca}(\text{OH})_2$ solution 1 to 5 times higher, 1.1 to 13.6 $\mu\text{Ci/g}$, compared to the water leach. The release remained relatively stable for the first five stages. The sixth stage with a longer contact time (43 days) showed another increase in the concentration of 20.7 to 35.1 $\mu\text{Ci/g}$ ^{137}Cs . The concentration of ^{137}Cs in the CaCO_3 leaches were lower than the concentrations measured in the water or $\text{Ca}(\text{OH})_2$ leaches with leachable quantities, 0.0025 to 2.17 $\mu\text{Ci/g}$, measured in the first five stages. In a manner similar to the $\text{Ca}(\text{OH})_2$ leach tests, the CaCO_3 leach showed a spike in the ^{137}Cs concentration in the sixth stage, 4.42 to 6.32 $\mu\text{Ci/g}$.

The ^{239}Pu , ^{237}Np , ^{241}Am , and ^{90}Sr leachable concentrations for the sequential contact tests are listed in Table 4.14. ^{239}Pu was not measured above its estimated quantitation limit (EQL) during any of the stages of leaching. Measurable quantities of leachable ^{237}Np were measured at most stages of the water leach test. No detectable ^{237}Np was measured in the $\text{Ca}(\text{OH})_2$ or CaCO_3 tests. ^{241}Am was only measured above its EQL during the first stage of the water test. The water leachability of ^{90}Sr for the first five stages is approximately constant within the range of 0.3 to 1.41 $\mu\text{g/g}$. (Stage 6 leaching data are not available for the water-leach or CaCO_3 -leach tests.) Leachable ^{90}Sr increases when $\text{Ca}(\text{OH})_2$ is used as the leaching solution. At each stage, the concentrations are higher than the corresponding water leach stage with a range of 0.3 to 7.78 $\mu\text{g/g}$ for the $\text{Ca}(\text{OH})_2$ leaches. The increase in Sr for the $\text{Ca}(\text{OH})_2$ leaches is likely due to cation exchange of Ca for Sr on the exchange sites. The CaCO_3 -leach tests show concentrations similar to the water leach tests. Because the CaCO_3 leaches follow the $\text{Ca}(\text{OH})_2$ leaches using the same sludge material, it appears that the majority of the exchangeable Sr has been desorbed by the initial $\text{Ca}(\text{OH})_2$ -leach tests.

Table 4.12. Anion Concentrations Leached During Sequential Contact Tests

	Fluoride (µg/g)	Chloride (µg/g)	Nitrite (µg/g)	Bromide (µg/g)	Nitrate (µg/g)	Carbonate (µg/g)	Sulfate (µg/g)	Oxalate (µg/g)	Phosphate (µg/g)
Stage 1									
C-106 Water Leach	3.06E+01 to 4.00E+01	7.96E+01 to 1.08E+2	<9.97E+01	<1.06E+02	<9.57E+01	1.16E+04 to 2.48E+04		2.68E+04 to 4.26E+04	<1.12E+02
C-106 Ca(OH) ₂	<1.28E+02	<2.59E+02	<4.95E+02	<5.28E+02	<4.75E+02	<5.49E+04	<4.49E+02	3.40E+2 to 5.87E+02	<6.52E+02
C-106 CaCO ₃	<1.28E+02	<2.59E+02	<4.95E+02	<5.28E+02	<4.75E+02	<5.49E+04	<4.49E+02	<3.79E+02	<5.54E+02
Stage 2									
C-106 Water Leach	<2.59E+01	3.93E+01 to 7.19E+01	<9.97E+01	<1.06E+02	<9.57E+01	<1.11E+04	<9.05E+01	1.77E+04 to 2.30E+04	<1.12E+02
C-106 Ca(OH) ₂	<1.51E+02	<3.05E+02	<5.82E+02	<6.21E+02	<5.59E+02	<6.45E+04	<5.28E+02	<4.45E+02	<6.52E+02
C-106 CaCO ₃	<1.28E+02	<2.59E+02	<4.95E+02	<5.28E+02	<4.75E+02	<5.49E+04	<4.49E+02	<3.79E+02	<5.54E+02
Stage 3									
C-106 Water Leach	<2.59E+01	3.00E+01 to 4.78E+01	<9.97E+01	<1.06E+02	<9.57E+01	<1.11E+04	<9.05E+01	1.18E+04 to 1.60E+04	<1.12E+02
C-106 Ca(OH) ₂	<1.51E+02	<3.05E+02	<5.82E+02	<6.21E+02	<5.59E+02	<6.45E+04	<5.28E+02	<4.45E+02	<6.52E+02
C-106 CaCO ₃	<1.28E+02	<2.59E+02	<4.95E+02	<5.28E+02	<4.75E+02	<5.49E+04	<4.49E+02	<3.79E+02	<5.54E+02
Stage 4									
C-106 Water Leach	<2.59E+01	<5.22E+01	<9.97E+01	<1.06E+02	<9.57E+01	<1.11E+04	<9.05E+01	6.06E+03 to 7.44E+03	<1.12E+02
C-106 Ca(OH) ₂	<1.51E+02	<3.05E+02	<5.82E+02	<6.21E+02	<5.59E+02	<6.45E+04	<5.28E+02	<4.45E+02	<6.52E+02
C-106 CaCO ₃	<1.28E+02	<2.59E+02	<4.95E+02	<5.28E+02	<4.75E+02	<5.49E+04	<4.49E+02	<3.79E+02	<5.54E+02
Stage 5									
C-106 Water Leach	<2.59E+01	<5.22E+01	<9.97E+01	<1.06E+02	<9.57E+01	<1.11E+04	<9.05E+01	1.73E+03 to 4.28E+03	<1.12E+02
C-106 Ca(OH) ₂	<1.51E+02	<3.05E+02	<5.82E+02	<6.21E+02	<5.59E+02	<6.45E+04	<5.28E+02	<4.45E+02	<6.52E+02
C-106 CaCO ₃	<1.28E+02	<2.59E+02	<4.95E+02	<5.28E+02	<4.75E+02	<5.49E+04	<4.49E+02	<3.79E+02	<5.54E+02
Stage 6									
C-106 Water Leach	<2.59E+01	<5.22E+01	<9.97E+01	<1.06E+02	<9.57E+01	<1.11E+04	<9.05E+01	3.80E+03	1.98E+02
C-106 Ca(OH) ₂	<1.51E+02	<3.05E+02	<5.82E+02	<6.21E+02	<5.59E+02	<6.45E+04	<5.28E+02	<4.45E+02	<6.52E+02
C-106 CaCO ₃	<1.28E+02	<2.59E+02	<4.95E+02	<5.28E+02	<4.75E+02	<5.49E+04	<4.49E+02	<3.79E+02	<5.54E+02

Table 4.13. ¹³⁷Cs Concentrations Leached During Sequential Contact Tests

	¹³⁷ Cs (μCi/g)	¹³⁷ Cs (μg/g)
Stage 1		
C-106 Water Leach	1.83E+00 to 2.88E+00	2.10E-02 to 3.31E-02
C-106 Ca(OH) ₂	1.10E+00 to 7.31E+00	1.26E-02 to 8.40E-02
C-106 CaCO ₃	6.25E-02 to 4.62E-01	7.18E-04 to 5.31E-03
Stage 2		
C-106 Water Leach	4.07E-02 to 2.15E-01	4.67E-04 to 2.47E-03
C-106 Ca(OH) ₂	5.25E+00 to 8.12E+00	6.04E-02 to 9.34E-02
C-106 CaCO ₃	1.80E-02 to 2.92E-02	2.07E-04 to 3.36E-04
Stage 3		
C-106 Water Leach	3.59E-02 to 4.20E-02	4.23E-04 to 4.82E-04
C-106 Ca(OH) ₂	2.87E+00 to 5.78E+00	3.30E-02 to 6.64E-02
C-106 CaCO ₃	2.25E-03 to 8.06E-03	2.59E-05 to 9.26E-05
Stage 4		
C-106 Water Leach	<4.27E-02	<4.90E-04
C-106 Ca(OH) ₂	7.44E+00 to 1.36E+01	8.55E-02 to 1.78E-01
C-106 CaCO ₃	7.41E-03 to 2.17E+00	8.52E-05 to 2.50E-02
Stage 5		
C-106 Water Leach	<4.27E-02	<4.90E-04
C-106 Ca(OH) ₂	4.72E+00 to 6.46E+00	5.42E-02 to 7.42E-02
C-106 CaCO ₃	2.79E-01 to 5.89E-01	3.21E-03 to 6.78E-03
Stage 6		
C-106 Water Leach	NA	NA
C-106 Ca(OH) ₂	2.07E+01 to 3.51E+01	2.56E-01 to 4.04E-1
C-106 CaCO ₃	4.42E+00 to 6.32E+00	5.07E-02 to 7.27E-02

Table 4.14. ⁹⁰Sr and Actinide Concentrations Leached During Sequential Contact Tests

	⁹⁰ Sr (μCi/g)	⁹⁰ Sr (μg/g)	²³⁹ Pu (μCi/g)	²³⁹ Pu (μg/g)	²³⁷ Np (μCi/g)	²³⁷ Np (μg/g)	²⁴¹ Am (μCi/g)	²⁴¹ Am (μg/g)
Stage 1								
C-106 Water Leach	4.34E+01 to 9.76E+01	3.10E-01 to 6.97E-01	<1.71E-03	<2.76E-02	5.06E-04 to 7.05E-4	7.13E-01 to 9.93E-01	2.57E-03	7.55E-04
C-106 Ca(OH) ₂	4.22E+01 to 2.34E+02	3.01E-01 to 1.67E+00	<4.00E-02	<6.45E-01	<4.58E-04	<6.45E-01	<1.10E+01	<3.23E+00
C-106 CaCO ₃	1.29E+02 to 3.79E+02	9.21E-01 to 2.71E+00	<6.81E-03	<1.10E-01	<7.79E-05	<1.10E-01	<1.87E+00	<5.49E-01
Stage 2								
C-106 Water Leach	7.13E+01 to 1.49E+02	5.94E-01 to 1.06E+00	<1.71E-03	<2.76E-02	2.08E-04 to 2.73E-04	2.93E-01 to 3.84E-01	<3.76E-03	<1.11E-03
C-106 Ca(OH) ₂	2.98E+02 to 4.01E+02	2.12E+00 to 2.86E+00	<4.00E-02	<6.45E-01	<4.58E-04	<6.45E-01	<1.10E+01	<3.23E+00
C-106 CaCO ₃	1.04E+02 to 1.58E+02	7.43E-01 to 1.12E+00	<6.81E-03	<1.10E-01	<7.79E-05	<1.10E-01	<1.87E+00	<5.49E-01
Stage 3								
C-106 Water Leach	1.02E+02 to 1.56E+02	7.26E-01 to 1.12E+00	<1.71E-03	<2.76E-02	1.36E-05 to 1.86E-05	1.92E-02 to 2.61E-02	<3.76E-03	<1.11E-03
C-106 Ca(OH) ₂	1.79E+02 to 3.97E+02	1.28E+00 to 2.84E+00	<4.00E-02	<6.45E-01	<4.58E-04	<6.45E-01	<1.10E+01	<3.23E+00
C-106 CaCO ₃	1.82E+01 to 9.56E+01	1.30E-01 to 6.83E-01	<6.81E-03	<1.10E-01	<7.79E-05	<1.10E-01	<1.87E+00	<5.49E-01
Stage 4								
C-106 Water Leach	8.79E+01 to 1.75E+02	6.28E-01 to 1.25E+00	<1.71E-03	<2.76E-02	7.65E-06 to 8.23E-06	1.08E-02 to 1.16E-02	<3.76E-03	<1.11E-03
C-106 Ca(OH) ₂	4.52E+02 to 8.56E+02	3.23E+00 to 6.11E+00	<4.00E-02	<6.45E-01	<4.58E-04	<6.45E-01	<1.10E+01	<3.23E+00
C-106 CaCO ₃	6.88E+01 to 1.54E+02	4.91E-01 to 1.08E+00	<6.81E-03	<1.10E-01	<7.79E-05	<1.10E-01	<1.87E+00	<5.49E-01

Table 4.14. (contd)

	⁹⁰ Sr (μCi/g)	⁹⁰ Sr (μg/g)	²³⁹ Pu (μCi/g)	²³⁹ Pu (μg/g)	²³⁷ Np (μCi/g)	²³⁷ Np (μg/g)	²⁴¹ Am (μCi/g)	²⁴¹ Am (μg/g)
Stage 5								
C-106 Water Leach	8.98E+01 to 1.97E+02	6.42E-01 to 1.41E+00	<1.71E-03	<2.76E-02	4.96E-06 to 5.37E-06	6.99E-03 to 7.56E-03	<3.76E-03	<1.11E-03
C-106 Ca(OH) ₂	3.71E+02 to 8.08E+02	2.65E+00 to 5.77E+00	<4.00E-02	<6.45E-01	<4.58E-04	<6.45E-01	<1.10E+01	<3.23E+00
C-106 CaCO ₃	3.83E+01 to 6.68E+01	2.74E-01 to 4.77E-01	<6.81E-03	<1.10E-01	<7.79E-05	<1.10E-01	<1.87E+00	<5.49E-01
Stage 6								
C-106 Water Leach	NA	NA	<1.71E-03	<2.76E-02	2.68E-04	3.78E-01	<3.76E-03	<1.11E-03
C-106 Ca(OH) ₂	4.20E+02 to 1.09E+03	3.00E+00 to 7.78E+00	<4.00E-02	<6.45E-01	<4.58E-04	<6.45E-01	<1.10E+01	<3.23E+00
C-106 CaCO ₃	NA	NA	<6.81E-03	<1.10E-01	<7.79E-05	<1.10E-01	<1.87E+00	<5.49E-01

4.2 XRD Results

This section describes the crystalline solids identified by XRD for the 1-month and Stage 6 sequential samples of residual waste from tank C-106 leached with $\text{Ca}(\text{OH})_2$ and CaCO_3 . The as-measured and background-subtracted XRD patterns for these samples are found in Appendix A. Phase identification was based on a comparison of the peak reflections and intensities observed in each pattern to the mineral powder diffraction files (PDFTM) published by the Joint Committee on Powder Diffraction Standards (JCPDS) International Center for Diffraction Data (ICDD). Phase identification from the XRD patterns was refined in an iterative fashion by considering phases with particle compositions that were determined by SEM/EDS (see Section 4.3) to be present in the residual waste samples. The XRD patterns in Appendix A show greater detail than those plotted in this section because they do not include the schematic PDF-XRD database patterns (as plotted in this section) used for phase identification.

Each pattern in this section and Appendix A is shown as a function of degrees 2θ based on $\text{Cu}_{K\alpha}$ radiation ($\lambda=1.5406 \text{ \AA}$). The vertical axis in each pattern represents the relative intensity of the XRD peaks. As noted in Section 3.3, trace quantities of reference-material corundum ($\alpha\text{-Al}_2\text{O}_3$, alumina) powder were added to each XRD mount to provide an internal 2θ standard for each XRD pattern. The schematic database (PDF) patterns considered for phase identification are shown, for comparison purposes, in the first two figures in this section. The height of each line in the schematic PDF patterns represents the relative intensity of an XRD peak (i.e., the most intense [the highest] peak has a relative intensity $[I/I_0]$ of 100%). Quantitative analyses of the relative masses of individual phases present in each solid sample were not estimated using these XRD patterns due to the factors discussed at the end of Section 3.3. Also, as noted previously in Section 3.3, a crystalline phase typically must be present at greater than 5 wt% of the total sample mass (greater than 1 wt% under optimum conditions) to be readily detected by XRD.

The as-measured XRD patterns (not background subtracted) measured for the 1-month and Stage 6 sequential $\text{Ca}(\text{OH})_2$ -leached and the 1-month and Stage 6 sequential CaCO_3 -leached samples are shown in Figure 4.1 and Figure 4.2, respectively. Minerals identified in the two $\text{Ca}(\text{OH})_2$ -leached samples (Figure 4.1) include gibbsite [$\text{Al}(\text{OH})_3$], whewellite (Ca oxalate monohydrate, $\text{CaC}_2\text{O}_4 \cdot \text{H}_2\text{O}$), calcite (CaCO_3), and corundum (the internal standard). The XRD patterns for the $\text{Ca}(\text{OH})_2$ -leached samples are also consistent with the possible presence of böhmite [$\text{AlO}(\text{OH})$]. Gibbsite, whewellite, calcite, and corundum (the internal standard) were also identified in the XRD patterns for the two CaCO_3 -leached samples (Figure 4.2). The XRD pattern for the 1-month CaCO_3 -leached sample also contained reflections that were consistent with the possible presence of dawsonite [$\text{NaAlCO}_3(\text{OH})_2$]. Calcite was identified in the $\text{Ca}(\text{OH})_2$ - and CaCO_3 -leached samples by the reflections at 29.40 , 39.57 , and $39.41^\circ 2\theta$. No other new carbonate phases were detected by XRD analysis of the $\text{Ca}(\text{OH})_2$ - and CaCO_3 -leached samples of C-106 residual waste.

There were no unassigned reflections in the background-subtracted XRD patterns for $\text{Ca}(\text{OH})_2$ - and CaCO_3 -leached samples (Figure 4.1 and Figure 4.2, respectively). This suggests that all crystalline phases present at greater than 5-10 wt% in these residual waste samples were identified by XRD. No other new carbonate phases were detected by XRD analysis of the $\text{Ca}(\text{OH})_2$ - and CaCO_3 -leached samples of C-106 residual waste.

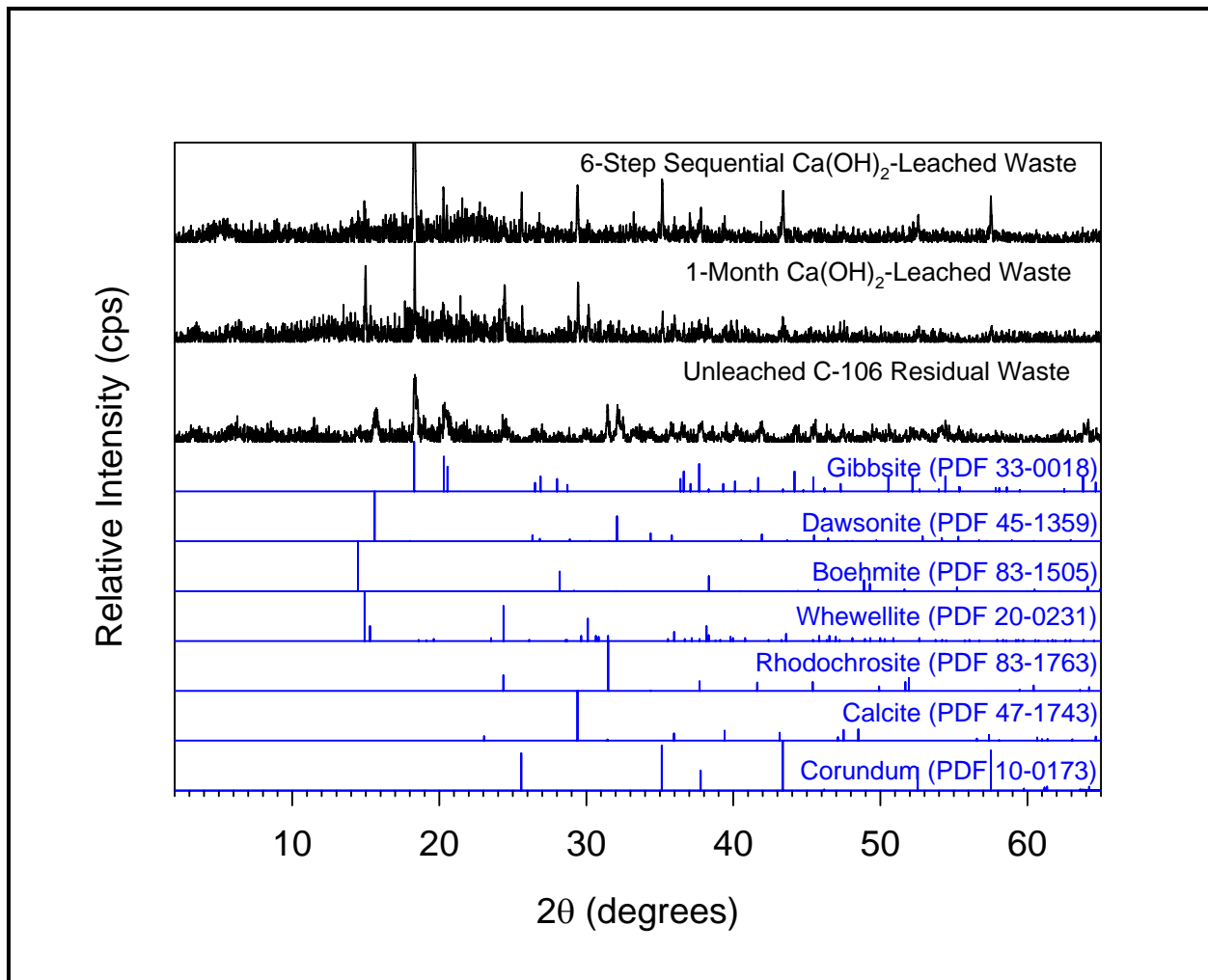


Figure 4.1. Background-Subtracted XRD Patterns (in black) for 1-Month and Stage 6 Sequential Ca(OH)₂-Leached and for Unleached C-106 Residual Waste Compared to the Matching PDF Database Patterns (in blue)

The background-subtracted XRD patterns for the Ca(OH)₂- and CaCO₃-leached samples are generally very similar to each other. Figure 4.3 shows a comparison of the XRD patterns for the 1-month Ca(OH)₂- and 1-month CaCO₃-leached samples of C-106 residual waste.

Table 4.15 gives a comparison of the XRD and SEM/EDS results for the Ca(OH)₂- and CaCO₃-leached samples relative to those from Deutsch et al. (2005b) for the C-106 residual waste used as starting material for these leaching tests. Except for the presence of calcite (CaCO₃), the phases identified from the XRD patterns for the Ca(OH)₂- and CaCO₃-leached samples were also present in the XRD patterns for the C-106 starting material. Absent from the XRD patterns for the leached samples, however, were hematite (Fe₂O₃), lindbergite (MnC₂O₄·2H₂O), rhodochrosite (MnCO₃), which were identified in the starting material. Identification of böhmite [AlO(OH)] and dawsonite [NaAlCO₃(OH)₂] in the Ca(OH)₂-leached and the 1-month leached CaCO₃-leached samples, respectively, was problematic and therefore need to also be considered as possibly absent in the Ca(OH)₂- and CaCO₃-leached samples. It was not possible from the XRD or SEM/EDS analyses (see Section 4.3) to determine if the lack of identification

of hematite, lindbergite, rhodochrosite (MnCO_3), böhmite, and dawsonite is due to their dissolution during contact with the $\text{Ca}(\text{OH})_2$ and CaCO_3 leachates and/or to their presence being at concentrations too low to be detected by bulk XRD.

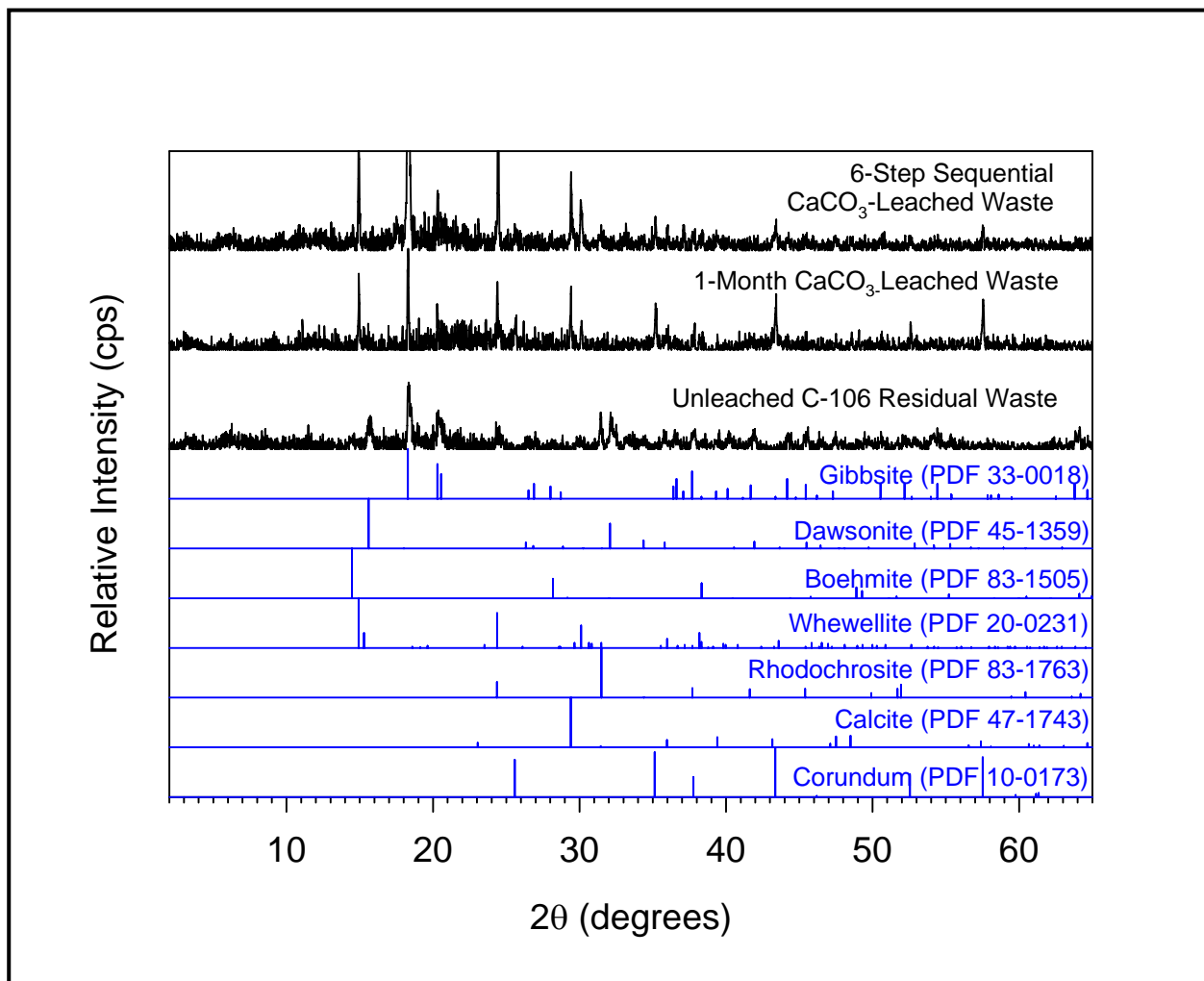


Figure 4.2. Background-Subtracted XRD Patterns (in black) for 1-Month and Stage 6 Sequential CaCO_3 -Leached and for Unleached C-106 Residual Waste Compared to the Matching PDF Database Patterns (in blue)

There are minor differences in peak intensities between the XRD patterns for the $\text{Ca}(\text{OH})_2$ - and CaCO_3 -leached samples and the pattern for the C-106 residual waste. Although some of these differences may be due to minor differences in the sample mounts, the XRD data suggests that the relative abundance of whewellite may be greater in the $\text{Ca}(\text{OH})_2$ -leached samples than in the unleached C-106 residual waste. Because of the hazardous nature of these sludge samples, it is not possible to control the exact amount of material used for each XRD mount. However, when these XRD mounts are prepared, a concerted effort is made to follow the same procedure and use the same amount of sludge material as closely as possible.

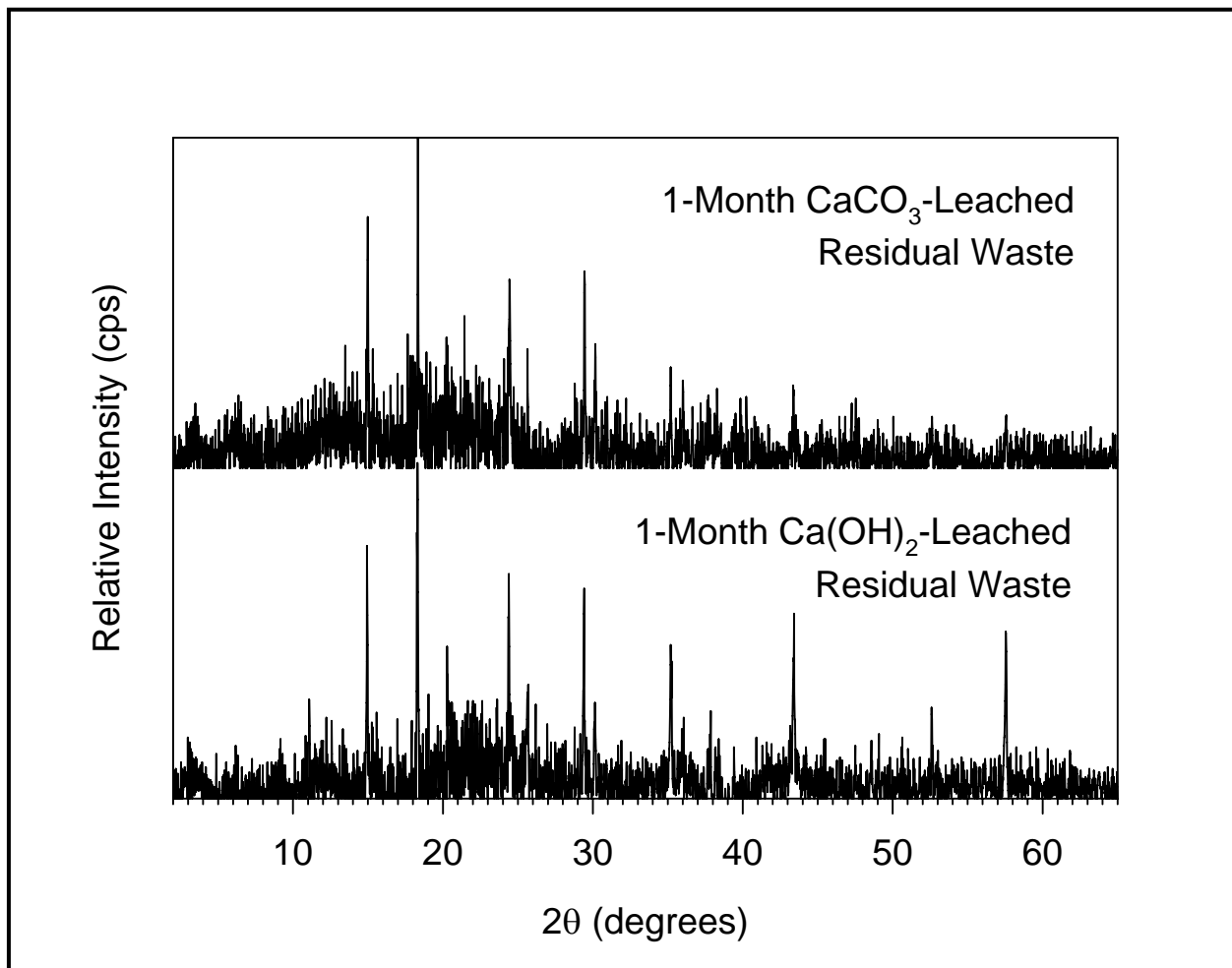


Figure 4.3. Comparison of Background-Subtracted XRD Patterns for 1-Month $\text{Ca}(\text{OH})_2$ - (bottom pattern) and 1-Month CaCO_3 - (top pattern) Leached Samples of Unleached C-106 Residual Waste

4.3 SEM/EDS Results

This section discusses the results of the SEM/EDS analyses for the 1-month and Stage 6 sequential $\text{Ca}(\text{OH})_2$ - and CaCO_3 -leached samples of residual waste from tank C-106. The SEM micrographs presented in this section show representative morphologies, sizes, surface textures, and composition data for particles in these samples. All of the SEM micrographs and EDS spectra obtained for these samples are shown in Appendices B [1-month $\text{Ca}(\text{OH})_2$ -leached], C [Stage 6 sequential $\text{Ca}(\text{OH})_2$ -leached], D [1-month CaCO_3 -leached], and E [Stage 6 sequential CaCO_3 -leached]. Each micrograph included in this section and Appendices B through E lists the identification number for the digital micrograph image file, descriptor for the type of sample, and a size scale bar, respectively, at the bottom left, center, and right of each SEM micrograph. Micrographs labeled BSE near the digital file identification number indicate that the micrographs were collected by backscattered electron imaging. Areas outlined by white dashed-line squares or particles marked by arrows in a micrograph designate material that is imaged at higher

Table 4.15. Comparison of XRD and SEM/EDS Results for the Unleached Samples of Residual Waste from Tank C-106 (from Deutsch et al. 2005a) to the Results for the Ca(OH)₂- and CaCO₃-Leached Samples

Unleached Oxalic Acid-Treated Residual Waste (from Deutsch et al. 2005b)		Ca(OH) ₂ -Leached Residual Waste: 1-Month and Stage 6 Sequential Leaches (from this study)		CaCO ₃ -Leached Residual Waste: 1-Month and Stage 6 Sequential Leaches (from this study)	
XRD Analyses	SEM/EDS Analyses	XRD Analyses	SEM/EDS Analyses	XRD Analyses	SEM/EDS Analyses
	Mn-Al-Fe-Na-P-Si-Ca- O±C±H				
			Ca-Mn-Al-Si-Fe- ±Pb±REE(Ce) ±Cr-P-O± C±H		Ca-Mn-Al-Si-Fe- ±Pb±REE(Ce) ±Cr -P-O± C±H
			Ca-Al-O-C±H (only in Stage 6 sequential leach)		Ca-Al-O-C±H
Gibbsite [Al(OH) ₃]	Al-O±H	Gibbsite	Al-O±H±C	Gibbsite	Al-O±H±C
Böhmite [AlO(OH)]		Böhmite (possibly)			
Dawsonite [NaAlCO ₃ (OH) ₂]	Al-Na-O-C±H			Dawsonite (only in 1-month leached)	
Hematite (Fe ₃ O ₄)	Fe-Cr-O±C±H Fe-Mn-O±C±H				
Rhodochrosite (MnCO ₃)	Mn-O-C±H (possibly two different phases based on morphology)				
Lindbergite (MnC ₂ O ₄ ·2H ₂ O)					
Whewellite (CaC ₂ O ₄ ·H ₂ O)	Ca-O±C±H	Whewellite	Ca-O±C±H	Whewellite	Ca-O±C±H
		Calcite (CaCO ₃)		Calcite	
Possible Ag-Hg phase	Possibly 1 or 2 phases with Ag-Hg±Fe±Pb±Cu±O±H		Ag-Hg (small particles)		Ag-Hg (small particles)

Table 4.15. (contd)

Unleached Oxalic Acid-Treated Residual Waste (from Deutsch et al. 2005b)		Ca(OH) ₂ -Leached Residual Waste: 1-Month and Stage 6 Sequential Leaches (from this study)		CaCO ₃ -Leached Residual Waste: 1-Month and Stage 6 Sequential Leaches (from this study)	
XRD Analyses	SEM/EDS Analyses	XRD Analyses	SEM/EDS Analyses	XRD Analyses	SEM/EDS Analyses
			Mn-Na-P-O±C±H (only one particle cluster in 1-month sequential leach)		
	Mn-O-P±Al±C±H				
	Si-Al-Na-O±C±H				
	REE-rich oxide				
	Ca-Si-Al-O±C±H				
	Pb-containing phase				

magnification. They are typically shown in the next several figures for that sample series. Micrographs presented in this section are typically reproduced at reduced size to conserve page space. For more detailed views of these micrographs, the reader is referred to Appendices B through E, where the micrographs are shown at a larger size.

Figure 4.4 shows SEM micrographs obtained at relatively low magnification of material present in $\text{Ca}(\text{OH})_2$ -leached (top row) and CaCO_3 -leached (bottom row) residual waste from tank C-106. The 1-month and Stage 6 sequential leaches for each of these treatments are shown in the left and right columns of Figure 4.4. Generally, the material in the 1-month $\text{Ca}(\text{OH})_2$ - and 1-month CaCO_3 -leached samples appear to be more disaggregated than the material in the Stage 6 sequential leaches of each treatment. It is not known if the disintegration resulted from dissolution of interstitial phases in the particle aggregates during the 1-month leach treatments or from solution sampling where more fines could have been discarded during leachate replenishment for the six stages of sequential leaches. The latter scenario seems unlikely because the sample tubes were centrifuged and spun at 4,000 rpm for 20 minutes prior to carefully decanting off each supernatant for chemical analysis.

Figure 4.5 shows for comparison low magnification SEM micrographs from Deutsch et al. (2005a) of particles in the unleached (top row), 1-month water-leached (left on bottom row), and HF stage 1 extract (right on bottom row) of residual waste from tank C-106. The unleached waste is the starting material for the $\text{Ca}(\text{OH})_2$ leach tests. Generally, the 1-month $\text{Ca}(\text{OH})_2$ - and 1-month CaCO_3 -leached samples (left column in Figure 4.4) appear to be more disintegrated than the unleached residual waste (top row of Figure 4.5). The materials resulting from the Stage 6 sequential leaches (right column in Figure 4.4) are more similar to the materials from the 1-month water-leached and HF stage 1 extract (bottom row of Figure 4.5) samples.

Figure 4.6 through Figure 4.11 show micrographs collected at higher magnification and spectra for areas analyzed by EDS of some of the more common particles and aggregates present in the $\text{Ca}(\text{OH})_2$ - and CaCO_3 -leached samples. The particles and aggregates are very similar to those presented in Deutsch et al. (2005b) for unleached C-106 residual waste. The EDS analyses are summarized in Table 4.1. The EDS results indicate that the $\text{Ca}(\text{OH})_2$ - and CaCO_3 -leached samples include particles consisting of primarily the following five compositions:

- Ca-Mn-Al-Si-Fe-±Pb±REE(Ce) ±Cr(trace)-P-O±C±H – Figure 4.6 (spectrum 2), Figure 4.7 (spectra 1 and 2), Figure 4.9 (spectra 1, 3, and 4), and Figure 4.10 (spectra 2 and 4)
- Al-O±H – Figure 4.6 (spectrum 1), Figure 4.7 (spectrum 3), Figure 4.9 (spectrum 2), Figure 4.10 (spectra 1 and 2), and Figure 4.11 (spectrum 2)
- Ca-Al-O-C±H – Figure 4.8 (spectra 1 and 2)
- Ca-O±C±H – Figure 4.11 (spectrum 1)
- Ag-Hg±O±H – Figure 4.11 (spectrum 3)

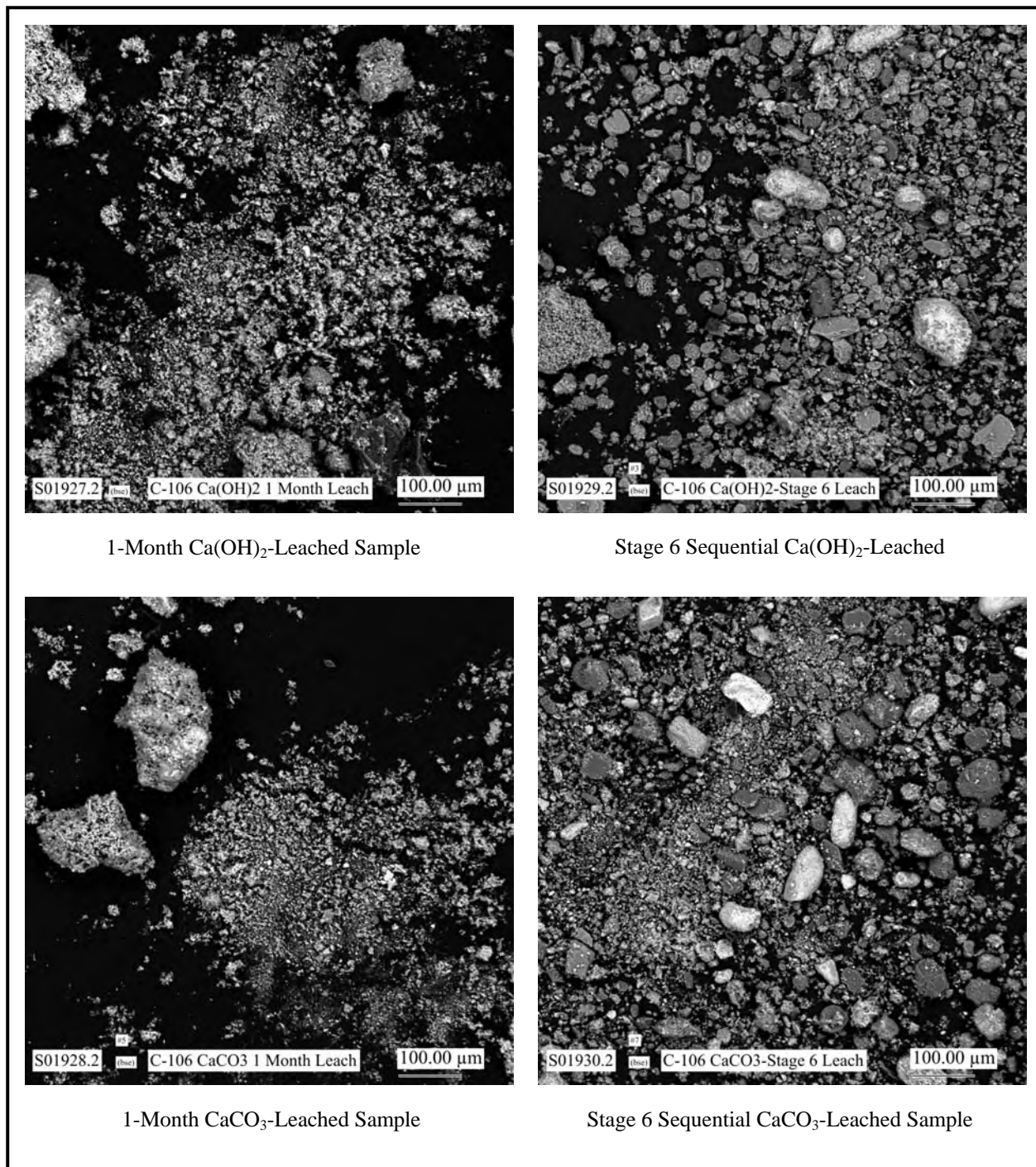


Figure 4.4. Low Magnification SEM Micrographs of Particles Present in 1-Month and Stage 6 Sequential Ca(OH)_2 -Leached (left and right top row, respectively) and 1-Month and Stage 6 Sequential CaCO_3 -Leached (left and right bottom row, respectively) C-106 Residual Waste

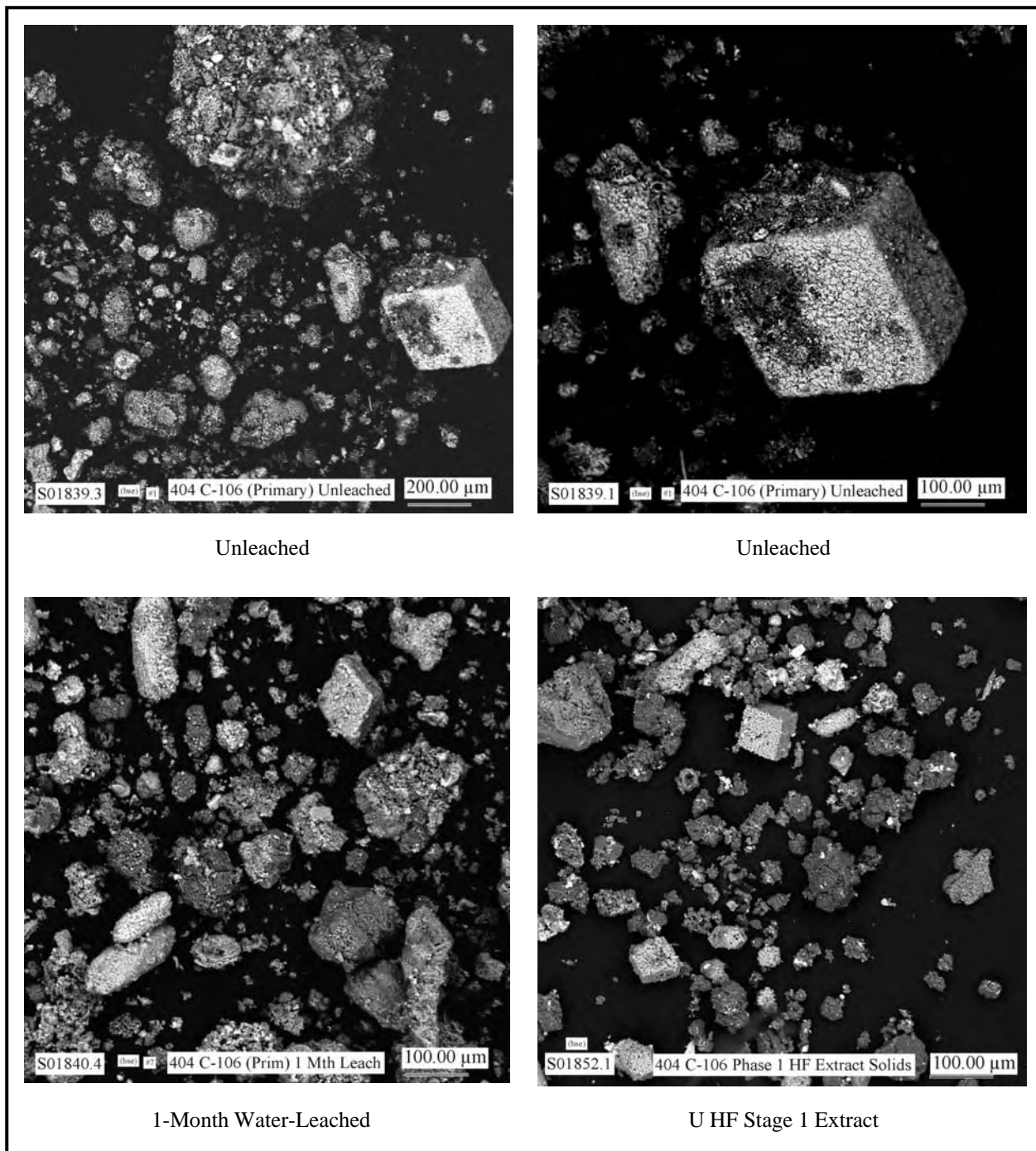


Figure 4.5. Low Magnification SEM Micrographs of Particles Present in the Unleached (top row), 1-Month Water-Leached (left on bottom row), and HF Stage 1 Extract (right on bottom row) of Oxalic Acid-Treated Residual Waste from Tank C-106 (from Deutsch et al. 2005b)

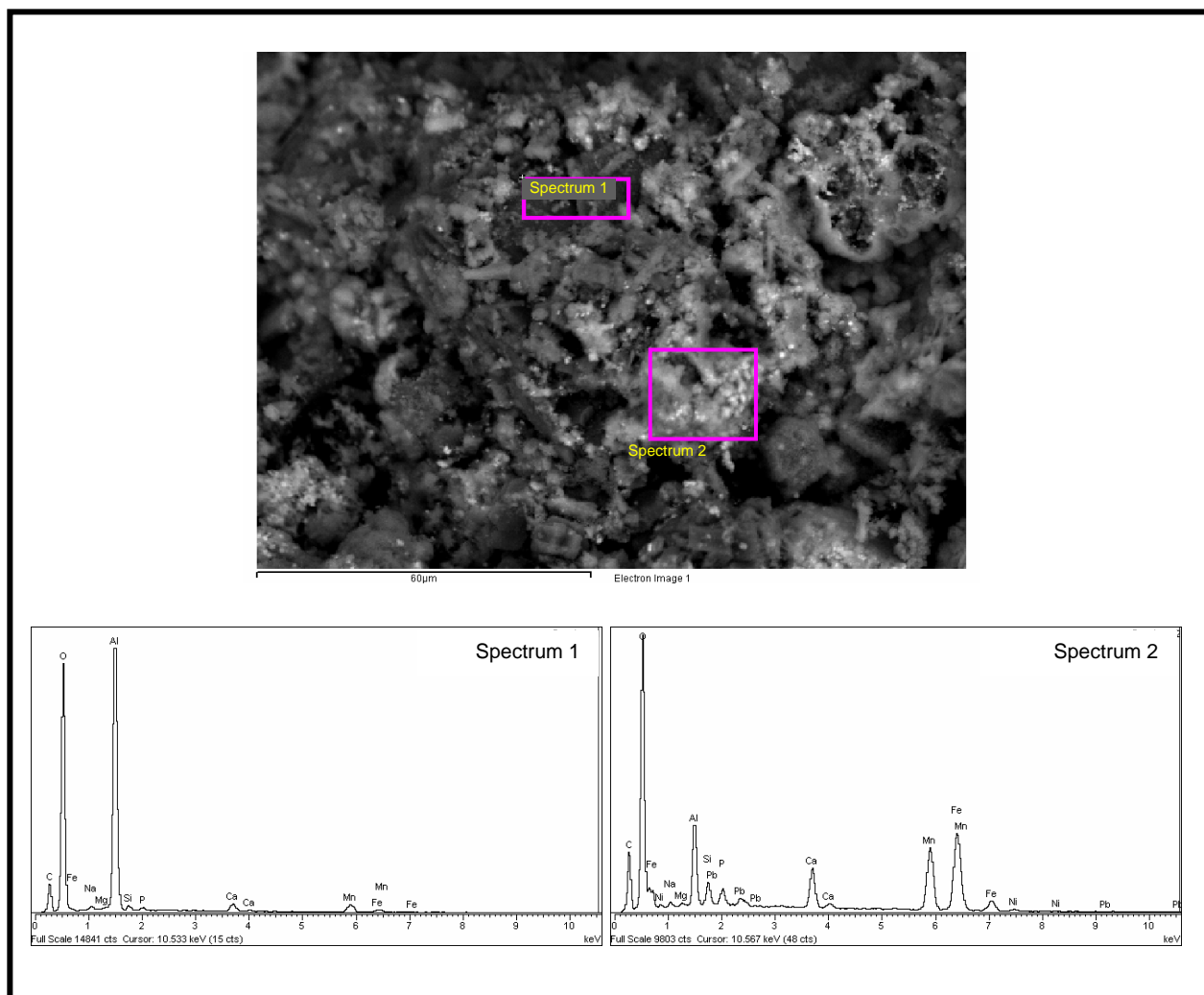


Figure 4.6. SEM Micrograph of Typical Particle Aggregates Present in 1-Month $\text{Ca}(\text{OH})_2$ -Leached C-106 Residual Waste and Spectra for Areas Analyzed by EDS

The $\text{Ca-Mn-Al-Si-Fe-}\pm\text{Pb}\pm\text{REE}(\text{Ce}) \pm\text{Cr}(\text{trace})\text{-P-O}\pm\text{C}\pm\text{H}$ and $\text{Al-O}\pm\text{H}$ were the most common phase compositions identified by EDS in the $\text{Ca}(\text{OH})_2$ - and CaCO_3 -leached samples. The $\text{Ca-Mn-Al-Si-Fe-}\pm\text{Pb}\pm\text{REE}(\text{Ce})\pm\text{Cr}(\text{trace})\text{-P-O}\pm\text{C}\pm\text{H}$ phase does not correspond to any phase identified by bulk XRD, and is compositionally different from the $\text{Mn-Al-Fe-Na-P-Si-Ca-O}\pm\text{C}\pm\text{H}$ phase identified by Deutsch et al. (2005b) in the unleached residual waste. In the $\text{Ca}(\text{OH})_2$ - and CaCO_3 -leached samples, Ca (based on EDS peak height) is usually the most or second most abundant element in these particles, whereas Mn and Al were the major components and Ca a minor component in the $\text{Mn-Al-Fe-Na-P-Si-Ca-O}\pm\text{C}\pm\text{H}$ phase found in the unleached residual solid. This phase in the $\text{Ca}(\text{OH})_2$ - and CaCO_3 -leached samples may also contain considerable concentrations of Pb (see spectra 3 and 4 in Figure 4.8) and/or trace concentrations of Ce (see spectrum 2 in Figure 4.10) and/or Cr. Because this phase is abundant in these leached samples and no compositionally similar phase was identified by bulk XRD, the $\text{Ca-Mn-Al-Si-Fe-}\pm\text{Pb}\pm\text{REE}(\text{Ce}) \pm\text{Cr}(\text{trace})\text{-P-O}\pm\text{C}\pm\text{H}$ phase is likely amorphous. Further analyses by transmission electron microscopy (TEM) or synchrotron-based x-ray microdiffraction (μXRD) would be required to verify the amorphous nature of this phase and ascertain if this phase is a homogenous single phase.

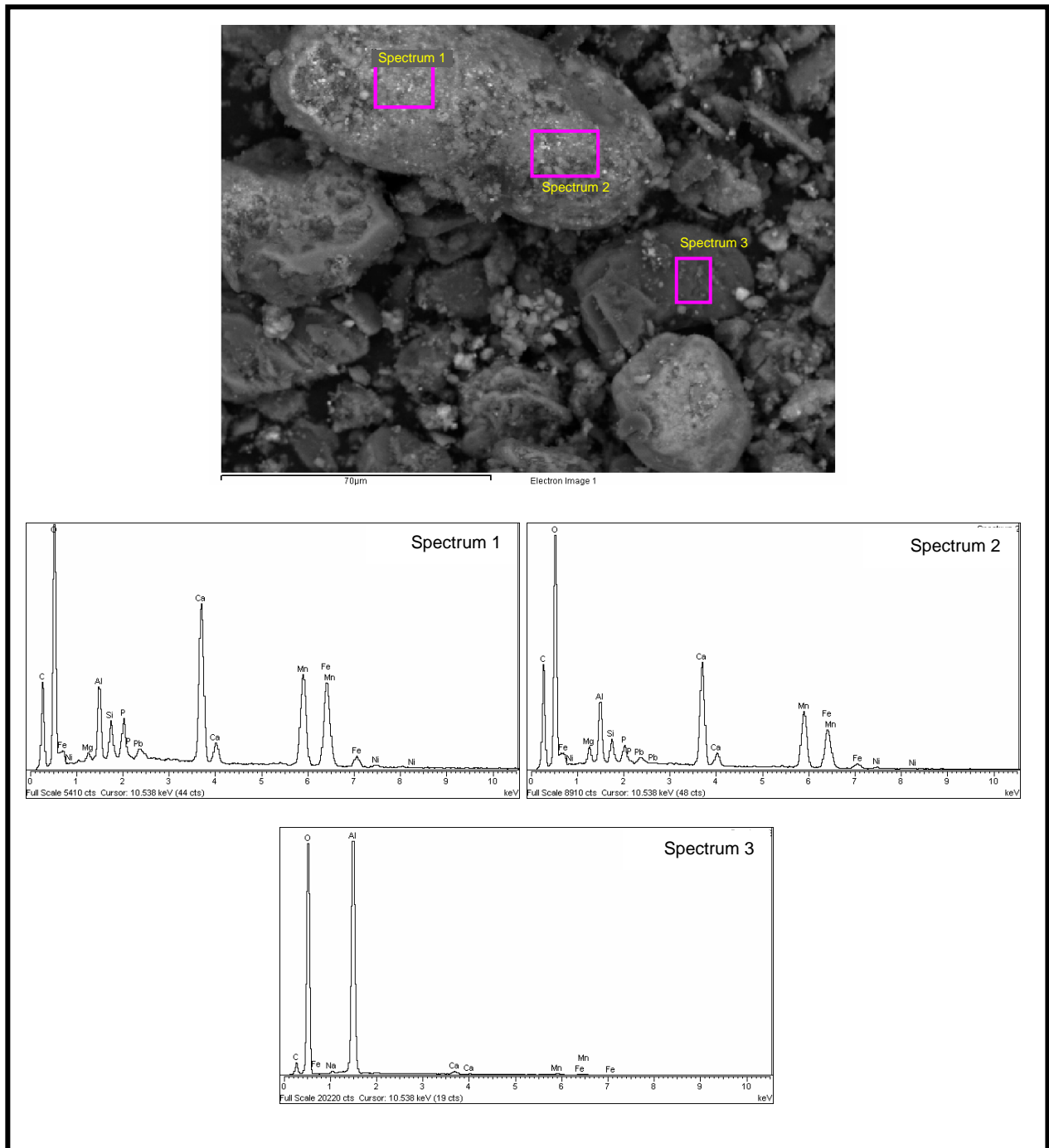


Figure 4.7. SEM Micrograph of Typical Particles Present in Stage 6 Sequential $\text{Ca}(\text{OH})_2$ -Leached C-106 Residual Waste and Spectra for Areas Analyzed by EDS

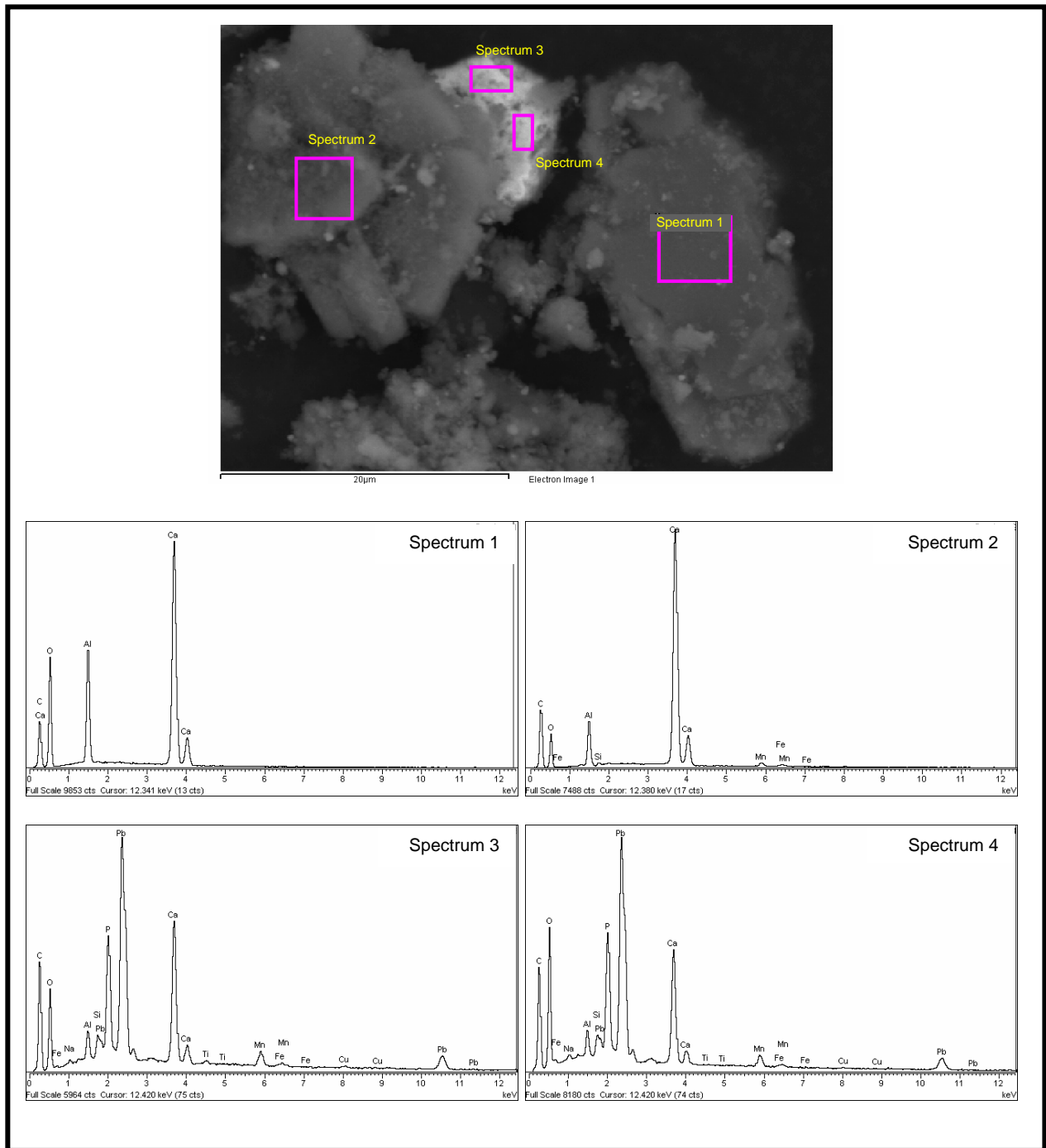


Figure 4.8. SEM Micrograph of Typical Particles Present in Stage 6 Sequential $\text{Ca}(\text{OH})_2$ -Leached C-106 Residual Waste and Spectra for Areas Analyzed by EDS

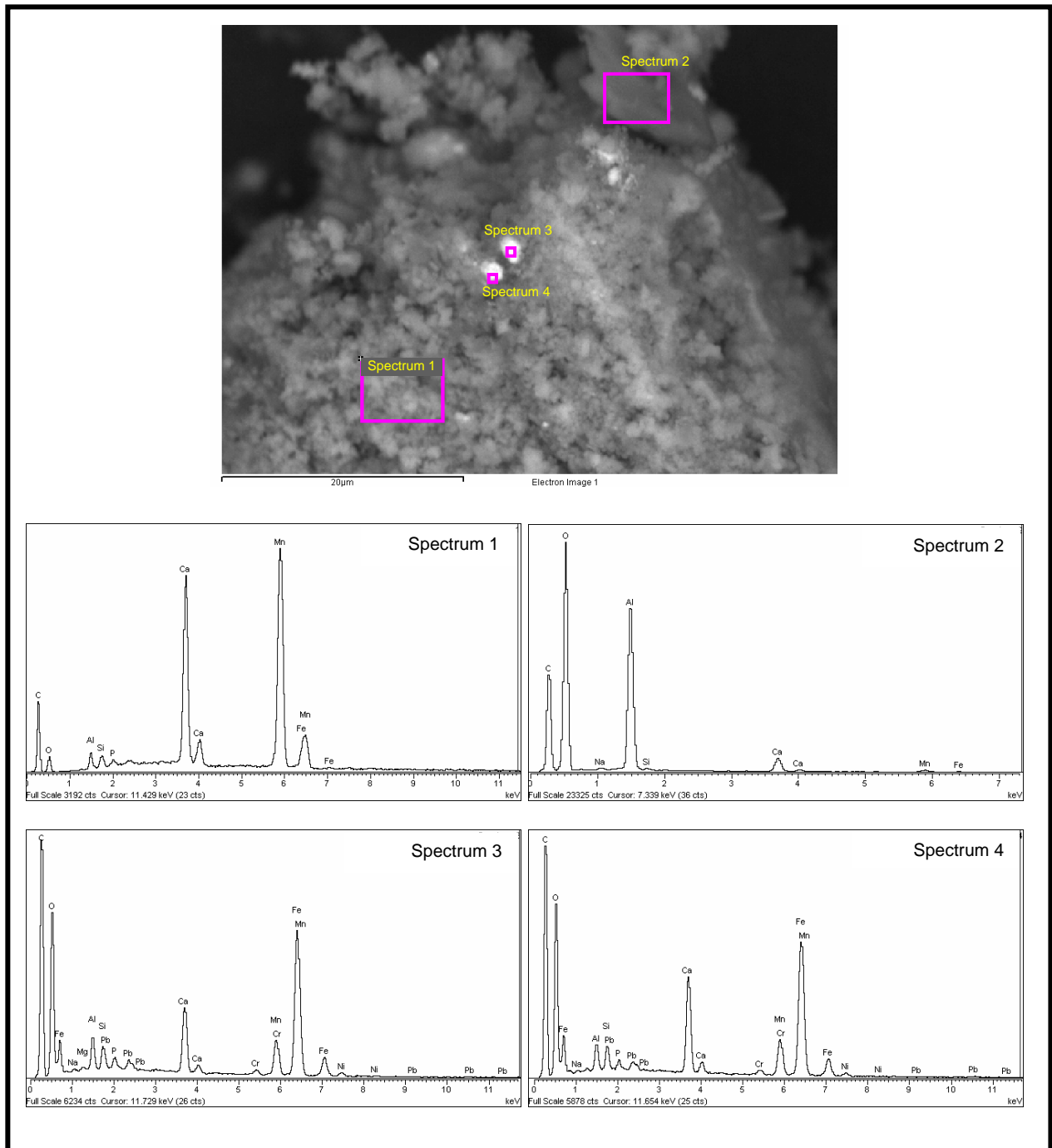


Figure 4.9. SEM Micrograph of Typical Particles Present in 1-Month CaCO_3 -Leached C-106 Residual Waste and Spectra for Areas Analyzed by EDS

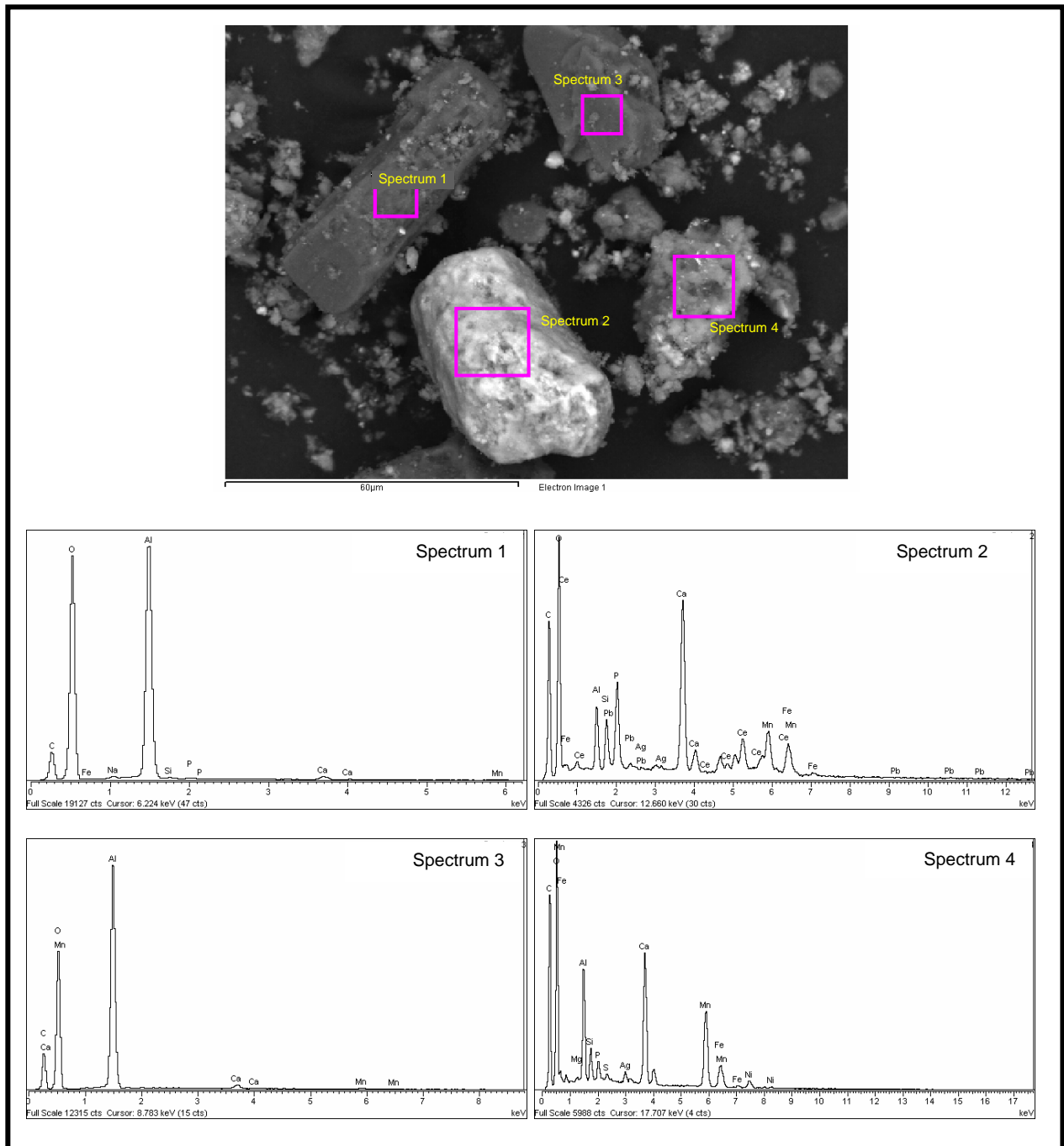


Figure 4.10. SEM Micrograph of Typical Particles Present in Stage 6 Sequential CaCO₃-Leached C-106 Residual Waste and Spectra for Areas Analyzed by EDS (Also see colored and black-and-white element distribution maps in Figures 4.19 and 4.20.)

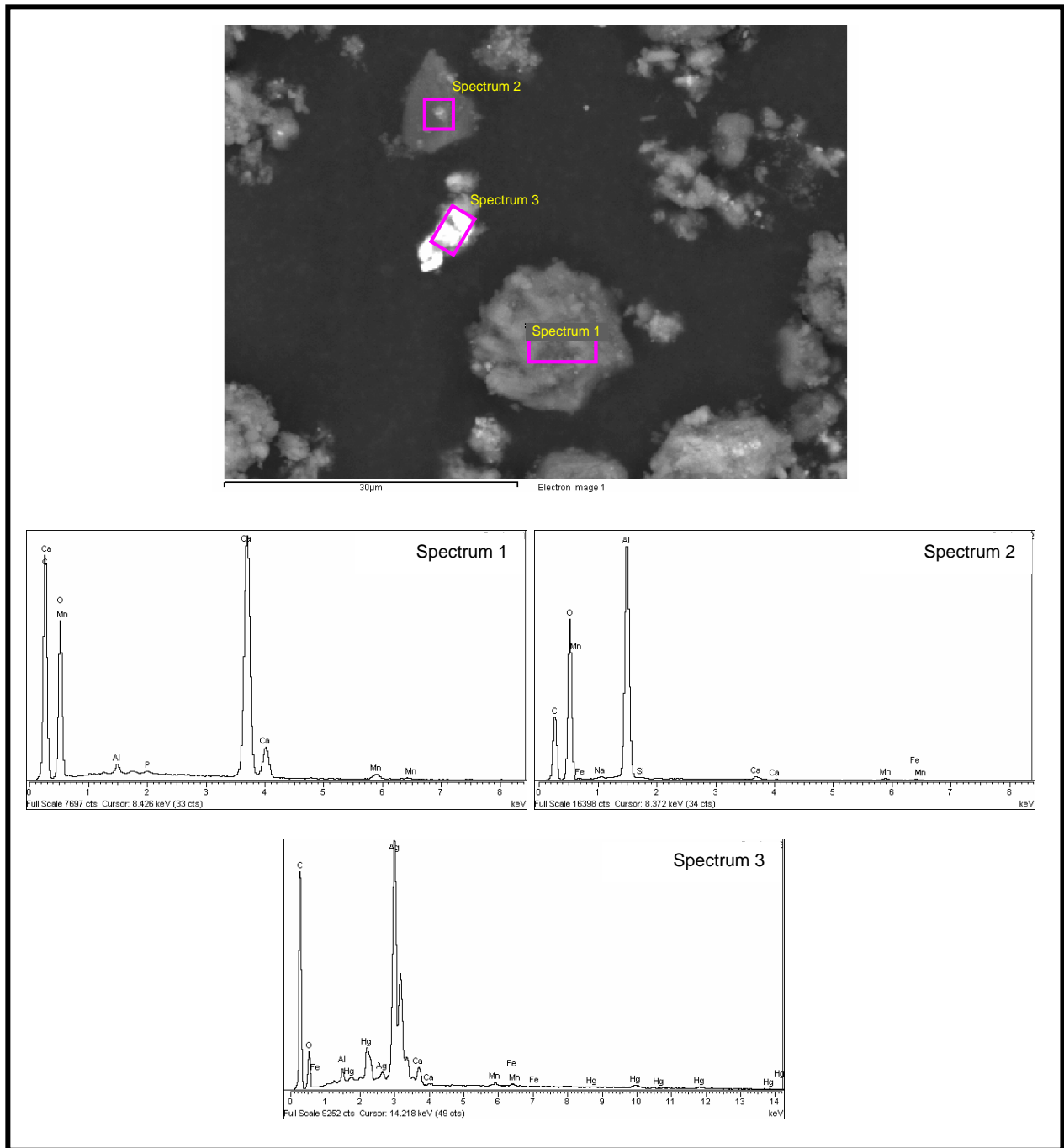


Figure 4.11. SEM Micrograph of Typical Particles Present in Stage 6 Sequential CaCO_3 -Leached C-106 Residual Waste and Spectra for Areas Analyzed by EDS

The Al-O±H and Ca-O±C±H phases also exist in the unleached residual waste studied by Deutsch et al. (2005b). The Al-O±H phase likely corresponds to gibbsite and/or böhmite which were identified by bulk XRD. The Ca-O±C±H phases probably correspond to either calcite or whewellite, which were also detected by bulk XRD.

The 1-month Ca(OH)₂- and 1-month and Stage 6 sequential CaCO₃-leached samples also contain another phase not previously identified by bulk XRD in these or the unleached residual waste samples. This phase consists of Ca-Al-O±C±H (spectra 1 and 2 in Figure 4.8). Based on a search of mineral composition databases on the Internet, the only phases found that match this composition include alumohydrocalcite [CaAl₂(CO₃)₂(OH)₄·3H₂O] and paraalumohydrocalcite [CaAl₂(CO₃)₂(OH)₄·6H₂O]. Also, a search of the PDF XRD mineral and inorganic solid database files for this composition or any similar oxides, hydroxides, or carbonates did not identify any phase with an XRD pattern that is consistent with the bulk XRD patterns for these samples. Moreover, as noted in Section 4.4, the measured XRD patterns did not contain any unassigned reflections. This suggests that all crystalline phases present at greater than 5 to 10 wt% in these Ca(OH)₂- and CaCO₃-leached residual waste samples were identified. Therefore, the Ca-Al-O±C±H phase may be present in the leached samples at less than 5-10 wt% or be amorphous. Additional analyses by TEM or synchrotron-based μXRD would be required to help identify this phase.

The SEM micrographs of the Ca(OH)₂- and CaCO₃-leached samples sometimes contained bright (white) particles or aggregates (see particles marked by spectrum 3 in Figure 4.11) a few micrometers to submicrometer in size that contained primarily Ag, Hg, O, and possibly C. These Ag-Hg particles were not as common or large in these samples as those identified by Deutsch et al. (2005a) in the unleached, water-leached, and HF-extracted residual waste samples.

One particle cluster with composition Mn-Na-P-O±C±H was also observed (see Figure B.24 in Appendix B) in the 1-month Ca(OH)₂-leached sample. This particle composition was not observed in any of the other leached samples analyzed by SEM/EDS. However, given the fine-grained nature of the particle aggregates in these samples, particles with this composition might be present elsewhere and not identified by EDS analyses, which often represented a composite composition of aggregates of several micrometer-size particles. Based on a search of mineral composition databases on the Internet, the composition Mn-Na-P-O±C±H could correspond to minerals such as kanonerovite (MnNa₃P₃O₁₀·12H₂O), natrophilite (NaMnPO₄), sidorenkite [Na₃Mn(PO₄)(CO₃)], and viitaniemiite [Na(Ca,Mn)Al(PO₄)(F,OH)₃]. No efforts were made to review the literature and determine if the conditions of formation for these minerals correspond to those associated with residual waste from tank C-106. However, Bechtold et al. (2003) reported the possible presence of sidorenkite in a baseline sample of C-106 sludge based on characterization by XRD and SEM/EDS.

Compared to the SEM/EDS results for the unleached residual solid presented by Deutsch et al. (2005a), SEM/EDS analyses of the Ca(OH)₂- and CaCO₃-leached samples did not indicate the presence of any obvious extensive coatings of newly precipitated phases on the particles and aggregates in the C-106 residual waste. If coatings existed that were only one or 2 micrometers thick, then EDS of such coatings would be difficult since the measured composition would be a composite of the coating and phase(s) under the coating.

The EDS analyses of the Ca(OH)₂- and CaCO₃-leached samples did not find any particles or aggregates with compositions corresponding to the Mn-O-C±H, Al-Na-O-C±H, Fe-Cr-O±C±H, and

Fe-Mn-O±C±H phases observed by SEM/EDS in the samples of C-106 residual waste analyzed by Deutsch et al. (2005a). The Fe-Cr and Fe-Mn oxide phases were not common in the samples of C-106 residual waste analyzed by Deutsch et al. (2005b), but were nonetheless observed by SEM/EDS. Although Fe was detected by EDS in the Ca-Mn-Al-Si-Fe-±Pb±REE(Ce) ±Cr(trace)-P-O±C±H phase and possibly enriched in areas in some particles at the submicrometer scale (see EDS element maps discussed later in this section), no distinct Fe-Cr or Fe-Mn oxide phases were identified by EDS or bulk XRD in the Ca(OH)₂- and Ca(OH)₂/CaCO₃-leached samples.

The SEM/EDS analyses did not indicate the presence of I, Tc, or U in any particles or aggregates present in the Ca(OH)₂- and CaCO₃-leached samples. This was due to their low concentrations in these residual waste samples and the high detection limits for analysis by EDS.

Colorized and black-and-white element distribution maps were also recorded for particles and aggregates present in the 1-month (Figure 4.12 and Figure 4.13) and Stage 6 sequential (Figure 4.14, Figure 4.15, and Figure 4.16) Ca(OH)₂-leached, and in 1-month (Figure 4.17 and Figure 4.18) and Stage 6 sequential (Figure 4.19 and Figure 4.20) CaCO₃-leached samples. The BSE SEM micrographs at the top of Figure 4.12 through Figure 4.20 show the particles included in the element distribution maps given in each figure. For the colorized element distribution maps, keys are given in each figure to indicate which elements correspond to each color. For the black-and-white element distribution maps, the concentration of each listed element is directly proportional to the regions of brightness (i.e., brighter the area, the higher the concentration of that element) in the corresponding distribution map.

The element distribution maps (Figure 4.14 through Figure 4.20) clearly show the complexity of the compositions of phases, especially for the mineral aggregates, in the Ca(OH)₂- and CaCO₃-leached samples. Like the EDS spectra in Figure 4.6 through Figure 4.11 and Appendices B through E, the element distribution maps illustrate the importance of Mn, Ca, and Al with respect to the particle compositions and bulk chemistry of these Ca(OH)₂- and CaCO₃-leached samples. Although the importance of Mn and Al in C-106 residual waste solids was previously shown in the SEM/EDS results in Deutsch et al. (2005a) and EDS element distribution maps in Deutsch et al. (2005b), the SEM/EDS results in this report, such as Figure 4.14 through Figure 4.20, suggest that the Ca concentrations have increased in the Ca(OH)₂- and CaCO₃-leached solid samples relative to the unleached residual waste from tank C-106. This includes the increase in Ca concentration detected by EDS in the Ca-Mn-Al-Si-Fe-±Pb±REE(Ce) ±Cr(trace)-P-O±C±H solids which are common in these leached materials and the identification by EDS of a Ca-Al-O-C±H phase, which was not previously observed in the unleached C-106 residual waste.

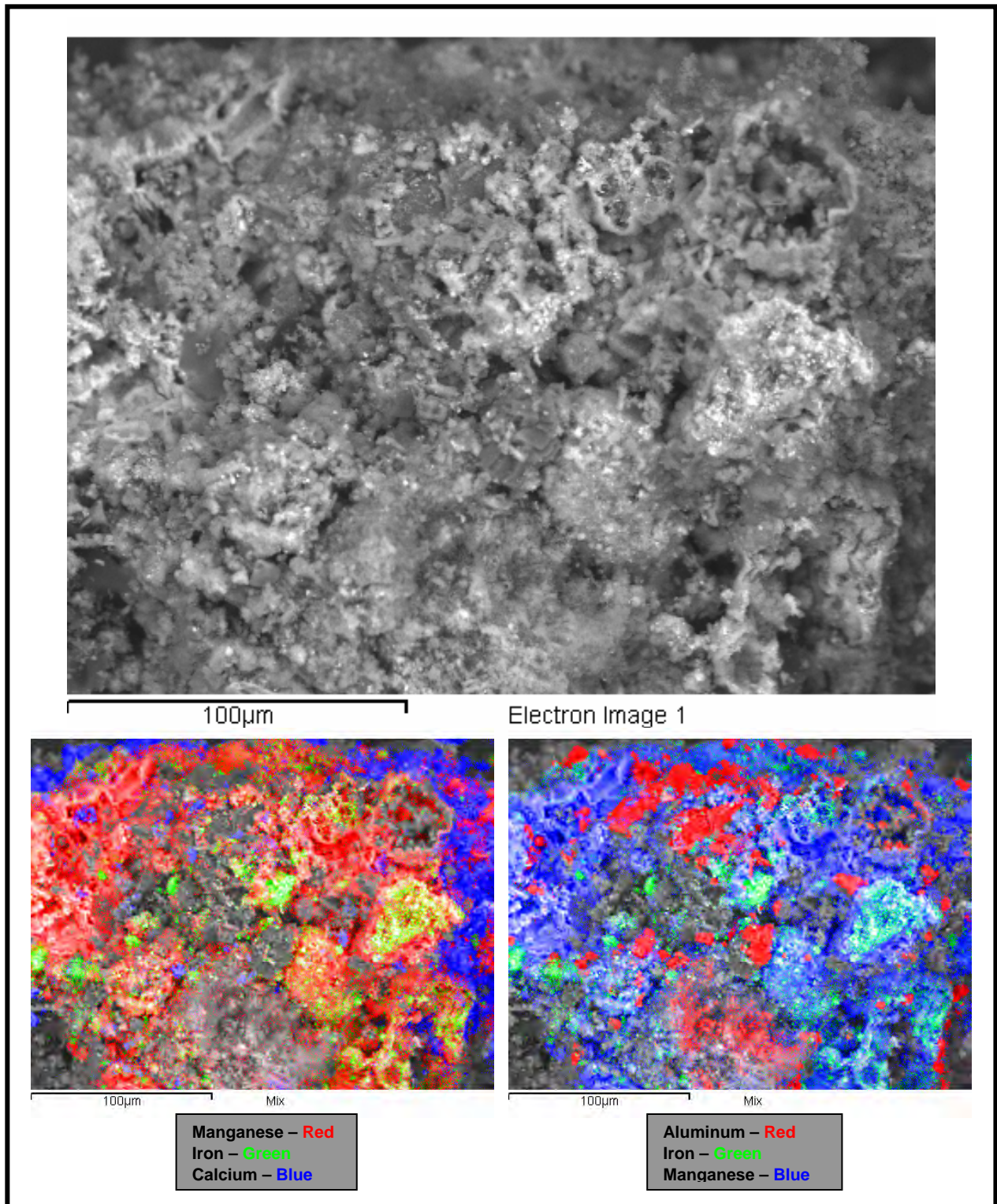


Figure 4.12. Backscatter-Electron SEM Image and Colorized Element Maps for a Particle Aggregate from the 1-Month $\text{Ca}(\text{OH})_2$ -Leached C-106 Residual Waste

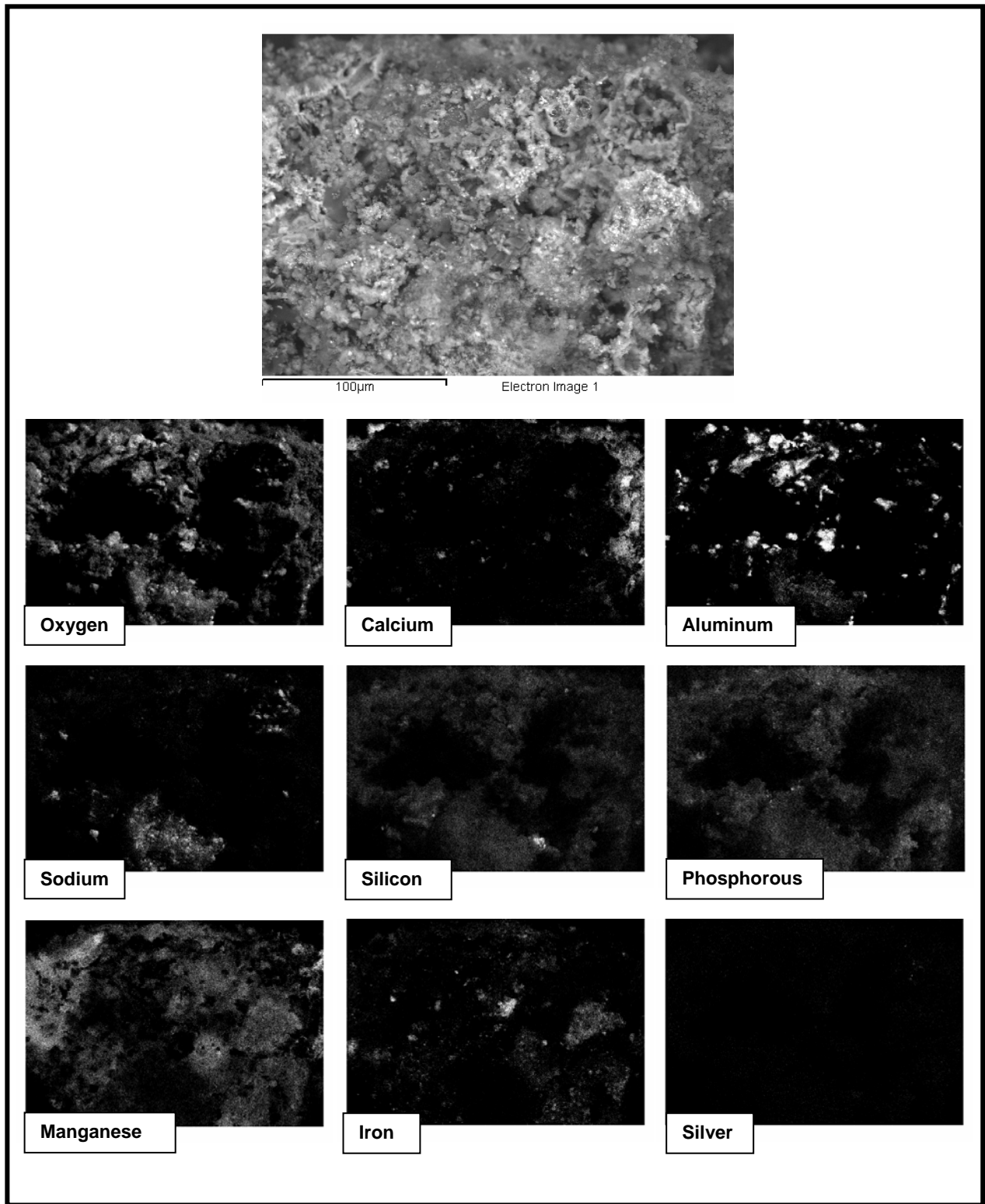


Figure 4.13. Backscatter-Electron SEM Micrograph and Element Distribution Maps for Particles in 1-Month $\text{Ca}(\text{OH})_2$ -Leached C-106 Residual Waste

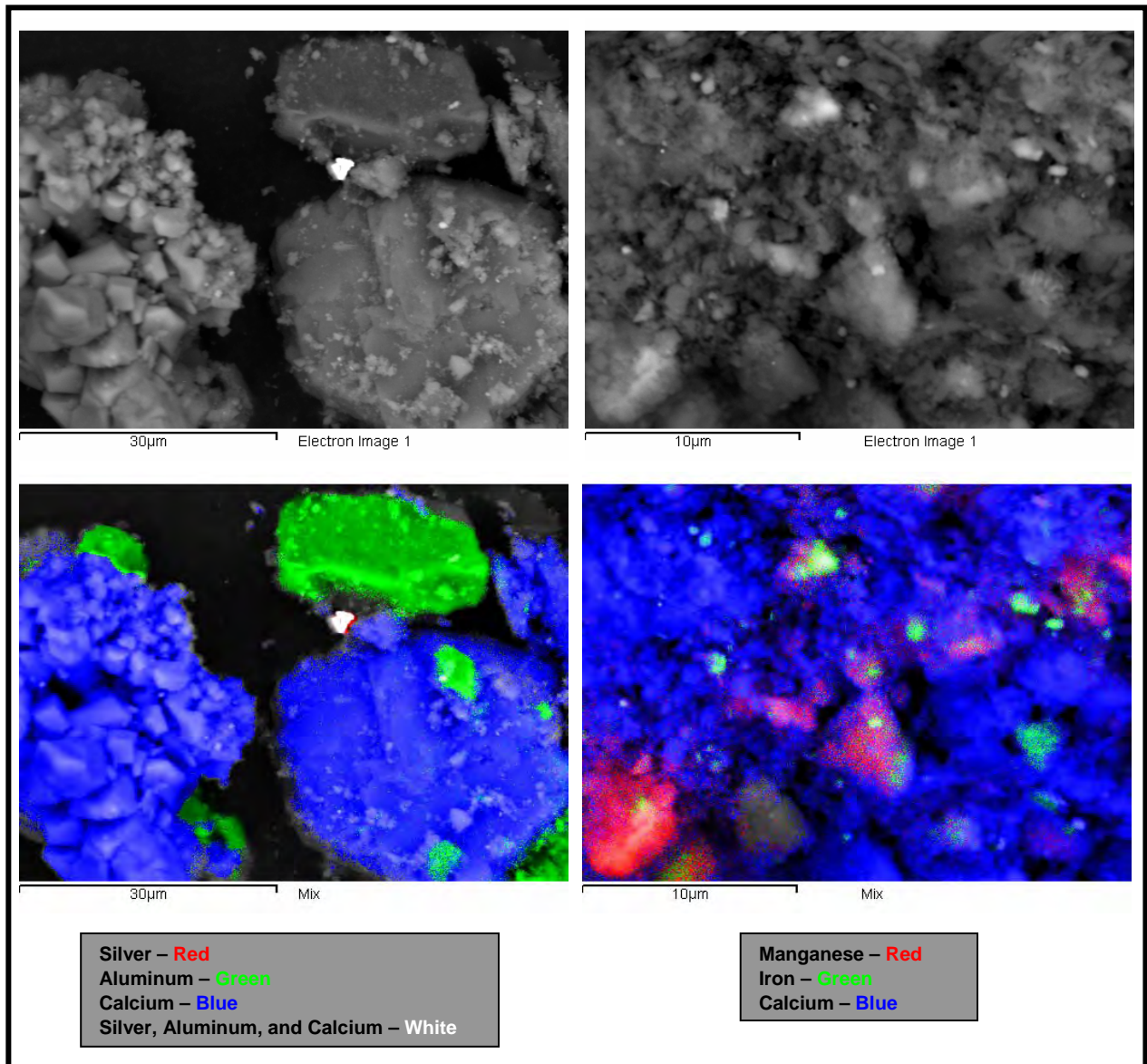


Figure 4.14. Backscatter-Electron SEM Image and Colorized Element Maps for a Particle Aggregate from the Stage 6 Sequential $\text{Ca}(\text{OH})_2$ -Leached C-106 Residual Waste

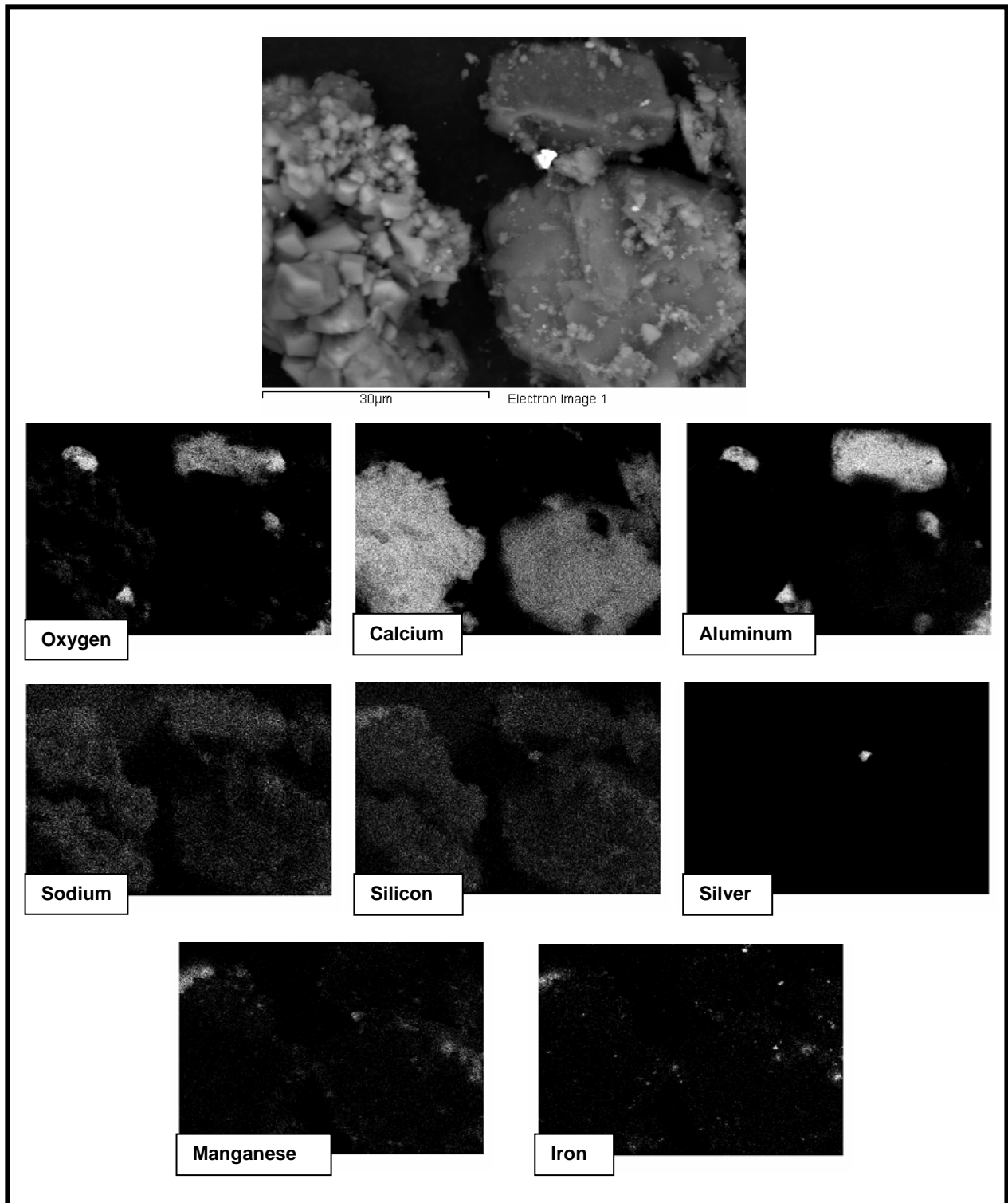


Figure 4.15. Backscatter-Electron SEM Micrograph and Element Distribution Maps for Particles in Stage 6 Sequential $\text{Ca}(\text{OH})_2$ -Leached C-106 Residual Waste

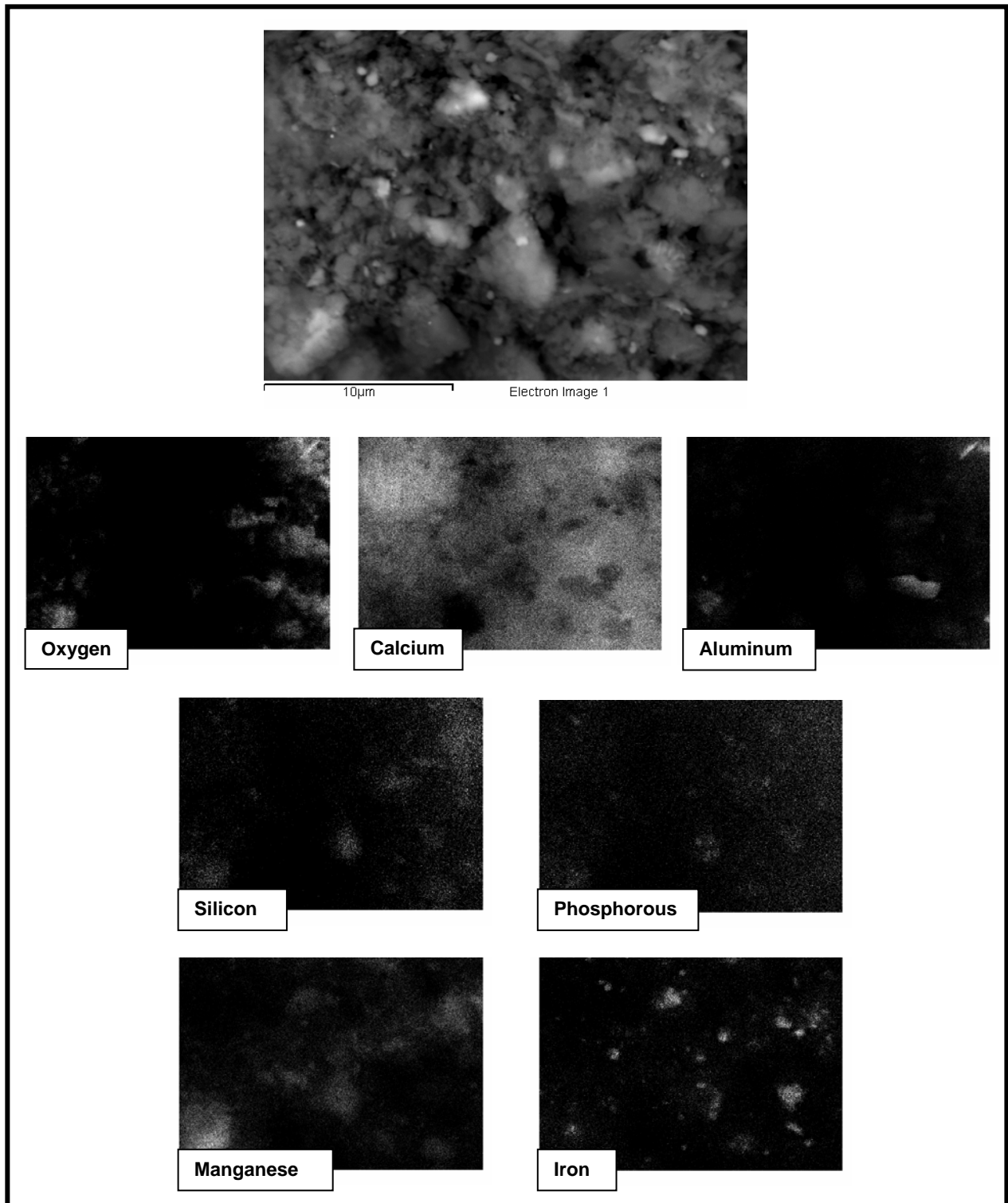


Figure 4.16. Backscatter-Electron SEM Micrograph and Element Distribution Maps for Particles in Stage 6 Sequential $\text{Ca}(\text{OH})_2$ -Leached C-106 Residual Waste

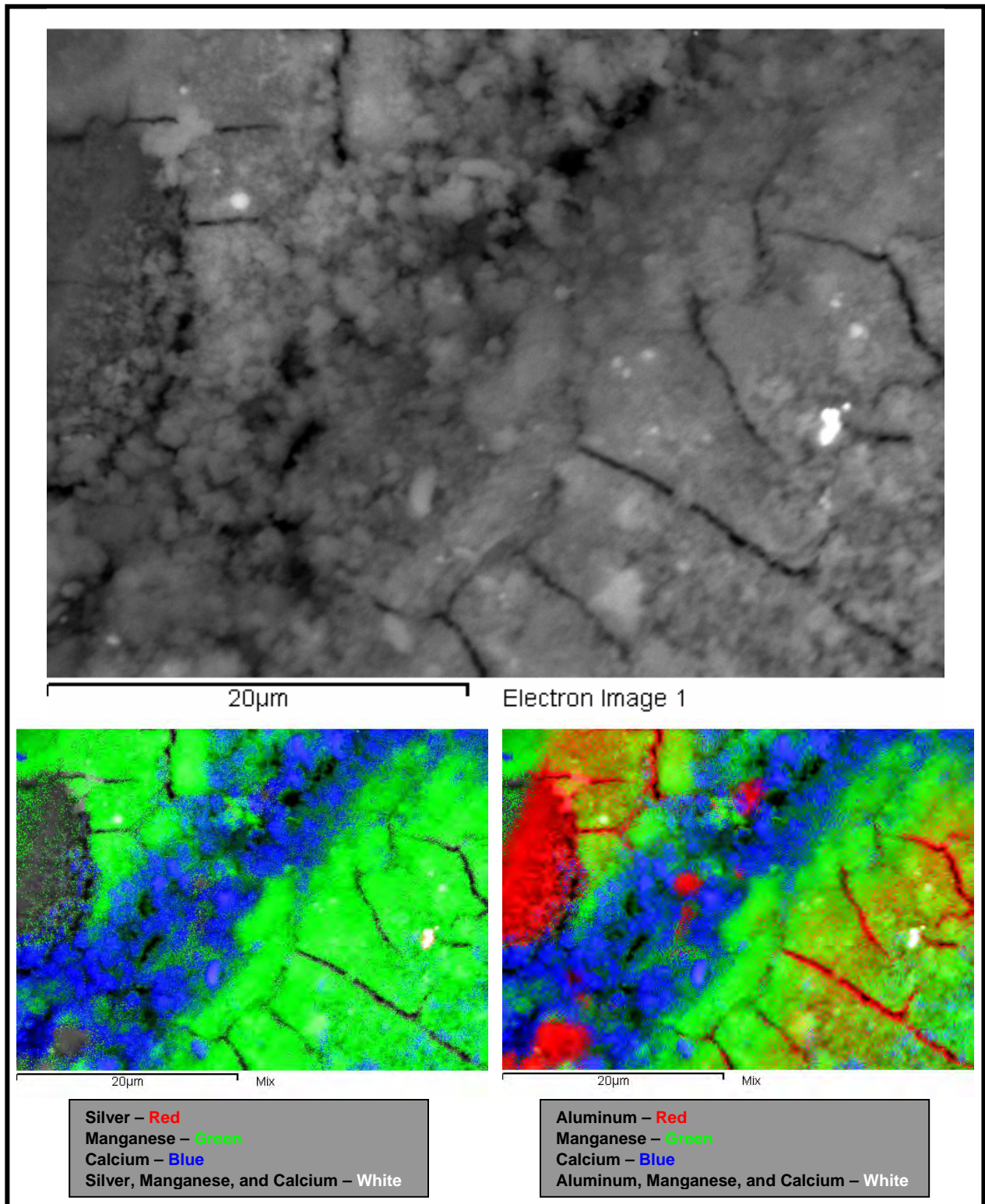


Figure 4.17. Backscatter-Electron SEM Image and Colorized Element Maps for a Particle Aggregate from the 1-Month CaCO_3 -Leached C-106 Residual Waste

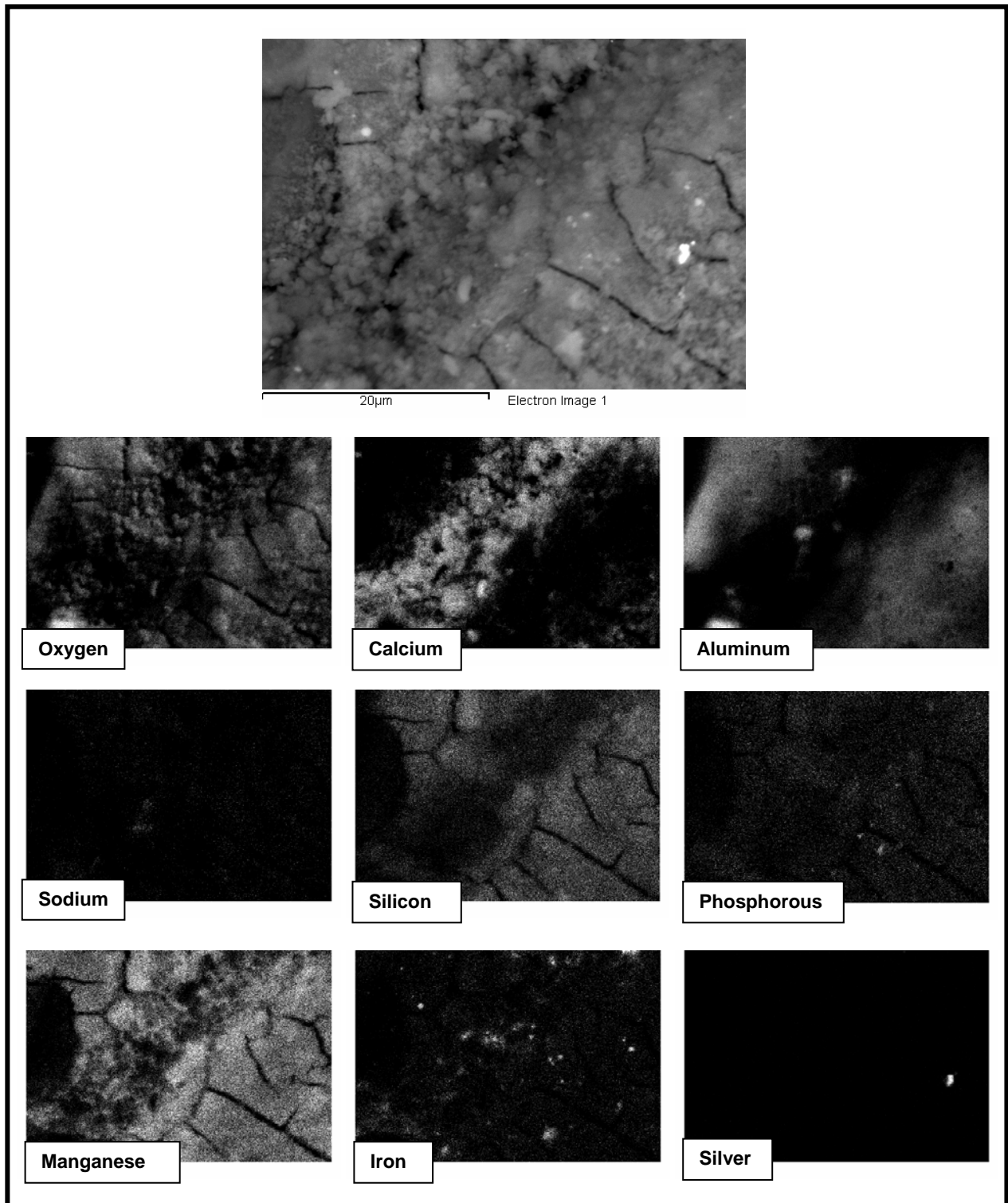


Figure 4.18. Backscatter-Electron SEM Micrograph and Element Distribution Maps for Particles in 1-Month CaCO_3 -Leached C-106 Residual Waste

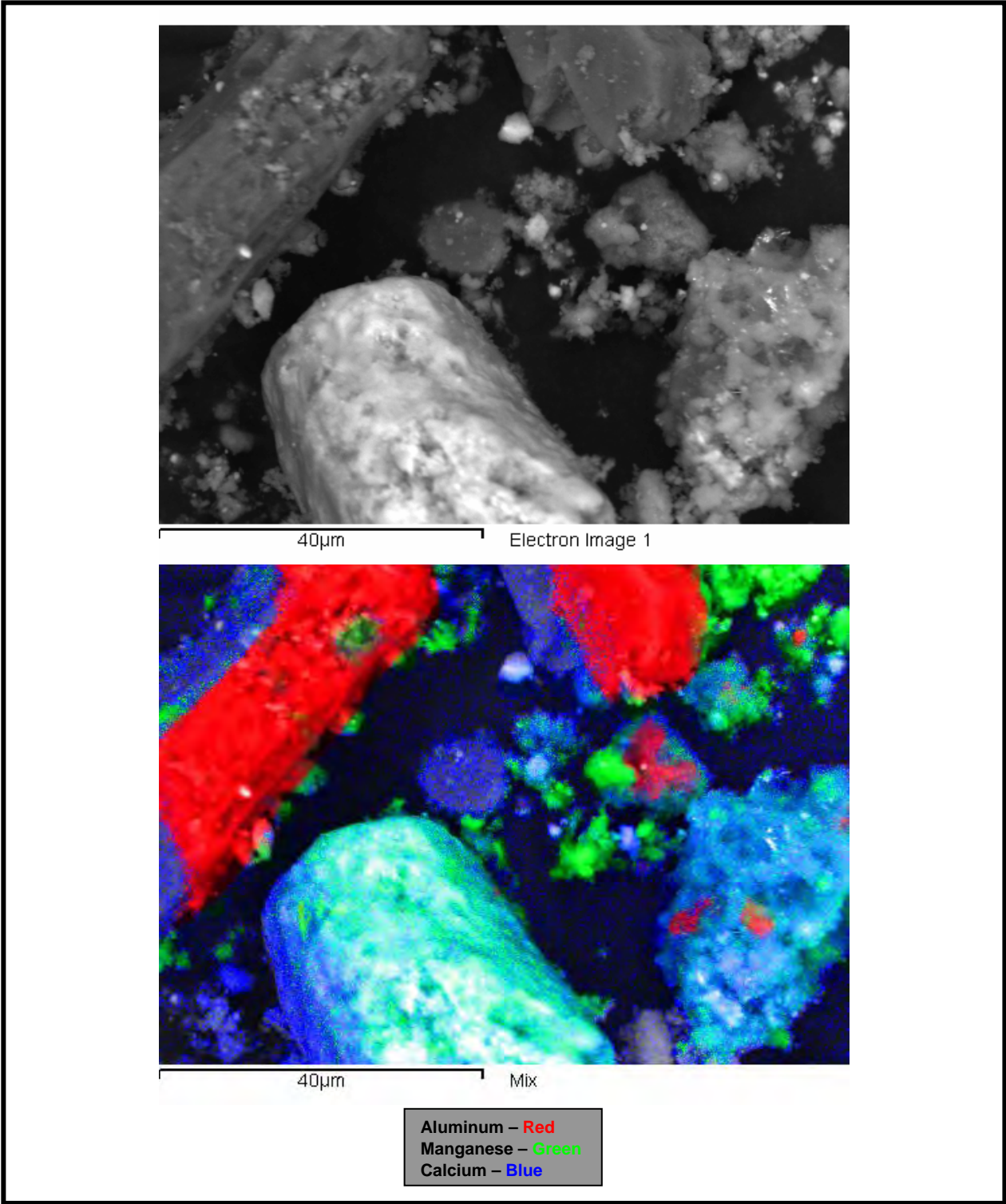


Figure 4.19. Backscatter-Electron SEM Image and a Colorized Element Map for a Particle Aggregate from the Stage 6 Sequential CaCO_3 -Leached C-106 Residual Waste

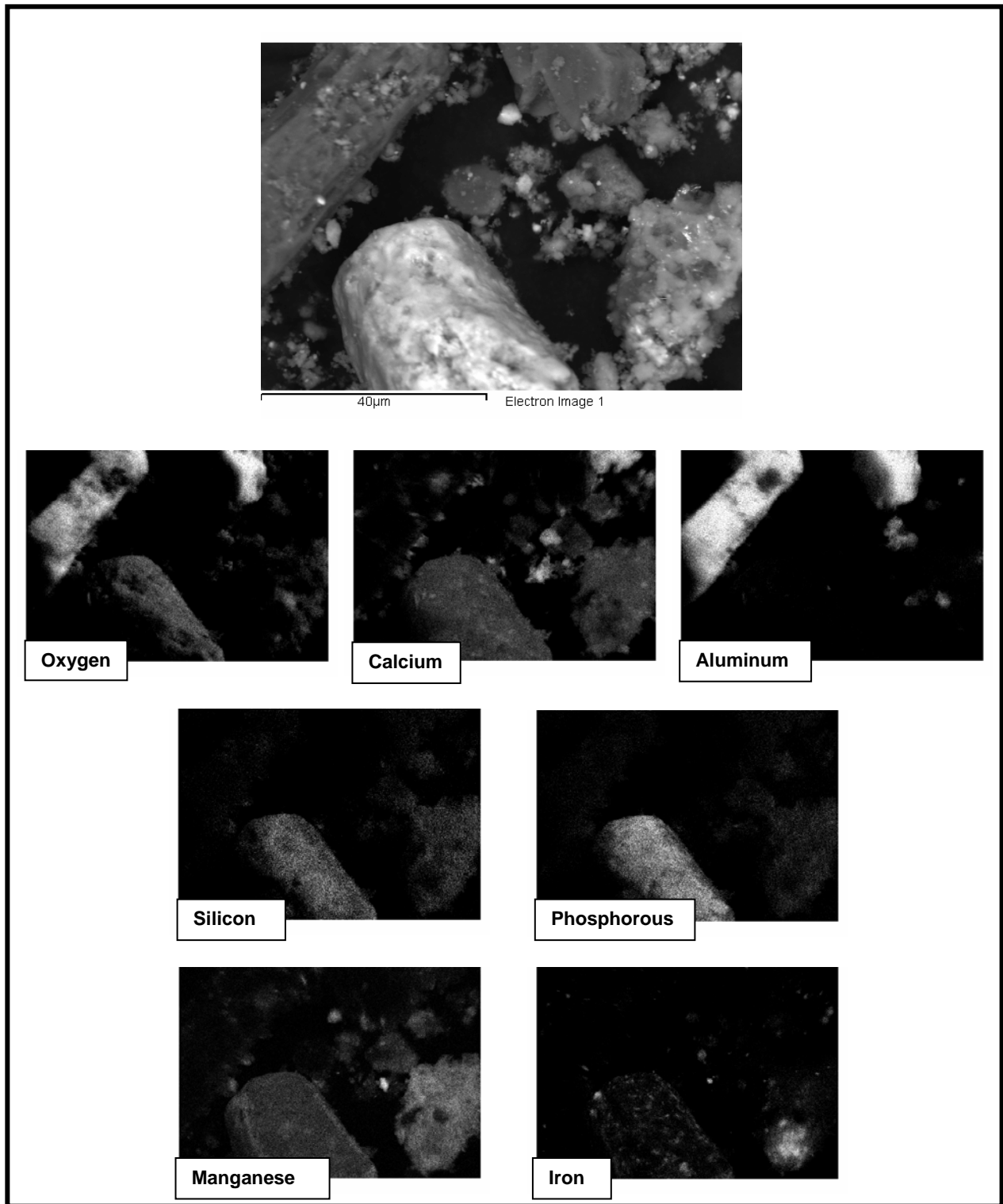


Figure 4.20. Backscatter-Electron SEM Micrograph and Element Distribution Maps for Particles in Stage 6 Sequential CaCO_3 -Leached C-106 Residual Waste

5.0 Contaminant Release Model

The primary objective of this project is to develop source release models for contaminants of concern present in residual waste upon closure of Hanford single-shell tanks. As shown in Figure 5.1, developing these models consists of laboratory testing to produce contaminant release data and a conceptual source release model. After development, the release model can be incorporated into a fate and transport model as part of a long-term risk/performance assessment for the closed tank. A previously developed release model for residual sludge from tank C-106 assumed that the sludge was contacted with dilute water meant to simulate rainwater that has infiltrated through the vadose zone to contact the sludge (Deutsch et al. 2005a). This section describes a new conceptual release model developed for ^{238}U , ^{99}Tc , Cr, and ^{129}I for a scenario in which the residual sludge is covered with cementitious grout, which is under consideration as a component of the closure process.

Data collected and analyses conducted in Deutsch et al. (2005a) and in this study indicated that contaminant release from tank C-106 residual sludge will be geochemically complex. Contaminant release from the sludge is expected to involve mineral dissolution and precipitation, oxidation-reduction reactions, solution phase complexation, and surface adsorption. Some of these reactions can be modeled as equilibrium reactions whereas others will be rate controlled. Although significant insight was gained in this study regarding the contaminant release mechanisms that will be important for tank C-106 sludge, it was not possible to adequately characterize the phase associations of the contaminants of concern in sufficient detail to produce a mechanistically rigorous geochemical release model. This could change with additional work; however, in the meantime, a release model based on empirical solubilities has been developed. The approach used is inherently conservative and will over-estimate contaminant release. Further characterization work could allow the development of a more mechanistically rigorous geochemical release model, if warranted.

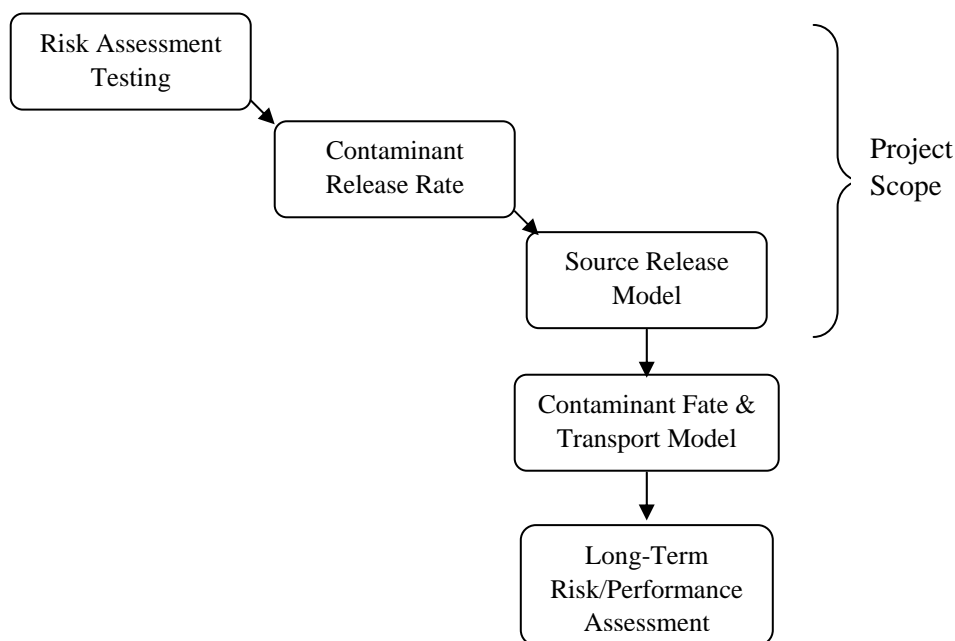


Figure 5.1. Source Release Model Development for Long-Term Risk/Performance Assessments

The contaminant release models that have been developed for residual sludge in tank C-106 are based on empirical solubilities of the contaminants of concern. Empirical solubilities can be influenced by many geochemical conditions (e.g., pH, Eh, ionic strength, presence/concentration of complexing species) that are potentially dynamic throughout the history of the evolving sludge environment. In addition, available data indicate that portions of the contaminants of concern are incorporated into slightly soluble phases. The dissolution of these relatively insoluble phases will likely control the long-term release of the contaminants of concern in the residual sludge. For these reasons, the release models described in this section are expected to be conservative only to tank conditions that are currently expected at closure and will need to be modified as additional information becomes available regarding different tank conditions.

5.1 Modification of the Conceptual Model of Chemical Transformations of Tank C-106 Sludge Resulting from a Cementitious Tank Filler

A conceptual model of the chemical transformations that have occurred in tank C-106 as a result of chemical treatments used in the sludge removal process has been described previously (Deutsch et al. 2005a). This model is shown schematically in Figure 4.2 of Deutsch et al. (2005b). The last box of that figure describing the water leaching process relevant to contaminant release has been modified here to account for the impact of cement. Figure 5.2 shows this modified portion of the figure.

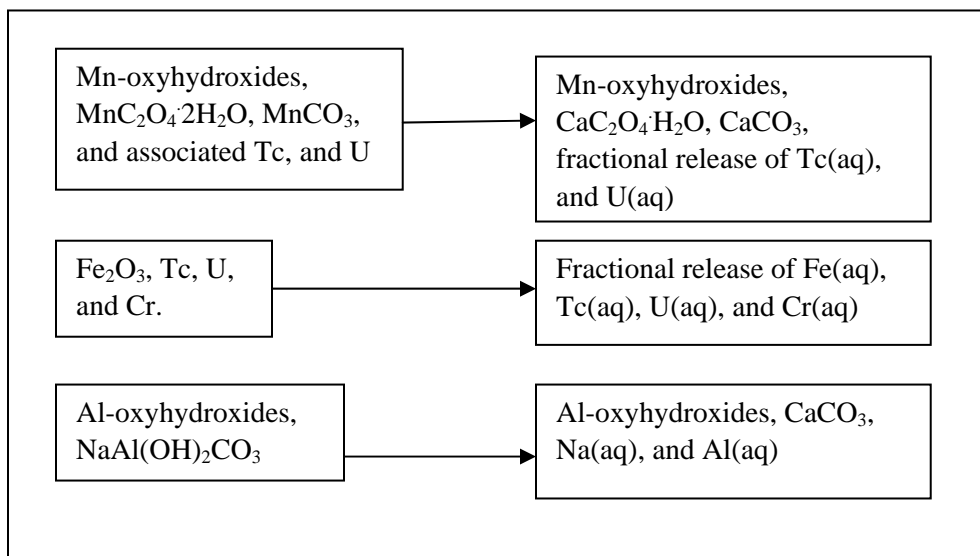


Figure 5.2. Chemical Transformations of Tank C-106 Residual Sludge Resulting from Contact with Cementitious Grout Leachate [0.01 M Ca(OH)₂]

The modifications shown here indicate that instead of a dilute water contacting the sludge, as assumed in Deutsch et al. (2005a), a solution with a composition of 0.01 M Ca(OH)₂ is assumed. The 0.01 M Ca(OH)₂ is used here as a surrogate for infiltration water modified by contact with a cementitious grout placed in the tank as part of the closure process.

The XRD results discussed in Section 4.2 indicate that rhodochrosite, lindbergite, dawsonite, and hematite, originally present in the post-retrieval C-106 sludge are no longer present after contact with the

0.01 M Ca(OH)₂ leachate. Calcite, which was not present in the unleached sample, was identified in the 0.01 M Ca(OH)₂ leachate samples. Analysis of the 0.01 M Ca(OH)₂ leachate solutions indicate that manganese, oxalate, and carbonate concentrations were below detection, suggesting that the majority of these components remain in the sludge during the leaching process. Significant concentrations of Al and Na were measured in the 0.01 M Ca(OH)₂ leachates. This information suggests that leaching of C-106 sludge with 0.01 M Ca(OH)₂ results in a number of phase transformations:

- Rhodochrosite (MnCO₃) is converted to calcite (CaCO₃) and a poorly defined amorphous Mn oxyhydroxide phase.
- Lindbergite (MnC₂O₄·2H₂O) is converted to whewellite (CaC₂O₄·H₂O), and the poorly defined amorphous Mn oxyhydroxide phase.
- Dawsonite (NaAl(OH)₂CO₃) is converted to calcite and dissolved Na and Al.

Chemical equilibrium modeling indicates that under oxidizing conditions, all these reactions are thermodynamically favorable in 0.01 M Ca(OH)₂. From a thermodynamic standpoint, the most stable Mn phase in equilibrium with air is pyrolusite (β-MnO₂). No Mn-oxyhydroxide phase was actually identified by XRD, so the phase is assumed to be amorphous. Although for the sake of simplicity this phase is referred to as an amorphous Mn-oxyhydroxide, SEM/EDS analysis suggests that this phase may actually be much more complicated: Ca-Mn-Al-Si-Fe±Pb±REE(Ce)±Cr-P-O±C±H.

The 1-month and six step 0.01 M Ca(OH)₂ sequential leaches produced very similar XRD and SEM/EDS results. The 1-month and six step 0.01 M CaCO₃ sequential leaches produced XRD and SEM/EDS results which were also very similar to the 1-month and six step 0.01 M Ca(OH)₂ sequential leaches with the exception that dawsonite was identified in the 1-month 0.01 M CaCO₃ leached sample. Based on these results, the transformations discussed above and outlined in Figure 5.2 will be used as the working hypothesis for the reaction of water contacting both fresh cement grout and aged cement grout and then contacting the residual sludge in tank C-106 after closure.

5.2 Release Models for Technetium, Uranium, Iodine, and Chromium in a Tank Filled with Cementitious Grout

Because of the highly complex chemical nature of tank C-106 residual sludge, clear and quantitative phase associations of the contaminants of concern with the phases known to exist in the residual sludge are difficult to specify. Although the various characterization methods employed in this study have revealed a number of important observations and have provided valuable data for constructing a scientifically defensible release model, many questions remain. Because a thorough understanding of all the important phase associations for the contaminants of concern cannot be developed at this time, an empirically based release model has been developed. Although less satisfying from a mechanistic point of view, this provides a release model that can be used now and is conservative in nature. Later work may provide a better understanding of the phase associations with the contaminants of concern and the release mechanisms from these phases; in this case, a less conservative, but more scientifically defensible release model could be developed.

Maximum release rates for ⁹⁹Tc, ²³⁸U, and Cr, from sludge extracts using Ca(OH)₂ (fresh cement stimulant) and CaCO₃ (aged cement stimulant) were determined from the 1-month water leachates. This

was done because the measured concentrations in these leachates were generally higher than those measured in the short term sequential leach extracts. Because it is necessary to rely on empirical release data for the release model, this more conservative approach is preferred. In addition, a longer leaching period is more representative of actual water/waste contact times expected in the future.

Table 5.1 is a summary of the contaminant release model data for tank C-106 for the fresh cement (0.01 M Ca(OH)₂) scenario. For ¹²⁹I and Cr, measured concentrations in the leachates were below the detection limits; therefore, the detection limit values were used for the release concentration. Total sludge concentrations are provided in column 2 of Table 5.1. These values were determined, as indicated in Deutsch et al. (2005a), from either the fusion or EPA Method 3050B acid digestions of the sludge, whichever had the highest concentration.

Table 5.1. Summary of Contaminant Release Model Data for Tank C-106, Fresh Cement (0.01 M Ca(OH)₂) Scenario

Contaminant	Sludge Concentration	Release Concentration	Release Control
⁹⁹ Tc	1.2 µg ⁹⁹ Tc/g-sludge (20,000 pCi ⁹⁹ Tc/g-sludge)	1.2 µg/L (20,000 pCi/L)	solubility
²³⁸ U	310 µg ²³⁸ U/g-sludge	36 µg/L	solubility
¹²⁹ I	0.62 µg ¹²⁹ I/g-sludge (110 pCi ¹²⁹ I/g-sludge)	0.17 µg/L (30 pCi/L)	solubility
Cr	897 µg Cr/g-sludge	<470 µg/L	solubility

Table 5.2 is a summary of the contaminant release model data for tank C-106 for the aged cement (CaCO₃-equilibrium) scenario. ¹²⁹I and Cr were not measured above their respective detection limits; therefore, the detection limit values were used for the release concentrations.

Table 5.2. Summary of Contaminant Release Model Data for Tank C-106, Aged Cement (CaCO₃-equilibrium) Scenario

Contaminant	Sludge Concentration	Release Concentration	Release Control
⁹⁹ Tc	1.2 µg ⁹⁹ Tc/g-sludge (20,000 pCi ⁹⁹ Tc/g-sludge)	0.39 µg/L (6,600 pCi/L)	solubility
²³⁸ U	310 µg ²³⁸ U/g-sludge	49 µg/L	solubility
¹²⁹ I	0.62 µg ¹²⁹ I/g-sludge (110 pCi ¹²⁹ I/g-sludge)	0.35 µg/L (61 pCi/L)	solubility
Cr	897 µg Cr/g-sludge	<283 µg/L	solubility

The data for the previous water leach release scenario from Deutsch et al. (2005a) are provided below in Table 5.3. Comparison of these data with the data in Table 5.1 and Table 5.2, indicate that for tank C-106 sludge, the presence of cement above the sludge does not have a large impact on contaminant mobility. The presence of cement has the biggest impact on ⁹⁹Tc. For the water leach scenario, the release concentration for ⁹⁹Tc is 0.21 µg/L, whereas the fresh cement concentration is 1.2 µg/L. For the aged cement scenario the ⁹⁹Tc release concentration is 0.39 µg/L; similar to that of the water release scenario. For ²³⁸U, both the fresh cement and aged cement scenarios have release concentrations which

are similar to that of the water release scenario. Comparisons for ^{129}I and Cr are not useful because the detection limits of these constituents in the cement leachates were higher than the water release scenario concentrations.

Table 5.3. Summary of Contaminant Release Model Data for C-106, Fresh Water Scenario

Contaminant	Sludge Concentration	Release Concentration	Release Control
^{99}Tc	1.2 $\mu\text{g } ^{99}\text{Tc/g-sludge}$ (20,000 pCi $^{99}\text{Tc/g-sludge}$)	0.21 $\mu\text{g/L}$ (3,600 pCi/L)	solubility
^{238}U	310 $\mu\text{g } ^{238}\text{U/g-sludge}$	46 $\mu\text{g/L}$	solubility
^{129}I	0.62 $\mu\text{g } ^{129}\text{I/g-sludge}$ (110 pCi $^{129}\text{I/g-sludge}$)	0.059 $\mu\text{g/L}$ (10 pCi/L)	solubility
Cr	897 $\mu\text{g Cr/g-sludge}$	19 $\mu\text{g/L}$	solubility

6.0 Conclusions

This report provides the results of laboratory tests on residual sludge from Hanford tank C-106 that has been contacted with solutions leaching from cementitious grout that may be used to fill the Hanford tanks. The impact of these leaching solutions on the long-term release of contaminants from the residual sludge has been evaluated. The major conclusions from this work are discussed in this section.

Contact of the residual tank sludge with the 0.01 M $\text{Ca}(\text{OH})_2$ solution that represents leachate from the grout produced the following mineral transformations:

- Rhodochrosite (MnCO_3) is converted to calcite (CaCO_3) and a poorly defined amorphous Mn oxyhydroxide phase.
- Lindbergite ($\text{MnC}_2\text{O}_4 \cdot 2\text{H}_2\text{O}$) is converted to whewellite ($\text{CaC}_2\text{O}_4 \cdot \text{H}_2\text{O}$), and a poorly defined amorphous Mn oxyhydroxide phase.
- Dawsonite ($\text{NaAl}(\text{OH})_2\text{CO}_3$) is converted to calcite and dissolved Na and Al.

The primary reasons for these transformations are the high Ca concentration of the leachate and its high pH (~12).

The effect of the cementitious leachate on the mobility of components in the sludge can be summarized as follows:

- ^{99}Tc is more leachable in the $\text{Ca}(\text{OH})_2$ leachant than in DDI water by a factor of 6; however, the amount of the total ^{99}Tc in the sludge that is leachable increases to only ~10%.
- ^{238}U is less leachable in the $\text{Ca}(\text{OH})_2$ leachant than in DDI water for the sequential contact leaching tests. Approximately 4% was water leachable through the six contact stages while <1% was leached during six stages with the $\text{Ca}(\text{OH})_2$ leachant.
- ^{129}I was not detected in any of the leaching tests showing its generally recalcitrant nature in this sludge material.
- ^{90}Sr is more leachable in the $\text{Ca}(\text{OH})_2$ leachant than in DDI water. This is likely a result of cation exchange of Ca for Sr on the solid phase ion exchange sites.
- ^{137}Cs is much more leachable in the sequential contact $\text{Ca}(\text{OH})_2$ leachant tests than in DDI water tests. The increase in leachability for some stages of these tests is a factor of 100. This may also be a result of cation exchange of Ca for Cs.
- Cr and Fe were also not detected in any of the leaching tests designed to simulate the impact of a cementitious cover on the sludge.

- Al is more leachable by a factor of about 10 for the cementitious leachants compared to DDI water leaches. This is due to the amphoteric behaviour of Al solution species and the high pH of these cementitious leach tests.
- Mn is less leachable in the cementitious leachants probably because the amorphous Mn oxyhydroxide phase listed above as a conversion product of rhodochrosite and lindbergite is less soluble in the high pH (~12) cementitious environment than its predecessors in the lower pH (~7) of the DDI water leachant.
- Oxalate is less leachable in the cementitious leachants because the high concentration of Ca (0.01 M) in these leachants depresses the solubility of whewellite ($\text{CaC}_2\text{O}_4 \cdot \text{H}_2\text{O}$).

A summary of the release models for the primary contaminants of concern is provided in Tables 5.1 through 5.3.

7.0 References

- 10 CFR 830.120. "Quality Assurance." *Code of Federal Regulations*, U.S. Department of Energy.
- ASME. 1989. *Quality Assurance Program Requirements for Nuclear Facilities/with Addenda*. NQA-1-1989. American Society of Mechanical Engineers, New York.
- ASTM. 1998. *D2216-98 Standard Test Method for Laboratory Determination of Water (Moisture) Content of Soil and Rock by Mass*. American Society for Testing and Materials, West Conshohocken, Pennsylvania.
- ASTM. 1999. *D3987-85 Standard Test Method for Shake Extraction of Solid Waste with Water*. American Society for Testing and Materials, West Conshohocken, Pennsylvania.
- Bechtold DB, GA Cooke, DL Herting, JC Person, RS Viswanath, and RW Warrant. 2003. *Laboratory Testing of Oxalic Acid Dissolution of Tank 241-C-106 Sludge*. RPP-17158, Rev. 0, Fluor Hanford, Inc. Richland, Washington.
- Clesceri LS, AE Greenberg, and AD Eaton. 1998. *Standard Methods for the Examination of Water and Wastewater*, 20th Edition. American Public Health Association, American Water Works Association, and Water Environment Federation, Washington, D.C.
- Conner JM. 1996. *Tank Characterization Report for Single-Shell Tank 241-C-204*. WHC-SD-WM-ER-479 Rev. 0, Westinghouse Hanford Company, Richland, Washington.
- Deutsch WJ, KM Krupka, MJ Lindberg, KJ Cantrell, CF Brown, and HT Schaeff. 2005a. *Hanford Tank C-106: Residual Waste Contaminant Release Model and Supporting Data*. PNNL-15187, Pacific Northwest National Laboratory, Richland, Washington.
- Deutsch WJ, KM Krupka, KJ Cantrell, CF Brown, MJ Lindberg, HT Schaeff, SM Heald, and BW Arey. 2005b. *Advances in Geochemical Testing of Key Contaminants in Residual Hanford Tank Waste*. PNNL-15372, Pacific Northwest National Laboratory, Richland, Washington.
- DOE. 1998. *Hanford Analytical Services Quality Assurance Requirements Documents*. HASQARD, DOE/RL-96-68, Volumes 1, 2, 3, and 4, U.S. Department of Energy, Richland, Washington.
- DOE Order 414.1A. *Management Assessment and Independent Assessment Guide*. U.S. Department of Energy, Washington, D.C. Available online at <http://www.directives.doe.gov/pdfs/doe/doetext/neword/414/g4141-1a.html>
- EPA. 1994a. "Method 6020. Inductively Coupled Plasma-Mass Spectrometry." In *Test Methods for Evaluating Solid Wastes: Physical/Chemical Methods*, EPA SW-846, Third Ed., Vol. I, Section A, Chapter 3 (Inorganic Analytes), pp. 6020-1 to 6020-18, U.S. Environmental Protection Agency, Office of Solid Waste and Emergency Response, Washington, D.C. Available at: <http://www.epa.gov/epaoswer/hazwaste/test/pdfs/6020.pdf>

EPA. 1994b. "Method 9056. Determination of Inorganic Anions by Ion Chromatography." In *Test Methods for Evaluating Solid Wastes: Physical/Chemical Methods*, EPA SW-846, Third Ed., Vol. I, Section C, Chapter 5 (Miscellaneous Test Methods), pp. 9056-1 to 9056-16, U.S. Environmental Protection Agency, Office of Solid Waste and Emergency Response, Washington, D.C. Available at: <http://www.epa.gov/epaoswer/hazwaste/test/pdfs/9056.pdf>

EPA. 1995. "Method 9040B. pH Electrometric Measurement." In *Test Methods for Evaluating Solid Wastes: Physical/Chemical Methods*, EPA SW-846, Third Ed., Vol. I, Section C, Chapter 8 (Methods for Determining Characteristics), pp. 9040B-1 to 9040B-5, U.S. Environmental Protection Agency, Office of Solid Waste and Emergency Response, Washington, D.C. Available at: <http://www.epa.gov/epaoswer/hazwaste/test/pdfs/9040b.pdf>

EPA. 1996. "Method 6010B. Inductively Coupled Plasma-Atomic Emission Spectrometry." In *Test Methods for Evaluating Solid Wastes: Physical/Chemical Methods*, EPA SW-846, Third Ed., Vol. I, Section A, Chapter 3 (Inorganic Analytes), pp. 6010B-1 to 6010B-25, U.S. Environmental Protection Agency, Office of Solid Waste and Emergency Response, Washington, D.C. Available at: <http://www.epa.gov/epaoswer/hazwaste/test/pdfs/6010b.pdf>

Krupka KM, WJ Deutsch, MJ Lindberg, KJ Cantrell, NJ Hess, HT Schaef, and BW Arey. 2004. *Hanford Tanks 241-AY-102 and 241-BX-101: Sludge Composition and Contaminant Release Data*. PNNL-14614, Pacific Northwest National Laboratory, Richland, Washington.

Strachan DM, HT Schaef, MJ Schweiger, KL Simmons, LJ Woodcock, and MK Krouse. 2003. "A Versatile and Inexpensive XRD Specimen Holder for Highly Radioactive or Hazardous Specimens." *Powder Diffraction* 18(1):23-28.

Appendix A

X-Ray Diffraction Patterns for Ca(OH)_2 - and $\text{Ca(OH)}_2/\text{CaCO}_3$ -Leached Tank C-106 Residual Waste

Appendix A

X-Ray Diffraction Patterns for Ca(OH)₂- and Ca(OH)₂/CaCO₃-Leached Tank C-106 Residual Waste

This appendix presents the as-measured (before background subtraction) x-ray powder diffraction (XRD) patterns for 1-month and stage 6 sequential Ca(OH)₂- and Ca(OH)₂/CaCO₃-leached residual waste from tank 241-C-106 (C-106). As noted in Section 3.3, trace quantities of reference-material corundum (α -Al₂O₃, alumina) [National Institute of Standards and Technology Standard Reference Material (NIST SRM) 676] powder were added to each XRD mount to provide an internal 2θ standard for each XRD pattern. The instrumentation and procedures used for measuring, subtracting background, and interpreting the XRD patterns for these materials are described in Section 3.3 of the main report.

The vertical axis in each of the following patterns represents the intensity in counts per second (cps) of the XRD peaks. The horizontal axis is in terms of degrees 2θ based on Cu_{K α} radiation ($\lambda=1.5406 \text{ \AA}$), and is related to d spacing according to the Bragg law (Cullity 1956).^(a) The as-measured XRD pattern for the unleached C-106 residual waste and the relevant schematic database (PDF) patterns are shown along with the as-measured XRD patterns for the 1-month and stage 6 sequential Ca(OH)₂-leached samples in Figure A.1, and with the patterns for the 1-month and stage 6 sequential Ca(OH)₂/CaCO₃-leached samples in Figure A.2. For comparison to the background signal in the as-measured XRD patterns included in this appendix, Figure A.3 shows the XRD pattern for collodion film measured in the absence of any sludge material and reported by Krupka et al. (2004).^(b) Figures A.4 through A.8 show, respectively, the individual as-measured XRD patterns for unleached, 1-month Ca(OH)₂-leached, stage 6 sequential Ca(OH)₂-leached, 1-month Ca(OH)₂/CaCO₃-leached, and stage 6 sequential Ca(OH)₂/CaCO₃-leached residual waste from tank C-106.

(a) Cullity BD. 1967. *Elements of X-Ray Diffraction*. Addison-Wesley Publishing Company, Inc., Reading, Massachusetts.

(b) Krupka KM, WJ Deutsch, MJ Lindberg, KJ Cantrell, NJ Hess, HT Schaef, and BW Arey. 2004. *Hanford Tanks 241-AY-102 and 241-BX-101: Sludge Composition and Contaminant Release Data*. PNNL-14614, Pacific Northwest National Laboratory, Richland, Washington.

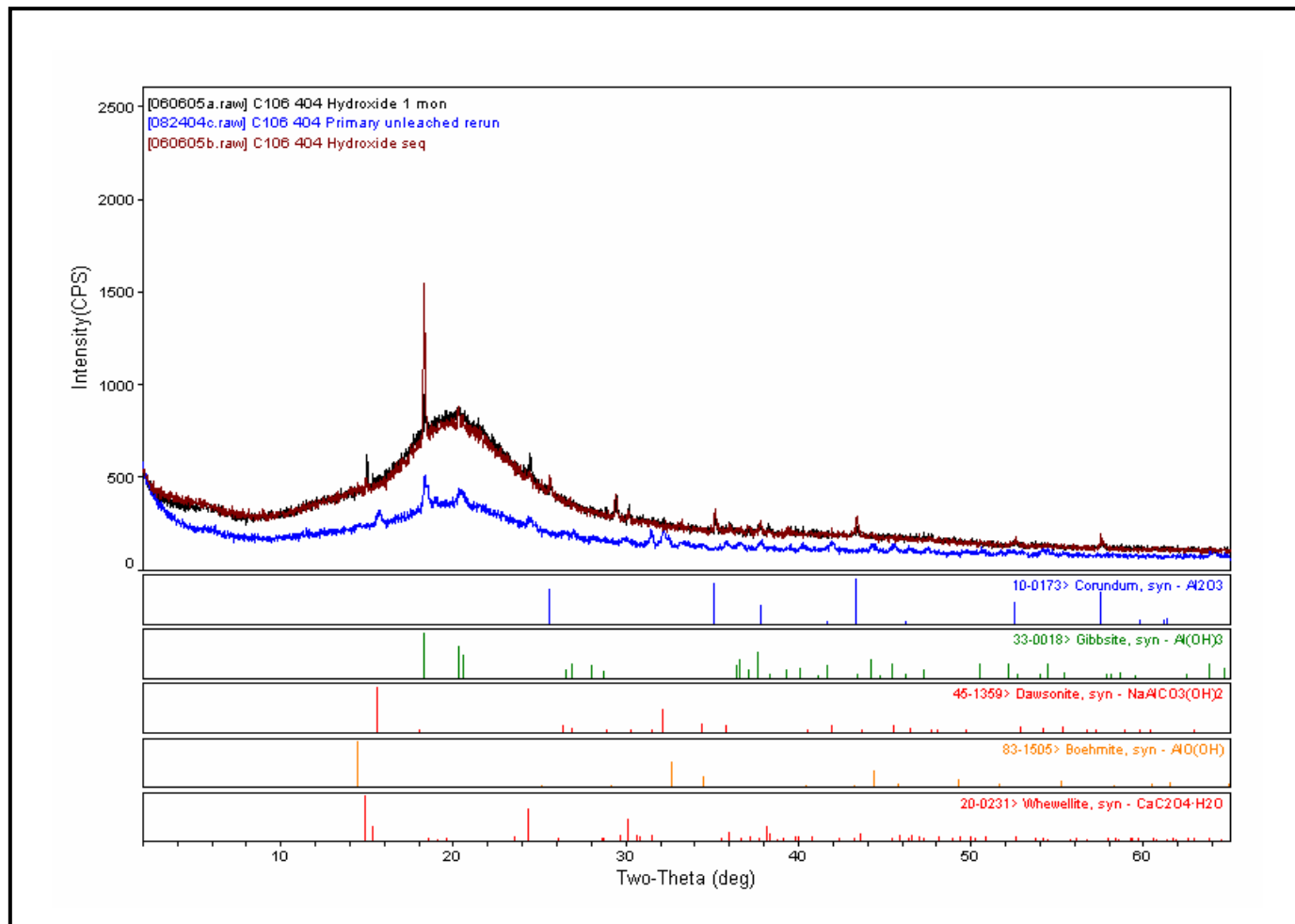


Figure A.1. As-Measured XRD Pattern (without background subtraction) for Unleached C-106 Residual Waste (blue trace) and Relevant Schematic Database (PDF) Patterns Compared to As-Measured XRD Patterns for the 1-Month (black trace) and Stage 6 Sequential Ca(OH)₂-Leached (maroon trace) C-106 Residual Waste

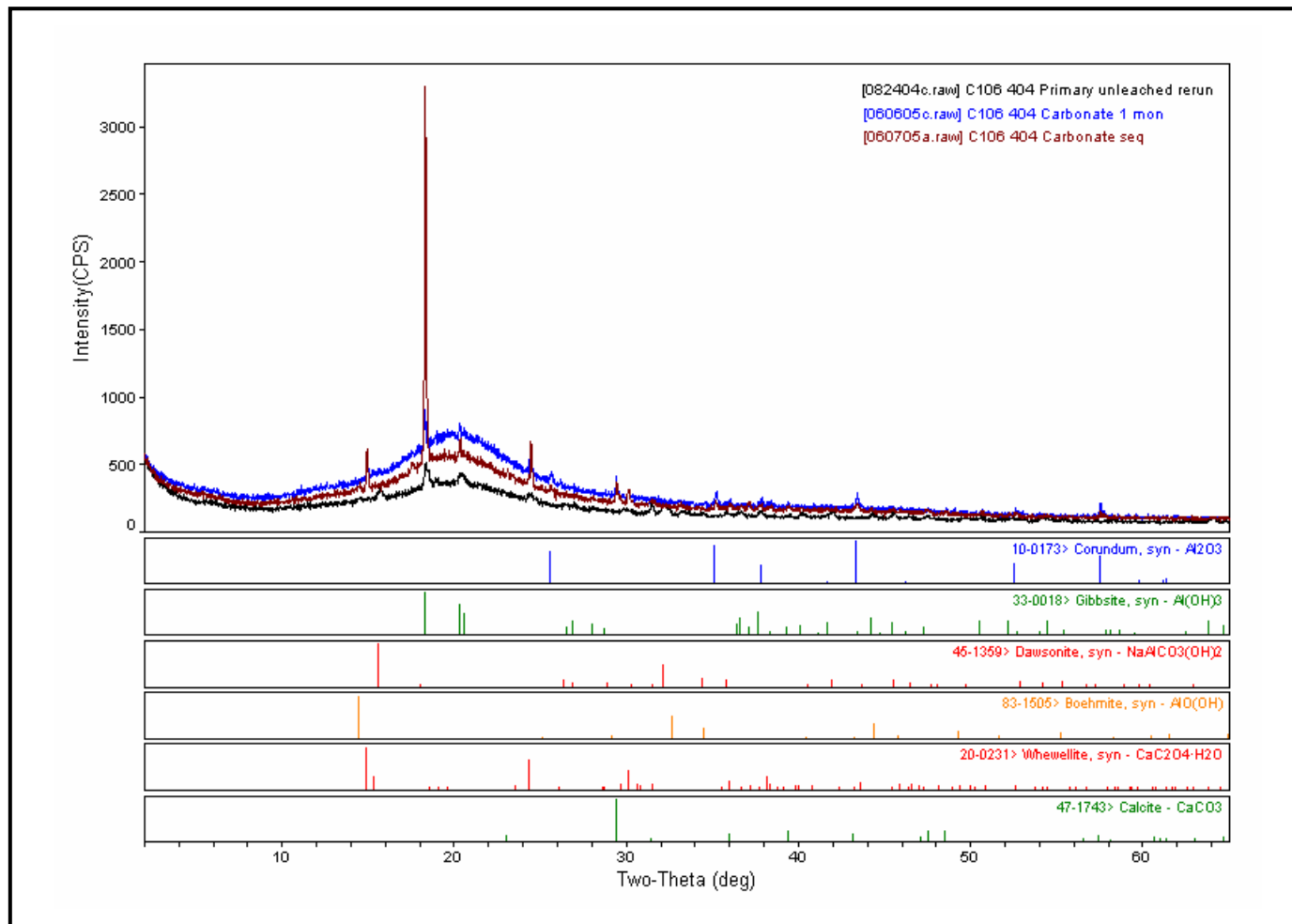


Figure A.2. As-Measured XRD Pattern (without background subtraction) for Unleached C-106 Residual Waste (black trace) and Relevant Schematic Database (PDF) Patterns Compared to As-Measured XRD Patterns for the 1-Month (blue trace) and Stage 6 Sequential $\text{Ca}(\text{OH})_2/\text{CaCO}_3$ -Leached (maroon trace) C-106 Residual Waste

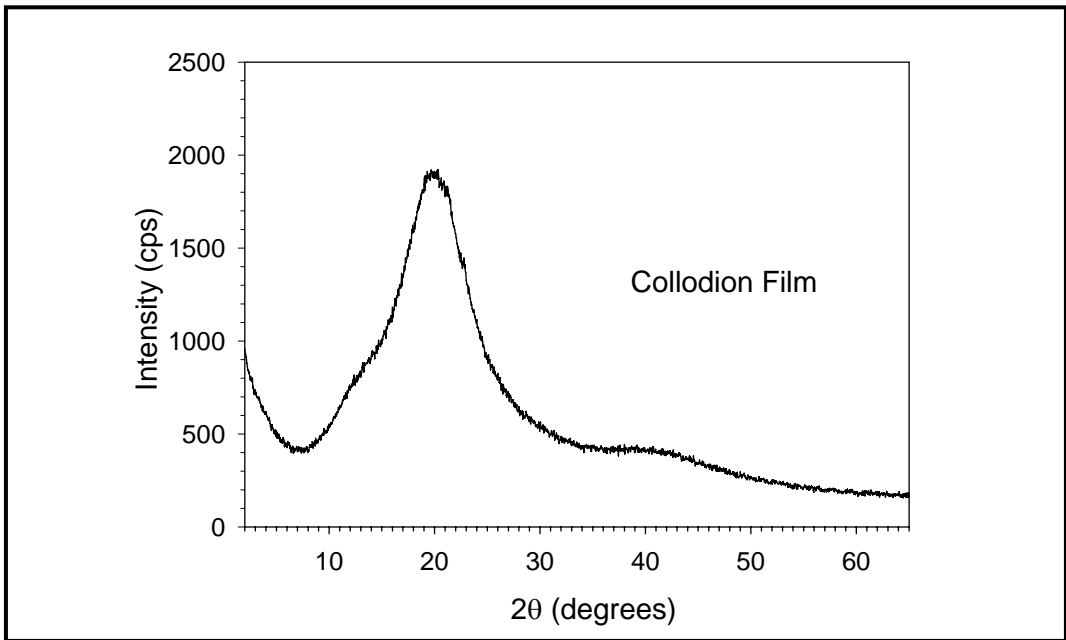


Figure A.3. XRD Pattern for Collodion-Solution Film (from Krupka et al. 2004)

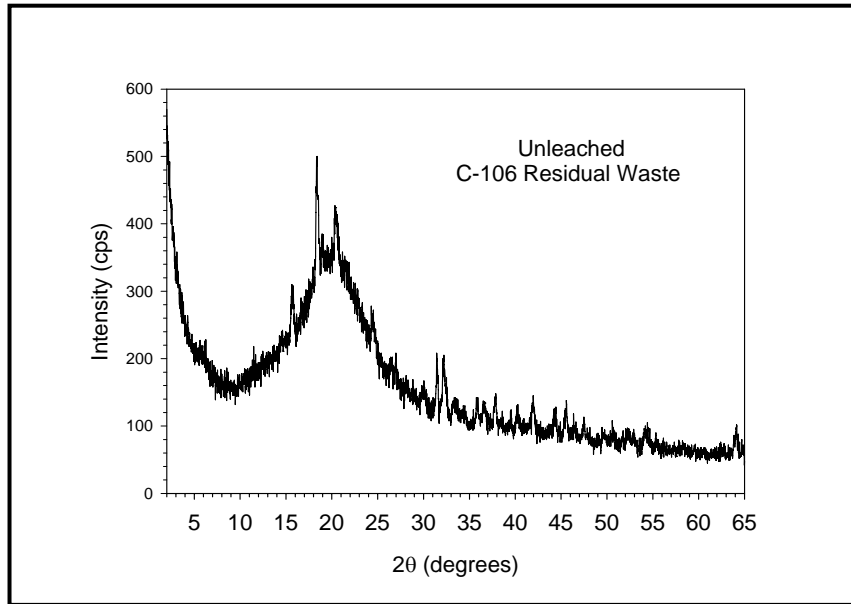


Figure A.4. As-Measured XRD Pattern (without background subtraction) for Unleached C-106 Residual Waste

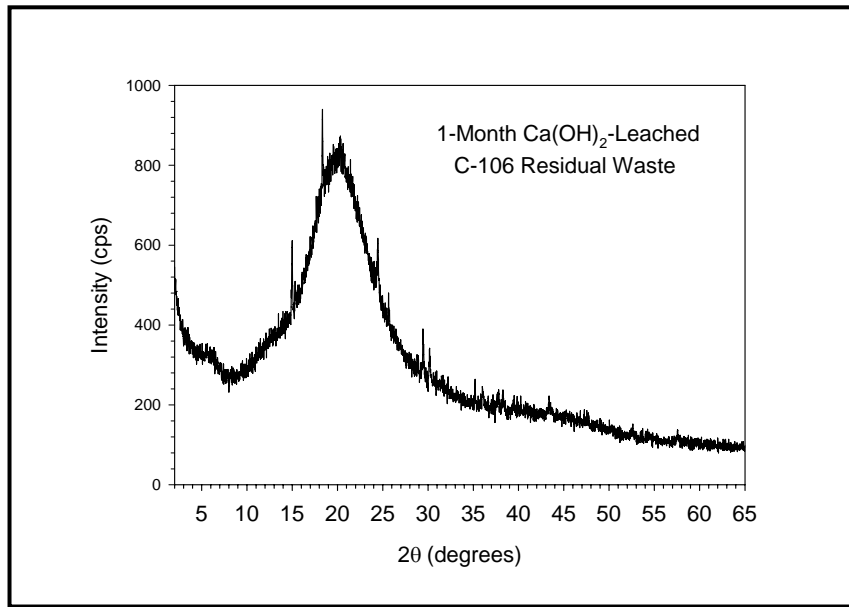


Figure A.5. As-Measured XRD Pattern (without background subtraction) for 1-Month Ca(OH)_2 -Leached Residual Waste from Tank C-106

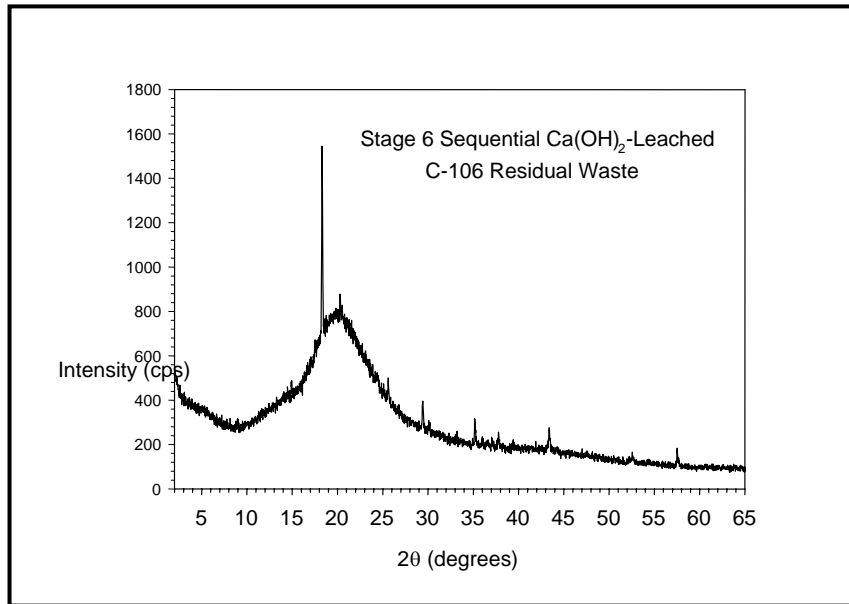


Figure A.6. As-Measured XRD Pattern (without background subtraction) for Stage 6 Sequential Ca(OH)_2 -Leached Residual Waste from Tank C-106

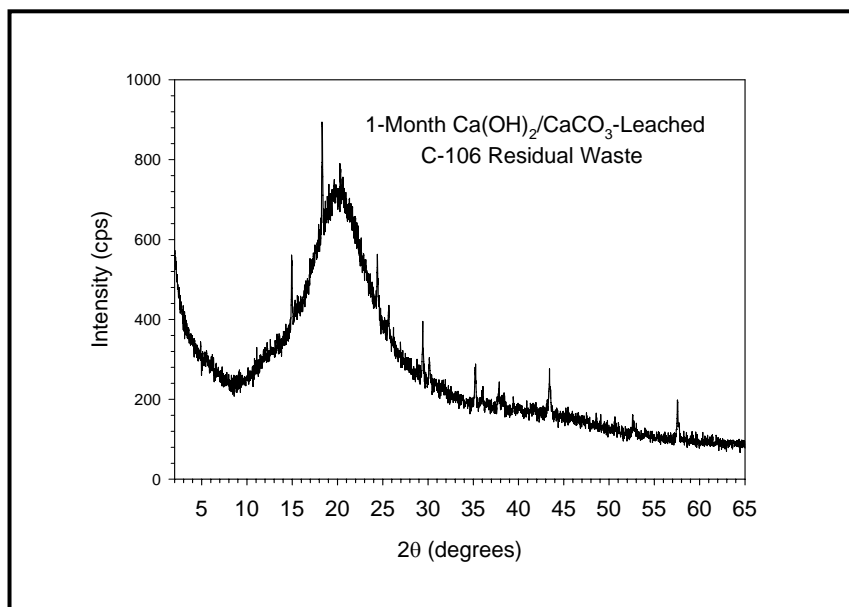


Figure A.7. As-Measured XRD Pattern (without background subtraction) for 1-Month $\text{Ca(OH)}_2/\text{CaCO}_3$ -Leached Residual Waste from Tank C-106

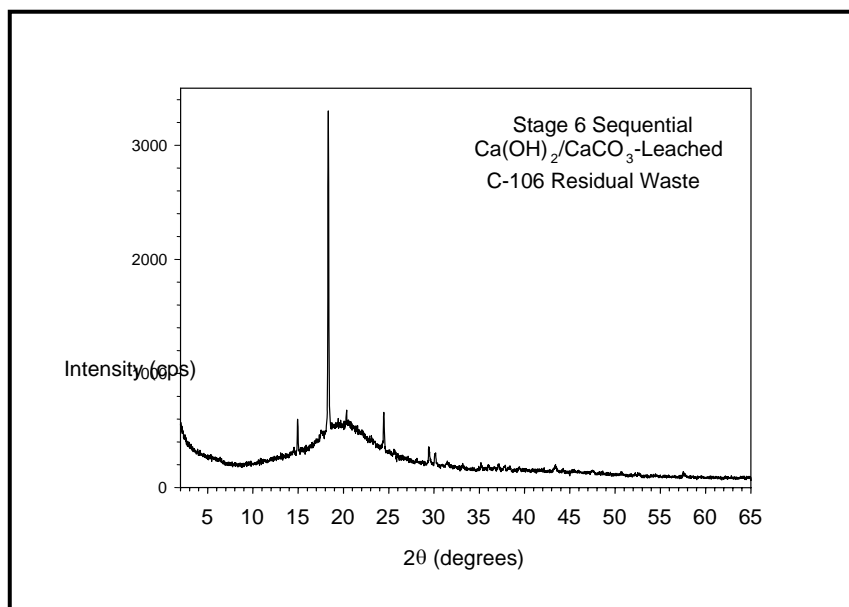


Figure A.8. As-Measured XRD Pattern (without background subtraction) for Stage 6 Sequential $\text{Ca(OH)}_2/\text{CaCO}_3$ -Leached Residual Waste from Tank C-106

Appendix B

SEM Micrographs and EDS Results for 1-Month Ca(OH)₂-Leached Tank C-106 Residual Waste

Appendix B

SEM Micrographs and EDS Results for 1-Month Ca(OH)₂ Leached Tank C-106 Residual Waste

This appendix includes the scanning electron microscope (SEM) micrographs and energy-dispersive x-ray spectrometry (EDS) spectra for samples of 1-month Ca(OH)₂-leached residual waste from tank C-106. The operating conditions for the SEM and procedures used for mounting the SEM samples are described in Section 3.4 of the main report.

The identification number for the digital micrograph image file, descriptor for the type of sample, and a size scale bar are given, respectively, at the bottom left, center, and right of each SEM micrograph in this appendix. Micrographs labeled by “BSE” to the immediate right of the digital image file number indicate that the micrograph was collected with backscattered electrons. Sample areas or particles identified by a letter, arrow, and/or outlined by white or black dotted-line squares in a micrograph designate sample material that was imaged at higher magnification and is typically shown in figure(s) that immediately follow in the series for that sample. The SEM micrographs for this leached material are shown in Figures B.1 through B.19. The EDS spectra for this material are given in Figures B.20 through B.30.

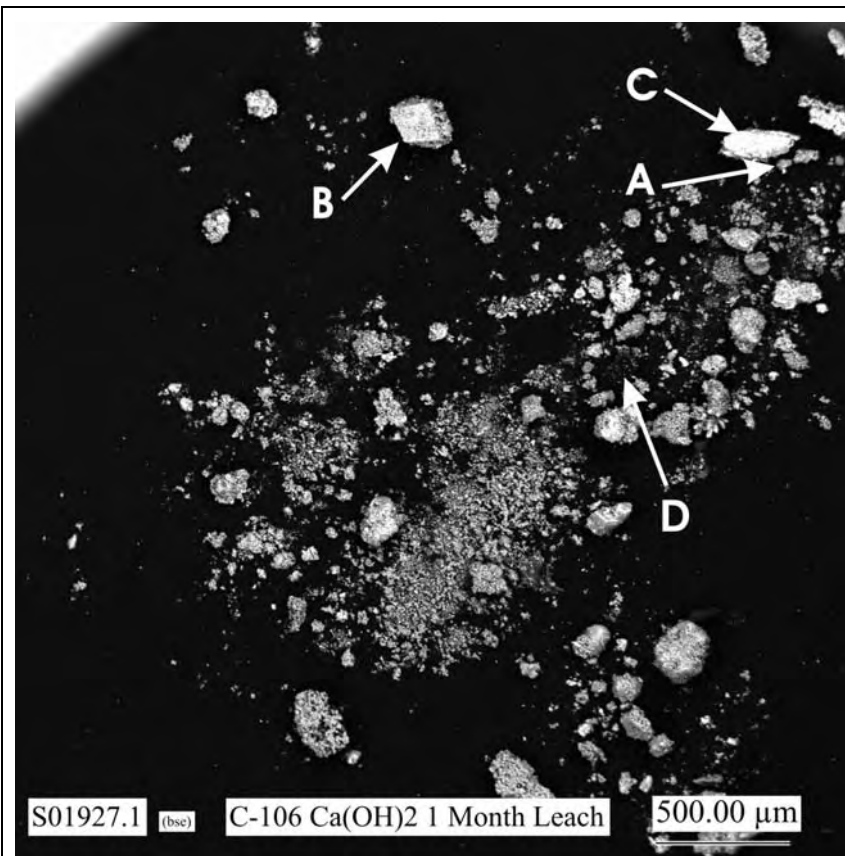


Figure B.1. Low Magnification SEM Micrograph Showing General Morphologies of Particles in the SEM Sample of the 1-Month $\text{Ca}(\text{OH})_2$ -Leached Residual Waste from Tank C-106

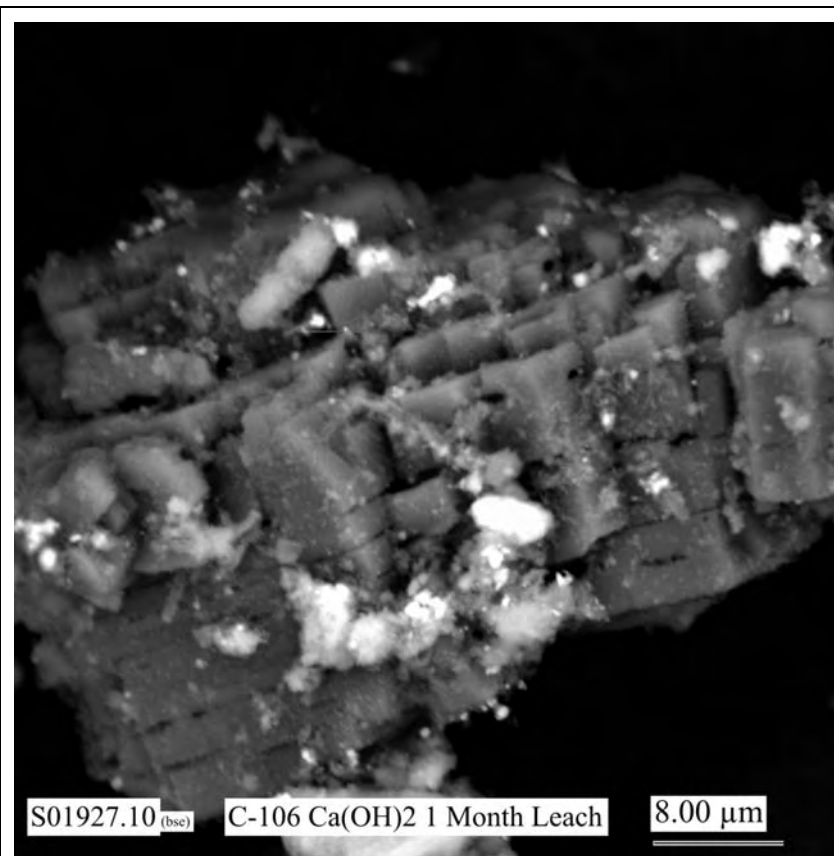


Figure B.2. Micrograph Showing at Higher Magnification the Particle Labeled A in Figure B.1 and the Area Indicated by the White Dashed-line Square Labeled A in Figure B.5 (areas where EDS analyses were made are shown in Figure B.23)

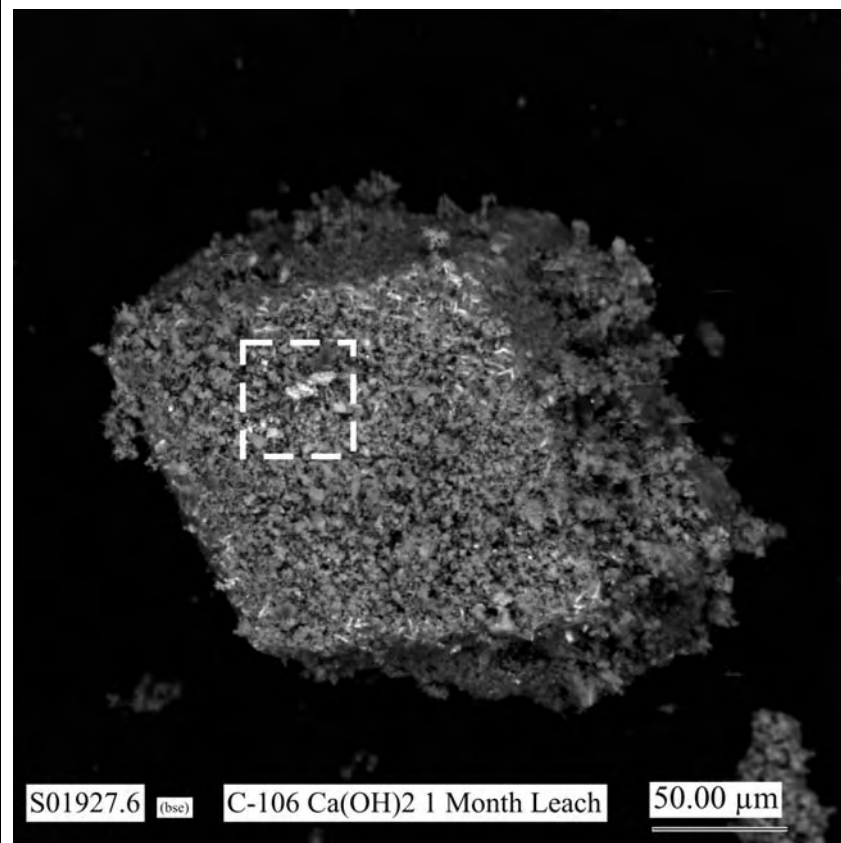


Figure B.3. Micrograph Showing at Higher Magnification the Particle Labeled B in Figure B.1.

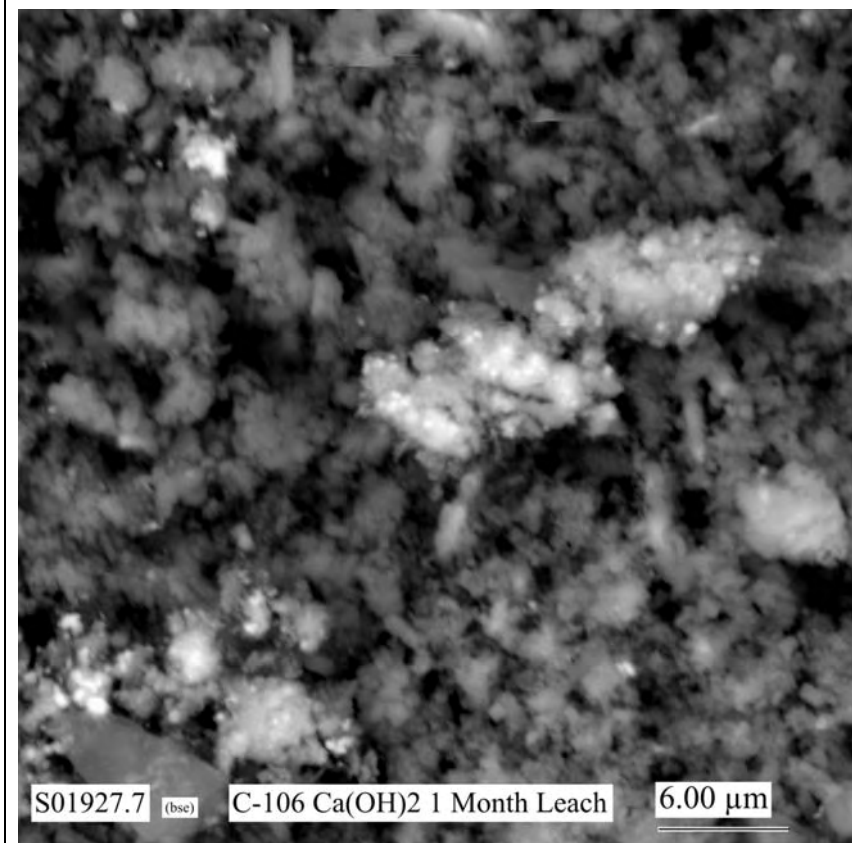


Figure B.4. Micrograph Showing at Higher Magnification the Area Indicated by the White Dashed-Line Square in Figure B.3 (areas where EDS analyses were made are shown in Figure B.22)

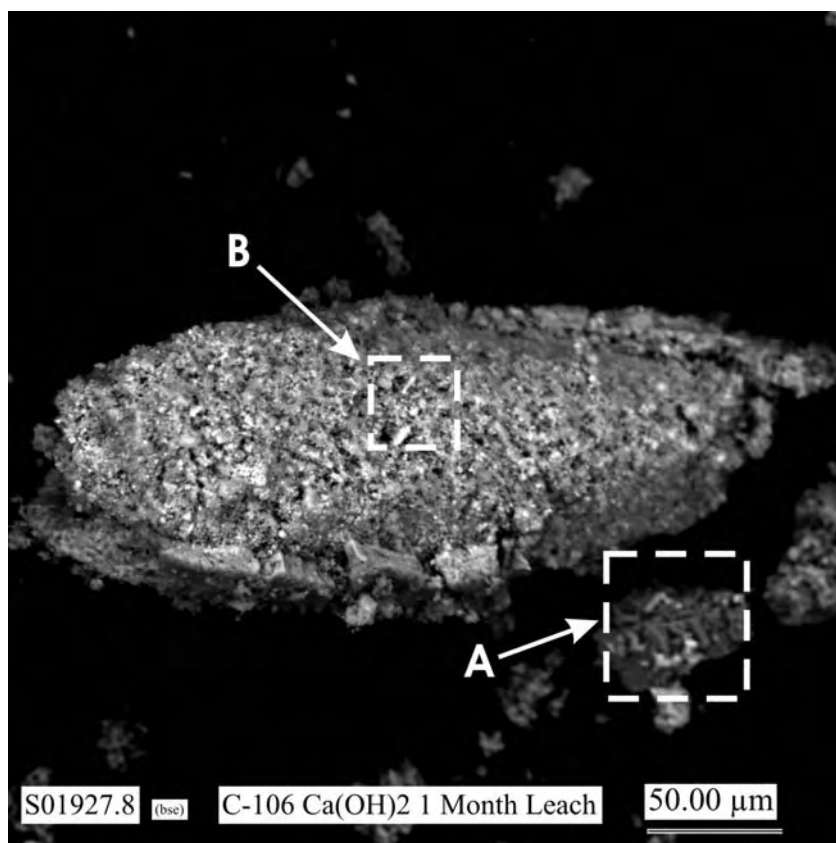


Figure B.5. Micrograph Showing at Higher Magnification the Particle Labeled C in Figure B.1

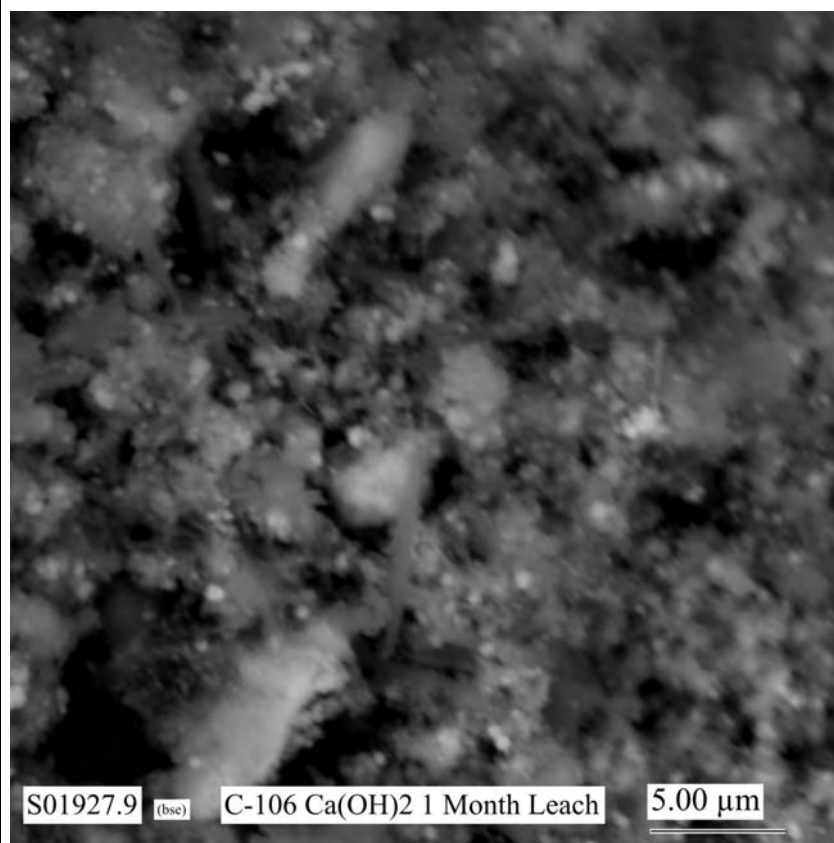


Figure B.6. Micrograph Showing at Higher Magnification the Area Indicated by the White Dashed-Line Square Labeled B in Figure B.5 (areas where EDS analyses were made are shown in Figure B.22)

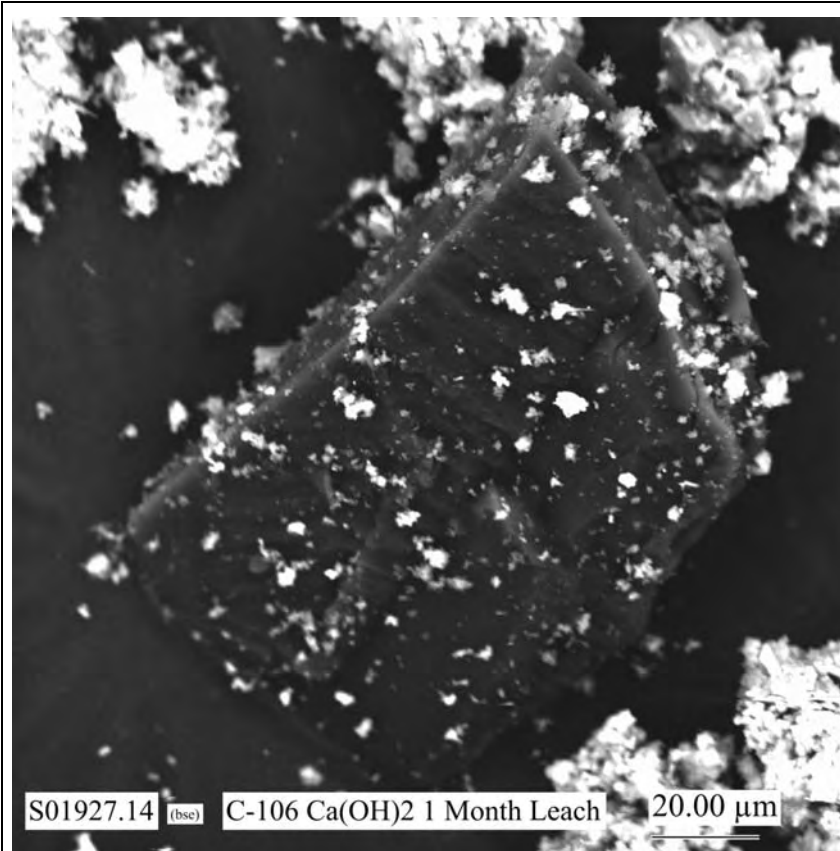


Figure B.7. Micrograph Showing at Higher Magnification the Dark Particle (hardly visible) Labeled D in Figure B.1 (areas where EDS analyses were made are shown in Figure B.27.)

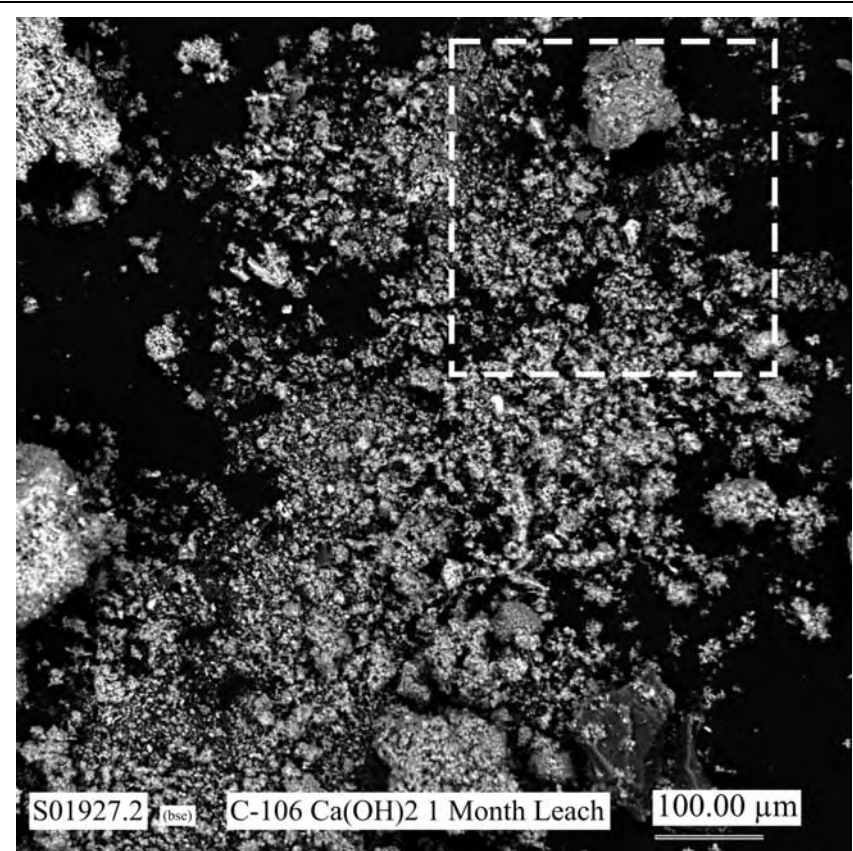


Figure B.8. Low Magnification SEM Micrograph Showing General Morphologies of Particles in the SEM Sample of the 1-Month Ca(OH)_2 -Leached Residual Waste from Tank C-106

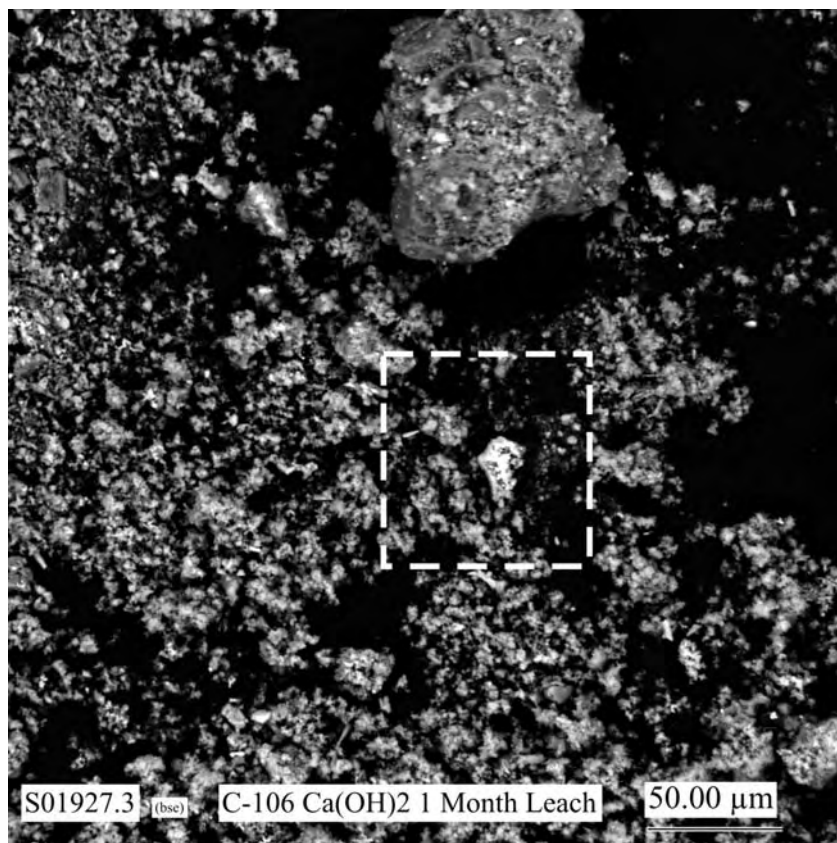


Figure B.9. Micrograph Showing at Higher Magnification the Area Indicated by the White Dashed-Line Square in Figure B.8

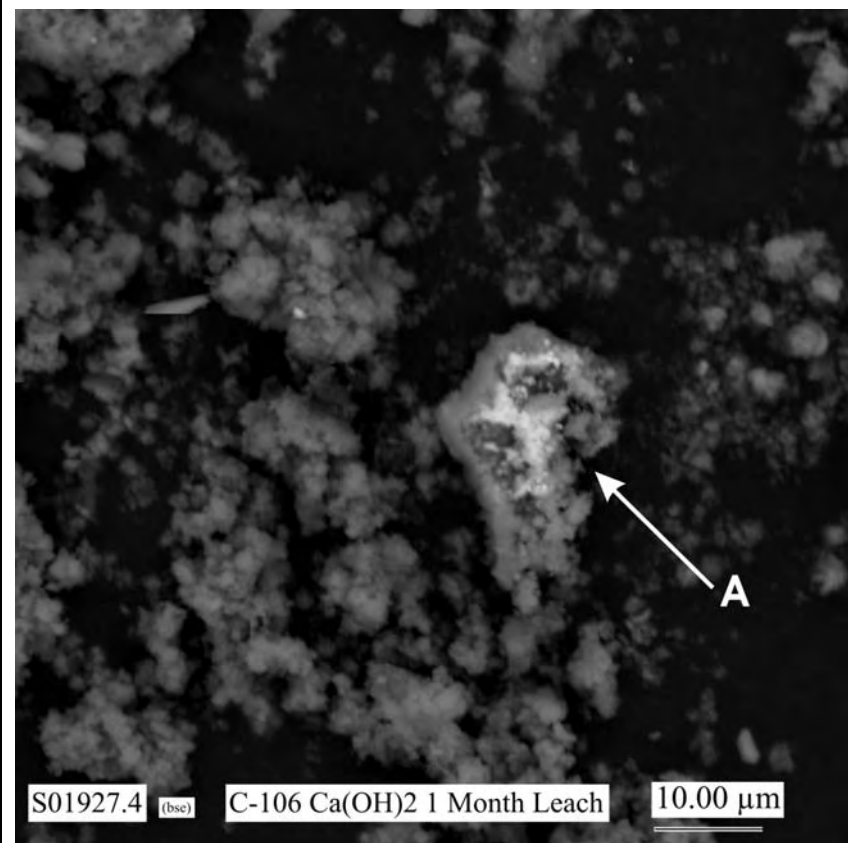


Figure B.10. Micrograph Showing at Higher Magnification the Area Indicated by the White Dashed-Line Square in Figure B.9 (areas where EDS analyses were made are shown in Figure B.20)

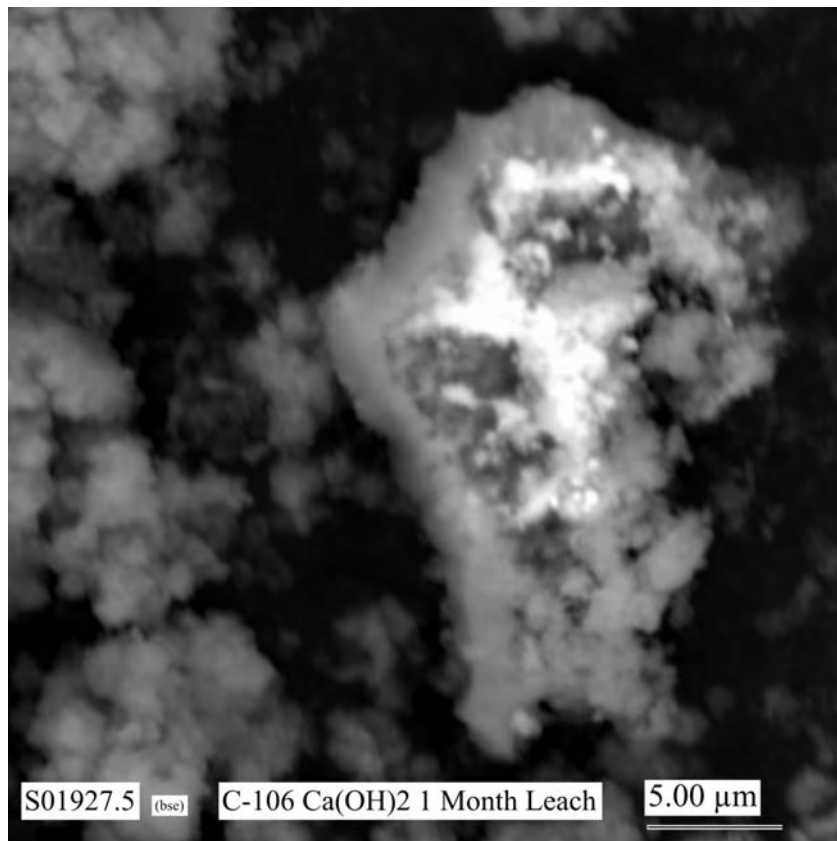


Figure B.11. Micrograph Showing at Higher Magnification the Particle Labeled A in Figure B.8

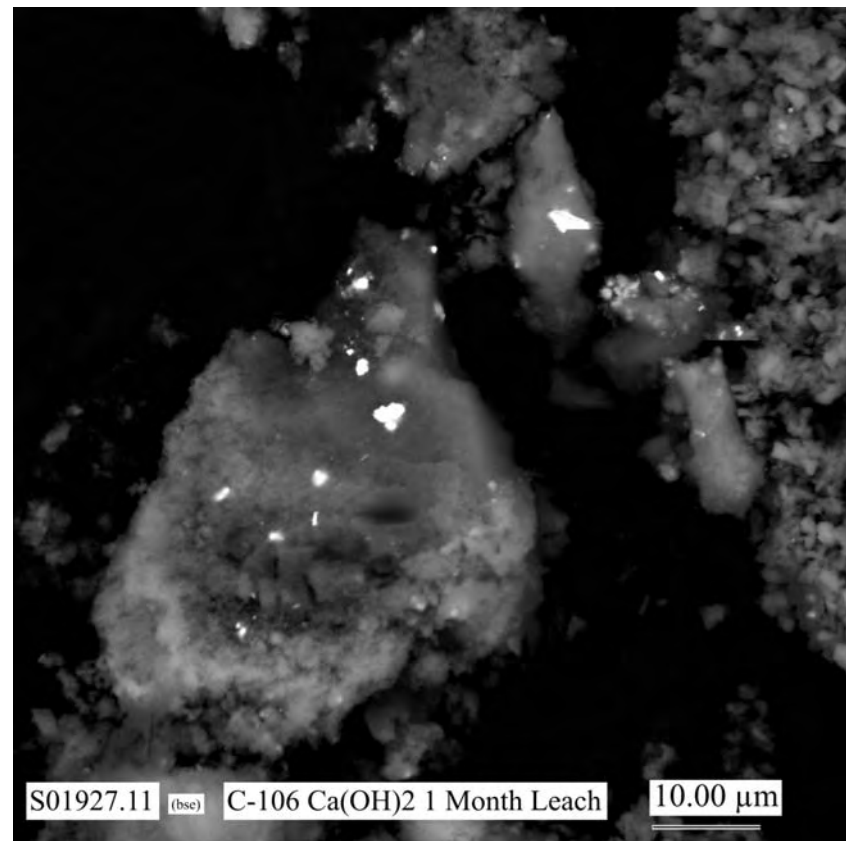


Figure B.12. Micrograph Showing Morphologies of Typical Particles in the SEM Sample of the 1-Month Ca(OH)_2 -Leached Residual Waste from Tank C-106 (areas where EDS analyses were made are shown in Figures B.22 and B.23)

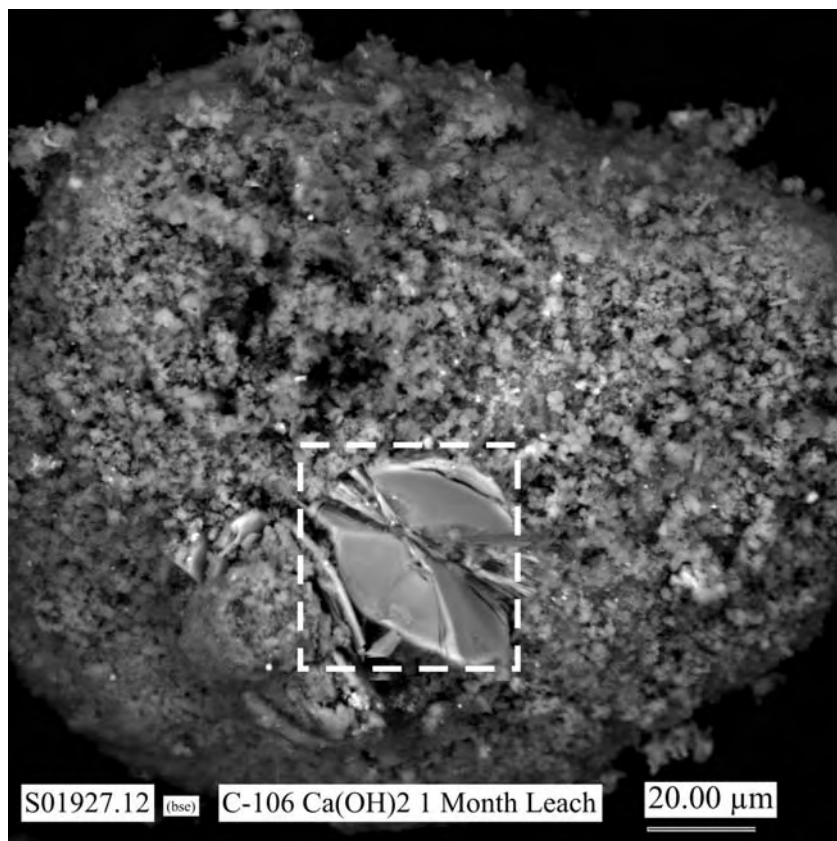


Figure B.13. Micrograph Showing Morphologies of Particles in the SEM of 1-Month Ca(OH)_2 -Leached Residual Waste from Tank C-106

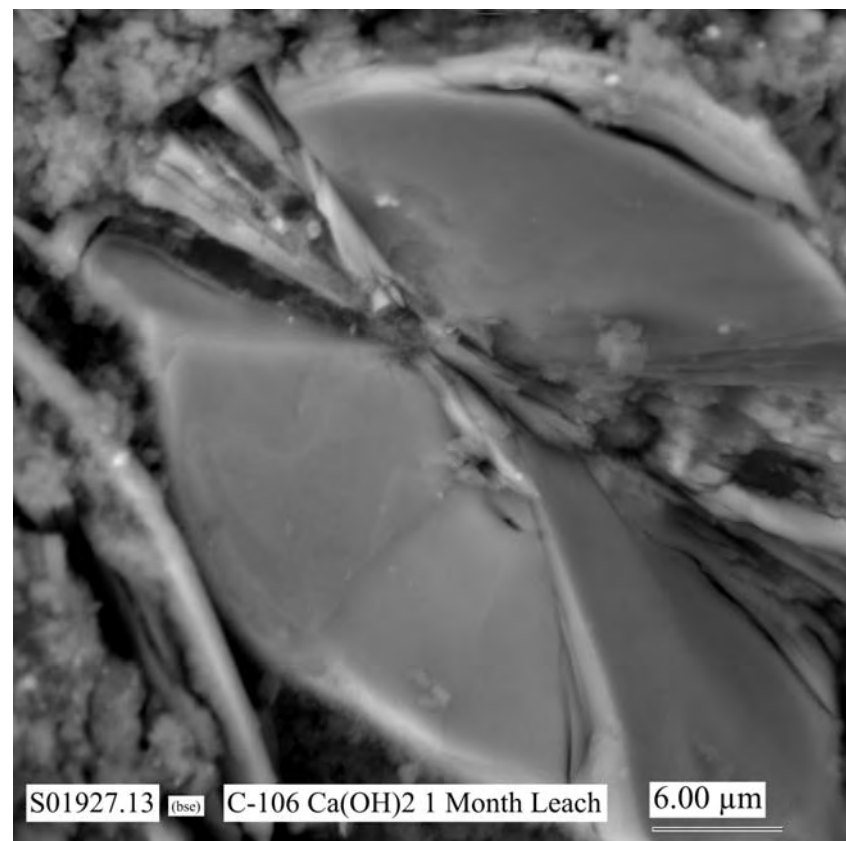


Figure B.14. Micrograph Showing at Higher Magnification the Area Indicated by the White Dashed-Line Square in Figure B.11 (areas where EDS analyses were made are shown in Figure B.24)

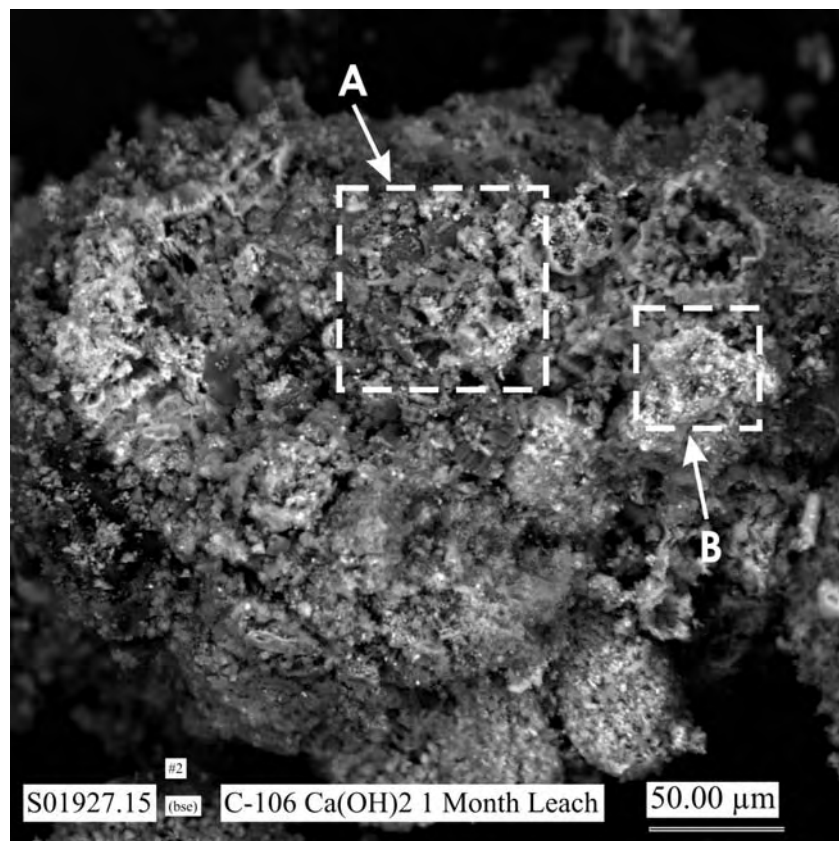


Figure B.15. Micrograph Showing Morphologies of Typical Particles in the SEM Sample of 1-Month $\text{Ca}(\text{OH})_2$ -Leached Residual Waste from Tank C-106

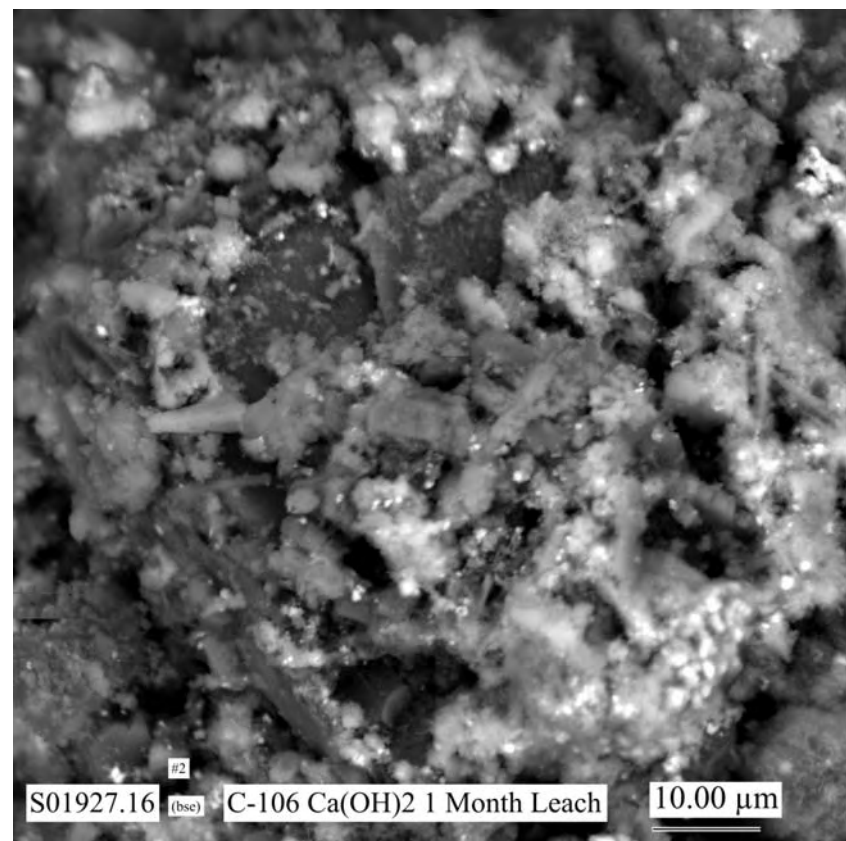


Figure B.16. Micrograph Showing at Higher Magnification the Area Indicated by the White Dashed-Line Square Labeled A in Figure B.13 (areas where EDS analyses were made are shown in Figure B.26)

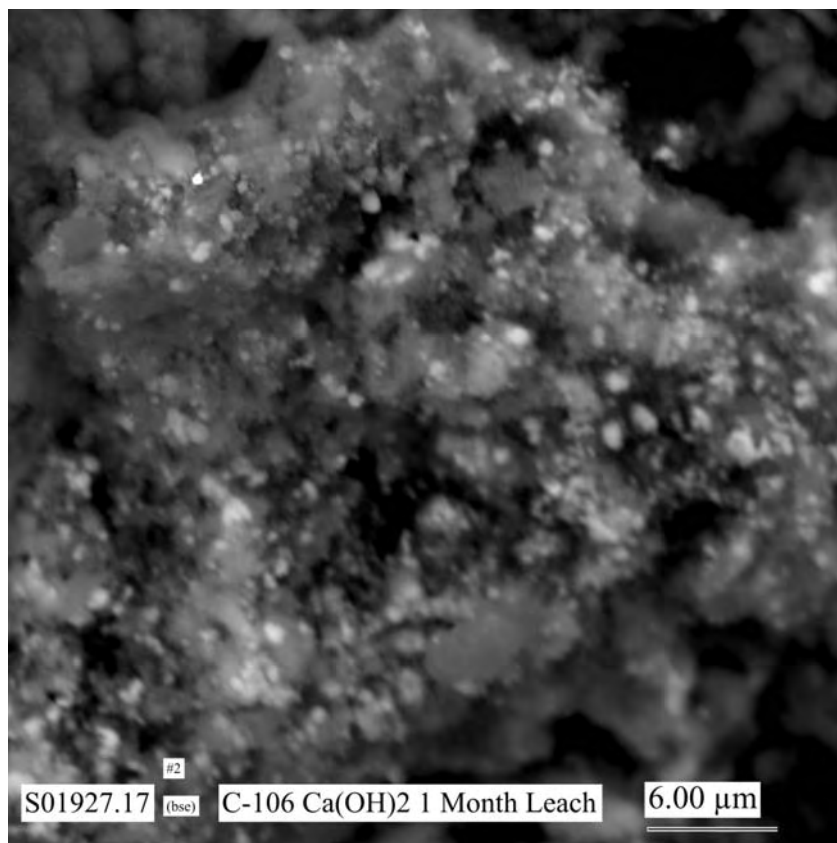


Figure B.17. Micrograph Showing at Higher Magnification the Area Indicated by the White Dashed-Line Square Labeled B in Figure B.13 (areas where EDS analyses were made are shown in Figure B.27)

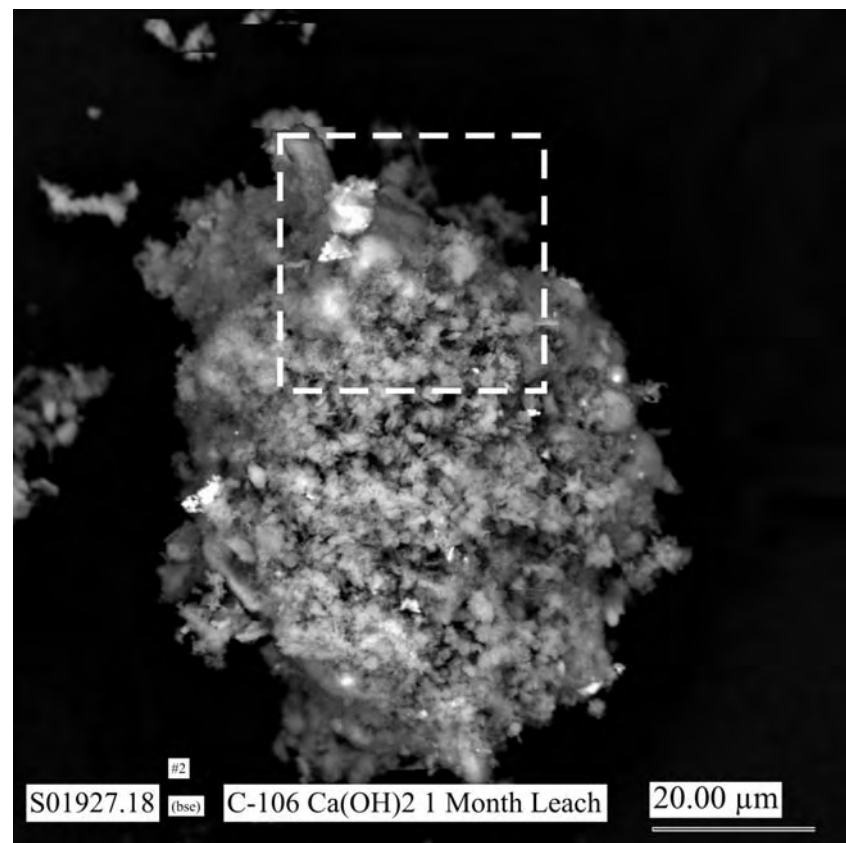


Figure B.18. Micrograph Showing Morphologies of Typical Particles in the SEM Sample of 1-Month Ca(OH)_2 -Leached Residual Waste from Tank C-106

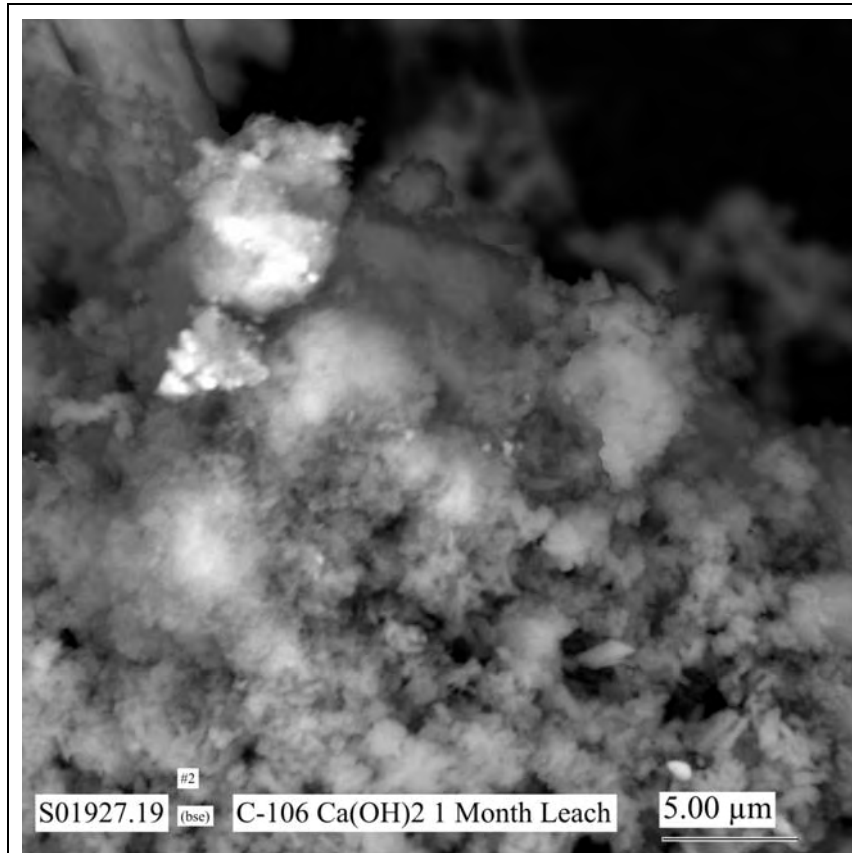


Figure B.19. Micrograph Showing at Higher Magnification the Area Indicated by the White Dashed-Line Square in Figure B.16 (areas where EDS analyses were made are shown in Figure B.21)

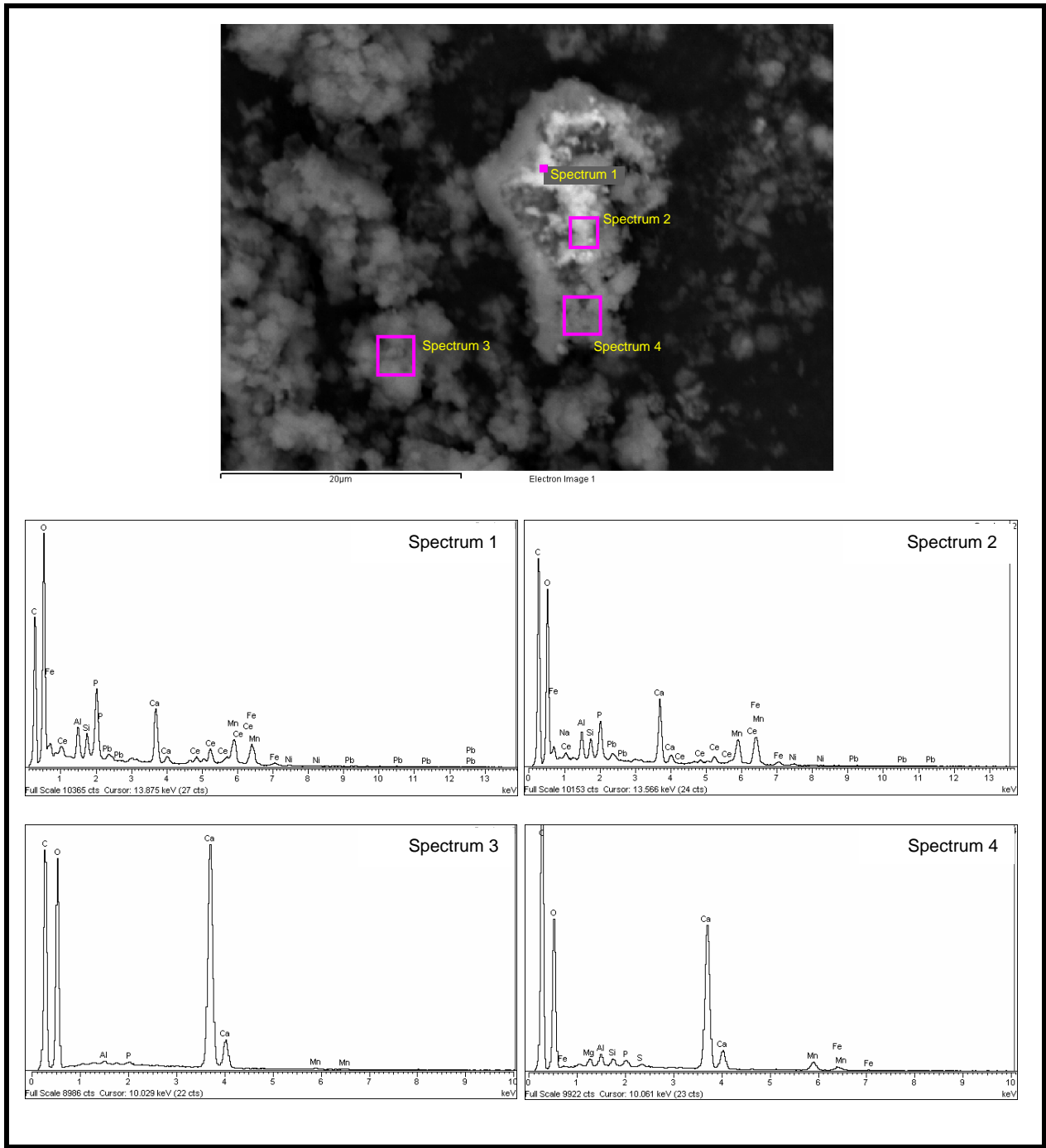


Figure B.20. EDS Spectra for Numbered Areas Marked in Pink in SEM Micrograph Shown at Top of Figure

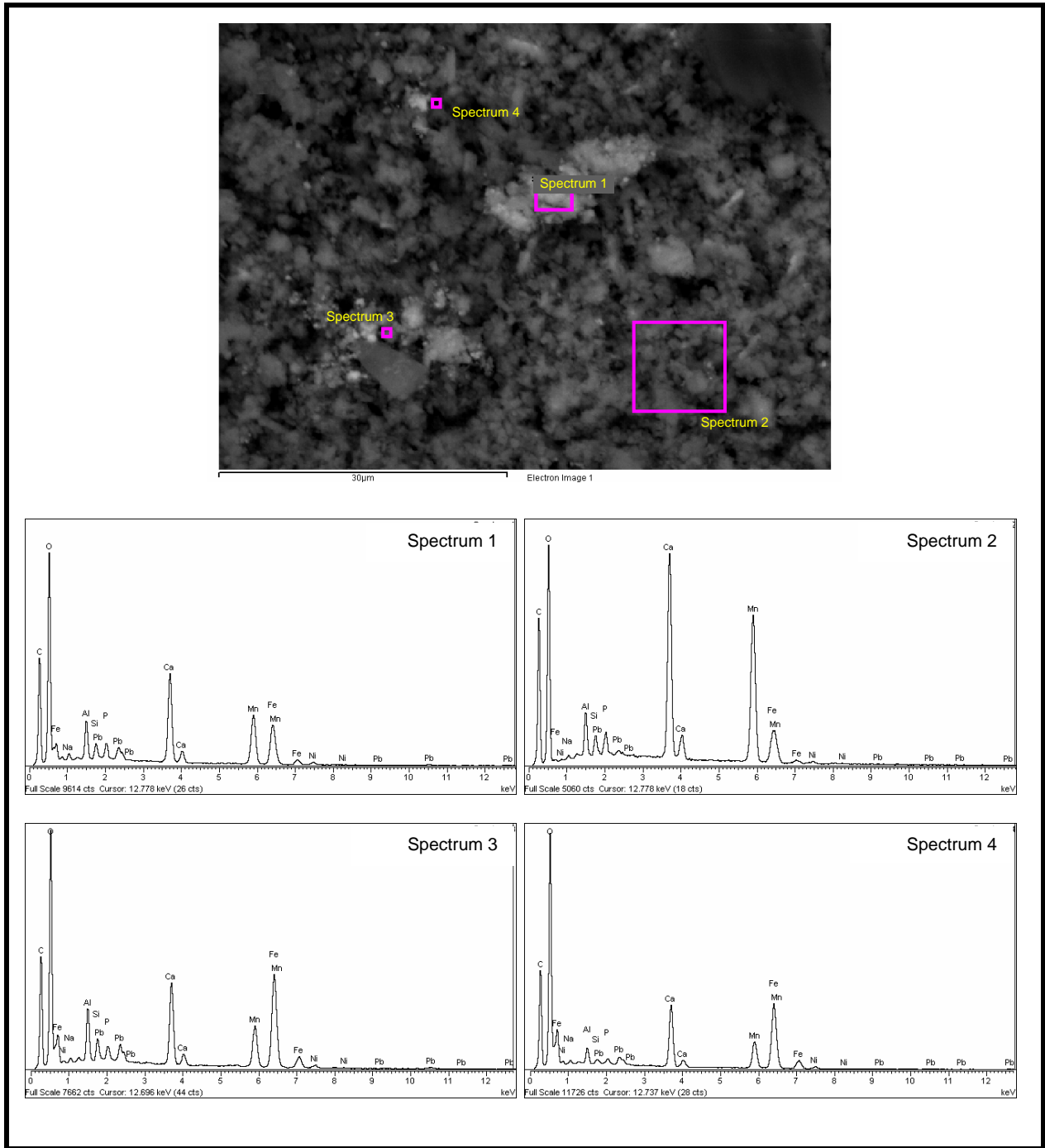


Figure B.21. EDS Spectra for Numbered Areas Marked in Pink in SEM Micrograph Shown at Top of Figure

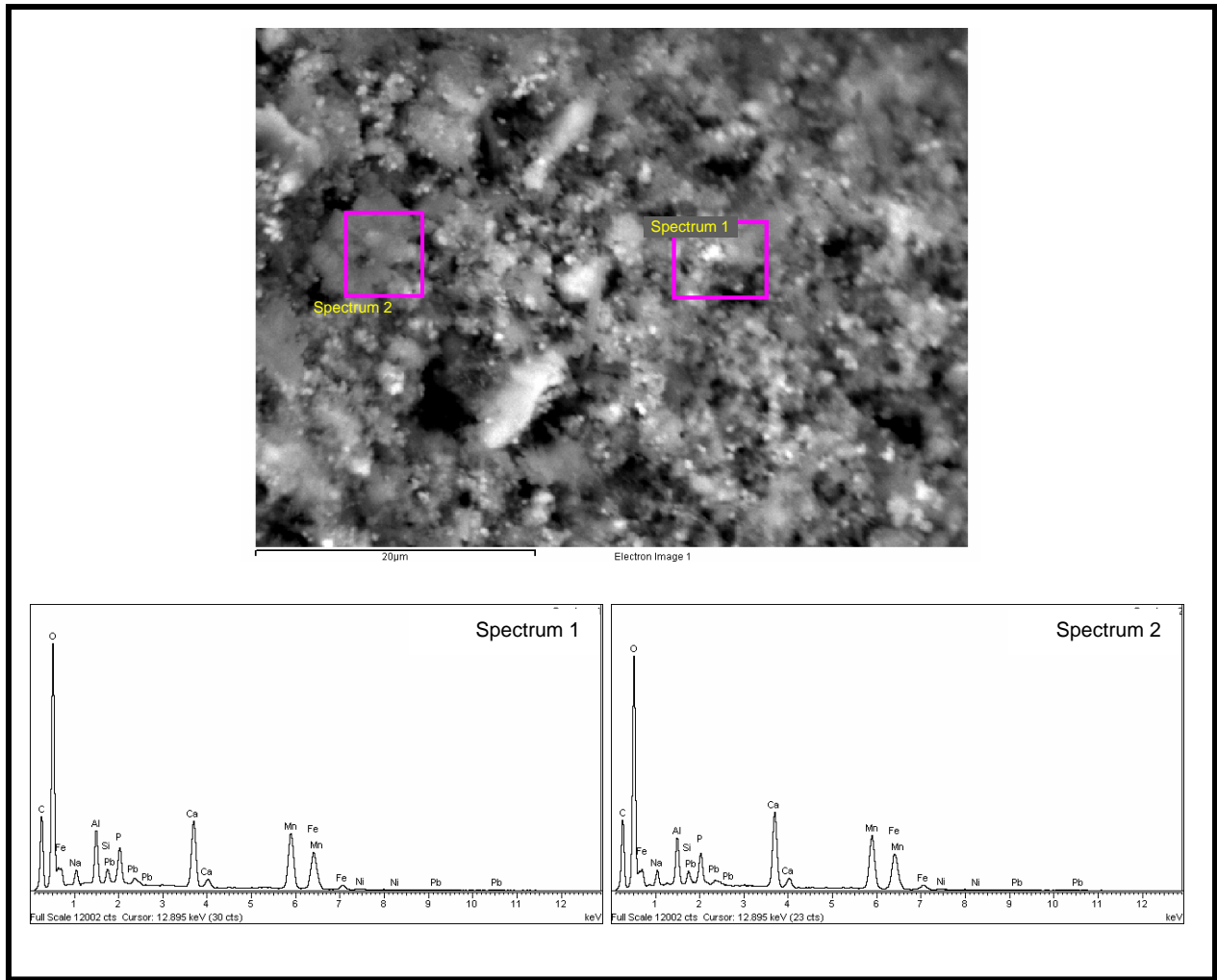


Figure B.22. EDS Spectra for Numbered Areas Marked in Pink in SEM Micrograph Shown at Top of Figure

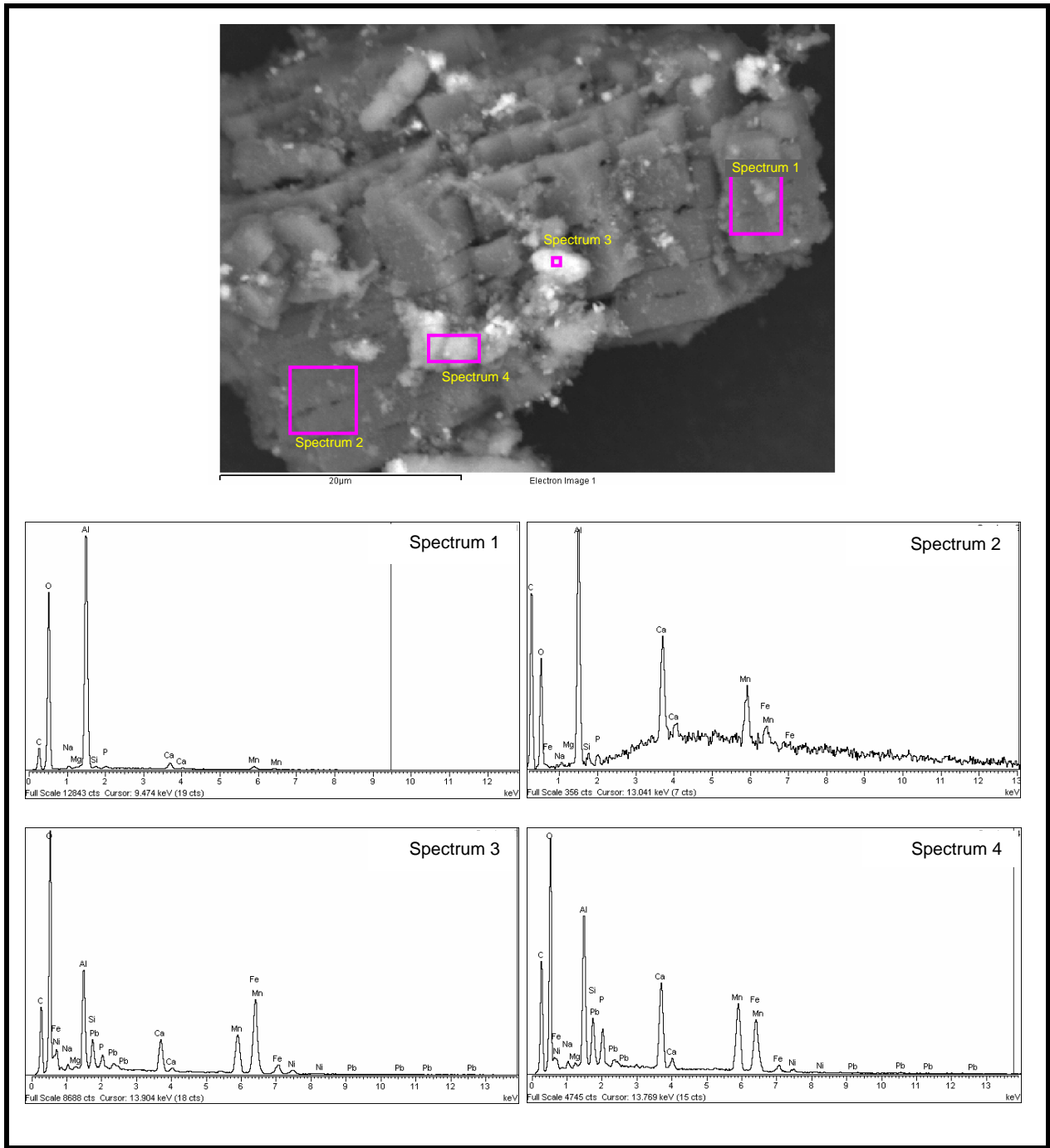


Figure B.23. EDS Spectra for Numbered Areas Marked in Pink in SEM Micrograph Shown at Top of Figure

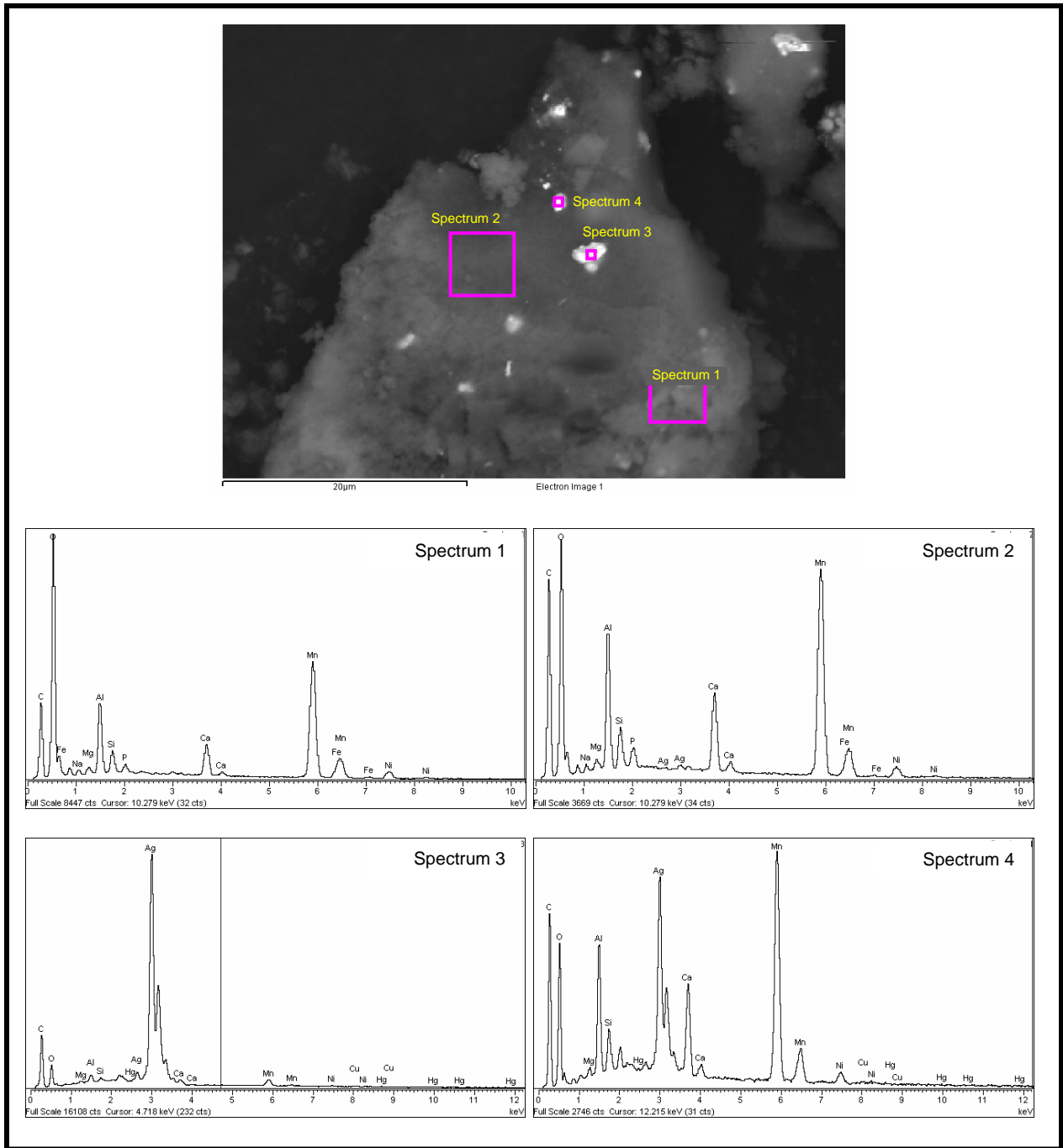


Figure B.24. EDS Spectra for Numbered Areas Marked in Pink in SEM Micrograph Shown at Top of Figure

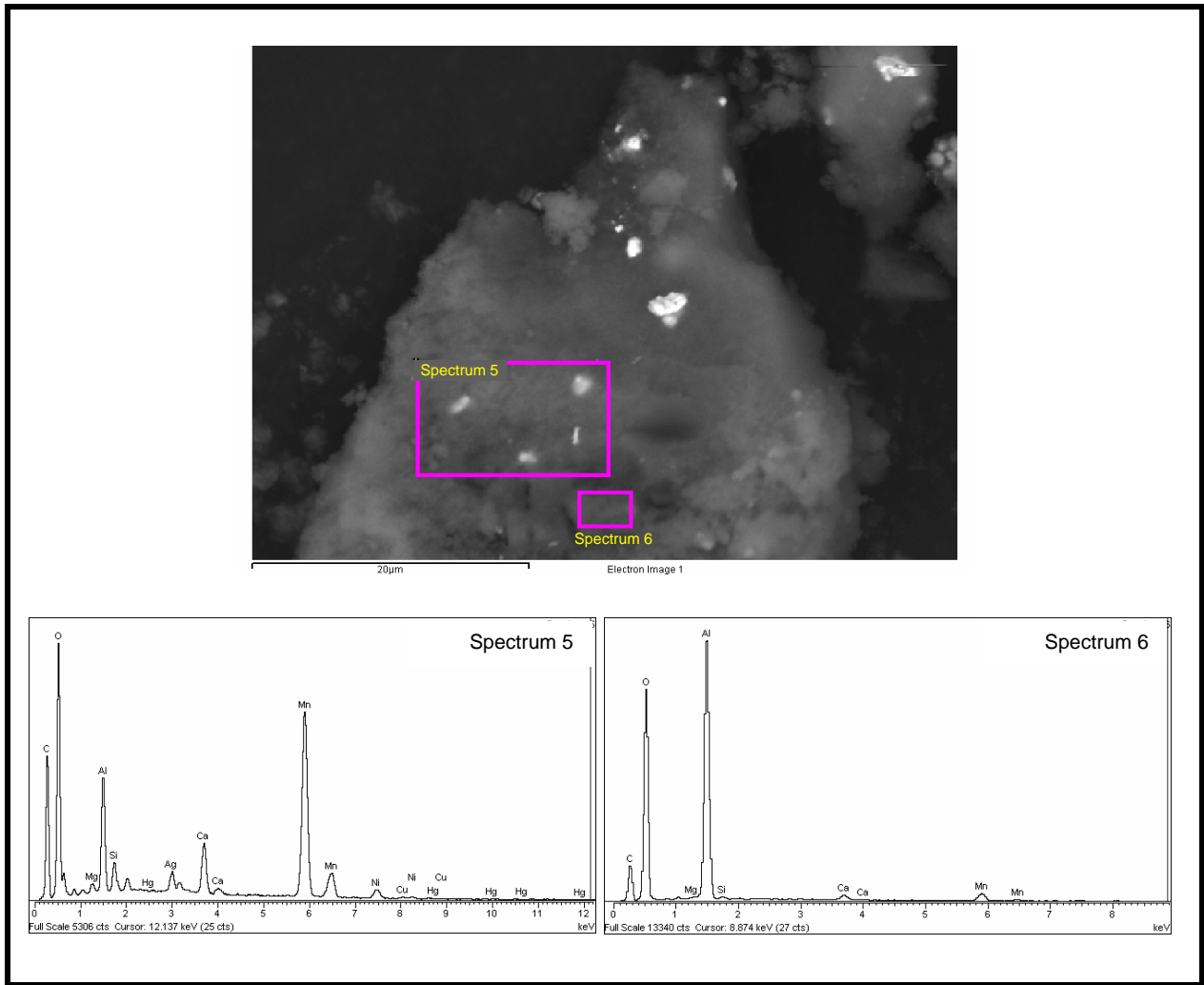


Figure B.25. EDS Spectra for Numbered Areas Marked in Pink in SEM Micrograph Shown at Top of Figure

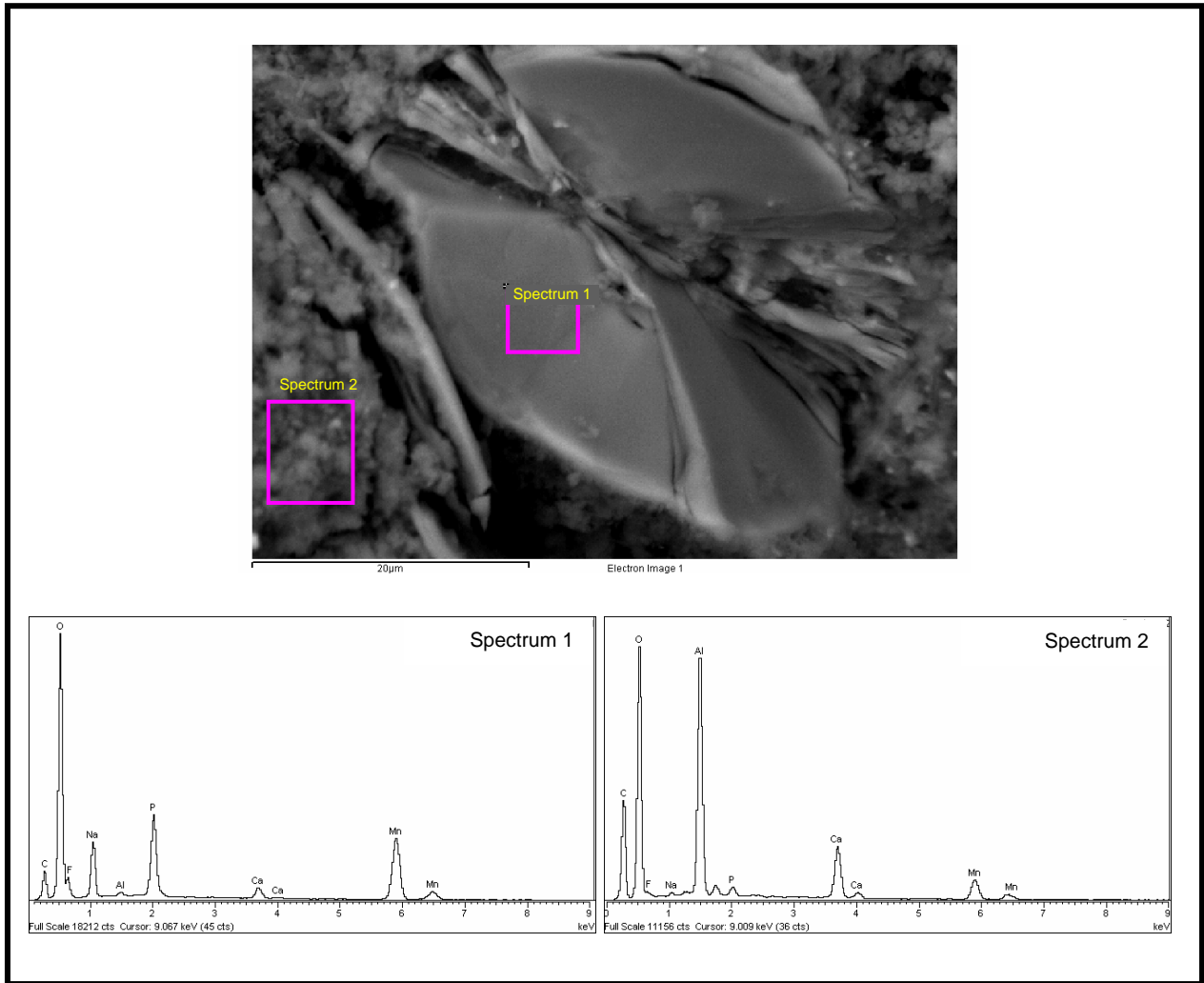


Figure B.26. EDS Spectra for Numbered Areas Marked in Pink in SEM Micrograph Shown at Top of Figure

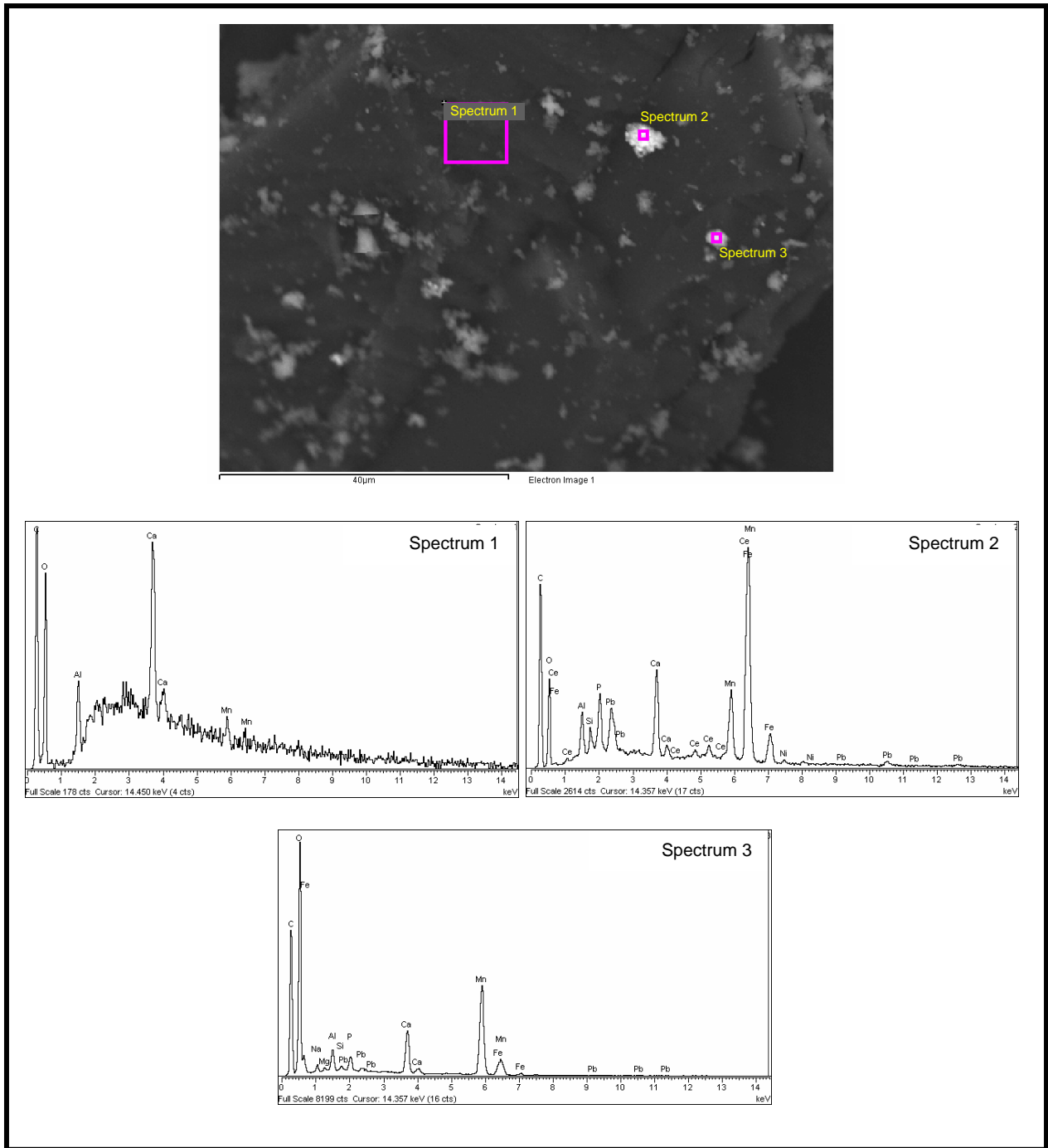


Figure B.27. EDS Spectra for Numbered Areas Marked in Pink in SEM Micrograph Shown at Top of Figure

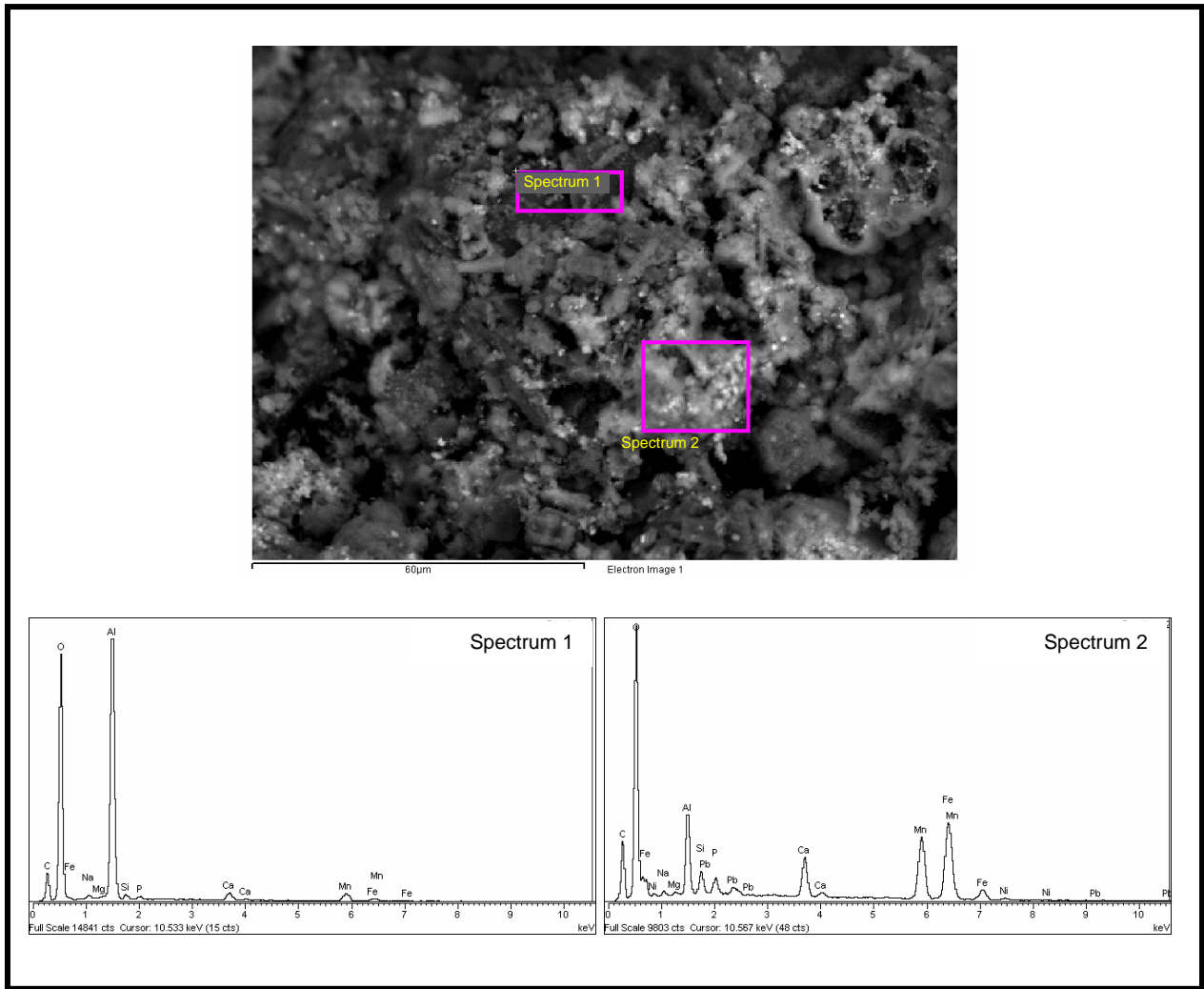


Figure B.28. EDS Spectra for Numbered Areas Marked in Pink in SEM Micrograph Shown at Top of Figure

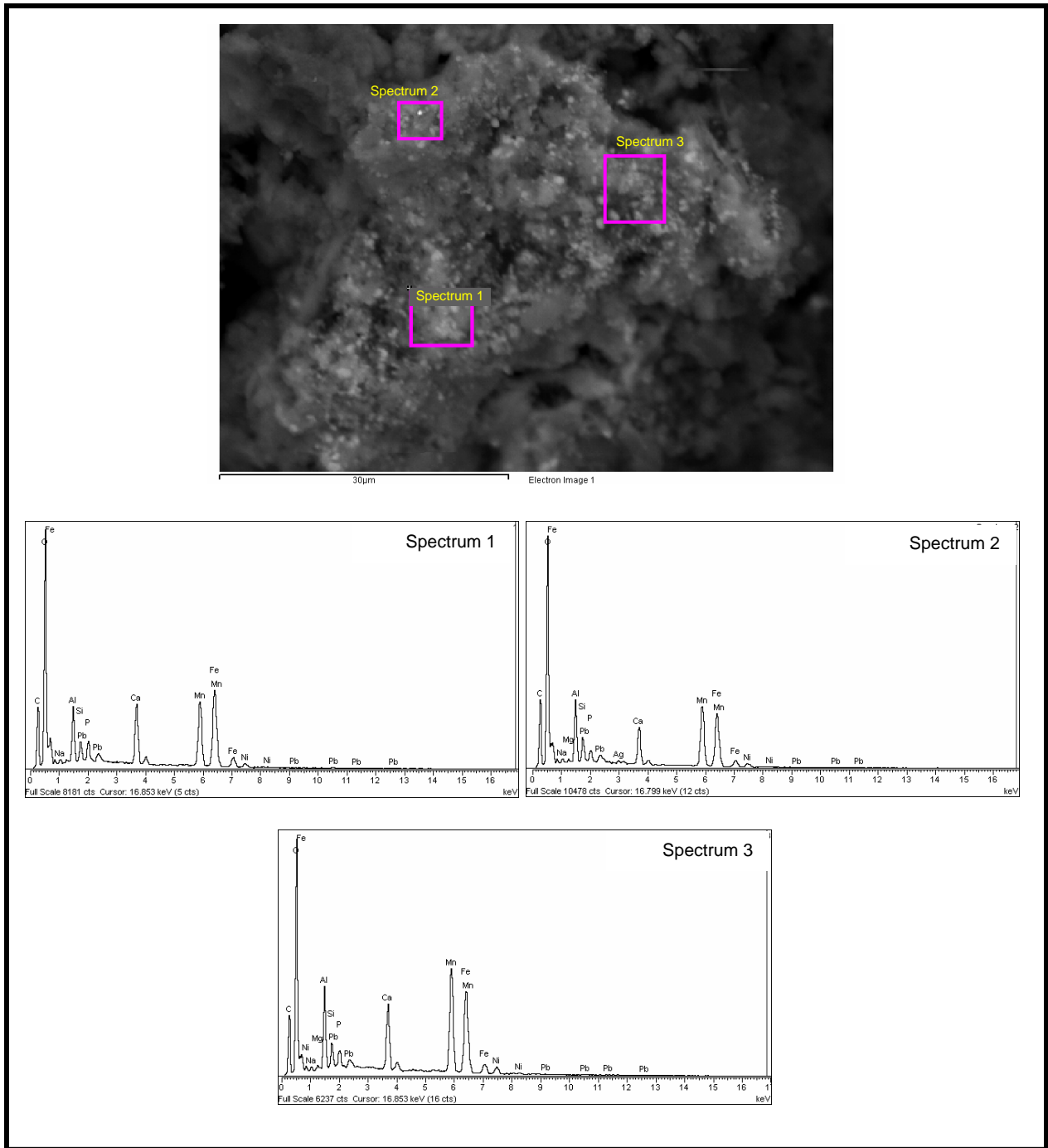


Figure B.29. EDS Spectra for Numbered Areas Marked in Pink in SEM Micrograph Shown at Top of Figure

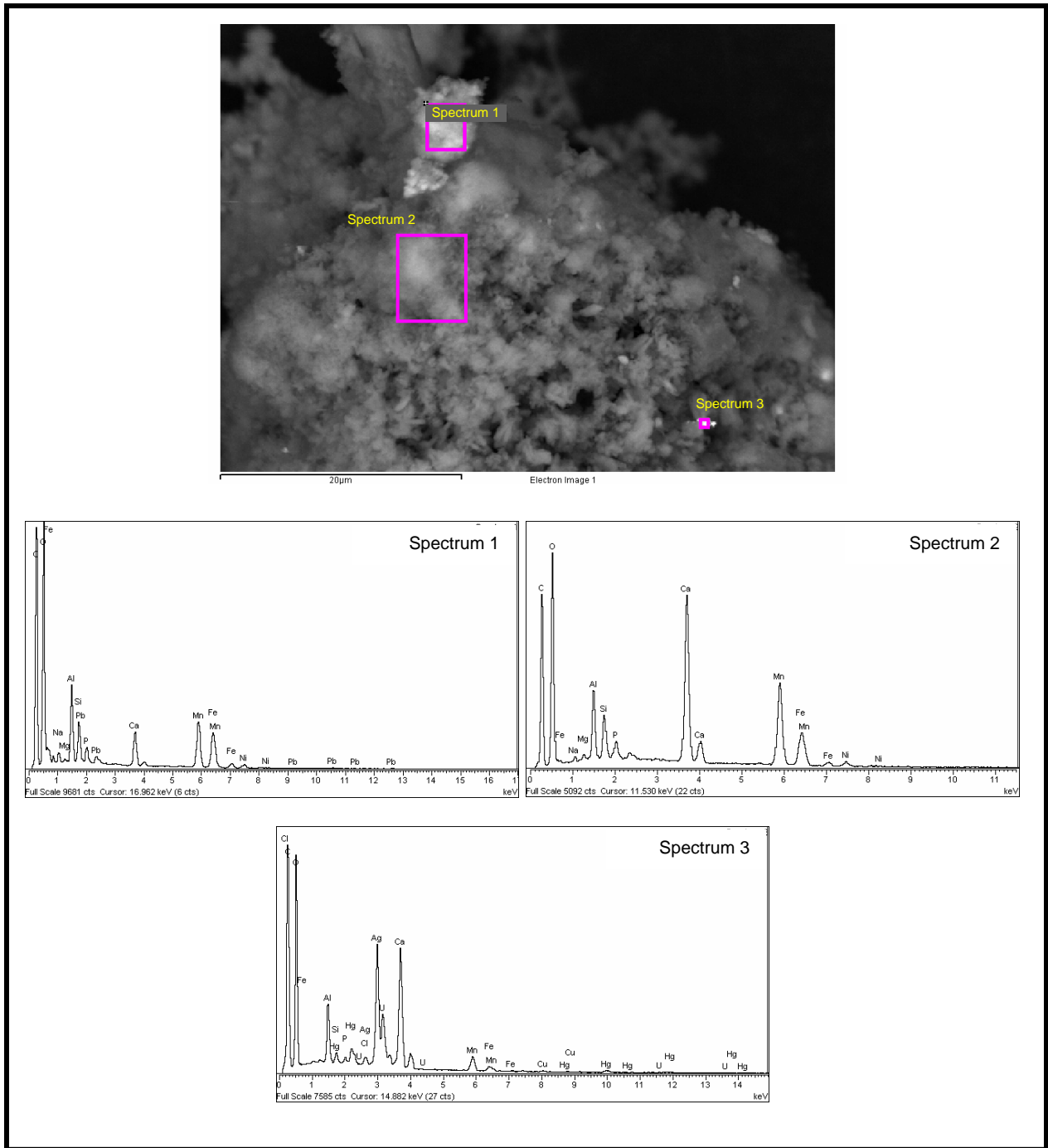


Figure B.30. EDS Spectra for Numbered Areas Marked in Pink in SEM Micrograph Shown at Top of Figure

Appendix C

SEM Micrographs and EDS Results for Stage 6 Sequential Ca(OH)₂-Leached Tank C-106 Residual Waste

Appendix C

SEM Micrographs and EDS Results for Stage 6 Sequential Ca(OH)₂-Leached Tank C-106 Residual Waste

This appendix includes the scanning electron microscope (SEM) micrographs and the energy-dispersive x-ray spectrometry (EDS) spectra, and element-distribution maps for samples of Stage 6 sequential Ca(OH)₂-leached residual waste from tank C-106. The operating conditions for the SEM and procedures used for mounting the SEM samples are described in Section 3.4 of the main report.

The identification number for the digital micrograph image file, descriptor for the type of sample, and a size scale bar are given, respectively, at the bottom left, center, and right of each SEM micrograph in this appendix. Micrographs labeled by “BSE” to the immediate right of the digital image file number indicate that the micrograph was collected with backscattered electrons. Sample areas or particles identified by a letter, arrow, and/or outlined by a white or black dotted-line squares in a micrograph designate sample material that was imaged at higher magnification, which is typically shown in figure(s) that immediately follow in the series for that sample. The SEM micrographs for this leached material are shown in Figures C.1 through C.12. The EDS spectra for this mount are given in Figures C.13 through C.23.

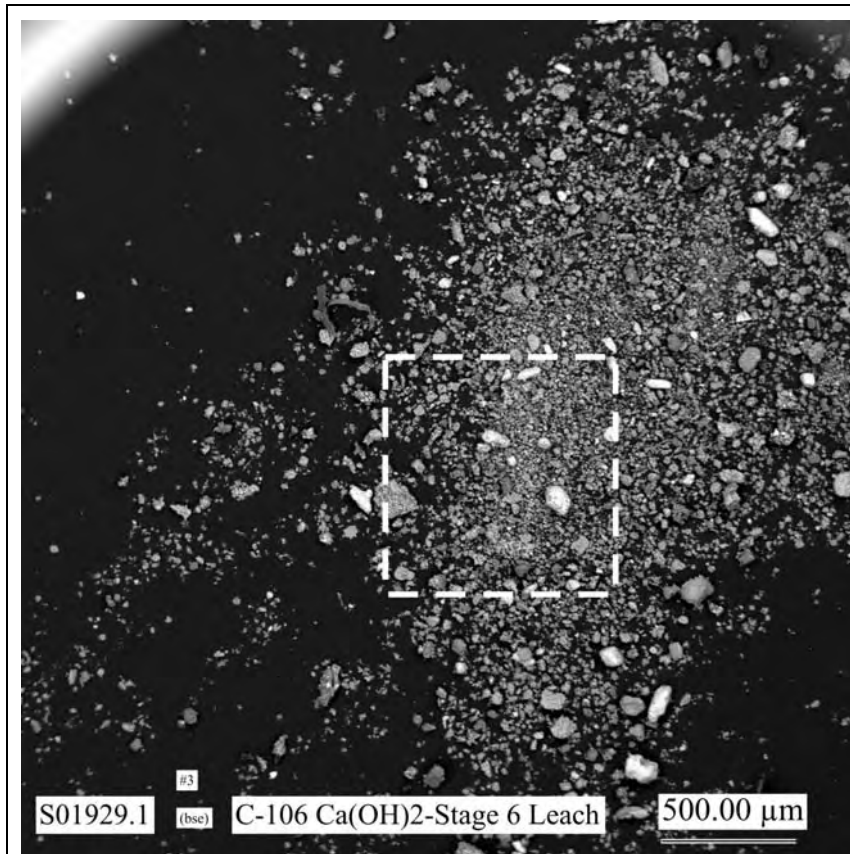


Figure C.1. Low Magnification SEM Micrograph Showing General Morphologies of Particles in the SEM Sample of the Stage 6 Sequential $\text{Ca}(\text{OH})_2$ -Leached Residual Waste from Tank C-106

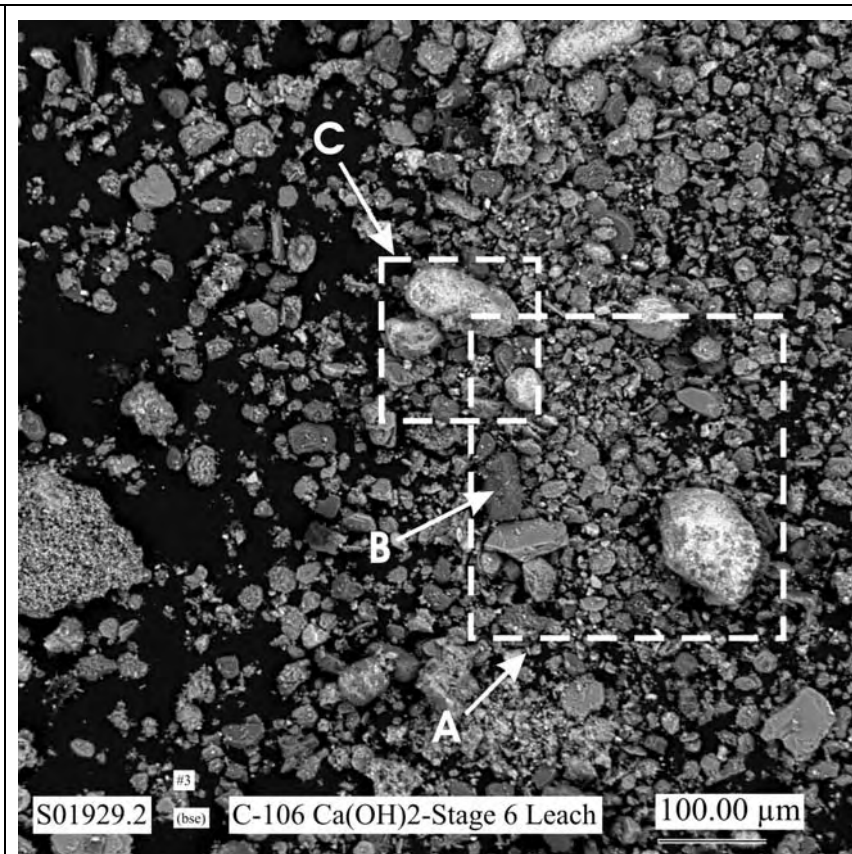


Figure C.2. Micrograph Showing at Higher Magnification the Particles in the Area Indicated by the White Dashed-Line Square in Figure C.1

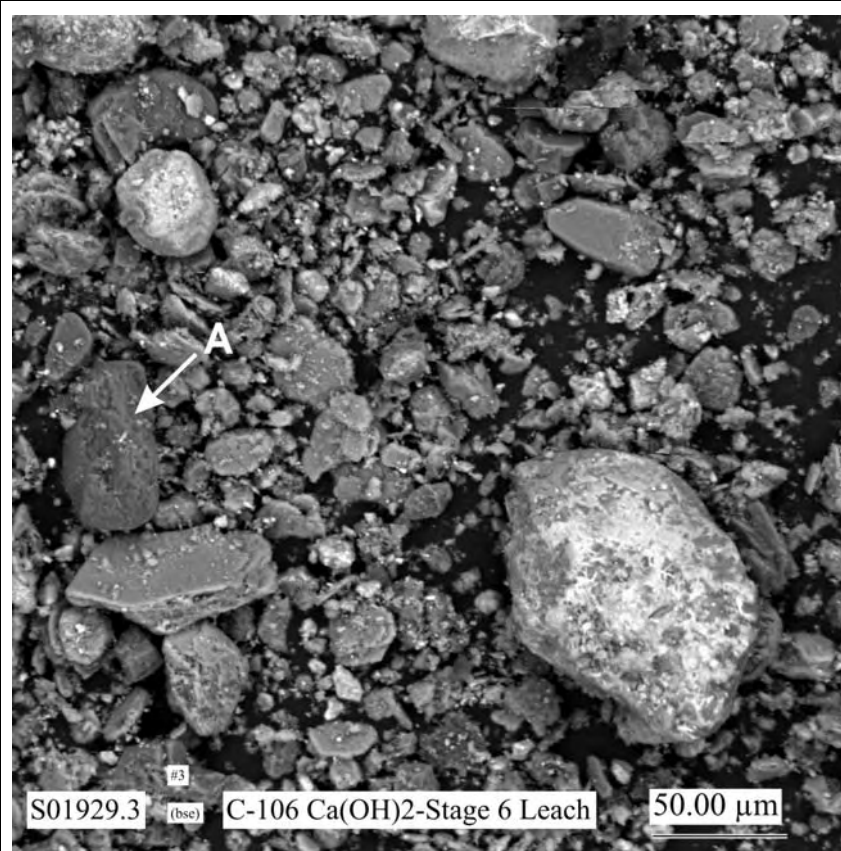


Figure C.3. Micrograph Showing at Higher Magnification the Particles in the Area Indicated by the White Dashed-Line Square Labeled A in Figure C.2 (particles in upper right of this figure where EDS analyses were made are shown in Figures C.14 and C.15)

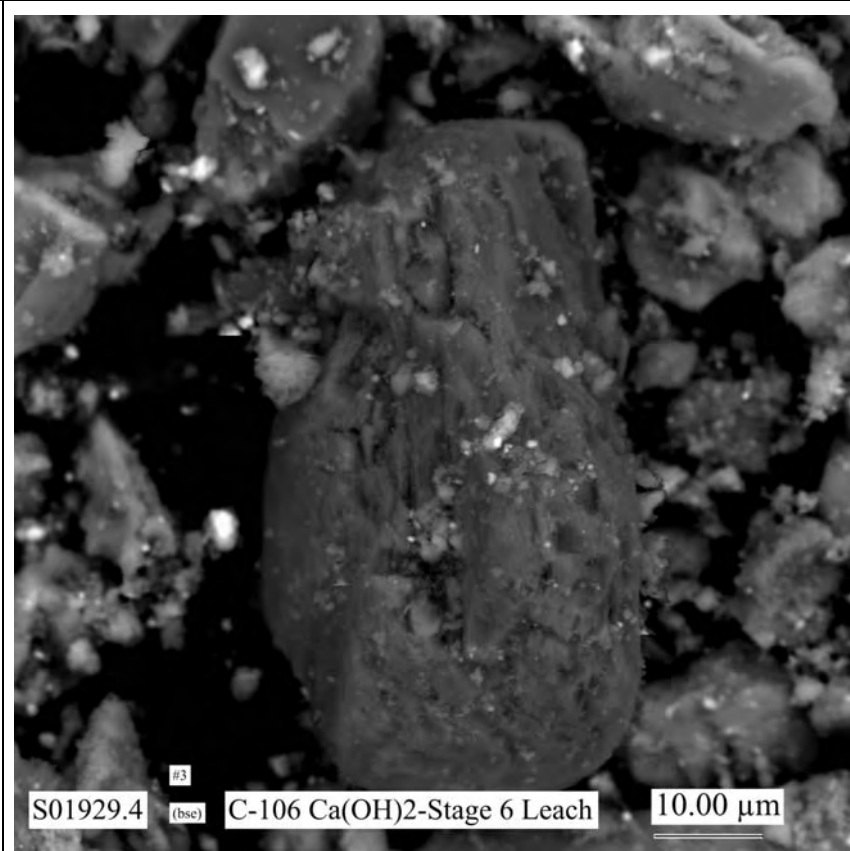


Figure C.4. Micrograph Showing at Higher Magnification the Particle Labeled B in Figure C.2 and A in Figure C.3 (areas where EDS analyses were made are shown in Figure C.13)

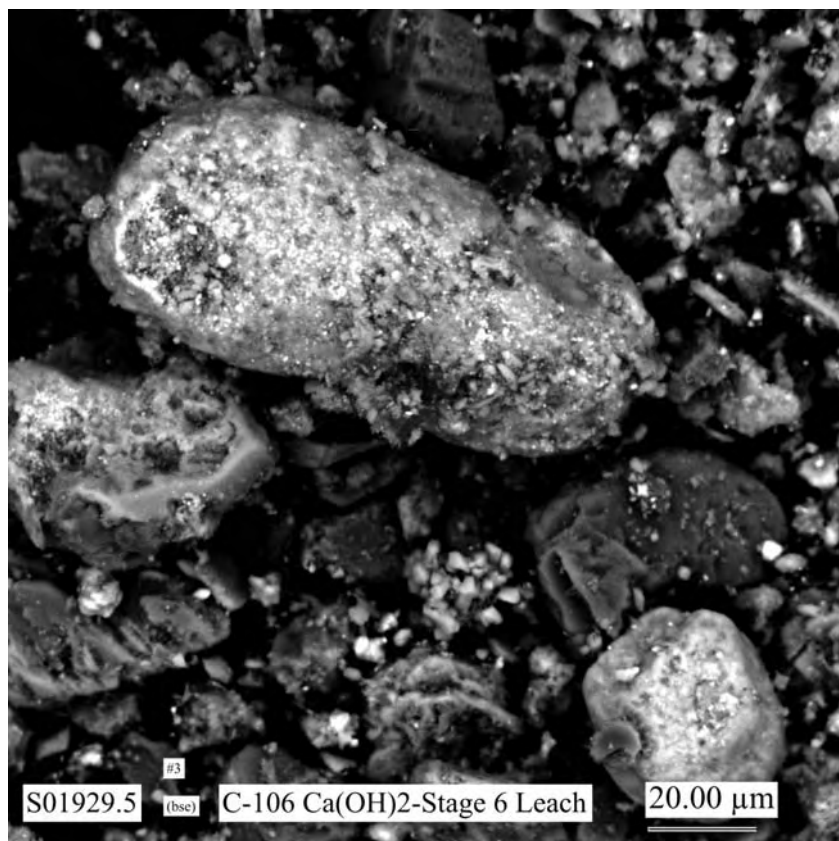


Figure C.5. Micrograph Showing at Higher Magnification the Particles in the Area Indicated by the White Dashed-Line Square Labeled C in Figure C.2 (areas where EDS analyses were made are shown in Figures C.16 and C.17)

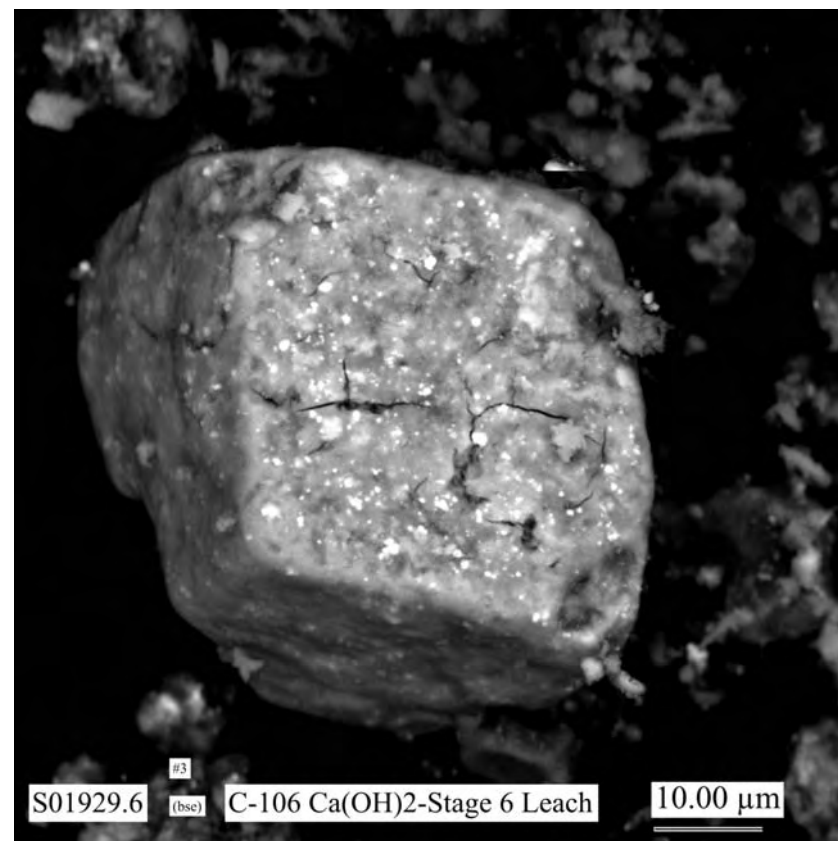


Figure C.6. Micrograph Showing Morphologies of Typical Particles in SEM Sample of the Stage 6 Sequential $\text{Ca}(\text{OH})_2$ -Leached Residual Waste from Tank C-106 (areas where EDS analyses were made are shown in Figure C.18)

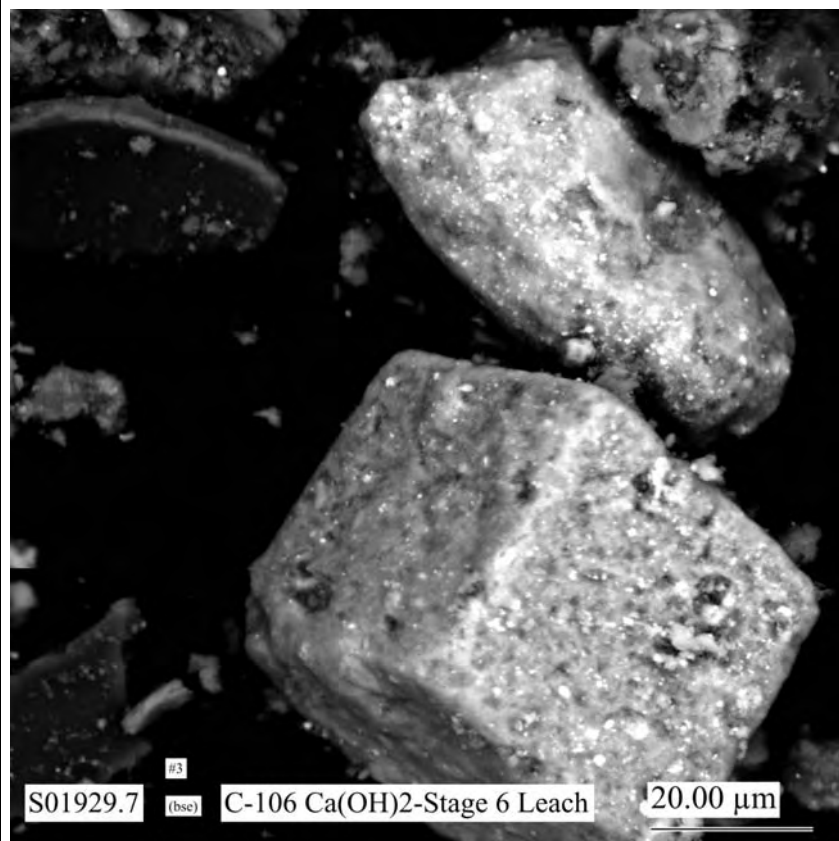


Figure C.7. Micrograph Showing Morphologies of Typical Particles in SEM Sample of the Stage 6 Sequential $\text{Ca}(\text{OH})_2$ -Leached Residual Waste from Tank C-106 (areas where EDS analyses were made are shown in Figure C.19)

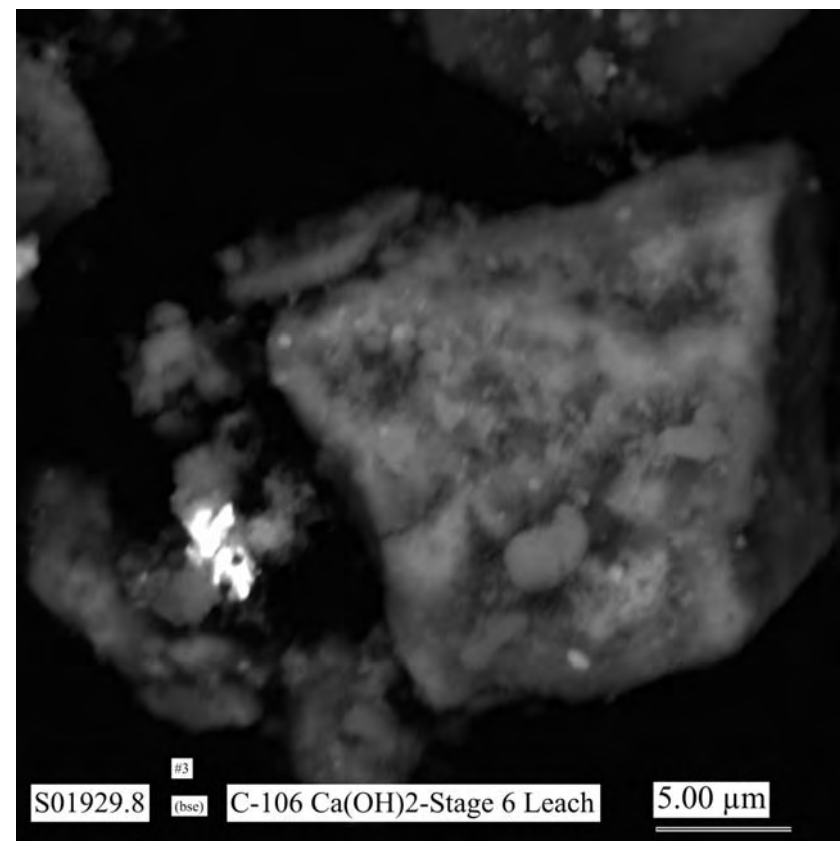


Figure C.8. Micrograph Showing Morphologies of Typical Particles in SEM Sample of the Stage 6 Sequential $\text{Ca}(\text{OH})_2$ -Leached Residual Waste from Tank C-106 (areas where EDS analyses were made are shown in Figure C.20)

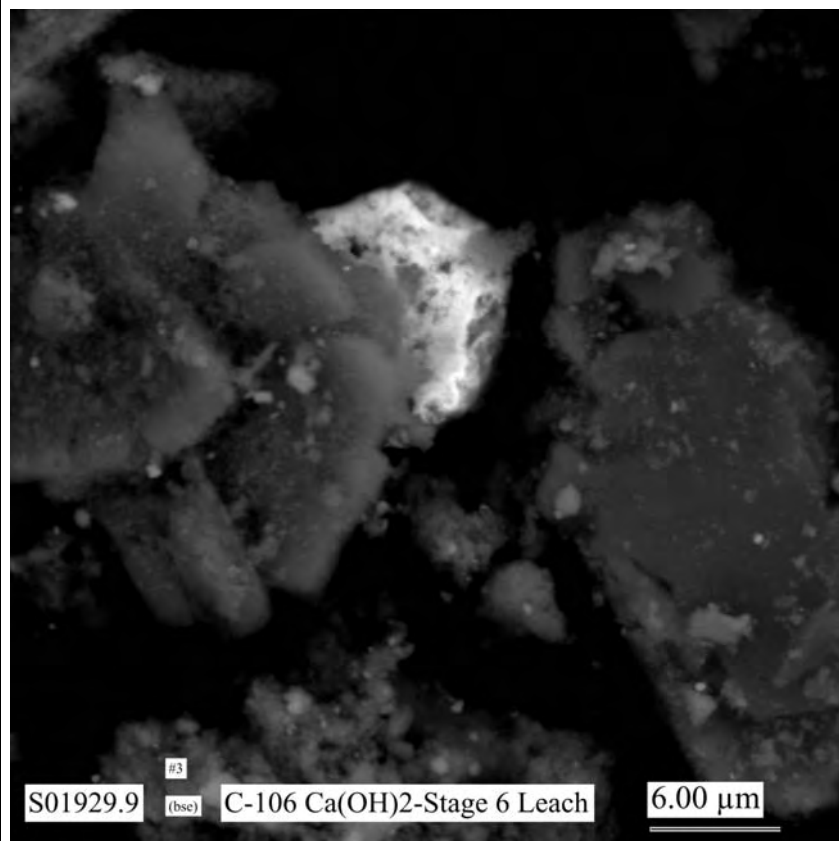


Figure C.9. Micrograph Showing Morphologies of Typical Particles in SEM Sample of the Stage 6 Sequential $\text{Ca}(\text{OH})_2$ -Leached Residual Waste from Tank C-106 (areas where EDS analyses were made are shown in Figure C.21)

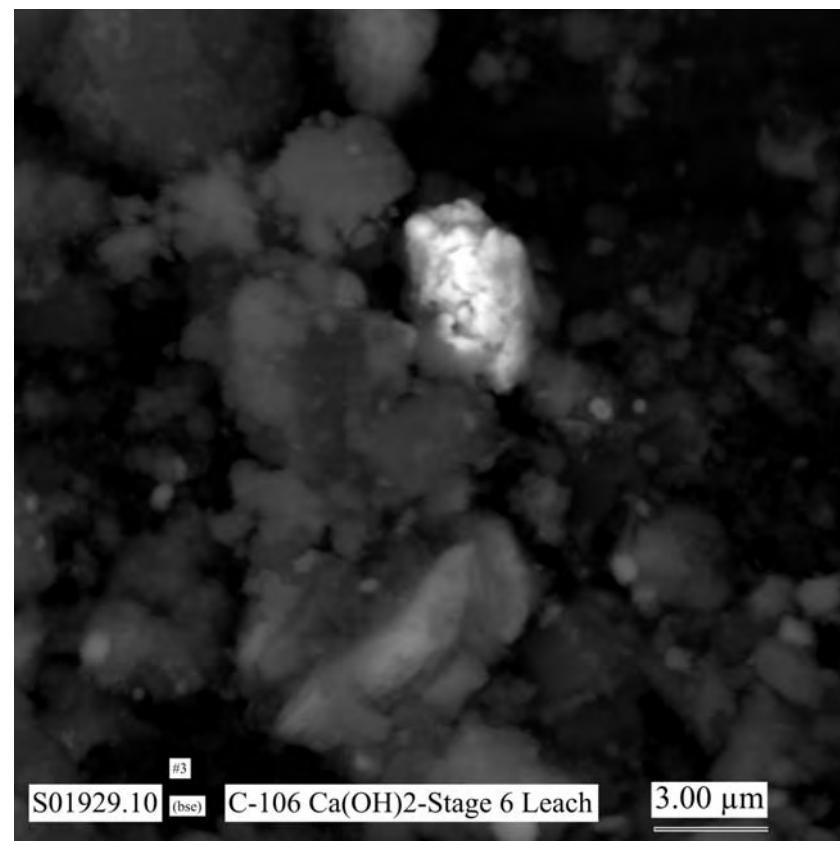


Figure C.10. Micrograph Showing Morphologies of Typical Particles in SEM Sample of the Stage 6 Sequential $\text{Ca}(\text{OH})_2$ -Leached Residual Waste from Tank C-106 (areas where EDS analyses were made are shown in Figure C.22)

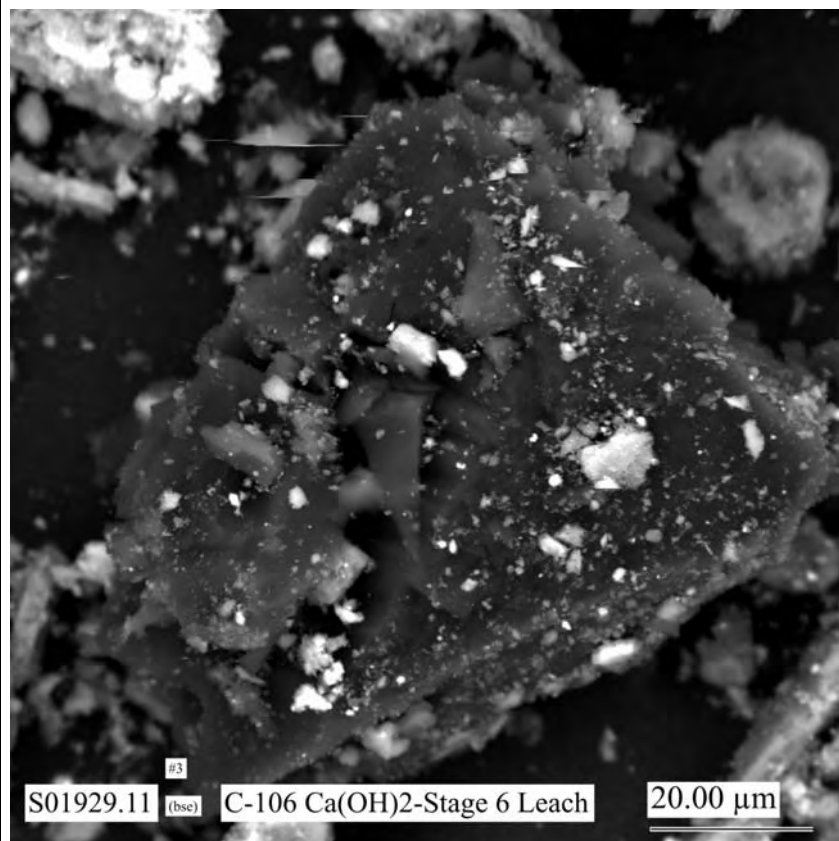


Figure C.11. Micrograph Showing Morphologies of Typical Particles in SEM Sample of the Stage 6 Sequential $\text{Ca}(\text{OH})_2$ -Leached Residual Waste from Tank C-106 (areas where EDS analyses were made are shown in Figure C.23)

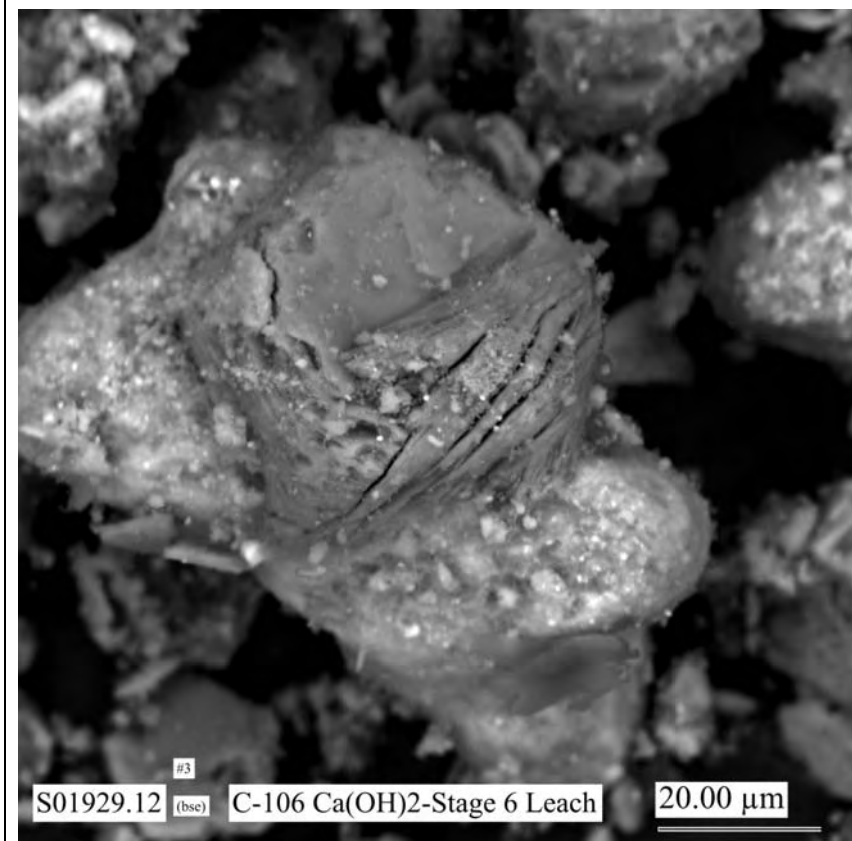


Figure C.12. Micrograph Showing Morphologies of Typical Particles in SEM Sample of the Stage 6 Sequential $\text{Ca}(\text{OH})_2$ -Leached Residual Waste from Tank C-106

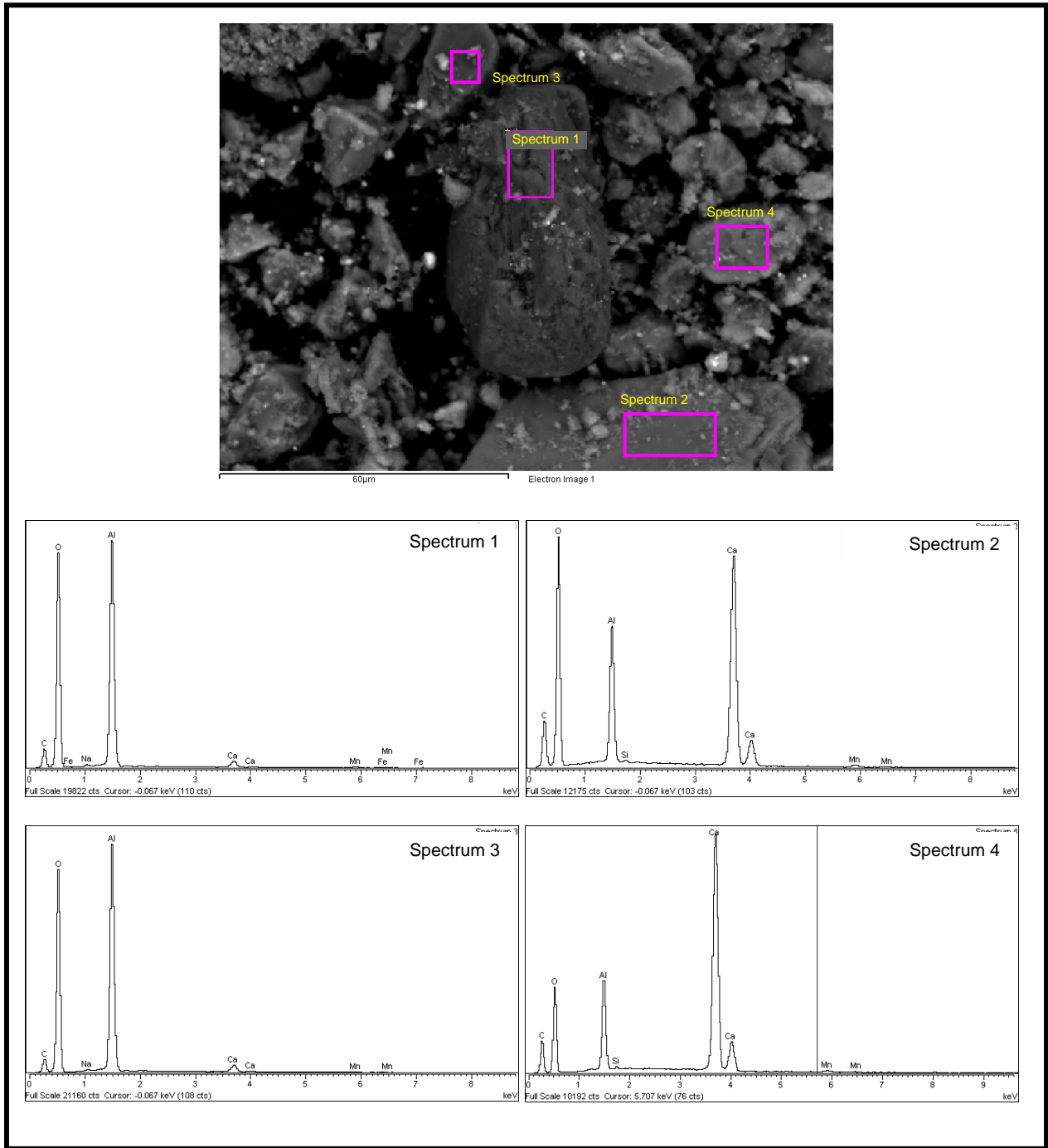


Figure C.13. EDS Spectra for Numbered Areas Marked in Pink in SEM Micrograph Shown at Top of Figure

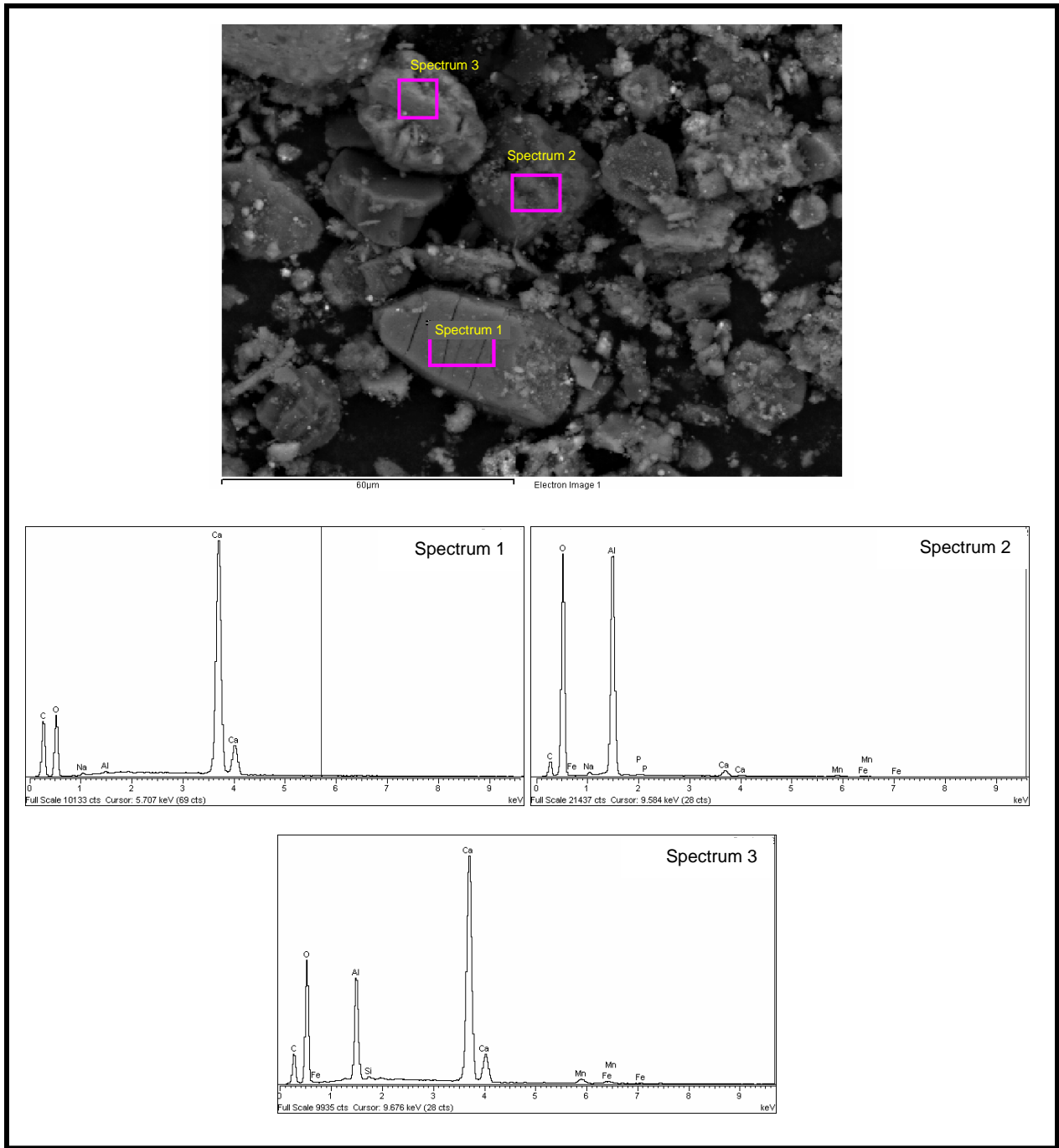


Figure C.14. EDS Spectra for Numbered Areas Marked in Pink in SEM Micrograph Shown at Top of Figure

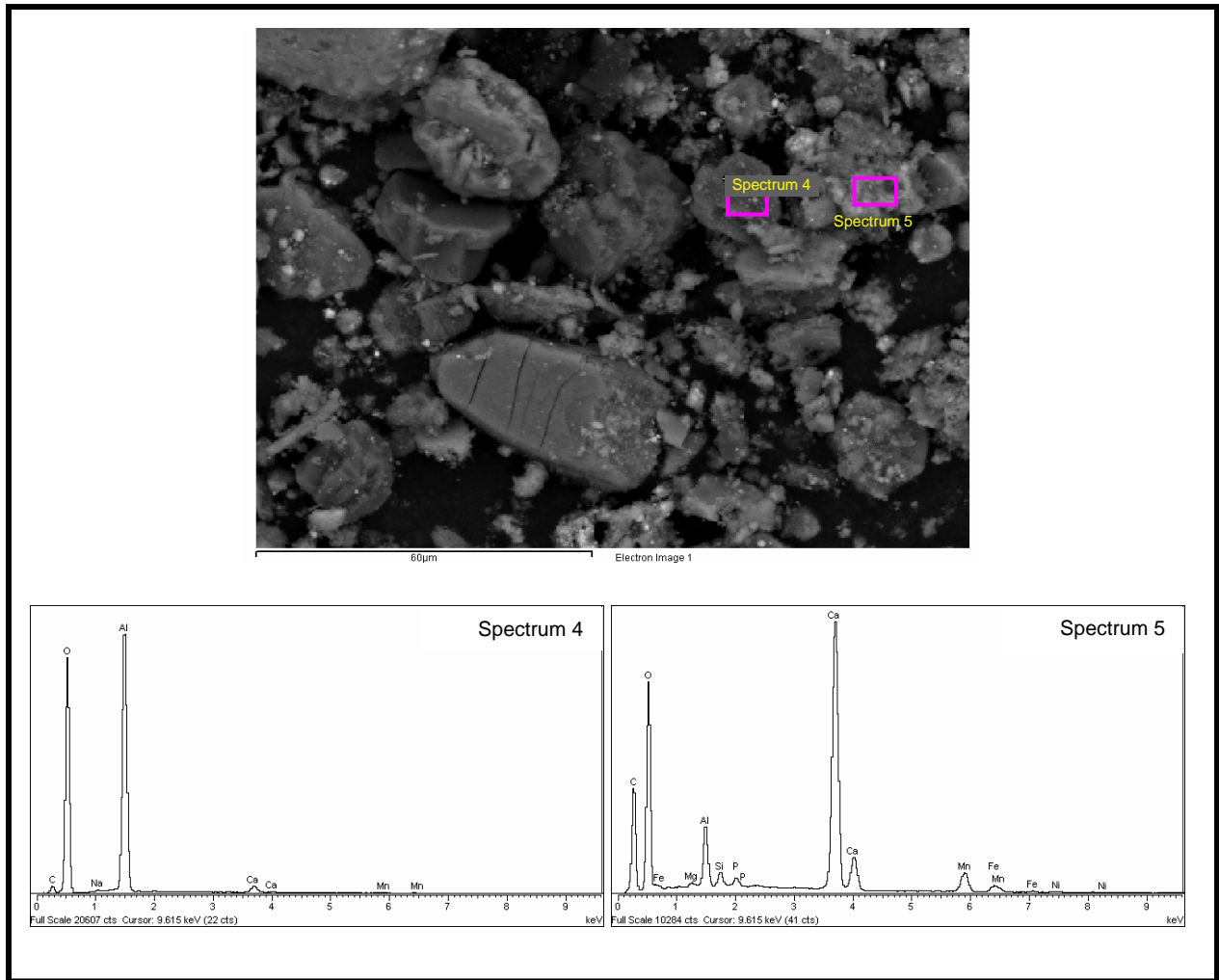


Figure C.15. EDS Spectra for Numbered Areas Marked in Pink in SEM Micrograph Shown at Top of Figure

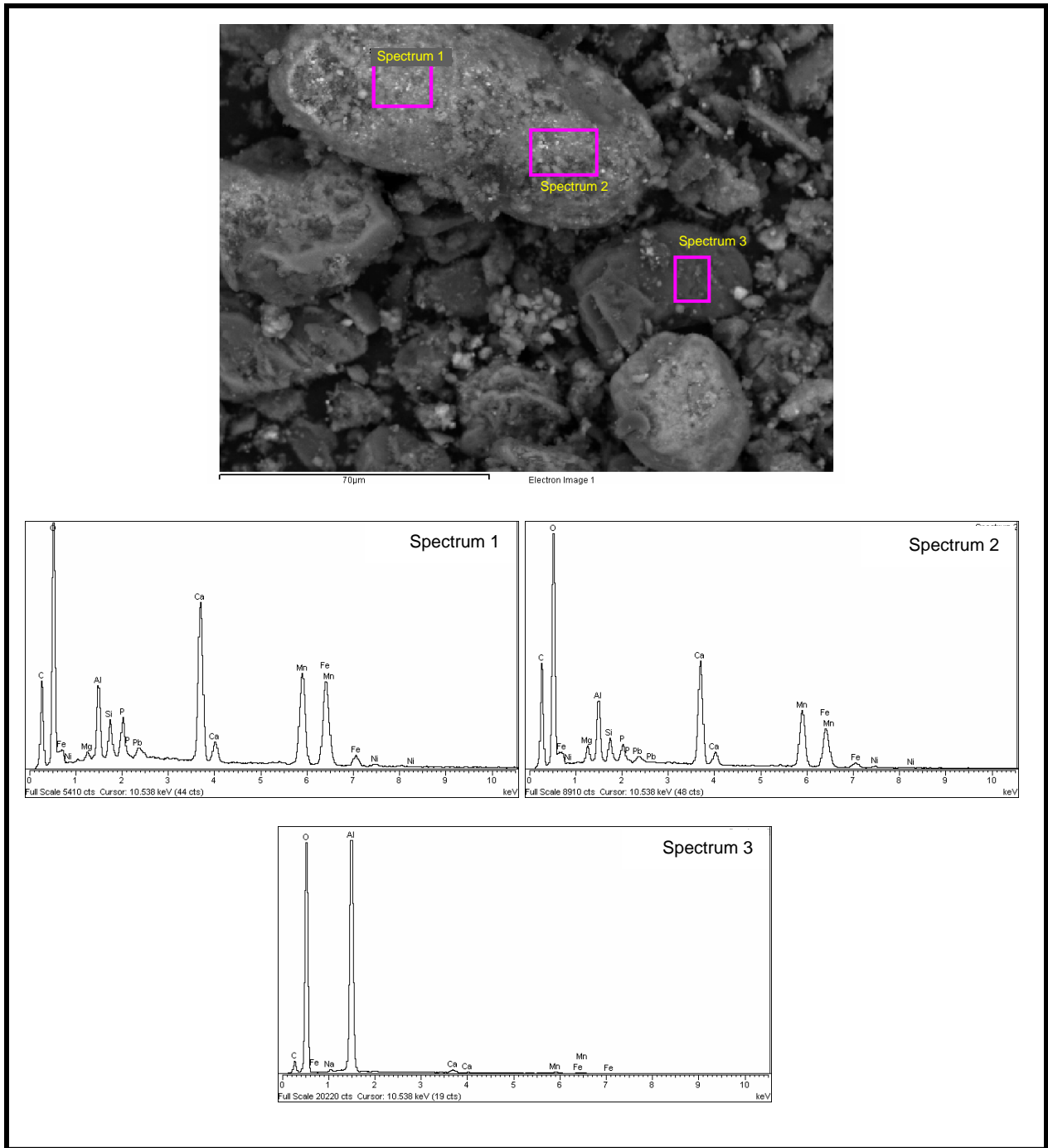


Figure C.16. EDS Spectra for Numbered Areas Marked in Pink in SEM Micrograph Shown at Top of Figure

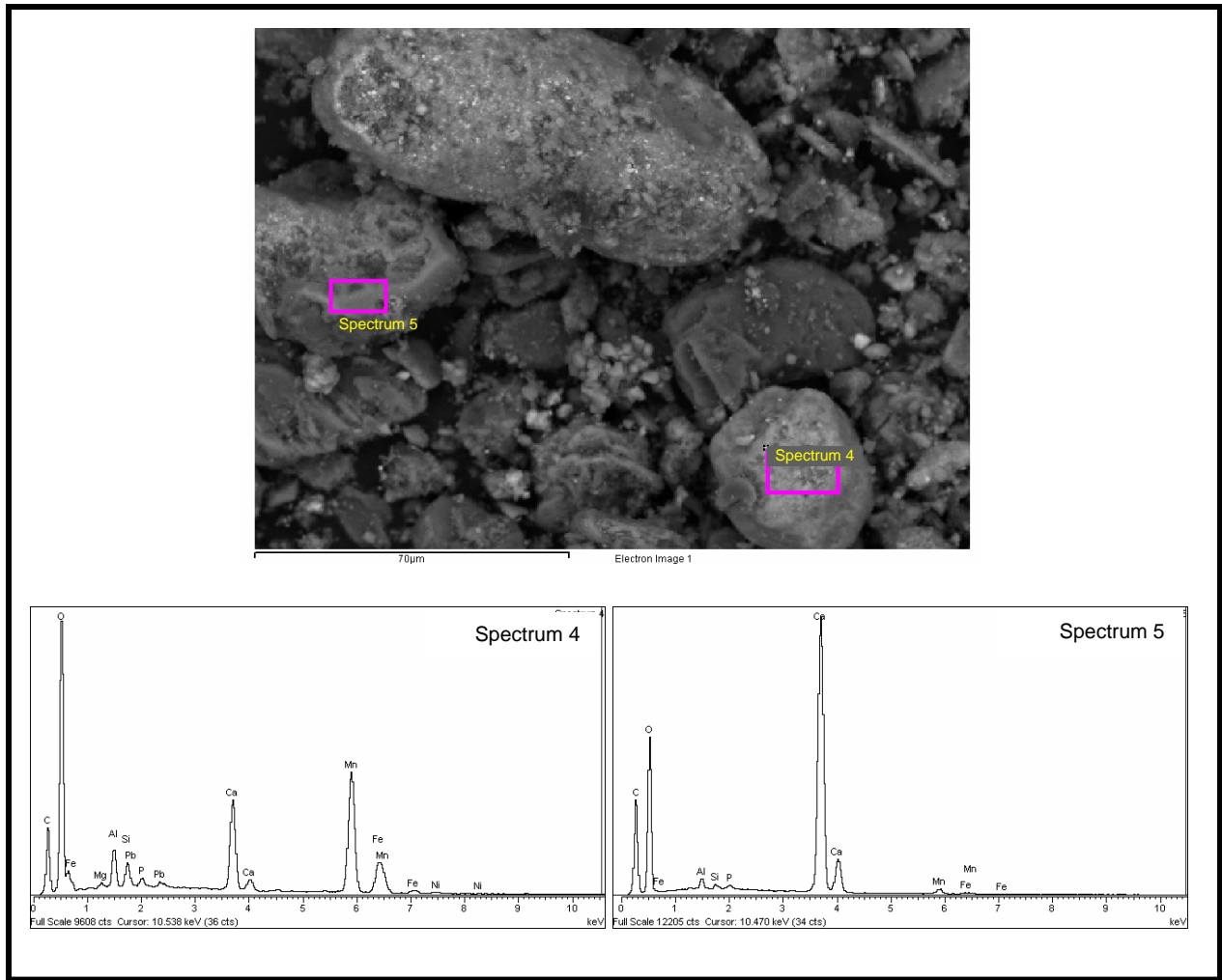


Figure C.17. EDS Spectra for Numbered Areas Marked in Pink in SEM Micrograph Shown at Top of Figure

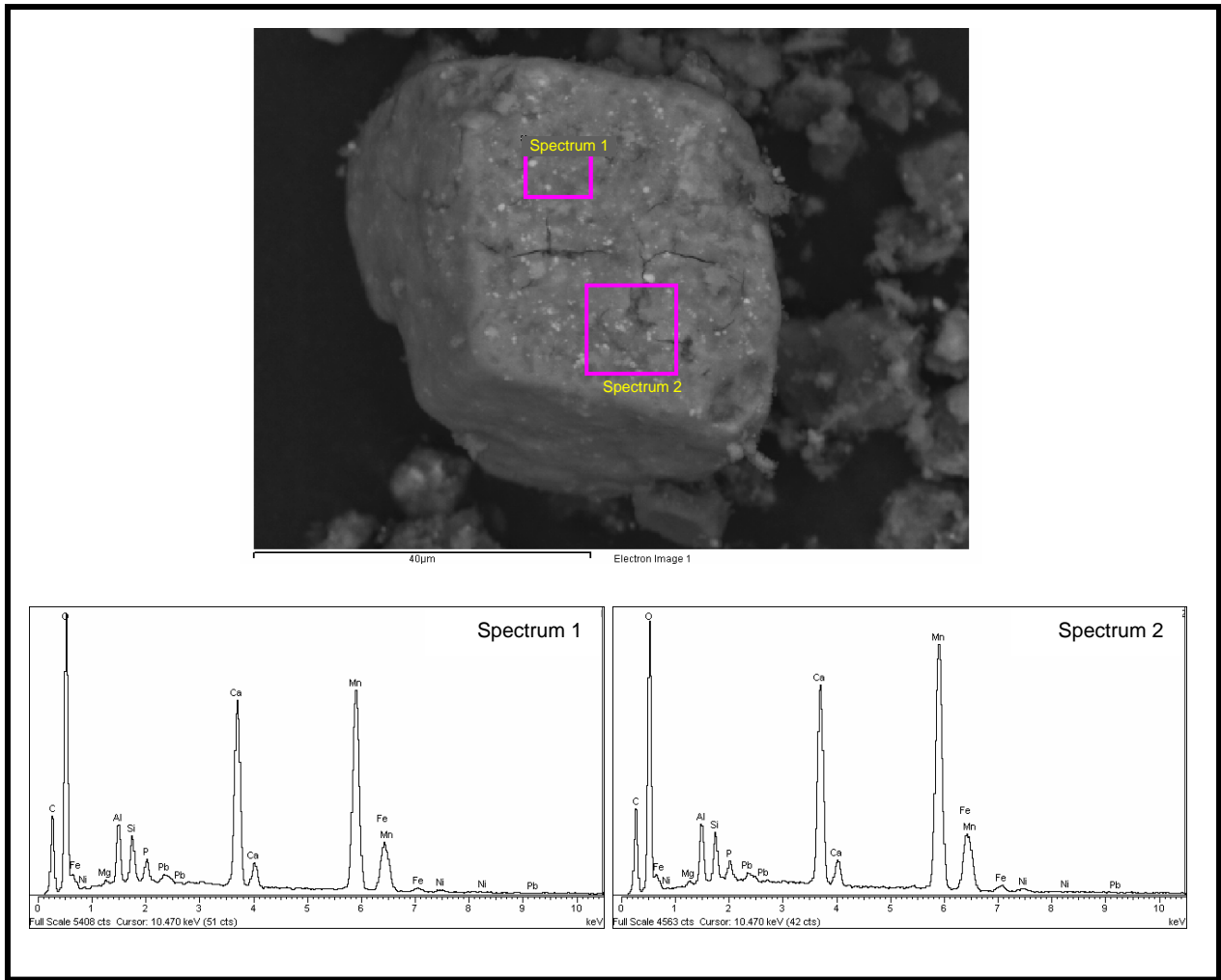


Figure C.18. EDS Spectra for Numbered Areas Marked in Pink in SEM Micrograph Shown at Top of Figure

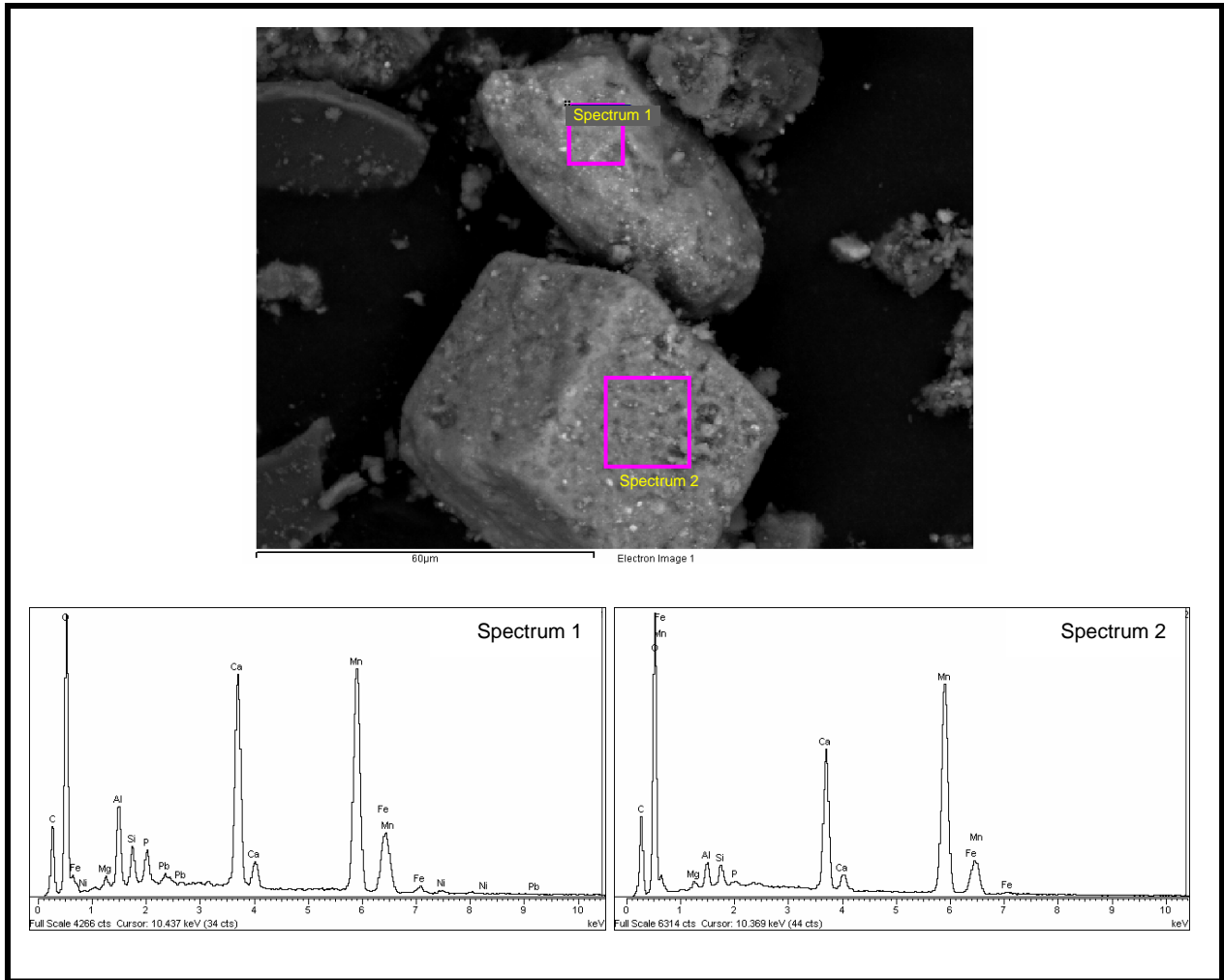


Figure C.19. EDS Spectra for Numbered Areas Marked in Pink in SEM Micrograph Shown at Top of Figure

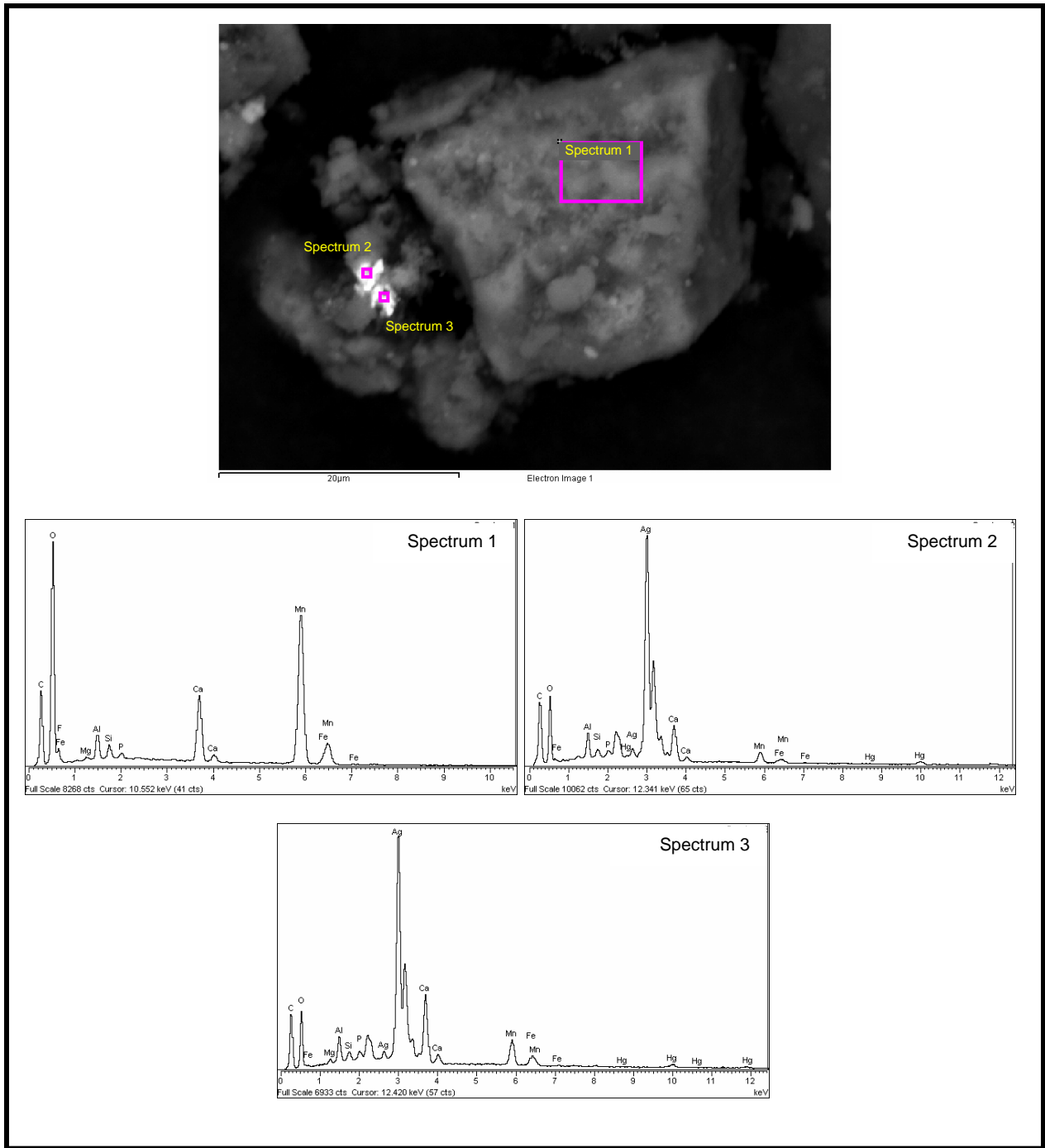


Figure C.20. EDS Spectra for Numbered Areas Marked in Pink in SEM Micrograph Shown at Top of Figure

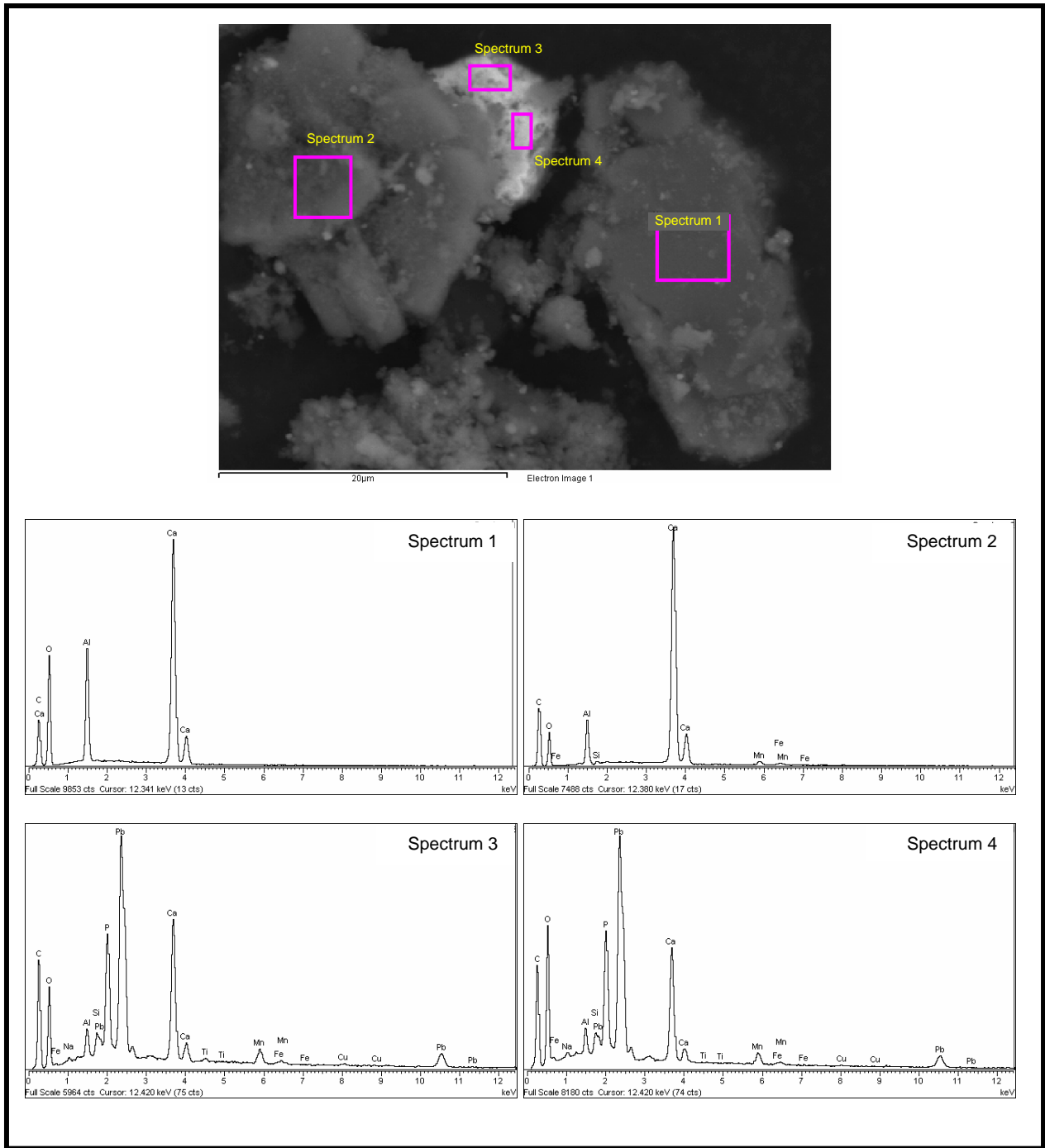


Figure C.21. EDS Spectra for Numbered Areas Marked in Pink in SEM Micrograph Shown at Top of Figure

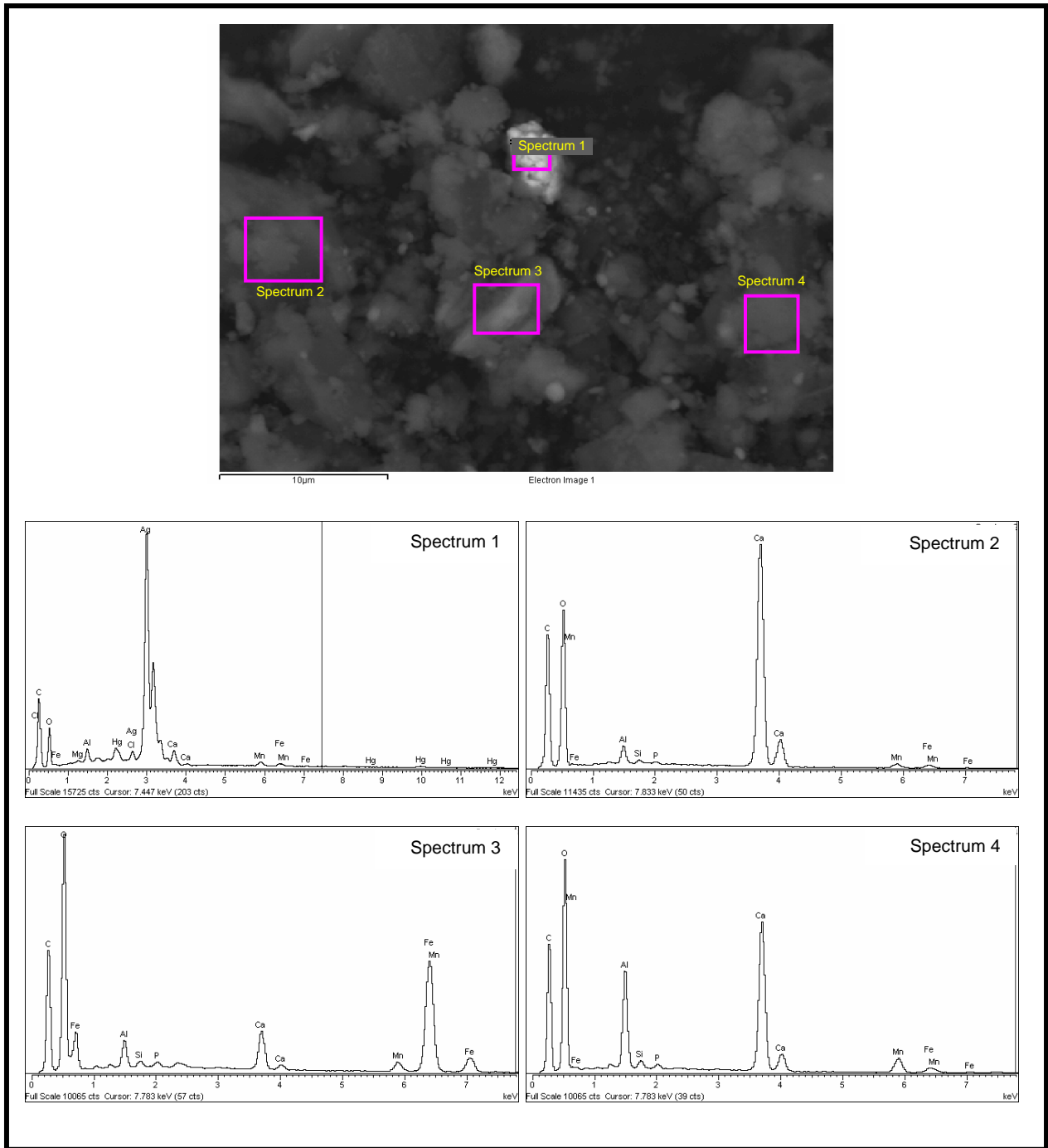


Figure C.22. EDS Spectra for Numbered Areas Marked in Pink in SEM Micrograph Shown at Top of Figure

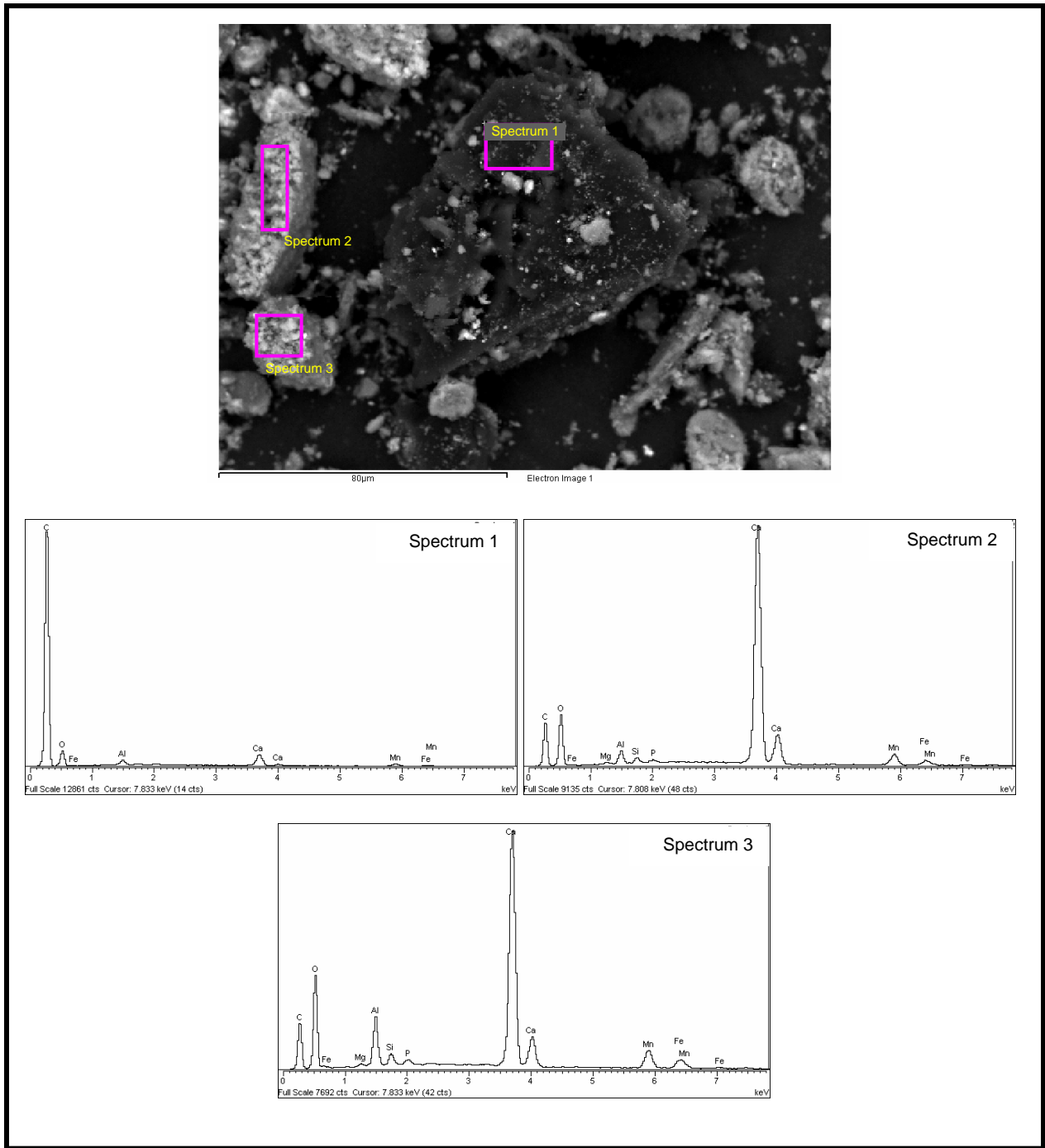


Figure C.23. EDS Spectra for Numbered Areas Marked in Pink in SEM Micrograph Shown at Top of Figure

Appendix D

SEM Micrographs and EDS Results for 1-Month $\text{Ca}(\text{OH})_2/\text{CaCO}_3$ -Leached Tank C-106 Residual Waste

Appendix D

SEM Micrographs and EDS Results for 1-Month Ca(OH)₂/CaCO₃-Leached Tank C-106 Residual Waste

This appendix includes the scanning electron microscope (SEM) micrographs and the energy-dispersive x-ray spectrometry (EDS) spectra, and element-distribution maps for samples of 1-month Ca(OH)₂/CaCO₃-leached residual waste from tank C-106. The operating conditions for the SEM and procedures used for mounting the SEM samples are described in Section 3.4 of the main report.

The identification number for the digital micrograph image file, descriptor for the type of sample, and a size scale bar are given, respectively, at the bottom left, center, and right of each SEM micrograph in this appendix. Micrographs labeled by “BSE” to the immediate right of the digital image file number indicate that the micrograph was collected with backscattered electrons. Sample areas or particles identified by a letter, arrow, and/or outlined by a white or black dotted-line squares in a micrograph designate sample material that was imaged at higher magnification, which is typically shown in figure(s) that immediately follow in the series for that sample. The SEM micrographs for this leached material are shown in Figures D.1 through D.16. The EDS spectra for this mount are given in Figures D.17 through D.24.

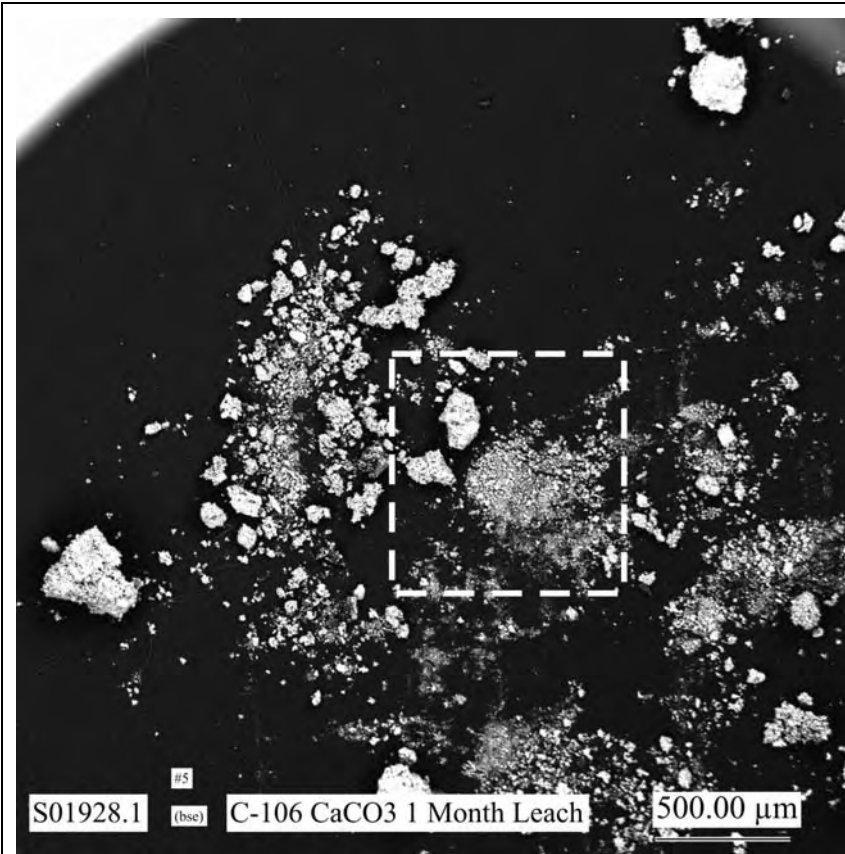


Figure D.1. Low Magnification SEM Micrograph Showing General Morphologies of Particles in SEM Sample of 1-Month $\text{Ca}(\text{OH})_2/\text{CaCO}_3$ -Leached Residual Waste from Tank C-106

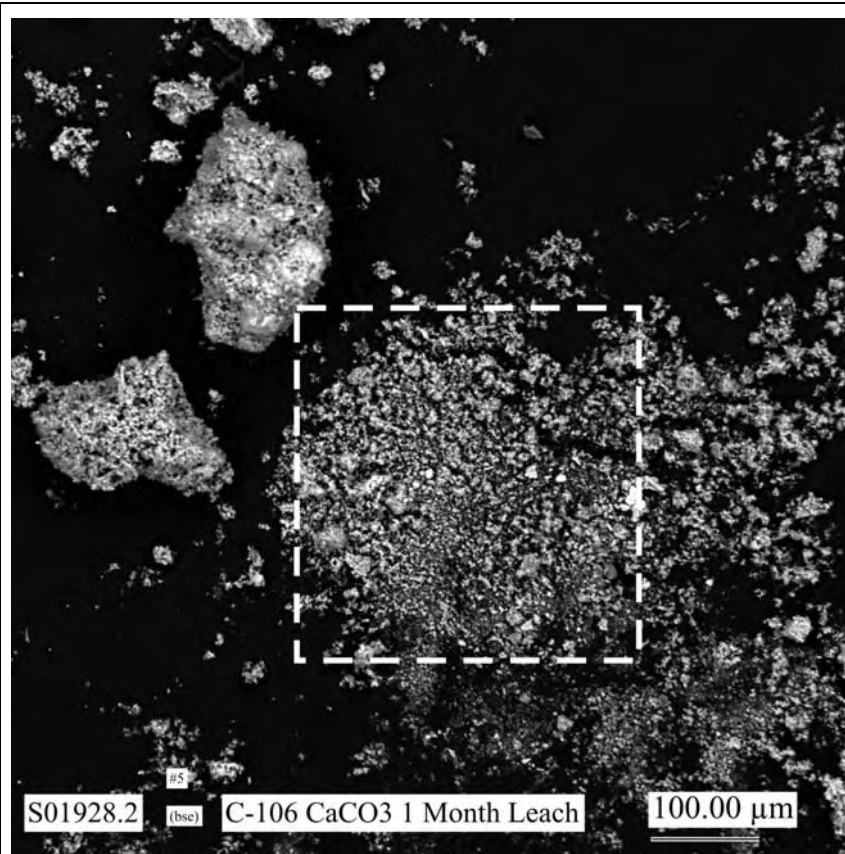


Figure D.2. Micrograph Showing at Higher Magnification the Area Indicated by the White Dashed-Line Square in Figure D.1

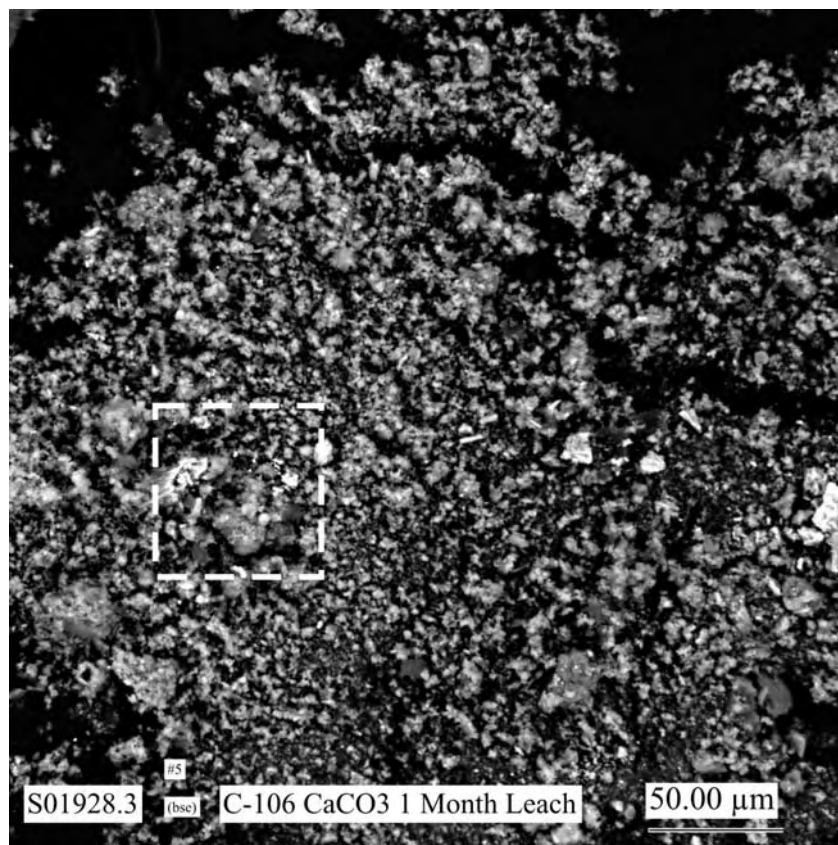


Figure D.3. Micrograph Showing at Higher Magnification the Area Indicated by the White Dashed-Line Square in Figure D.2

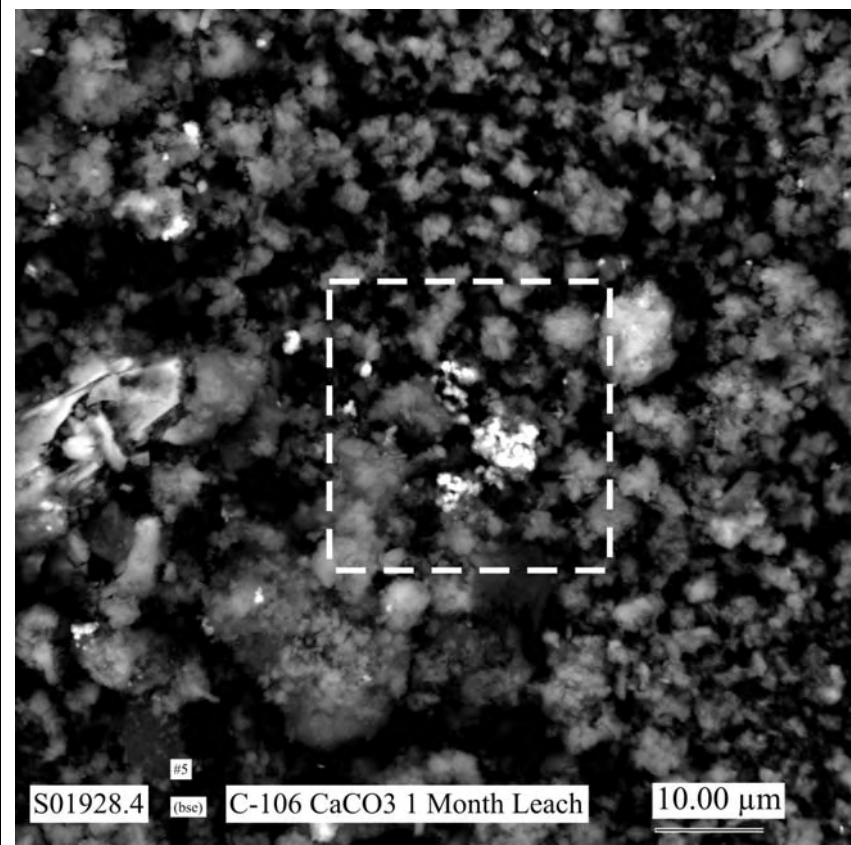


Figure D.4. Micrograph Showing at Higher Magnification the Area Indicated by the White Dashed-Line Square in Figure D.3

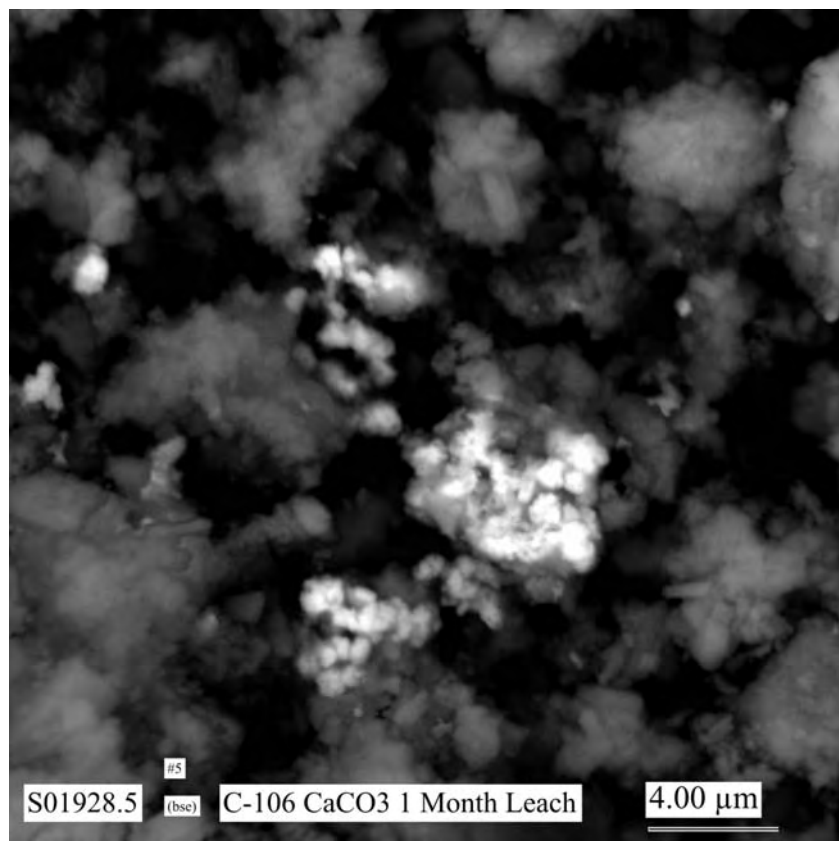


Figure D.5. Micrograph Showing at Higher Magnification the Area Indicated by the White Dashed-Line Square in Figure D.4 (areas where EDS analyses were made are shown in Figure D.17)

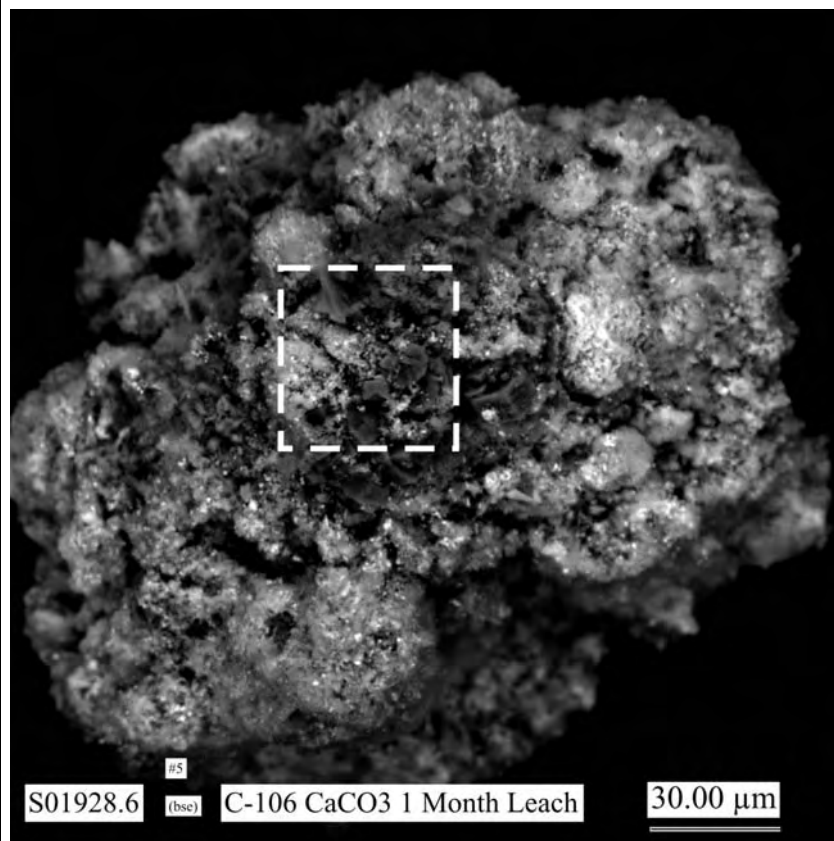


Figure D.6. Micrograph Showing Morphologies of Typical Particles in SEM Sample of 1-Month $\text{Ca}(\text{OH})_2/\text{CaCO}_3$ -Leached Residual Waste from Tank C-106

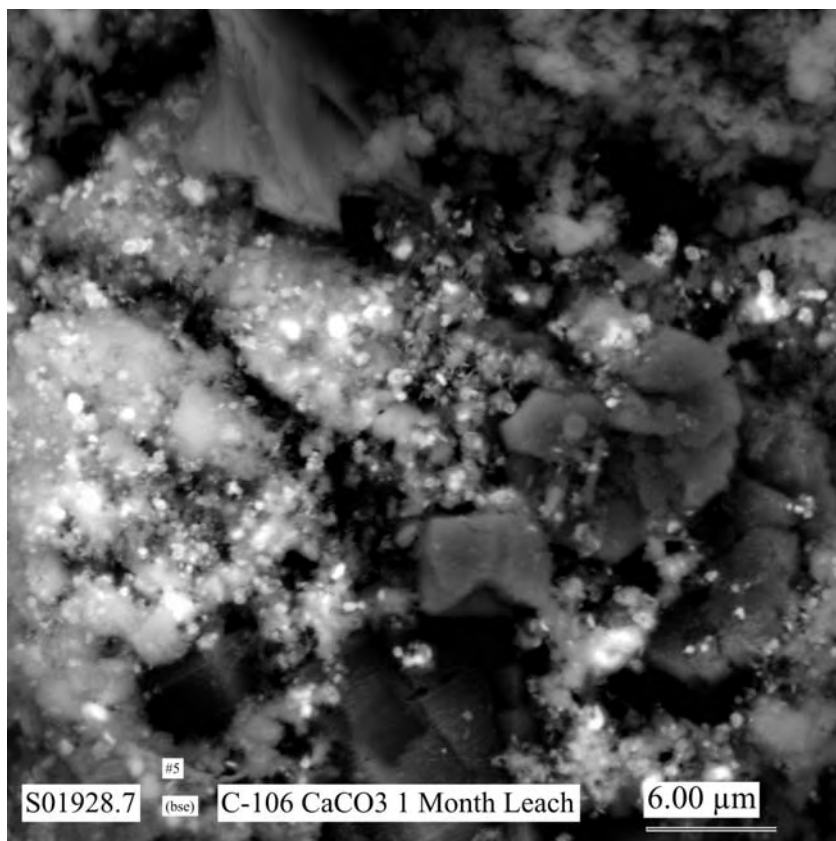


Figure D.7. Micrograph Showing at Higher Magnification the Area Indicated by the White Dashed-Line Square in Figure D.6 (areas where EDS analyses were made are shown in Figure D.18)

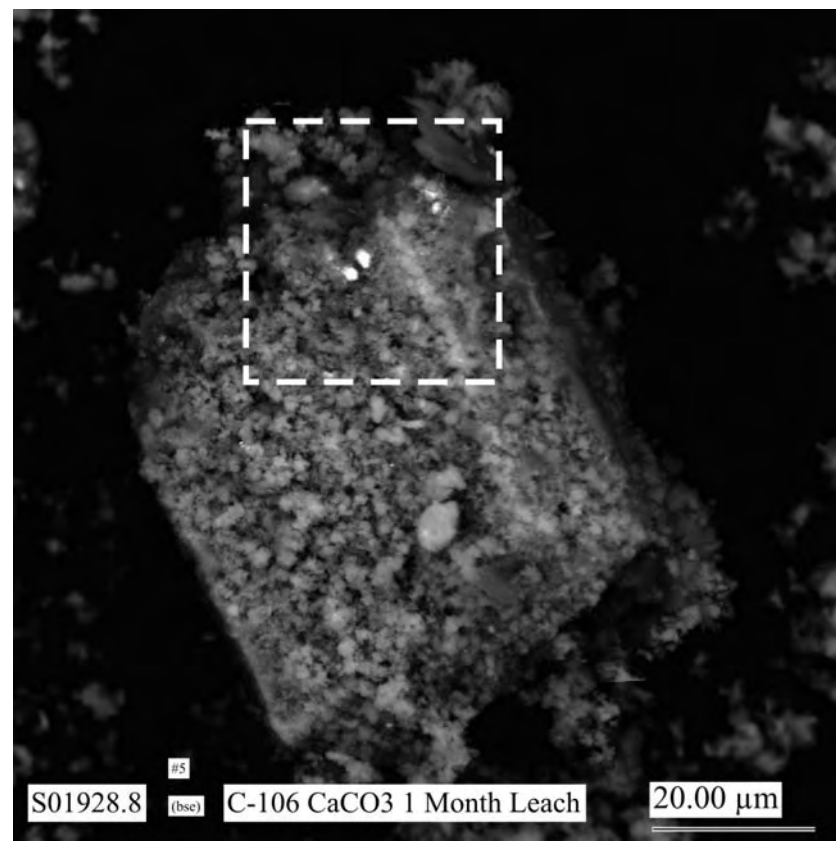


Figure D.8. Micrograph Showing Morphologies of Typical Particle Aggregates in SEM Sample of 1-Month $\text{Ca}(\text{OH})_2/\text{CaCO}_3$ -Leached Residual Waste from Tank C-106

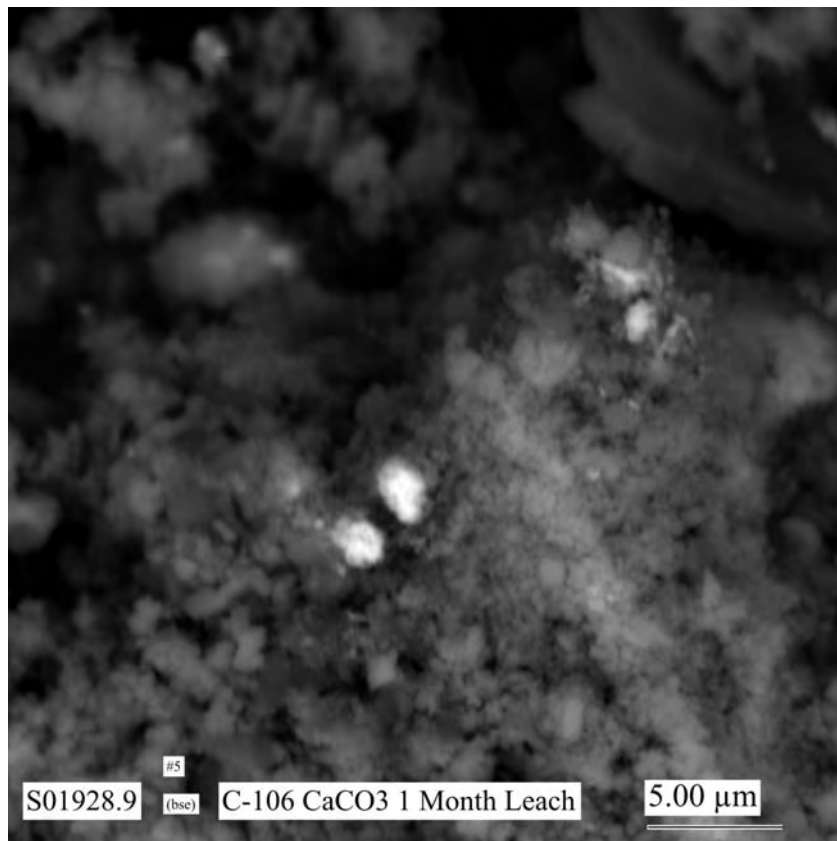


Figure D.9. Micrograph Showing at Higher Magnification the Area Indicated by the White Dashed-Line Square in Figure D.8 (areas where EDS analyses were made are shown in Figure D.19)

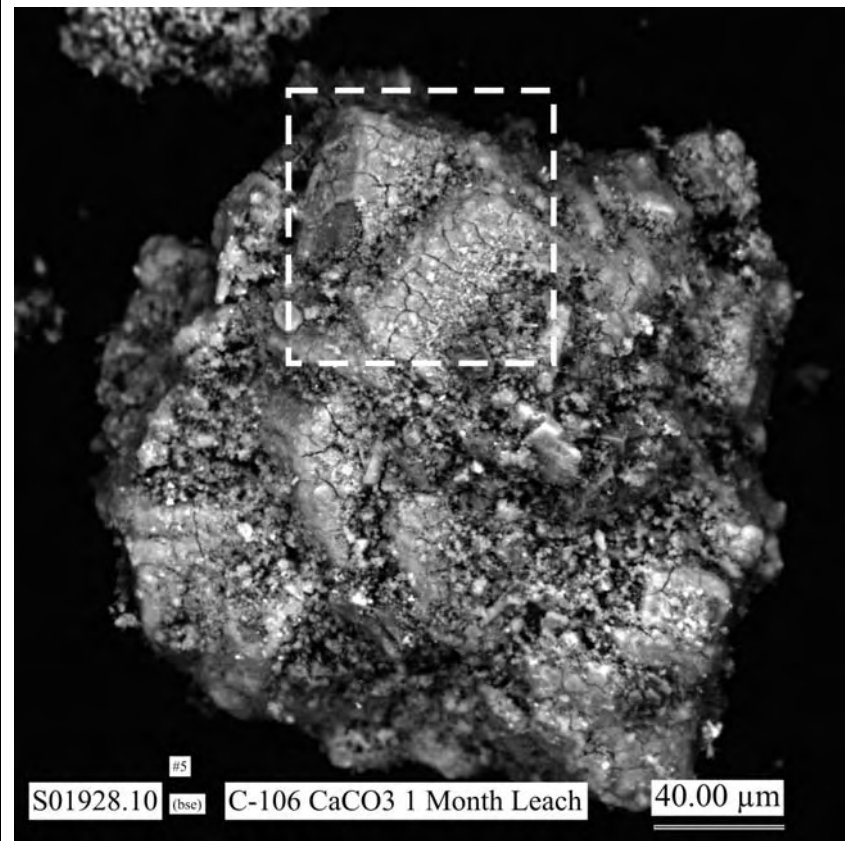


Figure D.10. Micrograph Showing Morphologies of Typical Particles in SEM Sample of 1-Month $\text{Ca}(\text{OH})_2/\text{CaCO}_3$ -Leached Residual Waste from Tank C-106

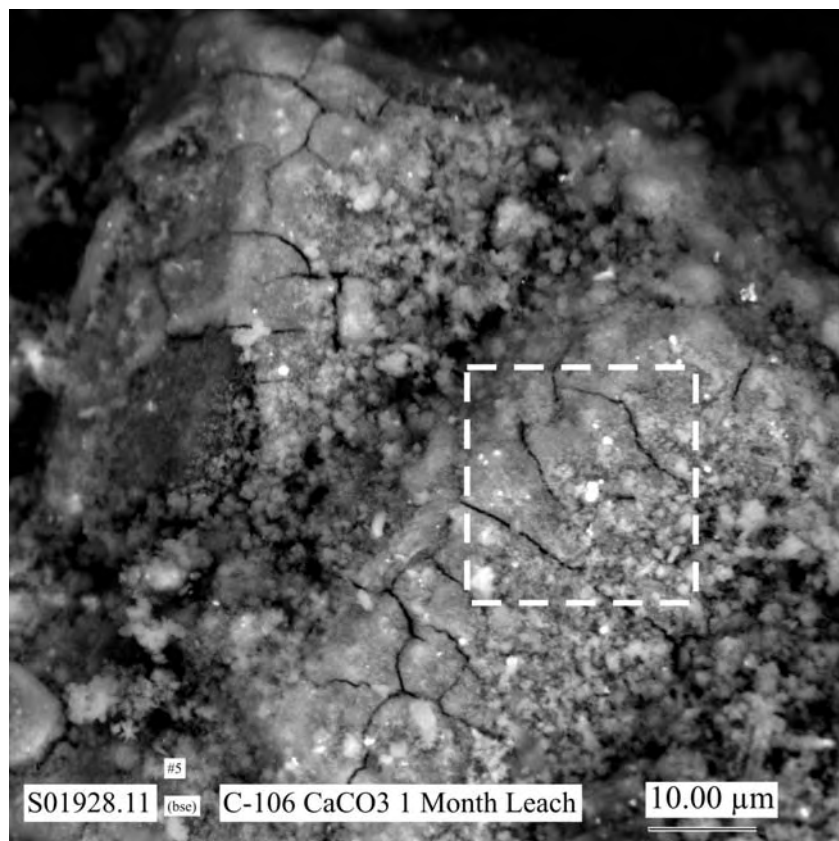


Figure D.11. Micrograph Showing at Higher Magnification the Area Indicated by the White Dashed-Line Square in Figure D.10 (areas where EDS analyses were made are shown in Figure D.20)

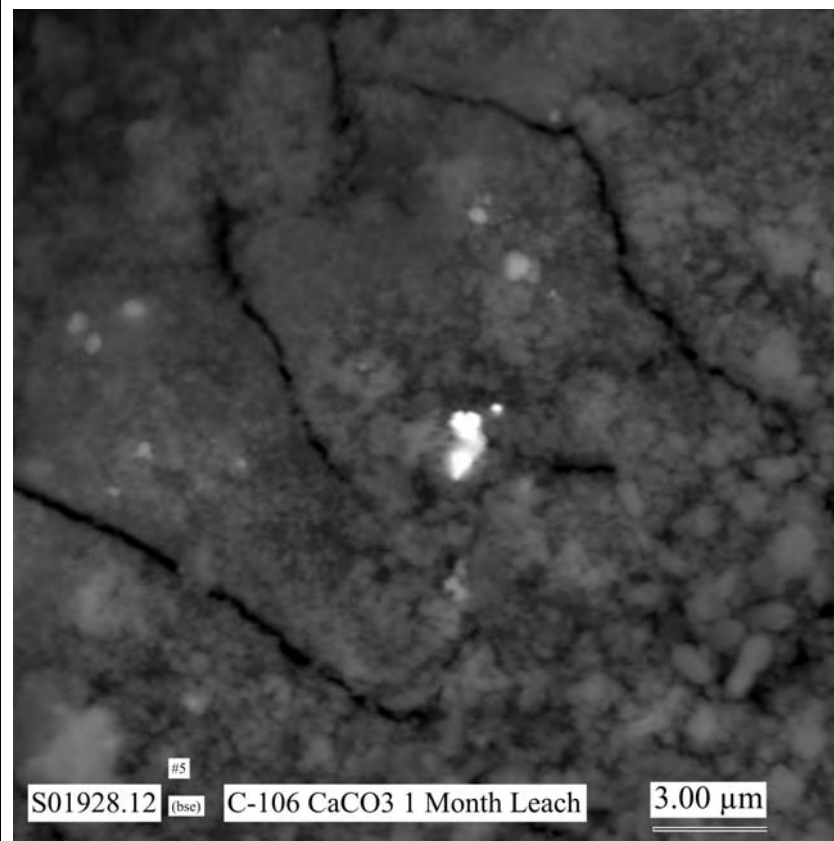


Figure D.12. Micrograph Showing at Higher Magnification the Area Indicated by the White Dashed-Line Square in Figure D.11 (areas where EDS analyses were made are shown in Figure D.21)

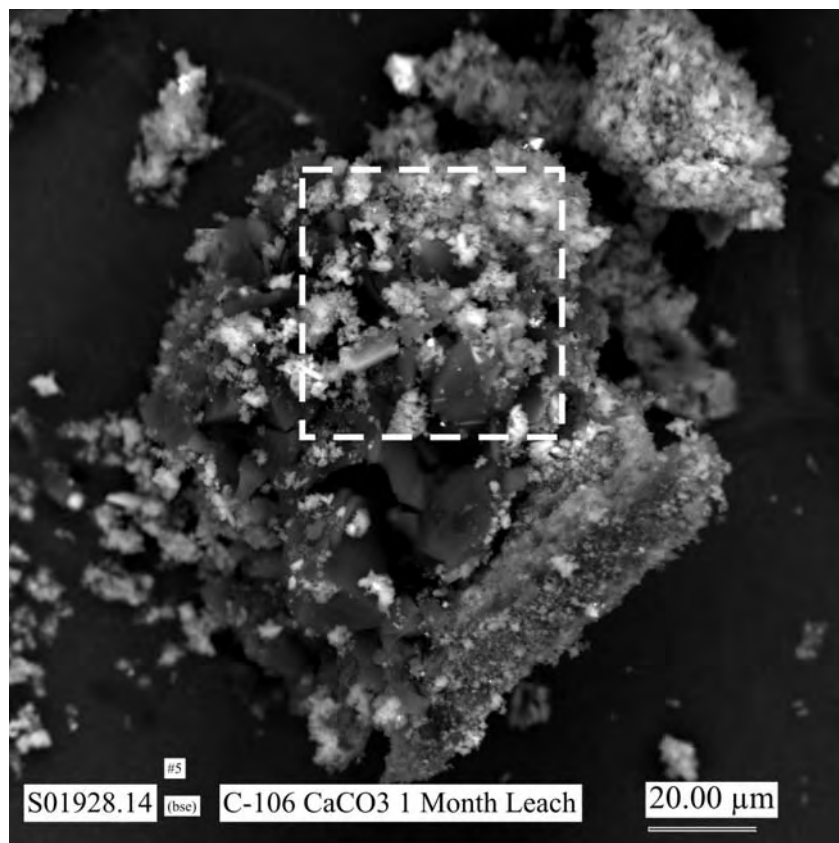


Figure D.13. Micrograph Showing Morphologies of Typical Particles in SEM Sample of 1-Month $\text{Ca}(\text{OH})_2/\text{CaCO}_3$ -Leached Residual Waste from Tank C-106

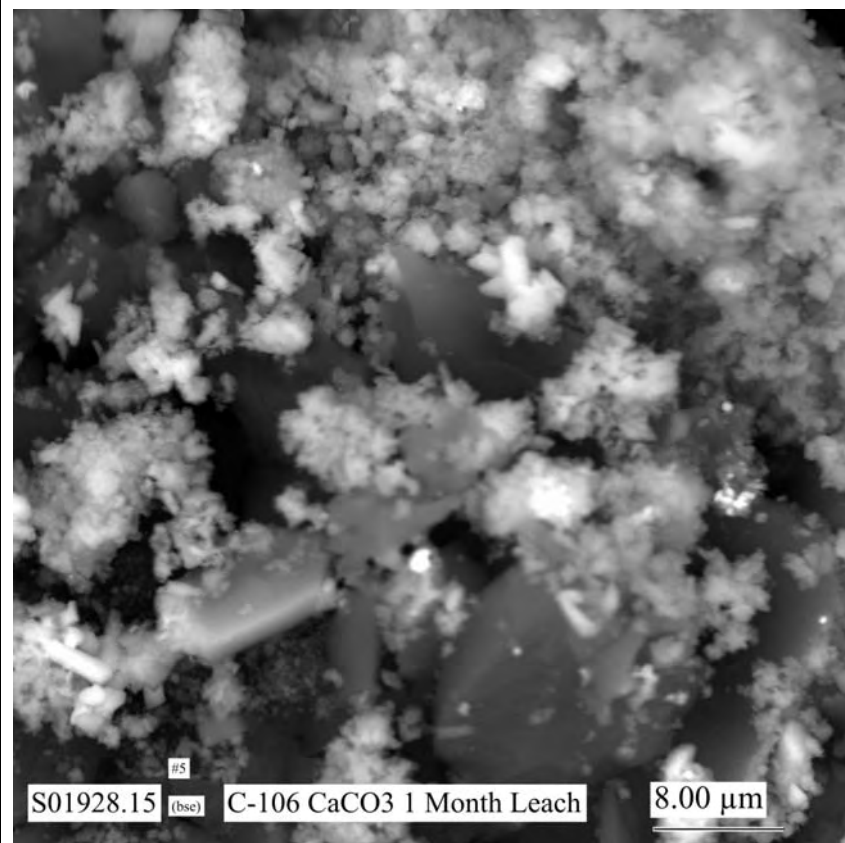


Figure D.14. Micrograph Showing at Higher Magnification the Area Indicated by the White Dashed-Line Square in Figure D.13 (areas where EDS analyses were made are shown in Figure D.23)

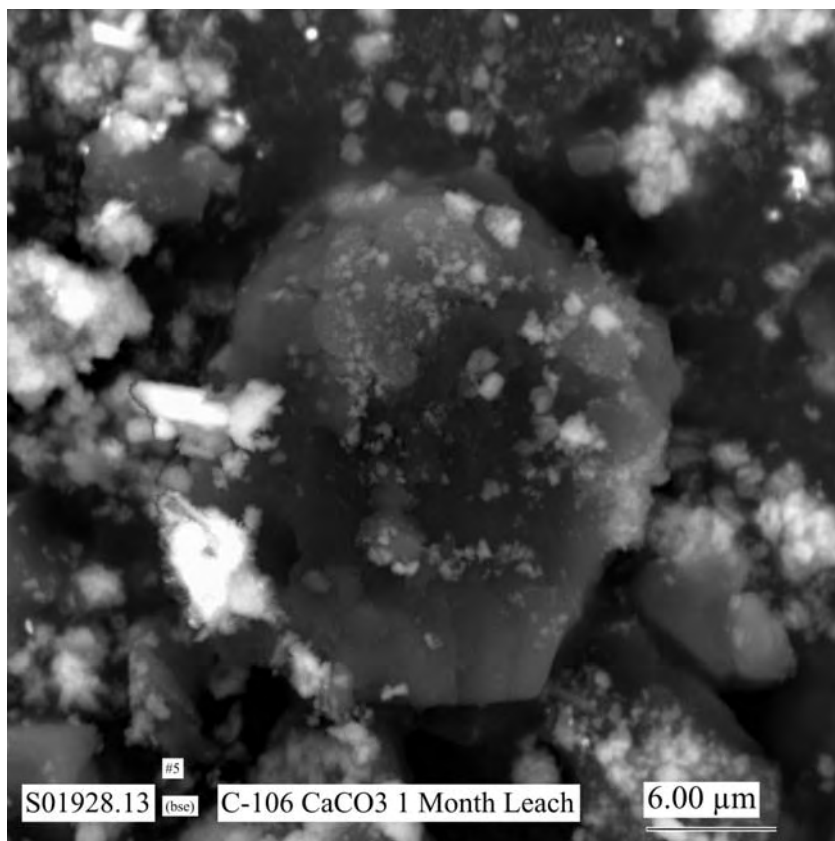


Figure D.15. Micrograph Showing Morphologies of Typical Particles in SEM Sample of 1-Month $\text{Ca}(\text{OH})_2/\text{CaCO}_3$ -Leached Residual Waste from Tank C-106 (areas where EDS analyses were made are shown in Figure D.22)

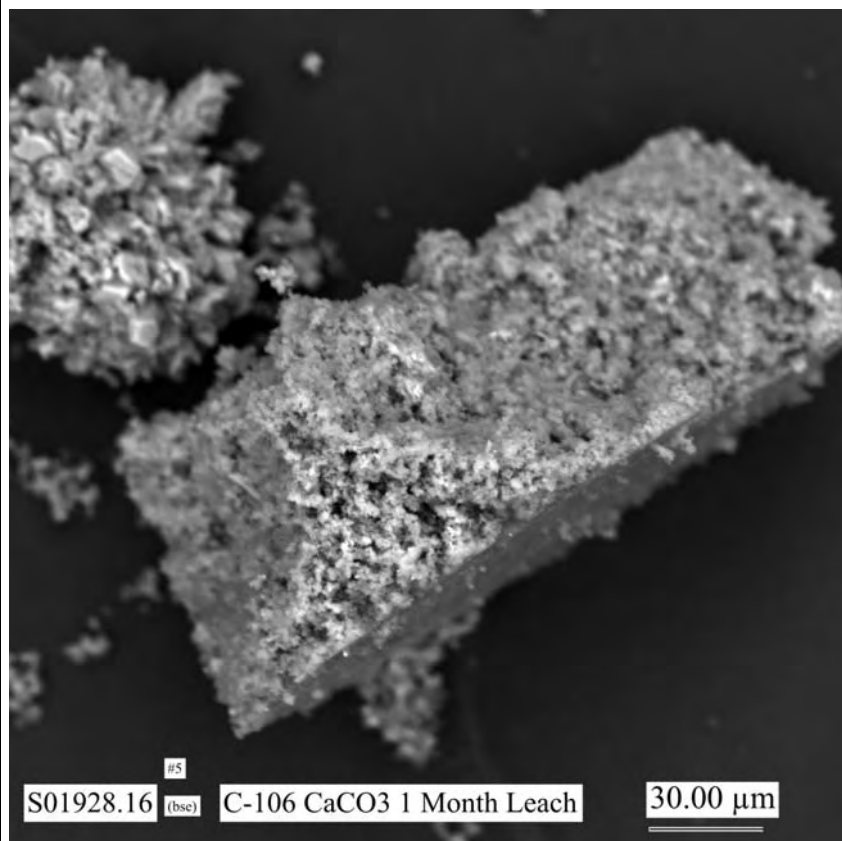


Figure D.16. Micrograph Showing Morphologies of Typical Particles in SEM Sample of 1-Month $\text{Ca}(\text{OH})_2/\text{CaCO}_3$ -Leached Residual Waste from Tank C-106 (areas just below center of the micrograph where EDS analyses were made are shown at higher magnification in Figure D.24)

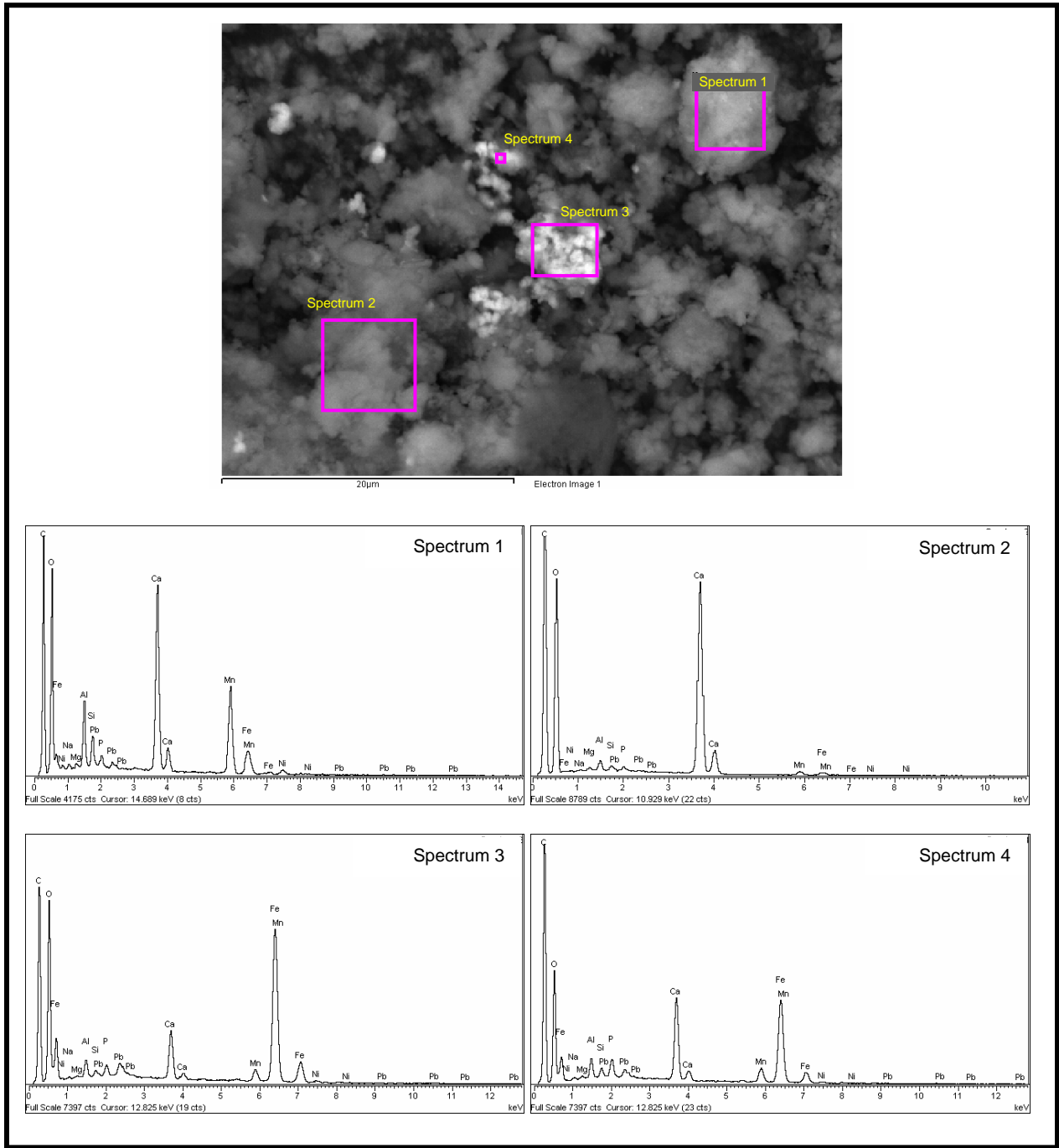


Figure D.17. EDS Spectra for Numbered Areas Marked in Pink in SEM Micrograph Shown at Top of Figure

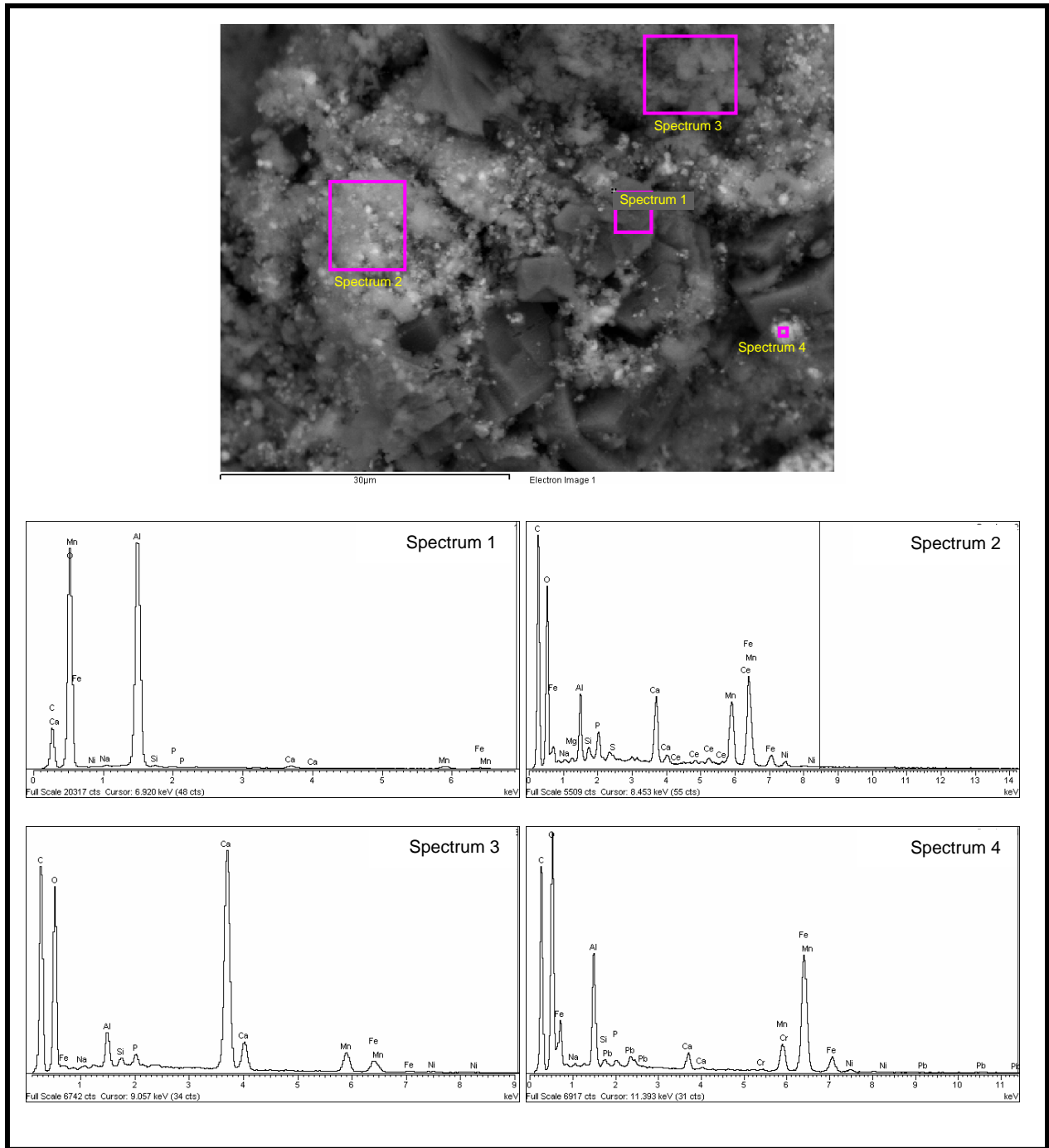


Figure D.18. EDS Spectra for Numbered Areas Marked in Pink in SEM Micrograph Shown at Top of Figure

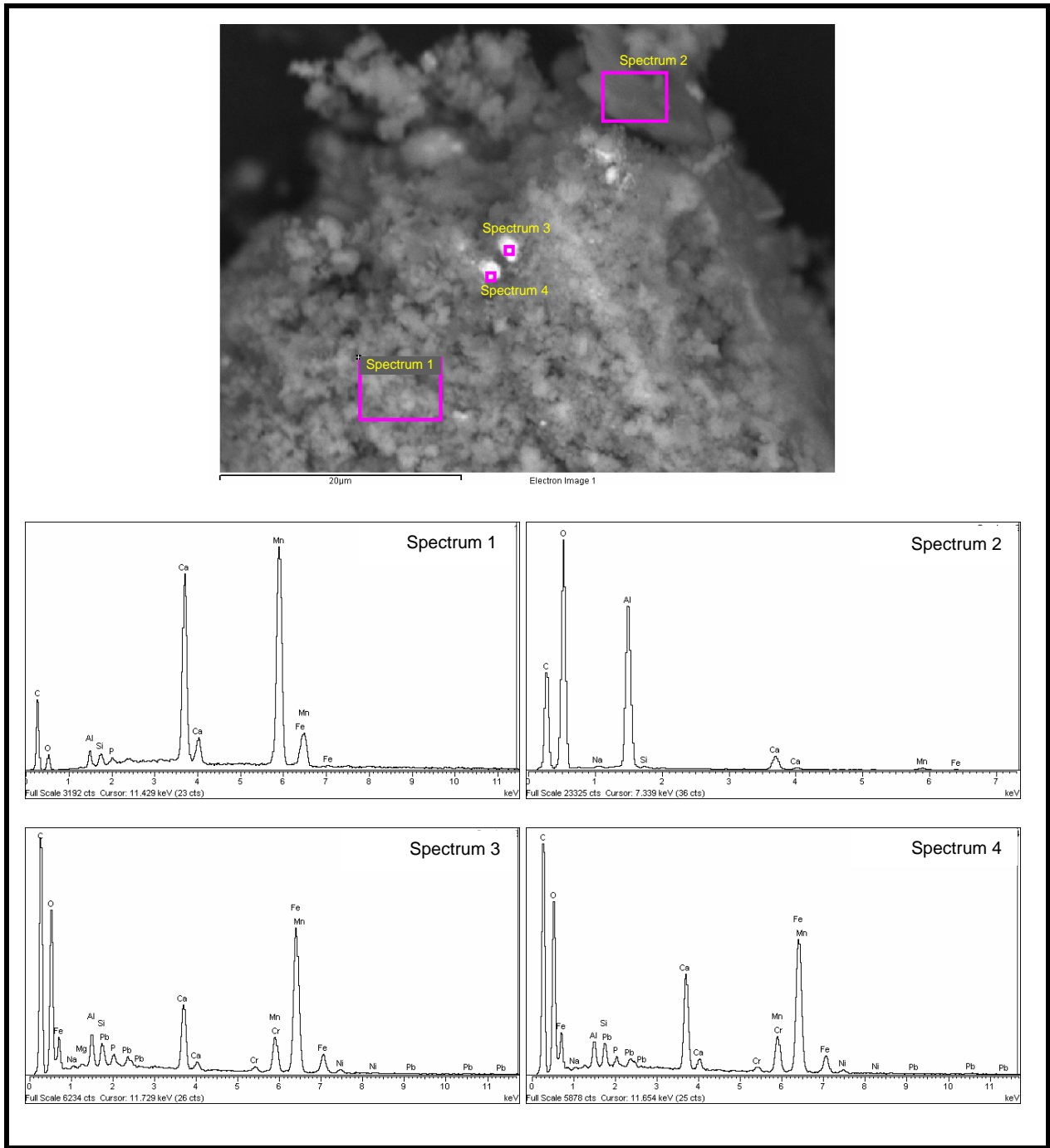


Figure D.19. EDS Spectra for Numbered Areas Marked in Pink in SEM Micrograph Shown at Top of Figure

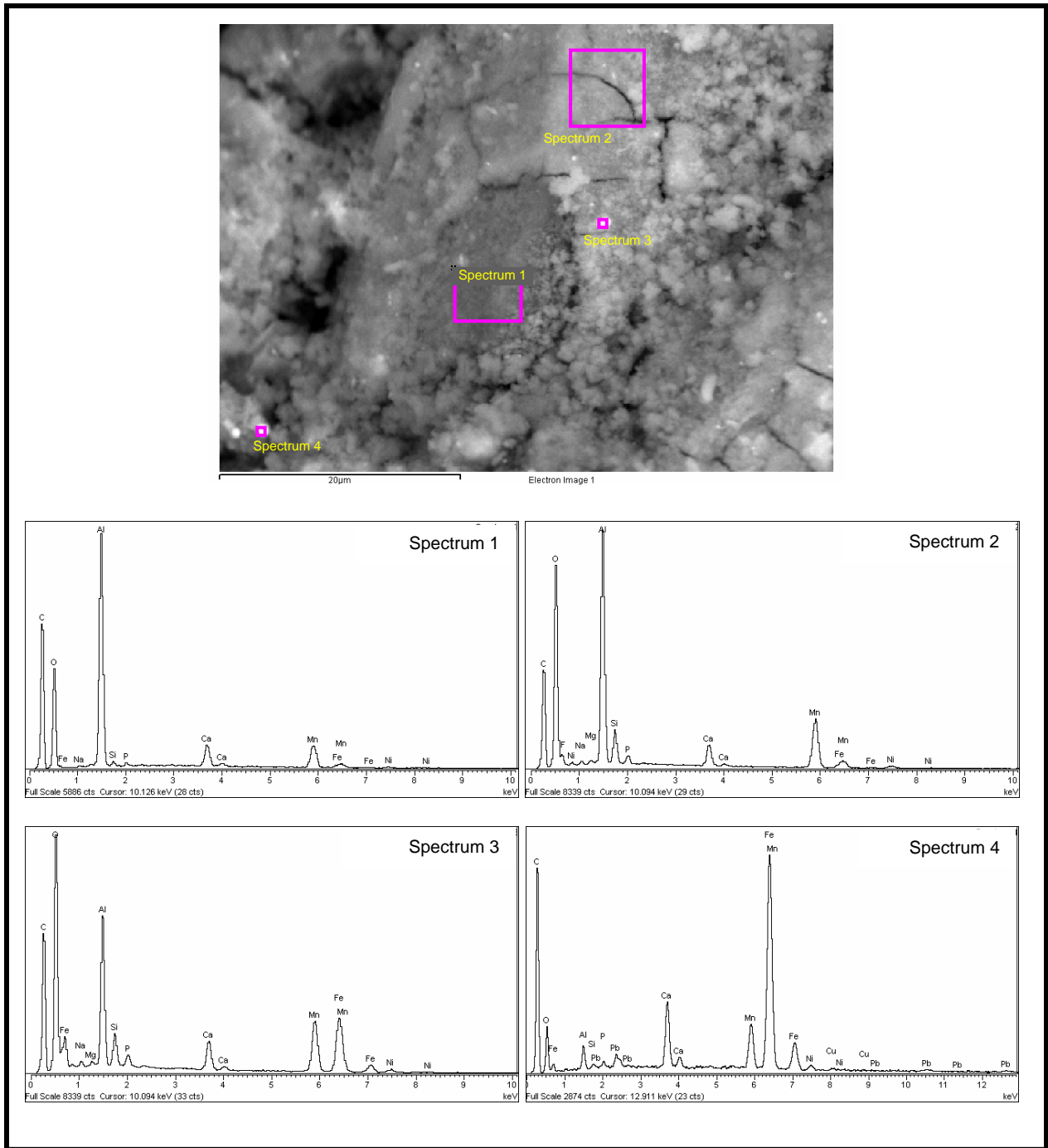


Figure D.20. EDS Spectra for Numbered Areas Marked in Pink in SEM Micrograph Shown at Top of Figure

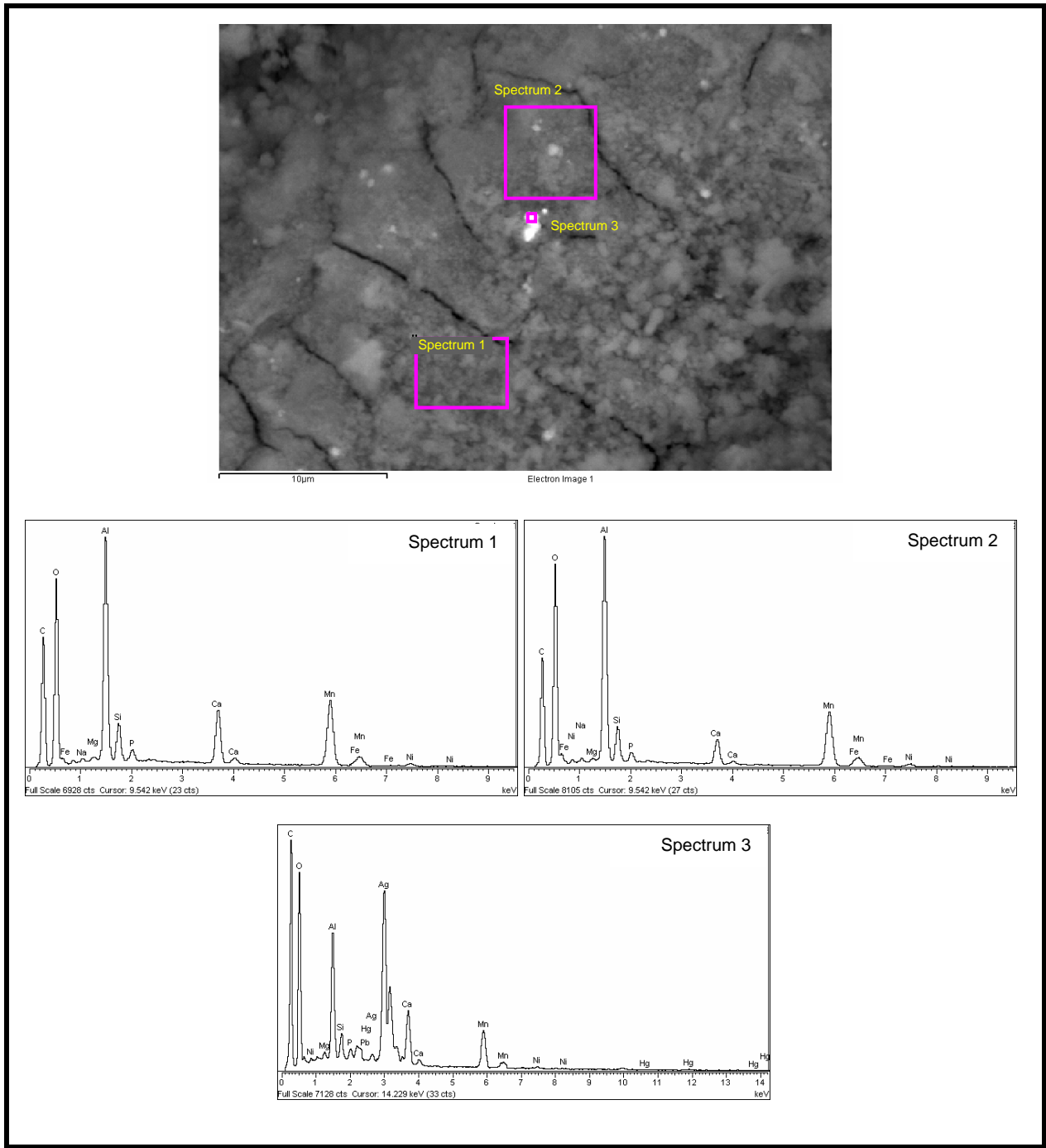


Figure D.21. EDS Spectra for Numbered Areas Marked in Pink in SEM Micrograph Shown at Top of Figure

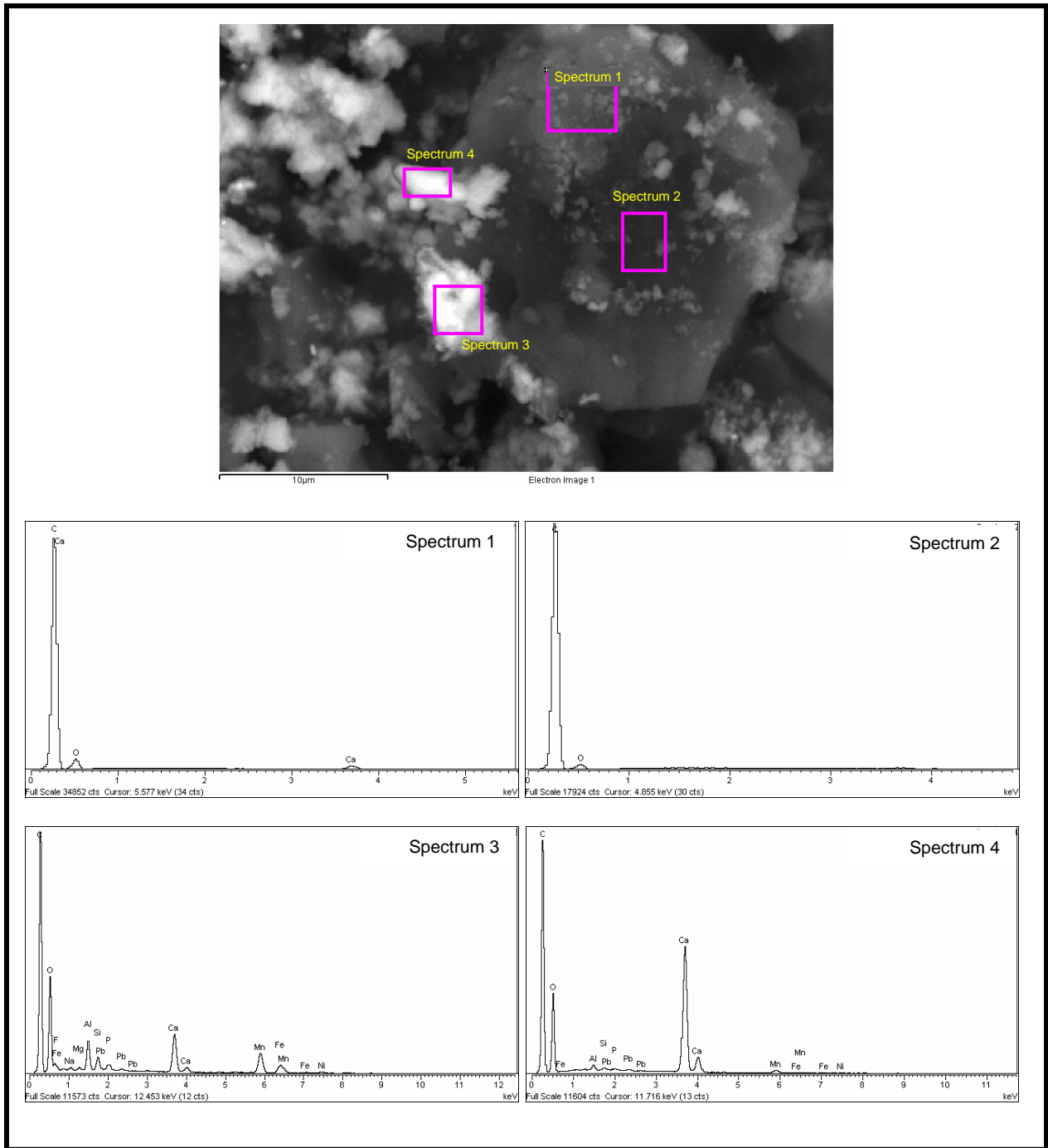


Figure D.22. EDS Spectra for Numbered Areas Marked in Pink in SEM Micrograph Shown at Top of Figure

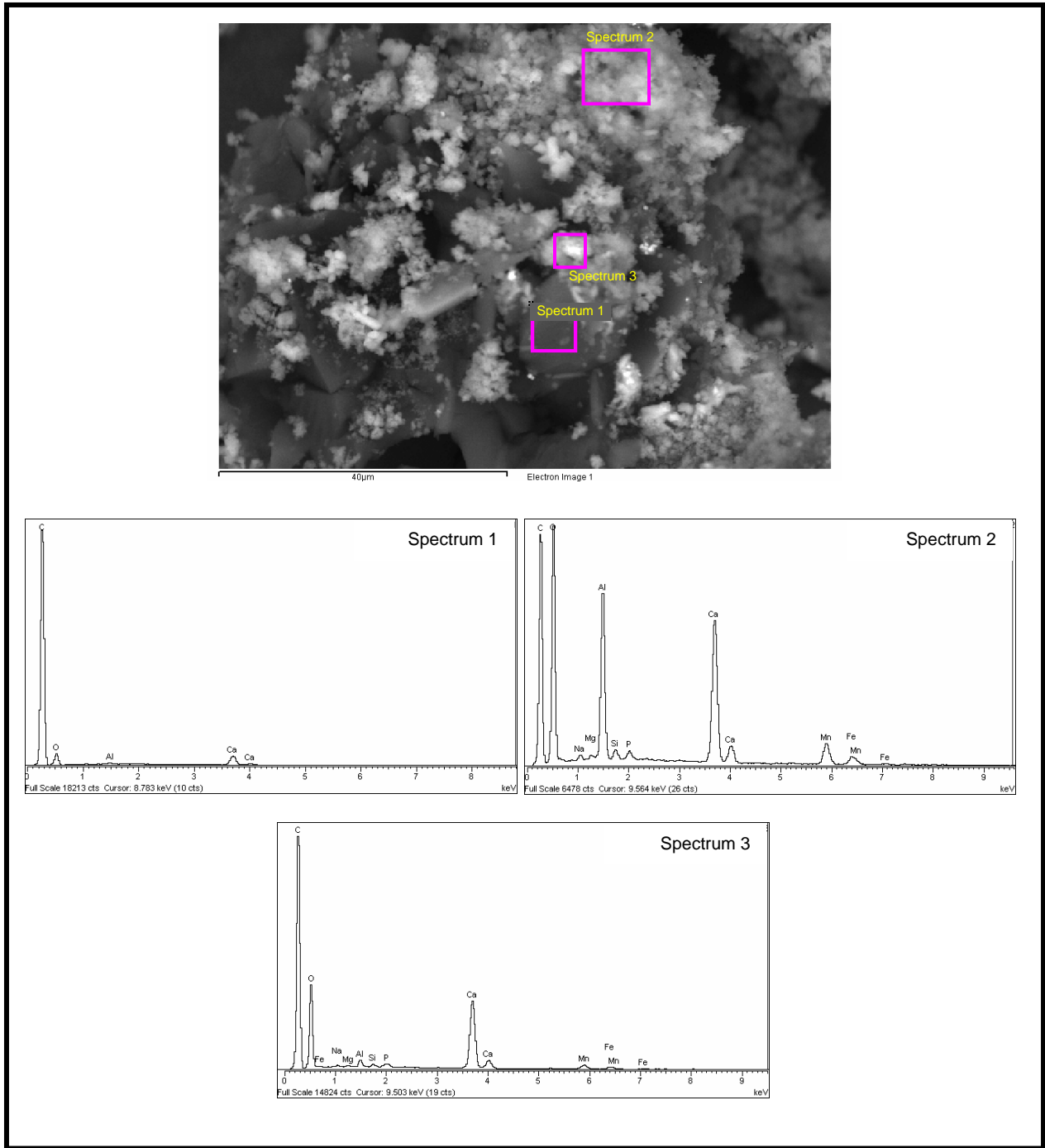


Figure D.23. EDS Spectra for Numbered Areas Marked in Pink in SEM Micrograph Shown at Top of Figure

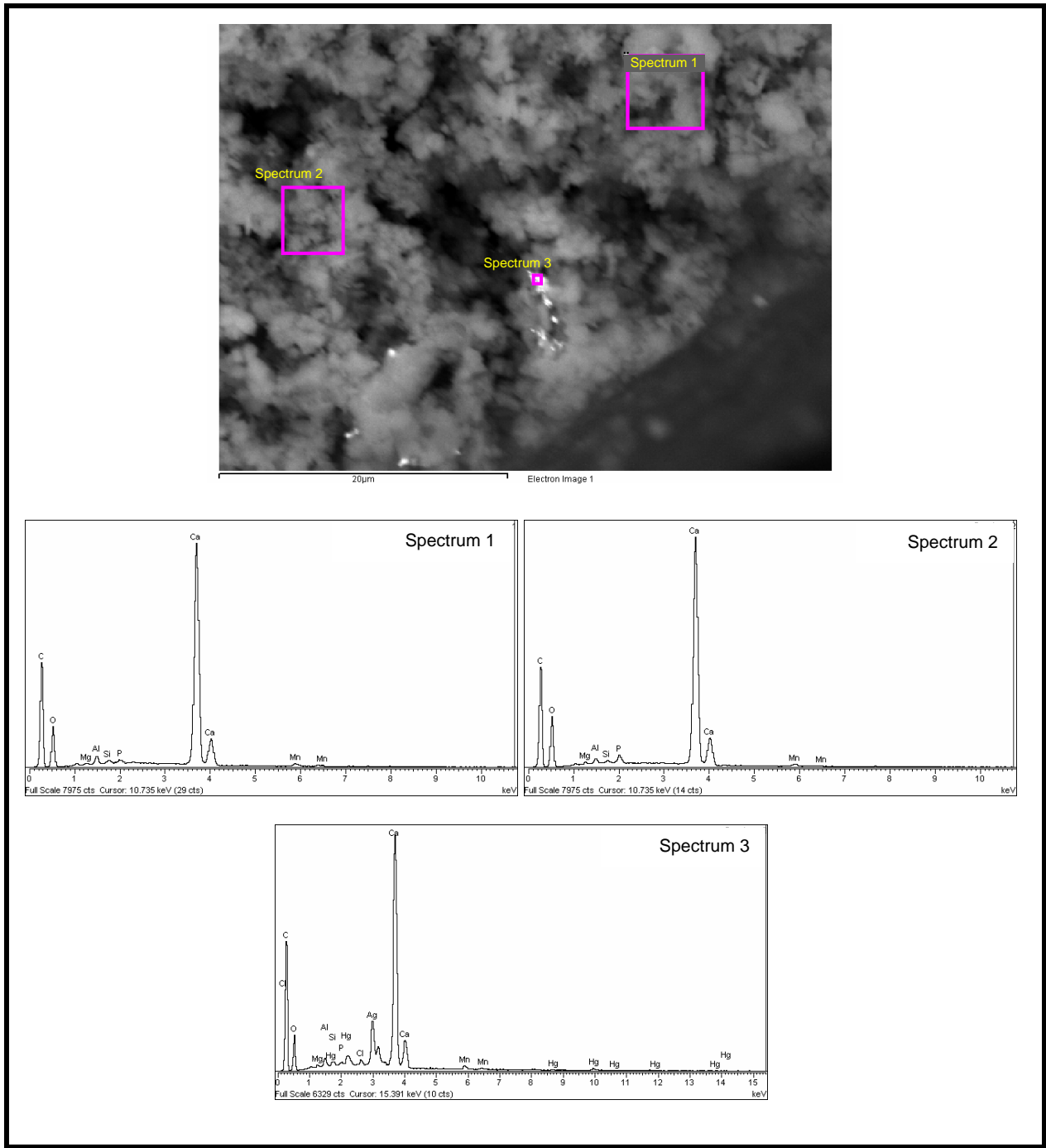


Figure D.24. EDS Spectra for Numbered Areas Marked in Pink in SEM Micrograph Shown at Top of Figure

Appendix E

SEM Micrographs and EDS Results for Stage 6 Sequential $\text{Ca}(\text{OH})_2/\text{CaCO}_3$ -Leached Tank C-106 Residual Waste

Appendix E

SEM Micrographs and EDS Results for Stage 6 Sequential Ca(OH)₂/CaCO₃-Leached Tank C-106 Residual Waste

This appendix includes the scanning electron microscope (SEM) micrographs and the energy-dispersive x-ray spectrometry (EDS) spectra, and element-distribution maps for samples of Stage 6 sequential Ca(OH)₂/CaCO₃-leached residual waste from tank C-106. The operating conditions for the SEM and procedures used for mounting the SEM samples are described in Section 3.4 of the main report.

The identification number for the digital micrograph image file, descriptor for the type of sample, and a size scale bar are given, respectively, at the bottom left, center, and right of each SEM micrograph in this appendix. Micrographs labeled by “BSE” to the immediate right of the digital image file number indicate that the micrograph was collected with backscattered electrons. Sample areas or particles identified by a letter, arrow, and/or outlined by a white or black dotted-line squares in a micrograph designate sample material that was imaged at higher magnification, which is typically shown in figure(s) that immediately follow in the series for that sample. The SEM micrographs for this leached material are shown in Figures E.1 through E.12. The EDS spectra for this mount are given in Figures E.13 through E.21.

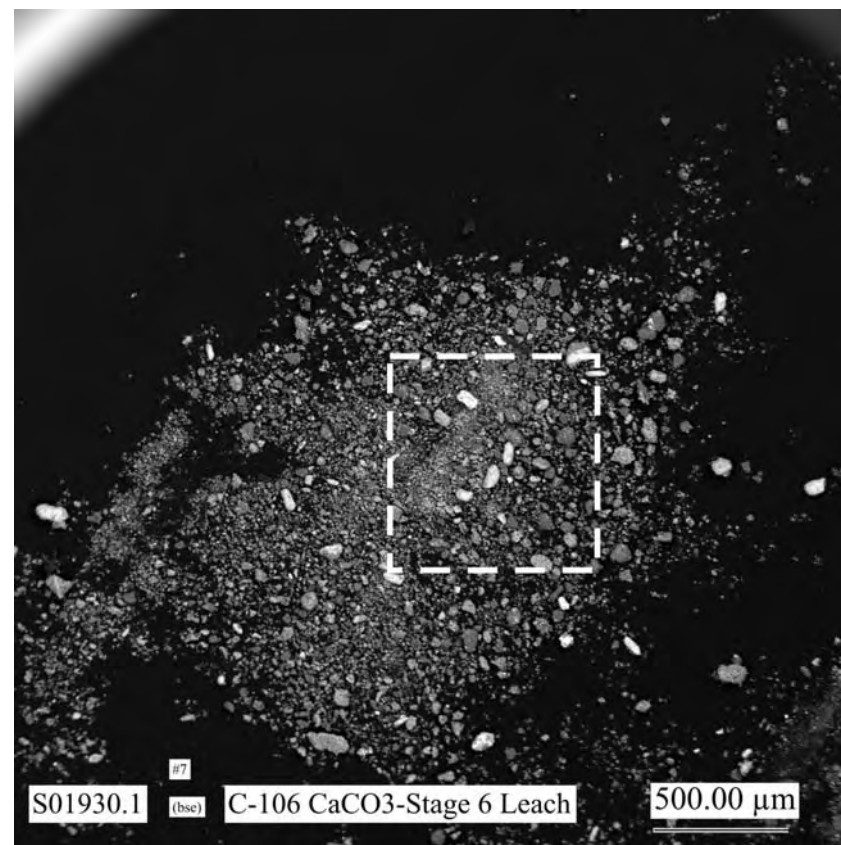


Figure E.1. Low Magnification SEM Micrograph Showing General Morphologies of Particles in the SEM Sample of Stage 6 Sequential $\text{Ca}(\text{OH})_2/\text{CaCO}_3$ -Leached Residual Waste from Tank C-106

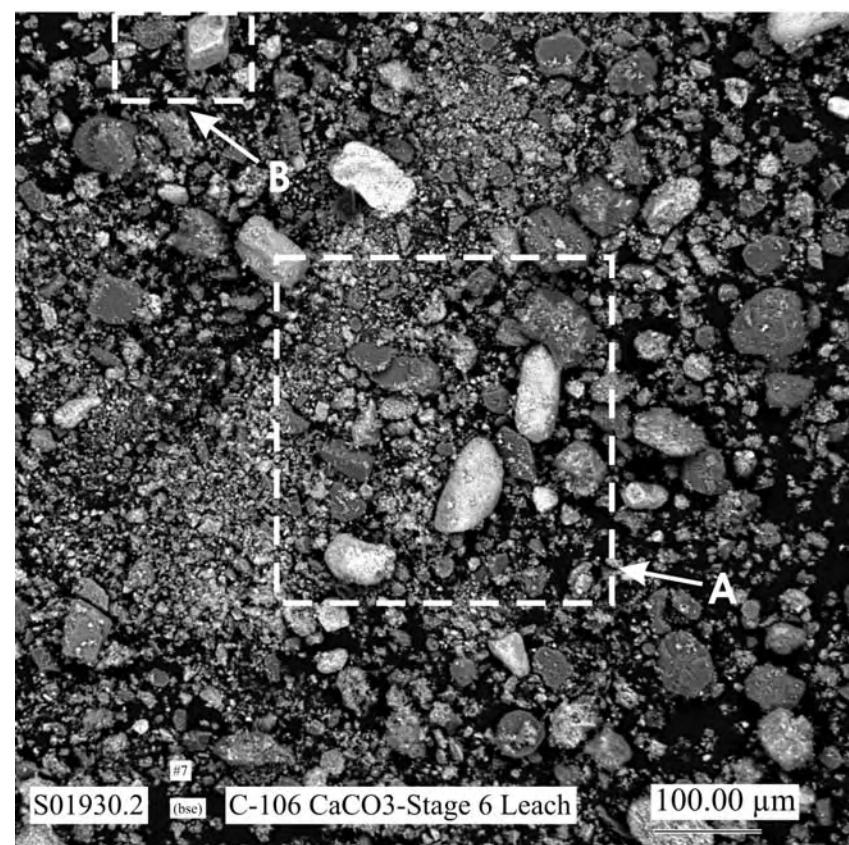


Figure E.2. Micrograph Showing at Higher Magnification the Area Indicated by the White Dashed-Line Square in Figure E.1

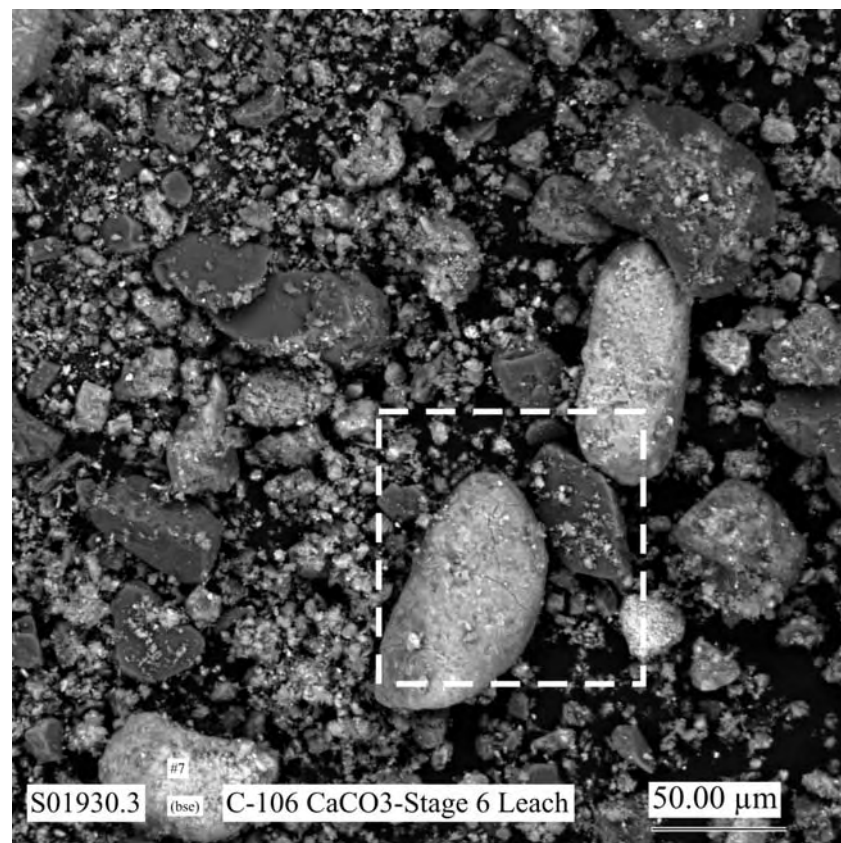


Figure E.3. Micrograph Showing at Higher Magnification the Particles the Area Indicated by the White Dashed-Line Square Labeled A in Figure E.2

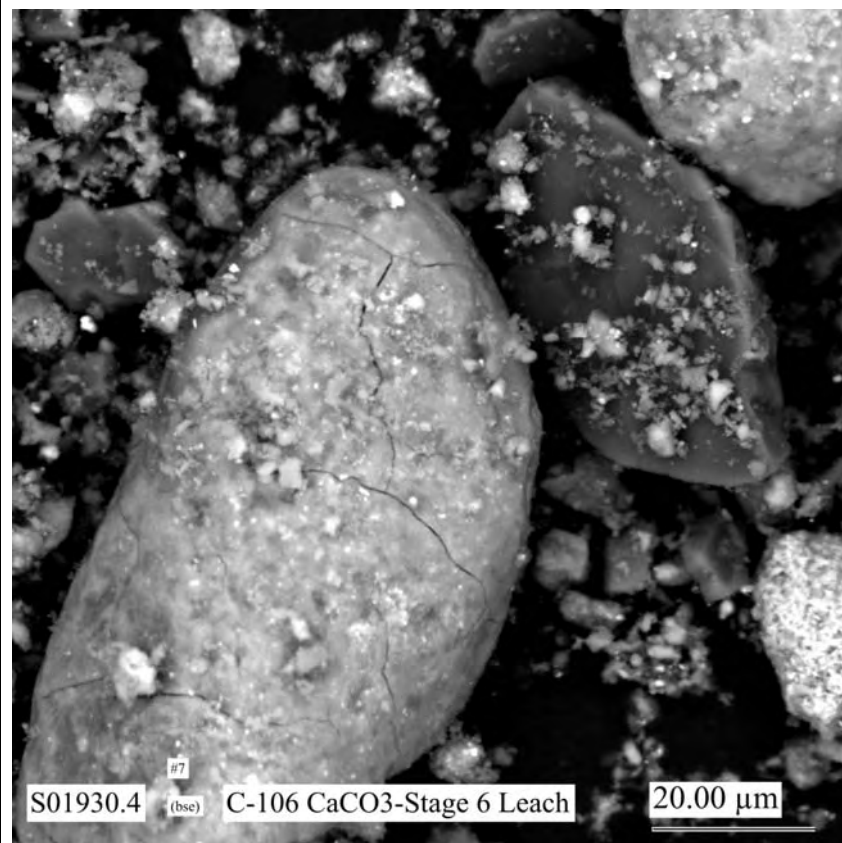


Figure E.4. Micrograph Showing at Higher Magnification the Area Indicated by the White Dashed-Line Square in Figure E.3 (areas where EDS analyses were made are shown in Figure E.13)

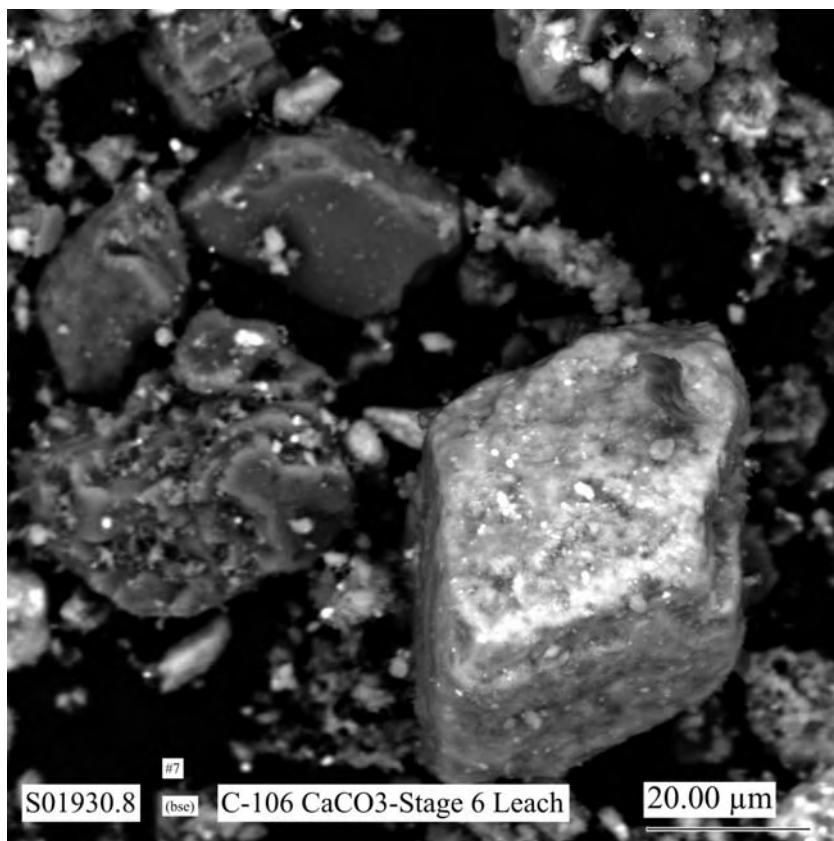


Figure E.5. Micrograph Showing at Higher Magnification the Particles the Area Indicated by the White Dashed-line Square Labeled B in Figure E.2 (areas where EDS analyses were made are shown in Figure E.17)

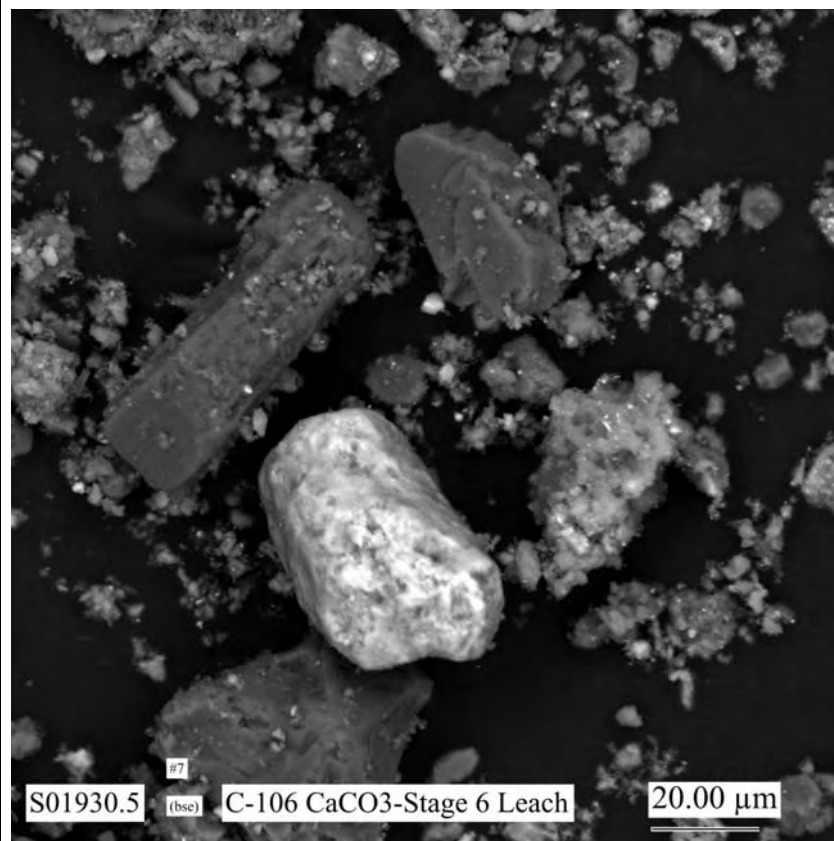


Figure E.6. Micrograph Showing Morphologies of Typical Particles in the SEM Sample of Stage 6 Sequential $\text{Ca(OH)}_2/\text{CaCO}_3$ -Leached Residual Waste from Tank C-106 (areas where EDS analyses were made are shown in Figure E.14)

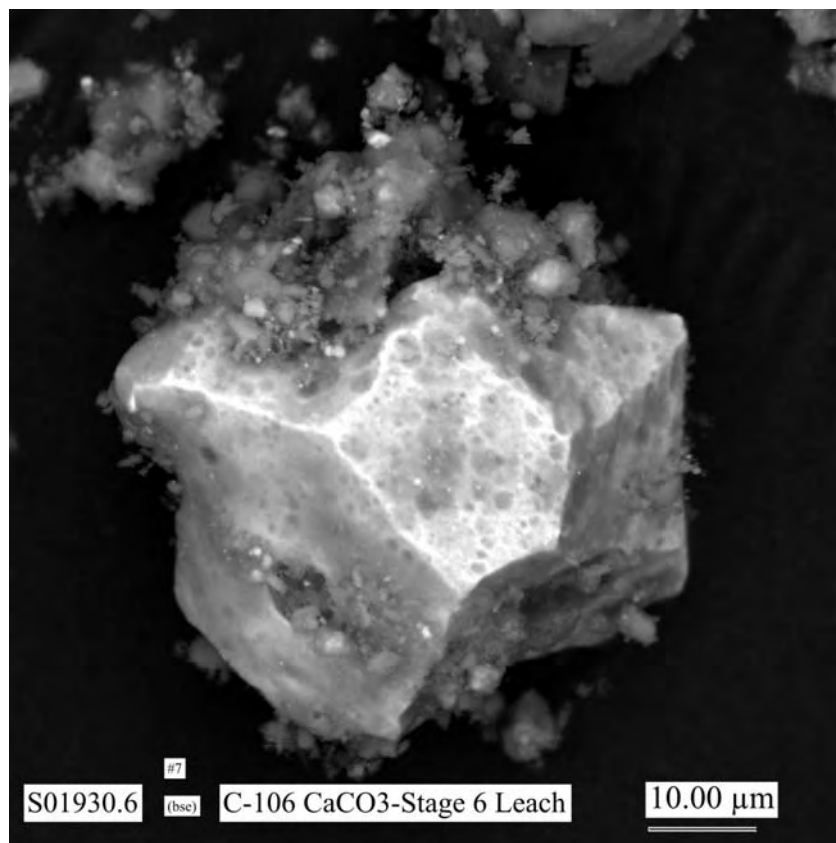


Figure E.7. Micrograph Showing Morphologies of Particles in the SEM Sample of Stage 6 Sequential $\text{Ca}(\text{OH})_2/\text{CaCO}_3$ -Leached Residual Waste from Tank C-106 (areas where EDS analyses were made are shown in Figure E.15)

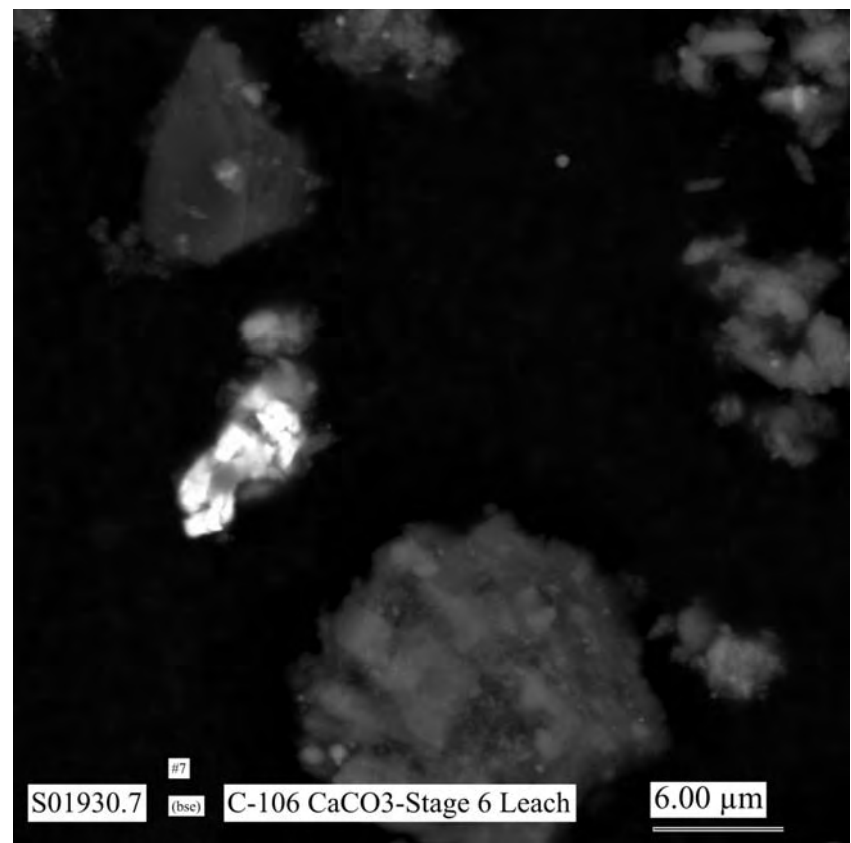


Figure E.8. Micrograph Showing Morphologies of Particles in the SEM Sample of Stage 6 Sequential $\text{Ca}(\text{OH})_2/\text{CaCO}_3$ -Leached Residual Waste from Tank C-106 (areas where EDS analyses were made are shown in Figure E.16)

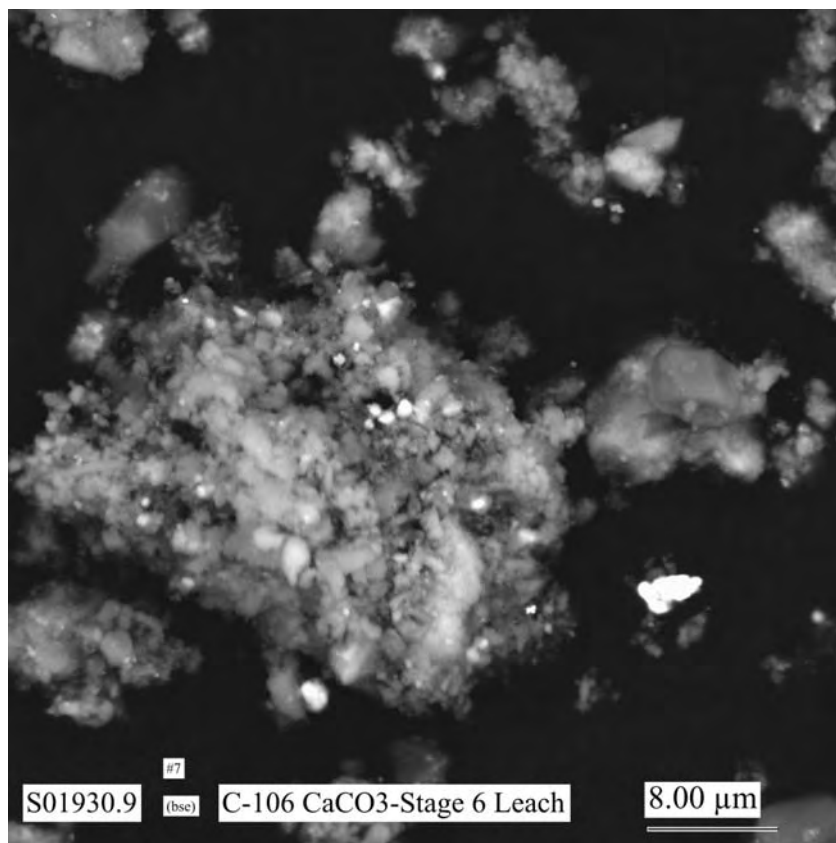


Figure E.9. Micrograph Showing Morphologies of Typical Particles in the SEM Sample of Stage 6 Sequential $\text{Ca}(\text{OH})_2/\text{CaCO}_3$ -Leached Residual Waste from Tank C-106 (areas where EDS analyses were made are shown in Figures E.18 and E.19)

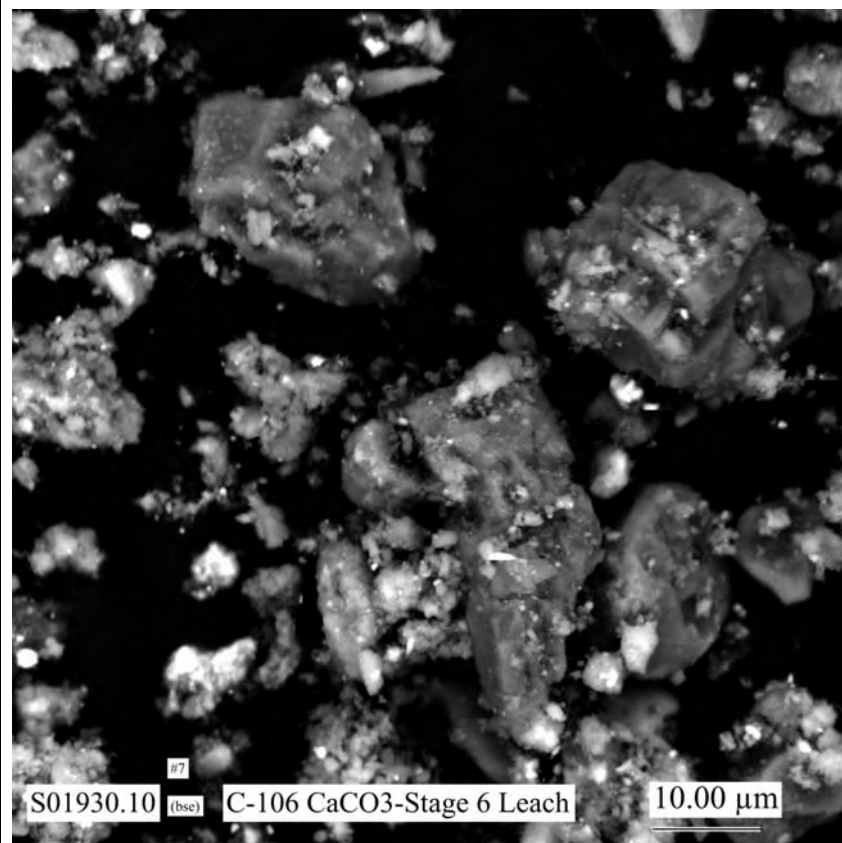


Figure E.10. Micrograph Showing Morphologies of Typical Particles in the SEM Sample of Stage 6 Sequential $\text{Ca}(\text{OH})_2/\text{CaCO}_3$ -Leached Residual Waste from Tank C-106

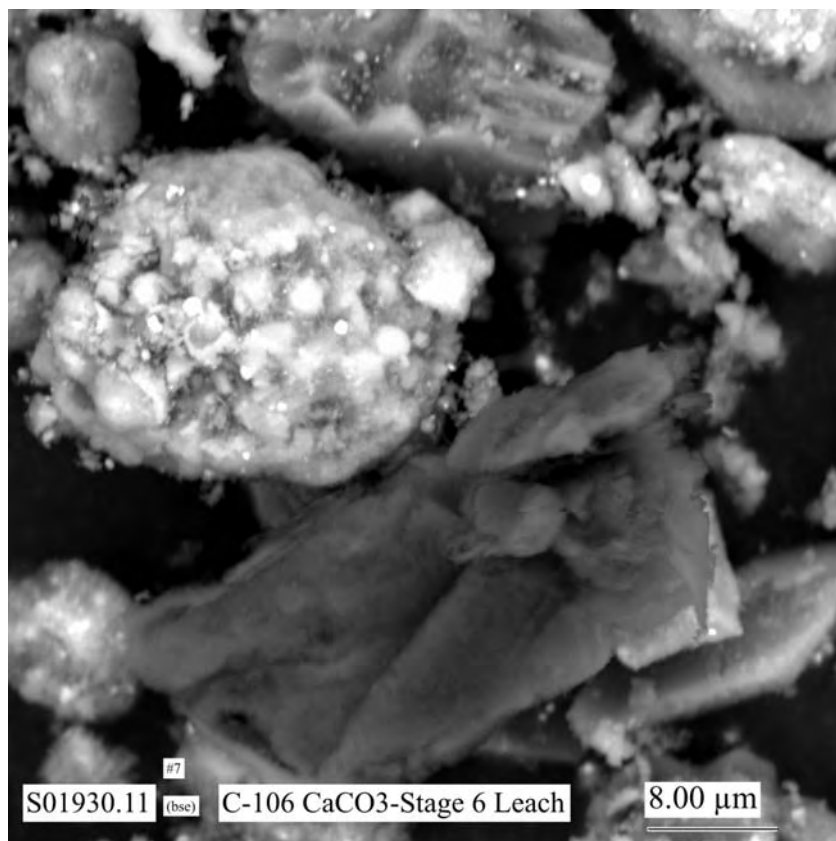


Figure E.11. Micrograph Showing Morphologies of Particles in the SEM Sample of Stage 6 Sequential $\text{Ca}(\text{OH})_2/\text{CaCO}_3$ -Leached Residual Waste from Tank C-106 (areas where EDS analyses were made are shown in Figure E.20)

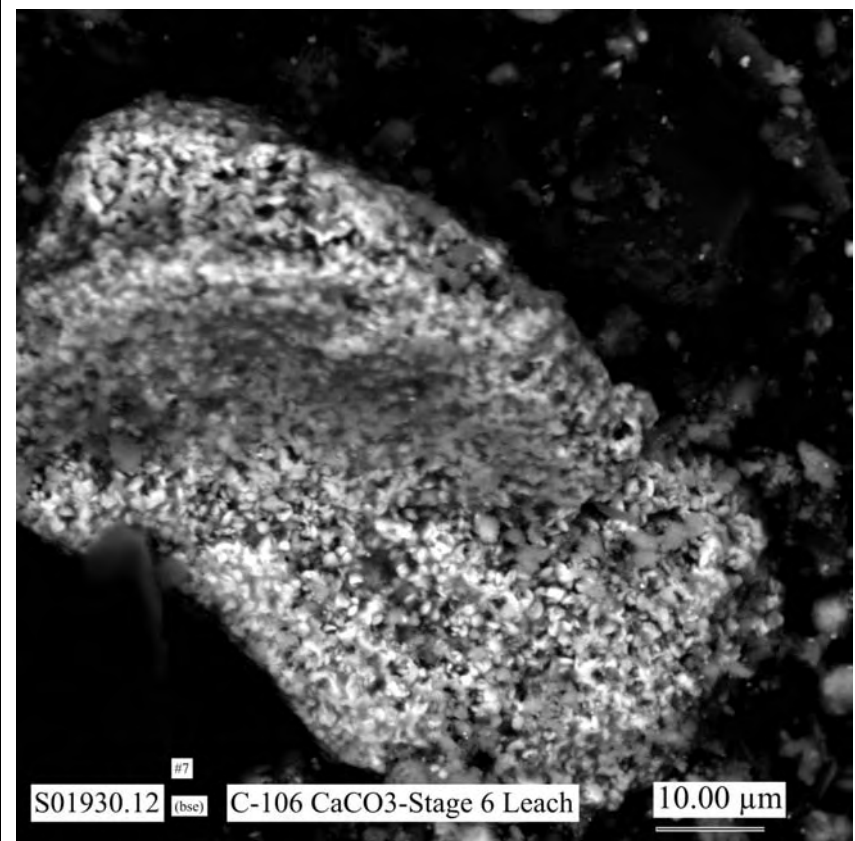


Figure E.12. Micrograph Showing Morphologies of Particles in the SEM Sample of Stage 6 Sequential $\text{Ca}(\text{OH})_2/\text{CaCO}_3$ -Leached Residual Waste from Tank C-106 (areas where EDS analyses were made are shown in Figure E.21)

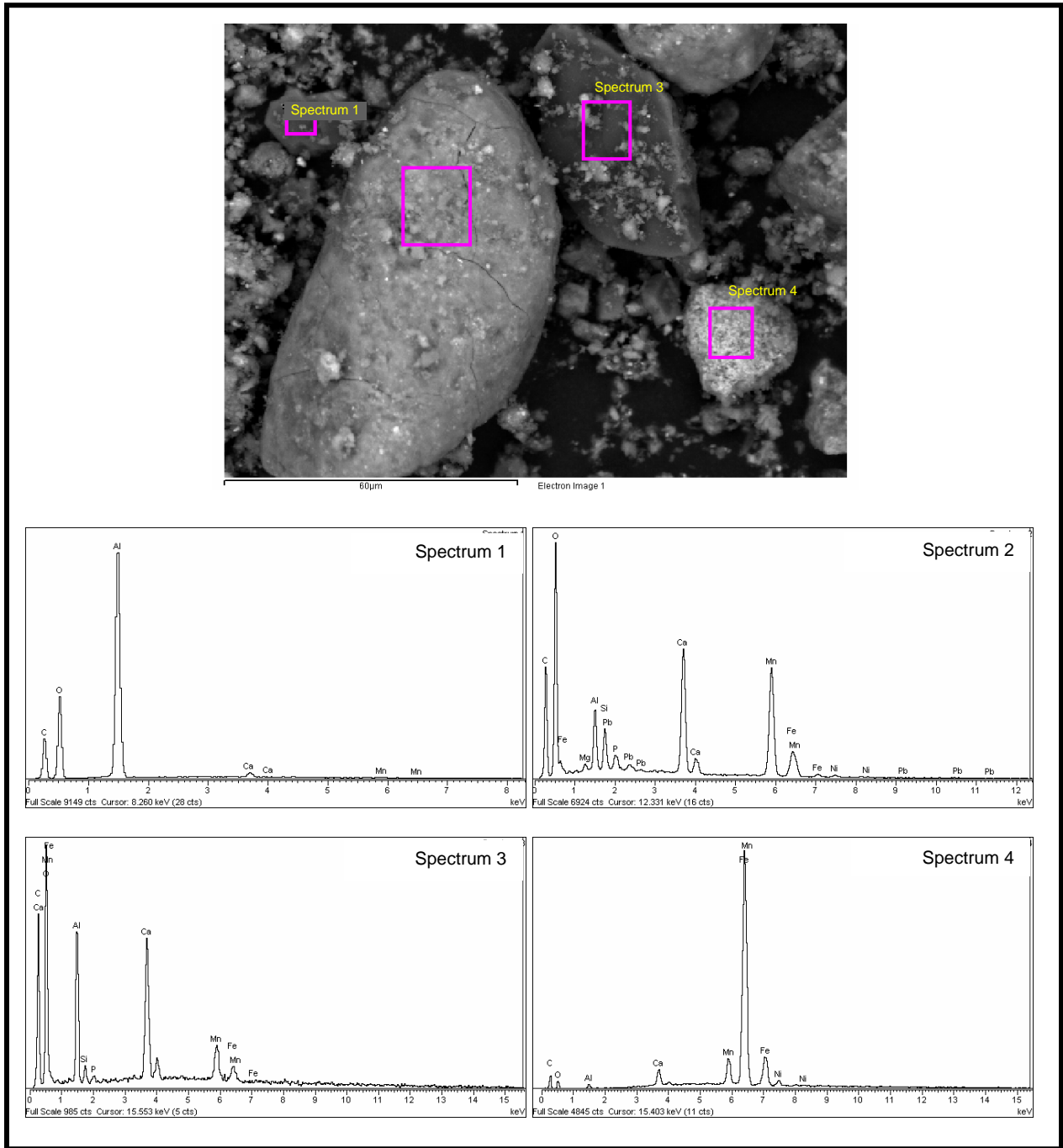


Figure E.13. EDS Spectra for Numbered Areas Marked in Pink in SEM Micrograph Shown at Top of Figure

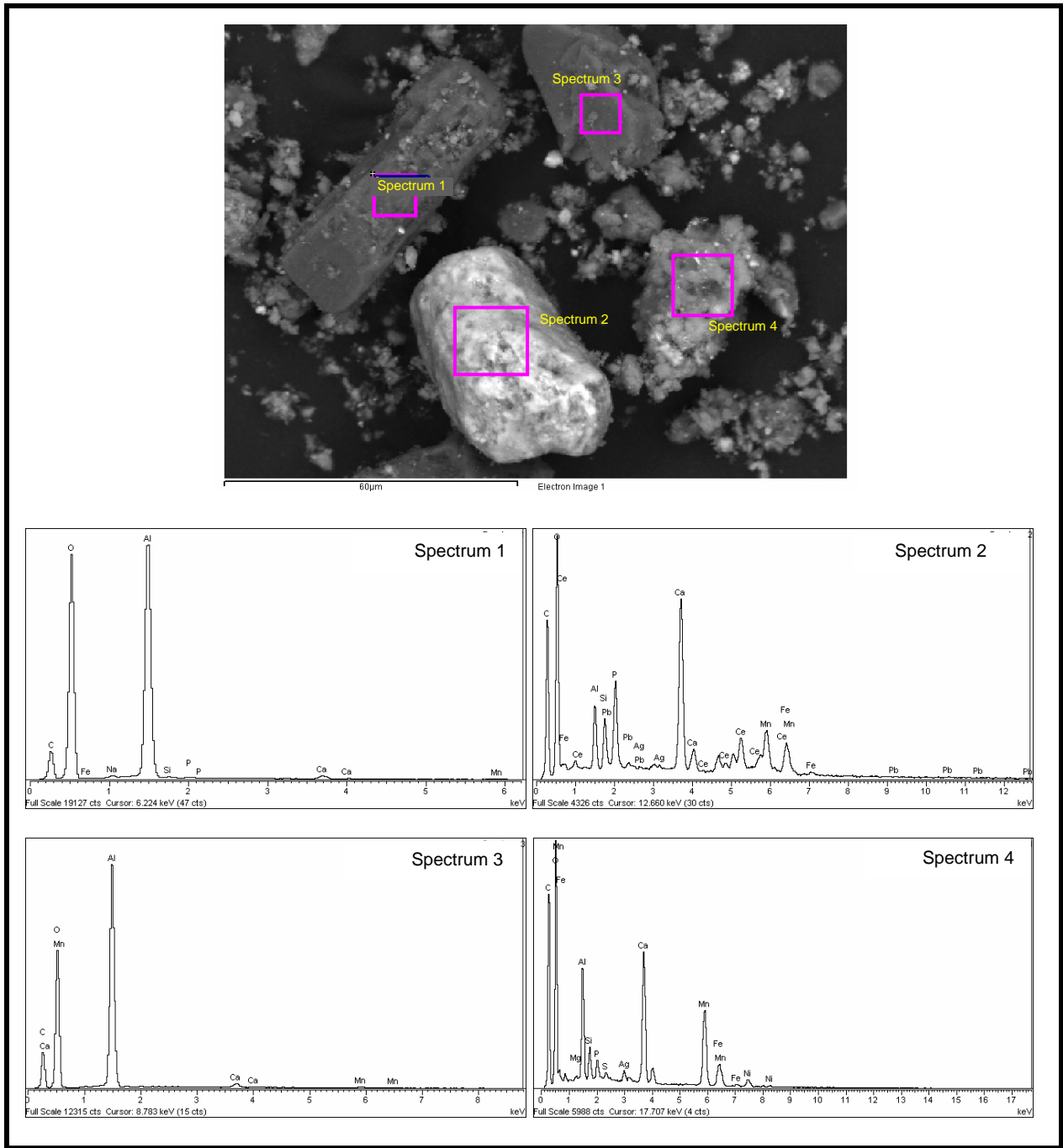


Figure E.14. EDS Spectra for Numbered Areas Marked in Pink in SEM Micrograph Shown at Top of Figure

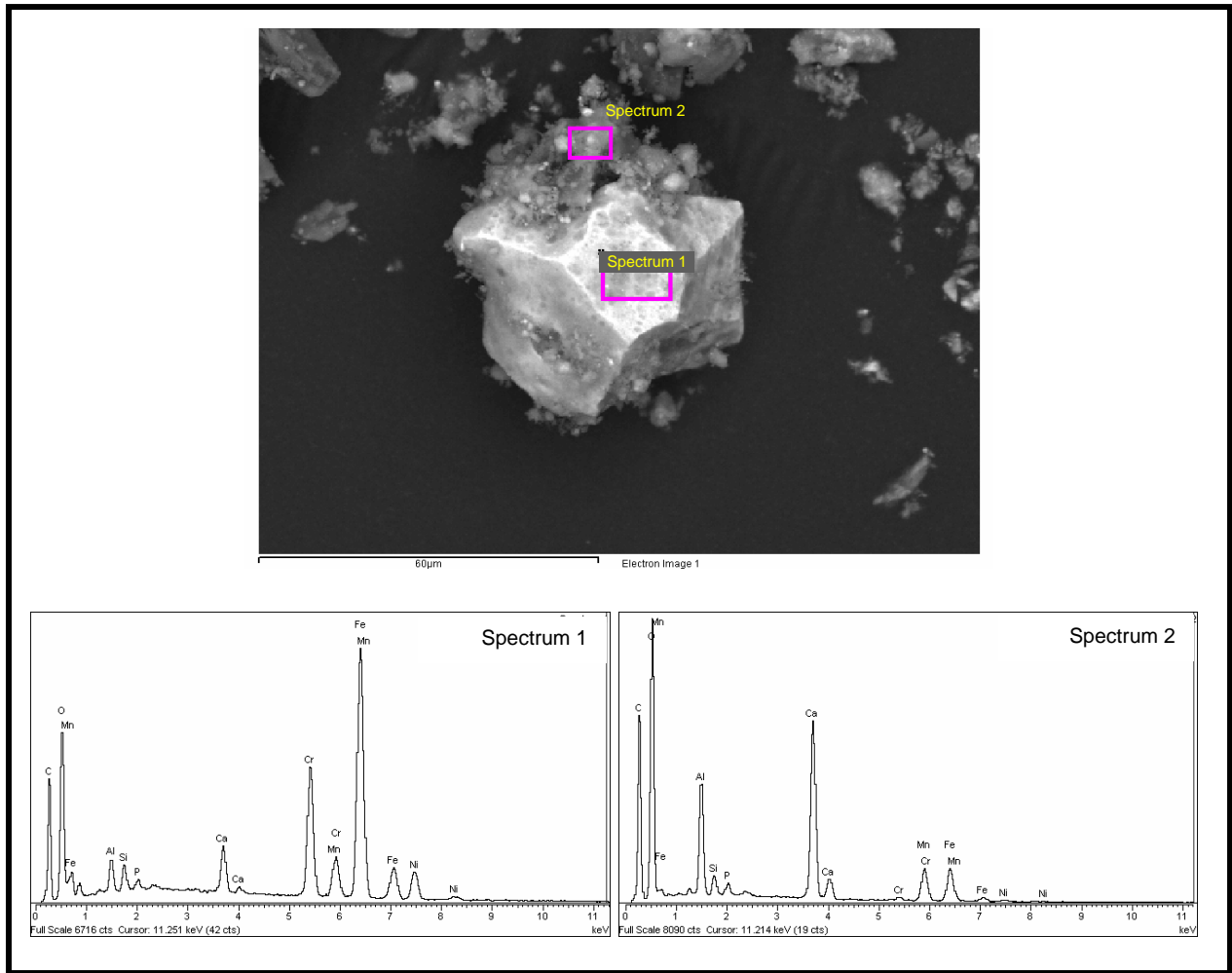


Figure E.15. EDS Spectra for Numbered Areas Marked in Pink in SEM Micrograph Shown at Top of Figure

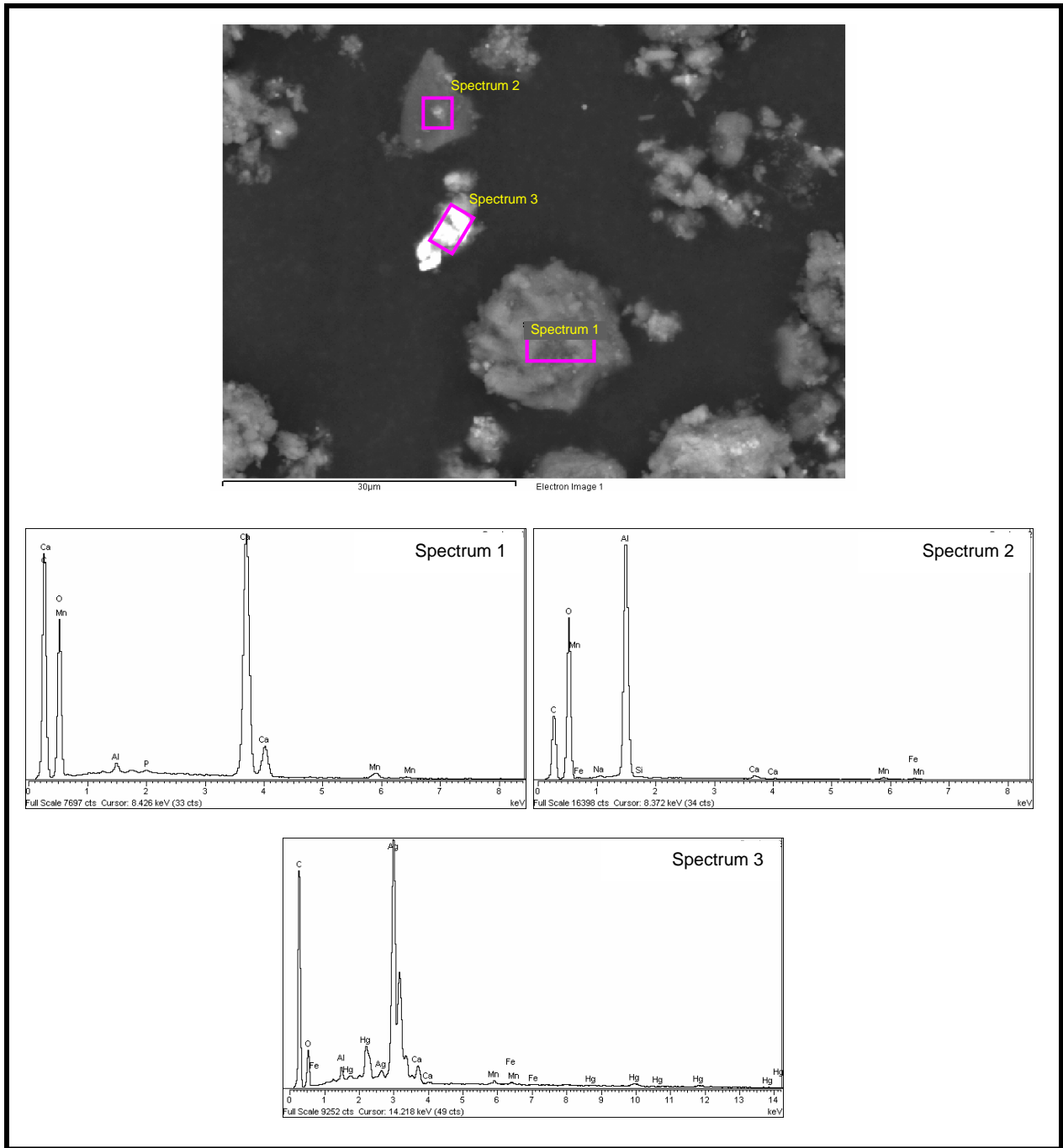


Figure E.16. EDS Spectra for Numbered Areas Marked in Pink in SEM Micrograph Shown at Top of Figure

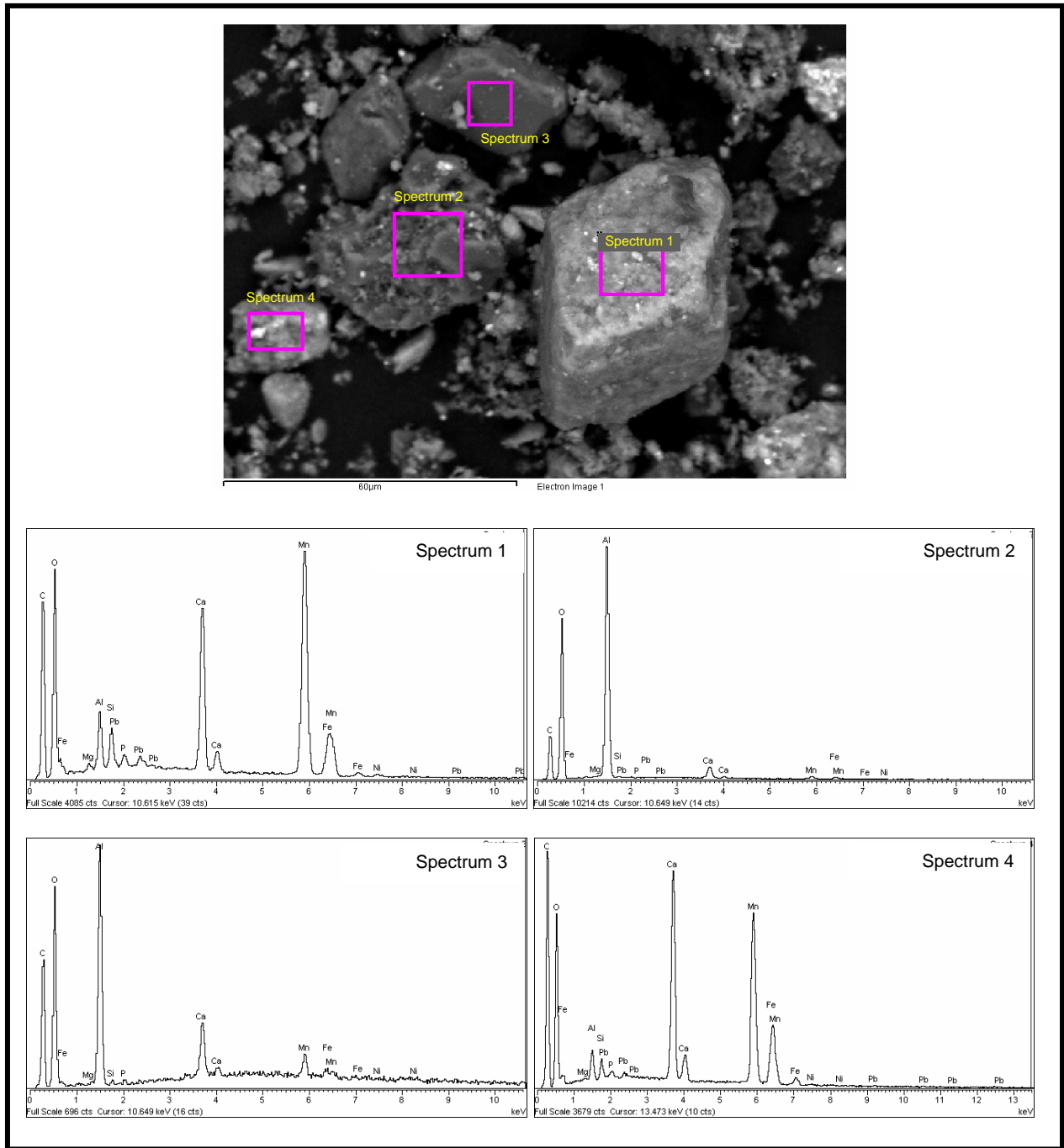


Figure E.17. EDS Spectra for Numbered Areas Marked in Pink in SEM Micrograph Shown at Top of Figure

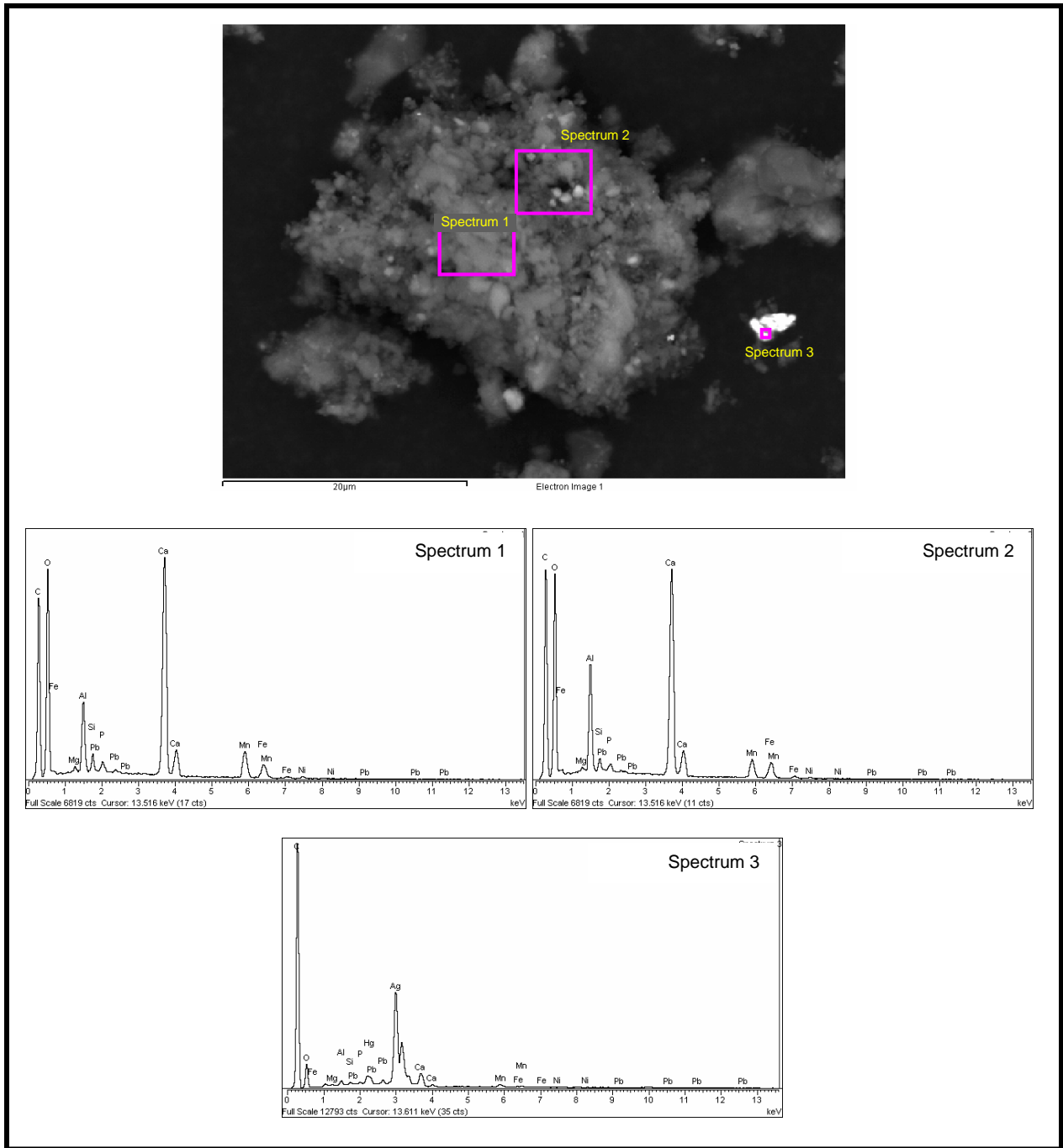


Figure E.18. EDS Spectra for Numbered Areas Marked in Pink in SEM Micrograph Shown at Top of Figure

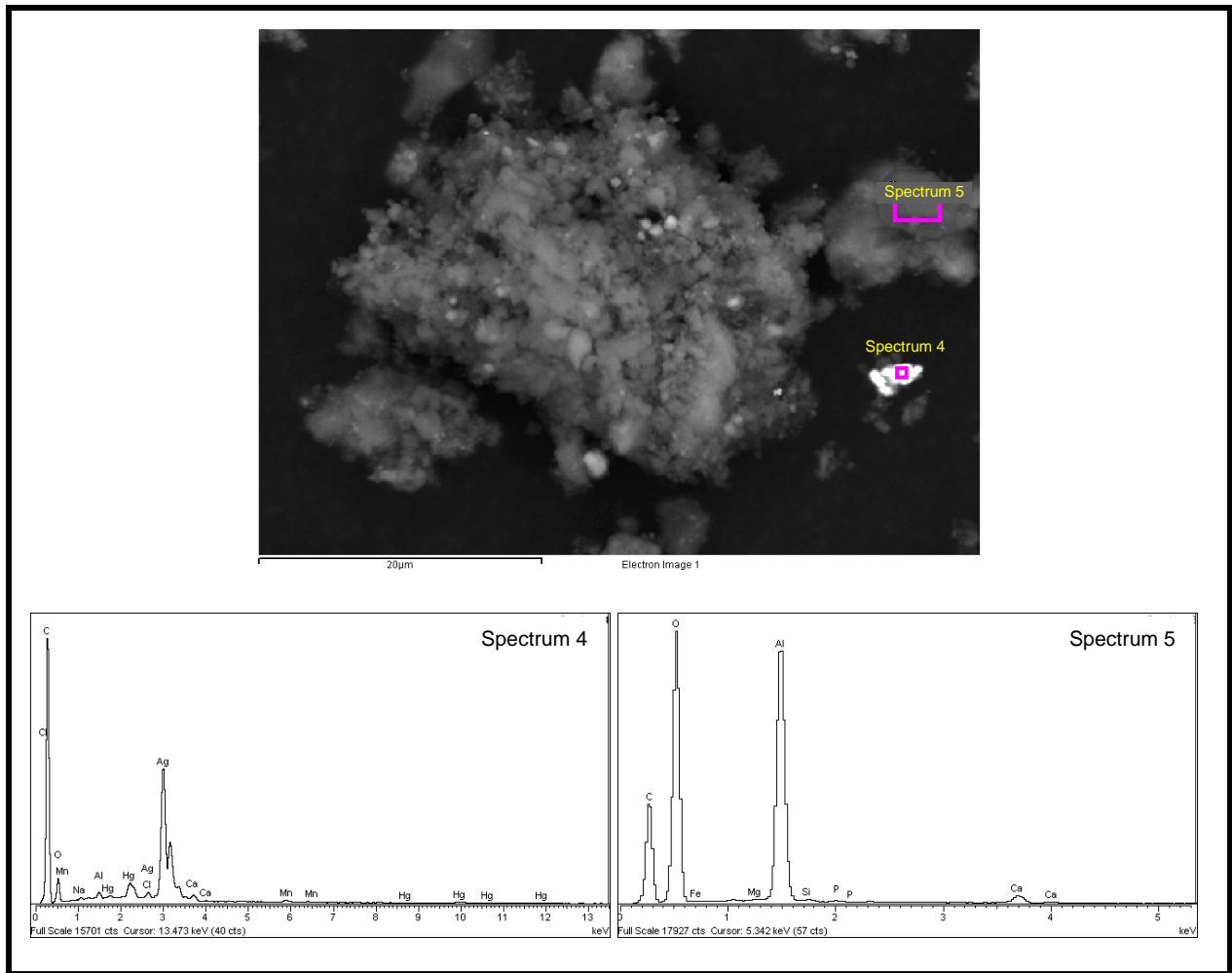


Figure E.19. EDS Spectra for Numbered Areas Marked in Pink in SEM Micrograph Shown at Top of Figure

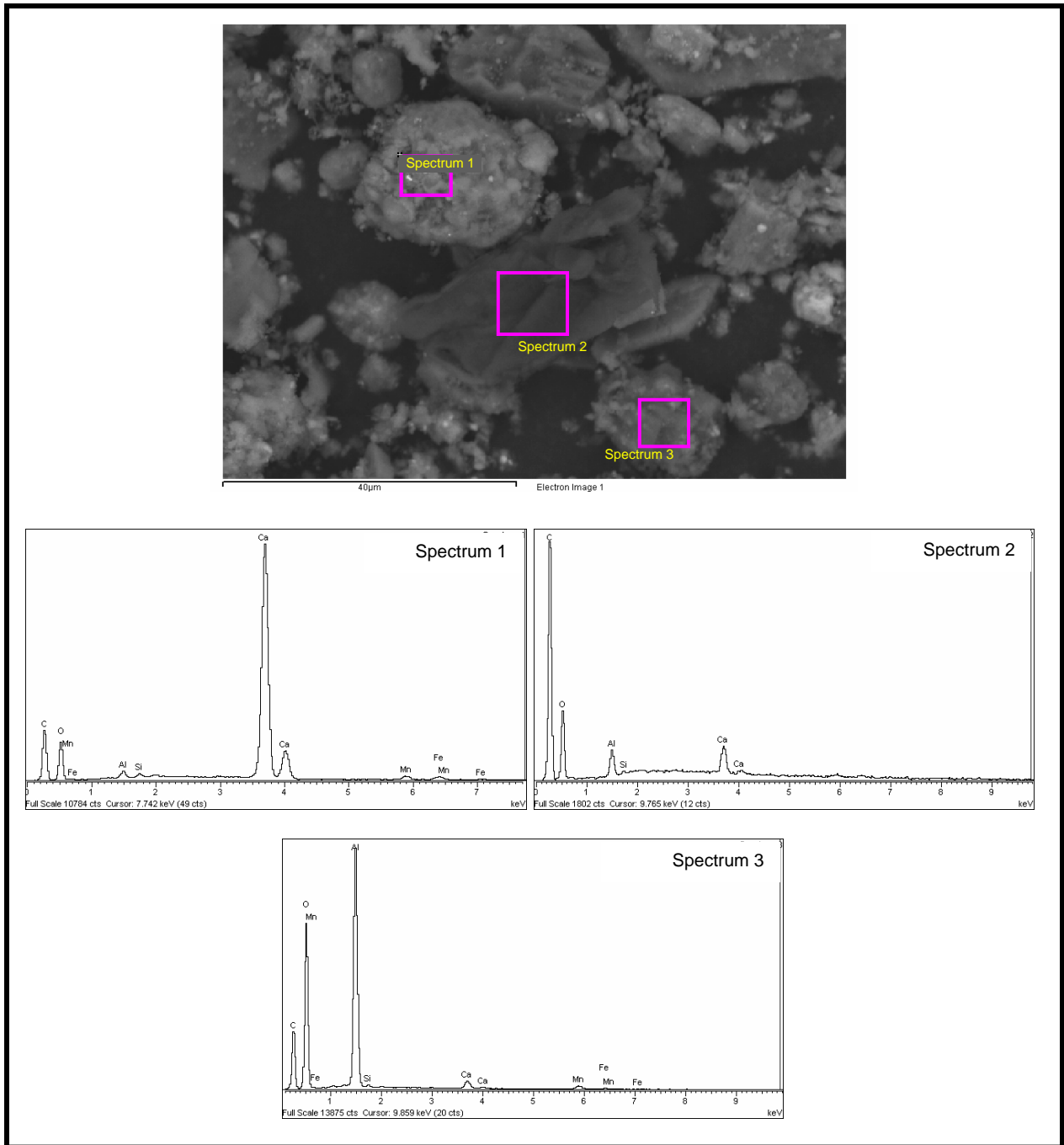


Figure E.20. EDS Spectra for Numbered Areas Marked in Pink in SEM Micrograph Shown at Top of Figure

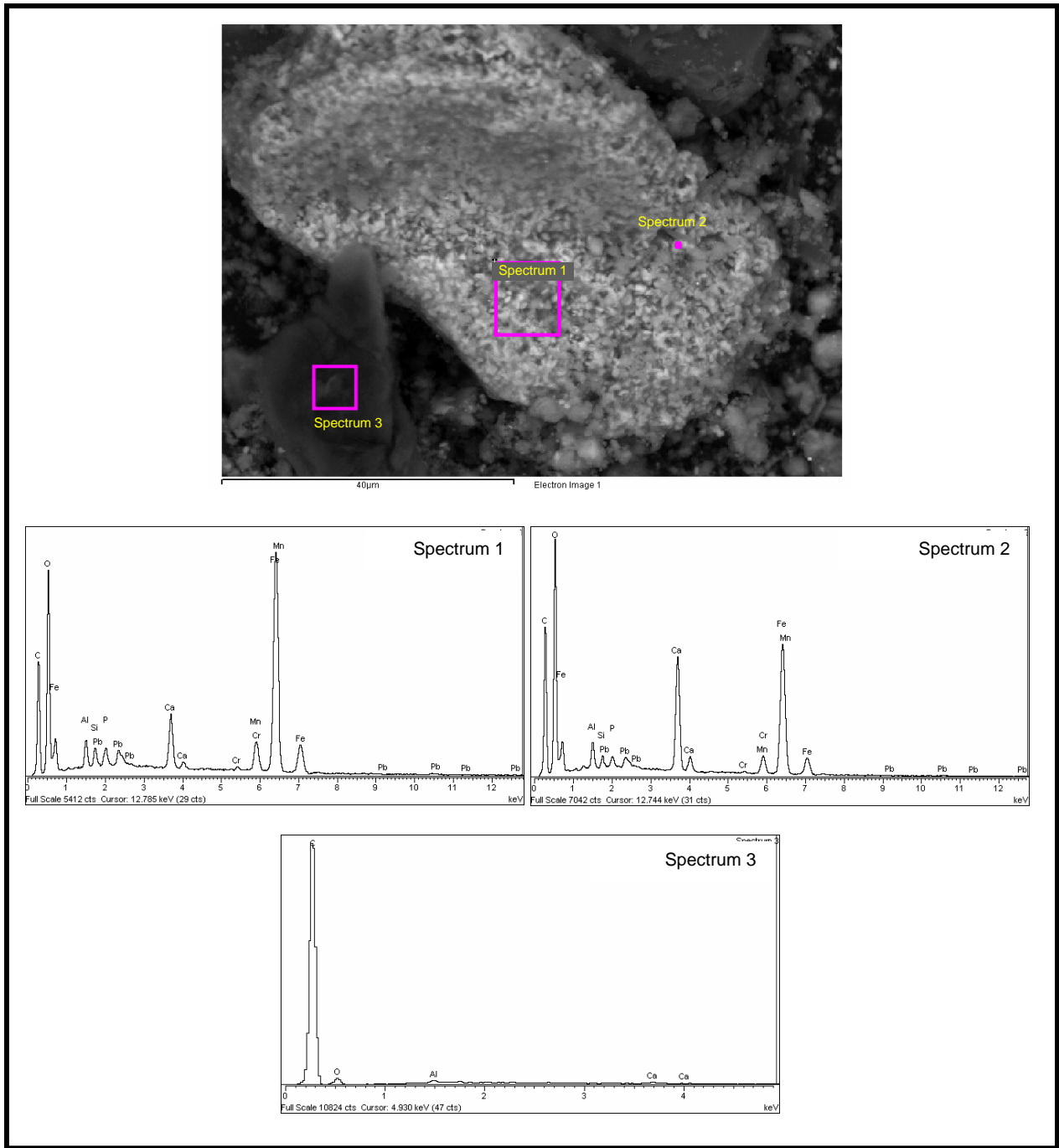


Figure E.21. EDS Spectra for Numbered Areas Marked in Pink in SEM Micrograph Shown at Top of Figure

Appendix F

Solution Concentrations of Tank C-106 Solution Contact Tests with Residual Sludge

Table F.1. Tank Chem 404 Ca(OH)₂

Tank C-106 (404) Ca(OH) ₂ Results																									
Parameter	Units	Single Contact						Periodic Replenishment Tests																	
		1 day	1 day (dup)	1 Day (triplicate)	1 month	1 month (dup)	1 month (triplicate)	Stage 1	Stage 1 (dup)	Stage 1 (triplicate)	Stage 2	Stage 2 (dup)	Stage 2 (triplicate)	Stage 3	Stage 3 (dup)	Stage 3 (triplicate)	Stage 4	Stage 4 (dup)	Stage 4 (triplicate)	Stage 5	Stage 5 (dup)	Stage 5 (triplicate)	Stage 6	Stage 6 (dup)	Stage 6 (triplicate)
pH	sd units	12.30	12.00	12.16			12.30	12.00	12.16	12.36	12.49	12.60	12.49	12.60	12.56	12.62	12.41	12.42	12.50	12.58	12.54	12.50	12.03	11.98	12.16
Alkalinity	mg/L as CaCO ₃	7,686	7,320	7,320	7,320	4,026	7,686	7,320	7,320	7,320	7,320	7,320	7,320	7,320	2,562	4,026	4,026	2,928	3,660	4,026	4,026	5,856	6,222	5,490	5,490
Radionuclides																									
⁹⁰ Sr	µCi/L	1.046E+03	1.556E+03	1.819E+03	6.737E+01	8.846E+01	6.932E+01	1.046E+03	1.556E+03	1.819E+03	2.812E+03	3.038E+03	2.305E+03	1.633E+03	3.226E+03	1.647E+03	6.323E+03	8.707E+03	3.506E+03	3.377E+03	5.241E+03	4.051E+03	4.654E+03	4.275E+03	7.612E+03
⁹⁹ Tc	mg/L	(4.15E-04)	6.53E-04	(3.70E-04)	1.19E-03	1.14E-03	(1.09E-03)	(4.15E-04)	6.53E-04	(3.70E-04)	(1.90E-04)	(1.70E-04)	(1.00E-04)	(8.00E-05)	(1.00E-04)	(7.00E-05)	(1.95E-04)	(2.50E-04)	(1.50E-04)	(1.20E-04)	(1.60E-04)	(1.00E-04)	1.20E-03	1.36E-03	5.85E-04
²³⁸ U	mg/L	(2.45E-04)	(4.80E-04)	(9.00E-05)	4.20E-02	2.15E-02	3.67E-02	(2.45E-04)	(4.80E-04)	(9.00E-05)	1.66E-03	1.19E-03	1.87E-03	1.16E-03	1.56E-03	1.62E-03	1.03E-03	9.60E-04	1.40E-03	7.30E-04	1.21E-03	1.73E-03	8.10E-04	7.40E-04	(3.20E-04)
²³⁹ Pu	mg/L	(4.66E-05)	(9.51E-05)	<1.00E-03	<1.00E-03	(7.07E-05)	<1.00E-03	(4.66E-05)	(9.51E-05)	<1.00E-03	(1.64E-05)	(4.32E-05)	(3.66E-05)	<1.00E-03	<1.00E-03	(6.96E-05)	<1.00E-03	(4.05E-05)	(1.68E-04)	(1.23E-04)	<1.00E-03	(8.46E-05)	(1.30E-04)	(6.92E-06)	(7.51E-06)
²⁴¹ Pu	µCi/L	(1.52E-02)	(2.98E-02)	(5.58E-03)	(2.60E+00)	(1.34E+00)	(2.28E+00)	(1.52E-02)	(2.98E-02)	(5.58E-03)	(1.03E-01)	(7.38E-02)	(1.16E-01)	(7.19E-02)	(9.67E-02)	(1.00E-01)	(6.36E-02)	(8.68E-02)	(4.53E-02)	(7.50E-02)	(1.07E-01)	(5.02E-02)	(4.59E-02)	(1.98E-02)	(1.98E-02)
²³⁷ Np	µCi/L	(1.07E-04)	(1.78E-04)	(1.07E-04)	(4.97E-05)	(2.84E-05)	(3.55E-05)	(1.07E-04)	(1.78E-04)	(1.07E-04)	(2.49E-04)	(1.07E-04)	(1.42E-04)	(1.07E-04)	(1.07E-04)	(1.42E-04)	(1.07E-04)	(2.13E-05)	(2.84E-05)	(2.13E-05)	(4.26E-05)	(2.13E-05)	(2.13E-05)	(2.13E-05)	(4.97E-05)
²⁴¹ Am	µCi/L	(4.08E+00)	(4.93E+00)	(3.57E+00)	(1.05E+00)	(5.61E-01)	(6.80E-01)	(4.08E+00)	(4.93E+00)	(3.57E+00)	(4.25E+00)	(4.25E+00)	(4.59E+00)	(4.25E+00)	(3.06E+00)	(3.91E+00)	(5.10E+00)	(1.05E+00)	(1.09E+00)	(8.84E-01)	(1.09E+00)	(7.14E-01)	(9.86E-01)	(8.50E-01)	(9.86E-01)
Metals																									
Al	mg/L	(5.11E+00)	2.34E+01	(8.59E+00)	9.47E+01	1.14E+02	1.02E+02	(5.11E+00)	2.34E+01	(8.59E+00)	(1.50E+00)	(1.15E+00)	(7.59E+01)	<1.25E+01	(1.23E-01)	<1.25E+01	(7.23E-01)	(1.40E+00)	(1.85E-01)	<1.25E+01	<1.25E+01	(5.44E-02)	1.79E+01	1.63E+01	(5.14E+00)
As	mg/L	(2.07E+00)	(9.22E-01)	(1.46E+00)	(4.49E+00)	(2.90E+00)	(3.35E+00)	(2.07E+00)	(9.22E-01)	(1.46E+00)	(2.34E+00)	(1.86E+00)	(2.53E+00)	(3.78E+00)	(1.84E+00)	(5.05E+00)	(4.67E+00)	(2.33E+00)	(5.69E-01)	(1.63E+00)	(1.84E+00)	(2.08E+00)	(1.83E+00)	(9.03E-01)	(1.04E+00)
B	mg/L	(8.69E+00)	(7.73E+00)	(7.90E+00)	(3.81E+00)	(3.44E+00)	(8.86E+00)	(8.69E+00)	(7.73E+00)	(7.90E+00)	(6.12E+00)	(6.24E+00)	(5.34E+00)	(5.30E+00)	(5.15E+00)	(4.98E+00)	(4.47E+00)	(9.78E+00)	(8.00E+00)	(6.97E+00)	(4.89E+00)	(4.89E+00)	(3.92E+00)	(3.98E+00)	(3.98E+00)
Ba	mg/L	(2.72E-01)	(2.49E-01)	(2.84E-01)	(1.83E-01)	(1.48E-01)	(2.43E-01)	(2.72E-01)	(2.49E-01)	(2.84E-01)	(2.18E-01)	(2.43E-01)	(1.94E-01)	(1.98E-01)	(1.79E-01)	(1.98E-01)	(1.60E-01)	(2.83E-01)	(1.86E-01)	(2.32E-01)	(1.93E-01)	(1.81E-01)	(1.39E-01)	(1.39E-01)	(1.37E-01)
Be	mg/L	(7.16E-02)	(4.42E-02)	(5.28E-02)	(3.12E-02)	(4.22E-02)	(1.44E-01)	(7.16E-02)	(4.42E-02)	(5.28E-02)	(3.73E-02)	(4.12E-02)	(4.20E-02)	(4.36E-02)	(4.45E-02)	(2.92E-02)	(4.02E-02)	(1.45E-01)	(5.99E-02)	(6.34E-02)	(4.39E-02)	(4.54E-02)	(3.95E-02)	(3.51E-02)	(3.19E-02)
Bi	mg/L	(1.11E+00)	(5.25E-01)	(1.11E+00)	(1.63E+00)	<1.25E+01	(1.22E+00)	(1.11E+00)	(5.25E-01)	(1.63E+00)	(4.94E-01)	(3.04E-01)	<1.25E+01	(7.36E-01)	(1.64E-02)	(2.69E-01)	<1.25E+01	(1.40E+00)	<1.25E+01	(5.65E-01)	(4.15E-01)	<1.25E+01	<1.25E+01	<1.25E+01	<1.25E+01
Ca	mg/L	2.65E+02	7.38E+01	1.80E+02	(2.12E+00)	2.51E+00	(2.03E+00)	2.65E+02	7.38E+01	1.80E+02	3.30E+02	3.61E+02	4.51E+02	5.84E+02	5.13E+02	6.14E+02	3.66E+02	3.65E+02	5.14E+02	6.11E+02	6.06E+02	6.45E+02	1.15E+02	1.20E+02	9.65E+01
Cd	mg/L	<2.50E+00	<2.50E+00	<2.50E+00	<2.50E+00	<2.50E+00	<2.50E+00	<2.50E+00	<2.50E+00	<2.50E+00	<2.50E+00	<2.50E+00	<2.50E+00	<2.50E+00	(1.60E-02)	<2.50E+00	(8.25E-03)	(5.15E-02)	<2.50E+00	<2.50E+00	<2.50E+00	<2.50E+00	(8.51E-03)	<2.50E+00	(6.13E-02)
Co	mg/L	(1.62E-01)	(2.64E-01)	(2.54E-01)	<2.50E+00	<2.50E+00	(1.68E-01)	(1.62E-01)	(2.64E-01)	(2.54E-01)	(1.95E-01)	(1.76E-01)	(1.85E-01)	(8.08E-03)	(7.55E-02)	(2.62E-01)	<2.50E+00	(2.58E-01)	<2.50E+00	(9.89E-03)	(3.32E-02)	<2.50E+00	(2.30E-02)	<2.50E+00	<2.50E+00
Cr	mg/L	(1.69E-01)	(6.08E-02)	(1.47E-01)	(3.67E-01)	(5.48E-01)	(6.02E-01)	(1.69E-01)	(6.08E-02)	(1.47E-01)	(6.02E-01)	(2.38E-01)	(2.17E-01)	(1.43E-01)	(2.19E-01)	(1.50E-01)	(2.04E-01)	(2.27E-01)	(2.08E-01)	(1.13E-01)	(3.20E-01)	(2.14E-01)	(2.45E-01)	(1.67E-01)	(1.67E-01)
Cu	mg/L	(1.56E+00)	(1.71E+00)	(1.36E+00)	<1.25E+01	<1.25E+01	(1.55E-01)	(1.56E+00)	(1.71E+00)	(1.36E+00)	(1.35E+00)	(1.09E+00)	(9.43E-01)	(7.99E-01)	(6.53E-01)	(6.03E-01)	(4.11E-01)	(7.35E-01)	(2.49E-01)	<1.25E+01	<1.25E+01	<1.25E+01	<1.25E+01	<1.25E+01	<1.25E+01
Fe	mg/L	(3.15E-01)	(2.75E-01)	(5.57E-01)	(4.42E-02)	(3.54E-01)	(3.54E-01)	(3.15E-01)	(2.75E-01)	(5.57E-01)	(2.99E-01)	(2.99E-01)	(2.09E-01)	(1.58E-01)	(1.57E-01)	(1.12E-01)	(1.20E-01)	(4.00E-01)	(2.17E-01)	(2.01E-01)	(1.11E-01)	(1.71E-01)	(8.11E-02)	(8.25E-02)	(8.25E-02)
K	mg/L	<6.25E+02	<6.25E+02	<6.25E+02	<6.25E+02	<6.25E+02	<6.25E+02	<6.25E+02	<6.25E+02	<6.25E+02	<6.25E+02	<6.25E+02	<6.25E+02	<6.25E+02	<6.25E+02	<6.25E+02	<6.25E+02	<6.25E+02	<6.25E+02	<6.25E+02	<6.25E+02	<6.25E+02	<6.25E+02	<6.25E+02	<6.25E+02
Li	mg/L	(5.38E-02)	(4.79E-01)	(7.96E-02)	<2.50E+01	<2.50E+01	<2.50E+01	(5.38E-02)	(4.79E-01)	(7.96E-02)	<2.50E+01	<2.50E+01	<2.50E+01	<2.50E+01	(3.02E-02)	<2.50E+01	<2.50E+01	<2.50E+01	<2.50E+01	<2.50E+01	<2.50E+01	<2.50E+01	<2.50E+01	<2.50E+01	<2.50E+01
Mg	mg/L	(7.81E-01)	(6.45E-01)	(6.26E-01)	(4.62E-01)	(5.00E-01)	(6.03E-01)	(7.81E-01)	(6.45E-01)	(6.26E-01)	(6.03E-01)	(6.61E-01)	(5.89E-01)	(5.50E-01)	(5.75E-01)	(4.57E-01)	(4.70E-01)	(6.48E-01)	(4.37E-01)	(5.16E-01)	(4.59E-01)	(4.82E-01)	(4.69E-01)	(4.72E-01)	(4.36E-01)
Mn	mg/L	<2.50E+00	<2.50E+00	<2.50E+00	<2.50E+00	<2.50E+00	<2.50E+00	<2.50E+00	<2.50E+00	<2.50E+00	<2.50E+00	<2.50E+00	<2.50E+00	<2.50E+00	<2.50E+00	<2.50E+00	<2.50E+00	<2.50E+00	<2.50E+00	<2.50E+00	<2.50E+00	<2.50E+00	<2.50E+00	<2.50E+00	<2.50E+00
Mo	mg/L	<5.00E+00	(1.15E-01)	<5.00E+00	<5.00E+00	(2.23E-01)	(2.45E-01)	<5.00E+00	(1.15E-01)	<5.00E+00	<5.00E+00	<5.00E+00	<5.00E+00	(1.08E-01)	(3.77E-01)	<5.00E+00	(1.05E-01)	(2.13E-01)	(5.50E-01)	(3.09E-02)	(1.90E-01)	<5.00E+00	(1.38E-01)	<5.00E+00	<5.00E+00
Na	mg/L	1.01E+02	1.37E+02	1.04E+02	2.31E+02	2.30E+02	5.77E+01	1.01E+02	1.37E+02	1.04E+02	1.04E+02	5.77E+01	6.05E+01	4.90E+01	2.72E+01	5.64E+01	5.96E+01	3.82E+01	2.51E+01	1.95E+01	1.04E+02	1.08E+02	1.08E+02	4.50E+01	4.50E+01
Ni	mg/L	(5.49E-01)	(5.13E-01)	(5.21E-01)	(4.98E-02)	<5.00E+00	(8.29E-01)	(5.49E-01)	(5.13E-01)	(5.21E-01)	(2.99E-01)	(4.19E-01)	(2.17E-01)	(2.96E-01)	(2.94E-01)	(4.68E-01)	(1.51E-01)	(8.33E-01)	(5.09E-01)	(3.40E-01)	<5.00E+00	<5.00E+00	(8.74E-02)	(1.12E-01)	(1.12E-01)
Pb	mg/L	<1.25E+01	<1.25E+01	<1.25E+01	<1.25E+01	<1.25E+01	<1.25E+01	<1.25E+01	<1.25E+01	<1.25E+01	<1.25E+01	<1.25E+01	<1.25E+01	<1.25E+01	<1.25E+01	<1.25E+01	<1.25E+01	<1.25E+01	<1.25E+01	<1.25E+01	<1.25E+01	<1.25E+01	<1.25E+01	<1.25E+01	<1.25E+01
S	mg/L	(3.69E+00)	<1.00E+02	<1.00E+02	<1.00E+02	<1.00E+02	<1.00E+02	(3.69E+00)	<1.00E+02	<1.00E+02	(3.65E+00)	(3.66E-01)	<1.00E+02	<1.00E+02	(4.54E+00)	<1.00E+02	<1.00E+02	(8.64E-01)	<1.00E+02	<1.00E+02	(1.71E+00)	<1.00E+02	<1.00E+02	<1.00E+02	<1.00E+02
Se	mg/L	(9.73E-01)	<2.50E+01	<2.50E+01	(6.41E+00)	(6.51E-01)	(4.05E-02)	(9.73E-01)	<2.50E+01	<2.50E+01	(6.51E-01)	(2.75E+00)	(3.48E+00)	(8.40E-02)	(2.57E+00)	(2.57E+00)	(4.44E+00)	(1.11E+00)	(2.02E+00)	(3.89E+00)	(3.41E+00)	(1.08E+00)	(3.41E+00)	(1.08E+00)	(4.62E+00)
Si	mg/L	<2.50E+02	<2.50E+02	<2.50E+02	<2.50E+02	<2.50E+02	<2.50E+02	<2.50E+02	<2.50E+02	<2.50E+02	<2.50E+02	<2.50E+02	<2.50E+02	<2.50E+02	<2.50E+02	<2.50E+02	<2.50E+02	<2.50E+02	<2.50E+02	<2.50E+02	<2.50E+02	<2.50E+02	<2.50E+02	<2.50E+02	<2.50E+02
Sr	mg/L	(2.27E-01)	(2.11E-01)	(2.60E-01)	<2.50E+00	(1.23																			

Table F.2. (contd)

Parameter	Units	Single Contact							Periodic Replenishment Tests																			
		1 day	1 day (dup)	1 Day (triplicate)	1 month	1 month (dup)	1 month (triplicate)	Stage 1	Stage 1 (dup)	Stage 1 (triplicate)	Stage 2	Stage 2 (dup)	Stage 2 (triplicate)	Stage 3	Stage 3 (dup)	Stage 3 (triplicate)	Stage 4	Stage 4 (dup)	Stage 4 (triplicate)	Stage 5	Stage 5 (dup)	Stage 5 (triplicate)	Stage 6	Stage 6 (dup)	Stage 6 (triplicate)			
pH	std units																											
Alkalinity	mM as CaCO3	40.2	36.6	40.2	36.6	40.2	36.6	40.2	36.6	40.2	25.6	73.1	40.2	36.6	73.1	40.2	58.5	40.2	73.1	29.3	54.9	43.9	36.6	40.2				
Radionuclides																												
⁹⁰ Sr	mM	3.581E-05	1.557E-04	8.439E-05	1.333E-05	1.086E-05	9.472E-06	3.581E-05	1.557E-04	8.439E-05	3.400E-04	2.326E-04	2.499E-04	3.368E-04	2.462E-04	2.163E-04	6.920E-04											
⁹⁹ Tc	mM	8.81E-06	6.24E-06	(2.93E-06)	1.03E-05	9.95E-06	1.20E-05	8.81E-06	6.24E-06	(2.93E-06)	4.04E-06	(1.52E-06)	(2.42E-06)	(1.21E-06)	(1.11E-06)	(1.11E-06)	(2.63E-06)	(2.12E-06)	(3.13E-06)	(1.92E-06)	(1.11E-06)	(1.82E-06)	1.52E-05	1.15E-05	1.16E-05			
²³⁸ U	mM	3.12E-05	(8.40E-08)	(8.40E-08)	1.07E-04	1.88E-04	3.14E-04	3.12E-05	(8.40E-08)	(8.40E-08)	(1.68E-07)	7.61E-06	(6.30E-07)	4.96E-06	5.76E-06	5.67E-06	(6.30E-07)	6.60E-06	(2.02E-06)	4.79E-06	6.51E-06	5.13E-06	2.90E-06	3.11E-06	2.44E-06			
²³⁹ U	mM	(1.26E-06)	(1.05E-06)	(1.15E-06)	(4.71E-08)	(4.15E-07)	(1.07E-06)	(1.26E-06)	(1.05E-06)	(1.15E-06)	(1.66E-07)	(8.11E-07)	(7.75E-06)	(7.75E-06)	(1.61E-07)	(2.00E-07)	(7.75E-06)	(7.75E-06)	(2.00E-07)	(9.96E-07)	(6.60E-07)	(5.11E-08)	(9.41E-07)	(5.31E-07)				
²³⁹ Pu	mM	(3.11E-04)	(8.37E-07)	(8.37E-07)	(1.07E-03)	(1.87E-03)	(3.11E-04)	(8.37E-07)	(8.37E-07)	(1.67E-06)	(7.57E-06)	(6.28E-06)	(4.94E-05)	(5.73E-05)	(5.65E-05)	(6.28E-06)	(6.28E-06)	(6.57E-05)	(2.01E-05)	(4.77E-05)	(6.49E-05)	(5.10E-05)	(2.89E-05)	(2.31E-05)	(2.43E-05)			
²³⁷ Np	mM	(1.27E-07)	(1.27E-07)	(1.27E-07)	(2.95E-07)	(2.11E-07)	(1.27E-07)	(1.27E-07)	(1.27E-07)	(1.27E-07)	(1.69E-07)	(1.27E-07)	(1.27E-07)	(1.69E-07)	(1.69E-07)	(8.44E-08)	(1.69E-07)	(8.44E-08)	(1.27E-07)	(1.69E-07)	(4.77E-07)	(1.27E-07)	(1.27E-07)	(1.27E-07)	(4.22E-07)			
²⁴¹ Am	mM	(1.08E-06)	(1.33E-06)	(9.96E-07)	(9.13E-07)	(1.29E-06)	(1.24E-06)	(1.08E-06)	(1.33E-06)	(9.96E-07)	(1.58E-06)	(6.64E-07)	<1.45E-06	<1.12E-06	<4.98E-07	(1.29E-06)	(1.08E-06)	<1.08E-06	<1.08E-06	(7.88E-07)	(1.16E-06)	(1.70E-06)	(1.16E-06)	(8.30E-07)	(1.16E-06)			
Metals																												
Al	mM	1.97E+00	1.02E+00	(1.45E-01)	4.48E+00	4.14E+00	3.19E+00	1.97E+00	1.02E+00	(1.45E-01)	(4.14E-01)	(4.36E-02)	(3.27E-01)	(6.88E-02)	(1.16E-02)	(3.79E-02)	(1.86E-01)	(3.08E-02)	(2.87E-01)	(5.20E-03)	<4.63E-01	(8.61E-03)	(3.42E-01)	(3.78E-01)	(6.26E-02)			
As	mM	(4.22E-02)	(5.66E-02)	(3.77E-02)	(1.39E-02)	(1.05E-02)	(2.07E-02)	(4.22E-02)	(5.66E-02)	(3.77E-02)	(2.51E-02)	(2.87E-02)	(1.76E-03)	(8.01E-03)	(3.53E-02)	<3.34E-01	(5.53E-02)	(1.22E-02)	(1.56E-02)	<3.34E-01	(1.80E-02)	(1.64E-02)	(5.64E-03)	(3.12E-02)	(2.13E-02)			
B	mM	(5.28E-01)	(4.42E-01)	(3.27E-01)	<2.31E+01	(4.12E-01)	(1.86E-01)	(5.28E-01)	(4.42E-01)	(3.27E-01)	(4.32E-01)	(2.06E-01)	(4.42E-01)	(1.33E-01)	(1.10E-01)	(5.77E-02)	(5.58E-01)	(3.20E-01)	(1.71E-01)	(1.17E-01)	(8.38E-02)	(5.41E-02)	<2.31E+01	<2.31E+01				
Ba	mM	(2.26E-03)	(1.15E-03)	(1.14E-03)	(1.13E-03)	(1.75E-03)	(1.19E-03)	(2.26E-03)	(1.15E-03)	(1.14E-03)	(1.67E-03)	(1.25E-03)	(1.45E-03)	(1.71E-03)	(1.33E-03)	(1.53E-03)	(1.68E-03)	(1.62E-03)	(1.18E-03)	(1.83E-03)	(1.26E-03)	(1.41E-03)	(1.24E-03)	(1.22E-03)	(1.61E-03)			
Be	mM	(8.78E-03)	(6.23E-03)	(5.44E-03)	(1.89E-03)	(1.89E-03)	(7.60E-03)	(8.78E-03)	(6.23E-03)	(5.44E-03)	(6.43E-03)	(4.42E-03)	(2.61E-03)	(3.14E-03)	(3.85E-03)	(3.29E-03)	(1.30E-02)	(6.47E-03)	(5.03E-03)	(4.57E-03)	(4.46E-03)	(2.89E-03)	(1.82E-03)	(2.83E-03)	(1.73E-03)			
Bi	mM	(2.75E-03)	(6.03E-03)	<5.98E-02	(6.42E-04)	(6.91E-04)	(8.38E-03)	(2.75E-03)	(6.03E-03)	<5.98E-02	<5.98E-02	<5.98E-02	<5.98E-02	(6.92E-04)	(1.07E-03)	<5.98E-02	<5.98E-02	(8.26E-04)	(1.77E-03)	(1.18E-03)	<5.98E-02	<5.98E-02	(6.72E-03)	<5.98E-02				
Ca	mM	3.51E-01	1.83E+00	2.83E+00	7.91E-02	6.23E-02	5.50E-02	3.51E-01	1.83E+00	2.83E+00	7.88E+00	9.43E+00	4.86E+00	3.74E+01	1.27E+01	1.02E+01	4.70E+00	1.16E+01	4.32E+00	1.27E+01	1.59E+01	4.12E+00	4.26E+00	8.07E+00				
Cd	mM	(1.85E-04)	<2.22E-02	<2.22E-02	(3.79E-04)	<2.22E-02	<2.22E-02	(1.85E-04)	<2.22E-02	<2.22E-02	(1.35E-04)	<2.22E-02	<2.22E-02	<2.22E-02	<2.22E-02	(2.77E-04)	(2.41E-04)	<2.22E-02	<2.22E-02	<2.22E-02	<2.22E-02	(7.70E-05)	<2.22E-02	(2.81E-04)	(1.68E-04)			
Co	mM	(2.31E-03)	(1.00E-03)	(3.36E-03)	<4.24E-02	(3.48E-03)	<4.24E-02	(2.31E-03)	(1.00E-03)	(3.36E-03)	(4.25E-04)	<4.24E-02	<4.24E-02	(7.76E-04)	<4.24E-02	(6.83E-03)	<4.24E-02	(3.08E-04)	(2.23E-04)	(1.16E-03)	<4.24E-02	<4.24E-02	<4.24E-02	<4.24E-02				
Cr	mM	(3.80E-03)	(4.04E-03)	(2.43E-03)	(7.06E-03)	(1.01E-02)	(6.82E-03)	(3.80E-03)	(4.04E-03)	(2.43E-03)	(4.09E-03)	(1.60E-03)	(2.23E-03)	(7.12E-04)	(2.45E-03)	(2.61E-03)	(5.69E-03)	(5.73E-03)	(3.43E-03)	(3.54E-03)	(1.63E-03)	(3.50E-03)	(6.51E-03)	(4.89E-03)	(4.48E-03)			
Cu	mM	<1.97E-01	<1.97E-01	<1.97E-01	<1.97E-01	<1.97E-01	<1.97E-01	<1.97E-01	<1.97E-01	<1.97E-01	<1.97E-01	<1.97E-01	<1.97E-01	<1.97E-01	<1.97E-01	<1.97E-01	<1.97E-01	<1.97E-01	<1.97E-01	<1.97E-01	<1.97E-01	<1.97E-01	<1.97E-01	<1.97E-01				
Fe	mM	(3.00E-03)	(2.26E-03)	(3.11E-03)	(8.56E-04)	(5.40E-03)	(2.40E-03)	(3.00E-03)	(2.26E-03)	(3.11E-03)	(1.20E-03)	(1.19E-03)	(2.00E-03)	(2.16E-03)	(2.19E-03)	(1.90E-03)	(5.67E-03)	(4.15E-03)	(2.47E-03)	(1.33E-03)	(1.57E-03)	(1.10E-03)	(1.61E-03)	(1.90E-03)	(1.30E-03)			
K	mM	<1.60E+01	<1.60E+01	<1.60E+01	<1.60E+01	<1.60E+01	<1.60E+01	<1.60E+01	<1.60E+01	<1.60E+01	<1.60E+01	<1.60E+01	<1.60E+01	<1.60E+01	<1.60E+01	<1.60E+01	<1.60E+01	<1.60E+01	<1.60E+01	<1.60E+01	<1.60E+01	<1.60E+01	<1.60E+01	<1.60E+01				
Li	mM	<3.60E+00	<3.60E+00	<3.60E+00	<3.60E+00	<3.60E+00	<3.60E+00	<3.60E+00	<3.60E+00	<3.60E+00	<3.60E+00	<3.60E+00	<3.60E+00	<3.60E+00	<3.60E+00	<3.60E+00	<3.60E+00	<3.60E+00	<3.60E+00	<3.60E+00	<3.60E+00	<3.60E+00	<3.60E+00	<3.60E+00				
Mg	mM	(2.08E-02)	(1.87E-02)	(1.59E-02)	(1.40E-02)	(2.40E-02)	(1.71E-02)	(2.08E-02)	(1.87E-02)	(1.59E-02)	(1.62E-02)	(1.76E-02)	(2.08E-02)	(1.20E-02)	(1.84E-02)	(1.44E-02)	(2.43E-02)	(1.72E-02)	(1.46E-02)	(1.48E-02)	(1.31E-02)	(1.56E-02)	(1.48E-02)	(1.38E-02)				
Mn	mM	<4.55E-02	<4.55E-02	<4.55E-02	<4.55E-02	(2.45E-04)	<4.55E-02	<4.55E-02	<4.55E-02	<4.55E-02	<4.55E-02	<4.55E-02	<4.55E-02	<4.55E-02	<4.55E-02	<4.55E-02	<4.55E-02	<4.55E-02	<4.55E-02	<4.55E-02	<4.55E-02	<4.55E-02	<4.55E-02	<4.55E-02				
Mo	mM	<5.21E-02	(2.28E-04)	<5.21E-02	<5.21E-02	(7.93E-03)	(5.97E-03)	<5.21E-02	(2.28E-04)	<5.21E-02	(1.64E-04)	<5.21E-02	(7.43E-04)	(4.88E-03)	(3.24E-03)	(1.13E-03)	(1.39E-03)	<5.21E-02	(2.03E-03)	<5.21E-02	<5.21E-02	<5.21E-02	<5.21E-02					
Na	mM	6.46E+00	5.29E+00	2.37E+00	9.34E+00	9.08E+00	8.59E+00	6.46E+00	5.29E+00	2.37E+00	2.60E+00	2.70E+00	2.60E+00	2.70E+00	2.60E+00	2.70E+00	2.60E+00	2.70E+00	2.60E+00	2.70E+00	2.60E+00	2.70E+00	2.60E+00	2.70E+00				
Ni	mM	(8.35E-03)	(1.61E-03)	<8.52E-02	<8.52E-02	(7.30E-03)	(8.52E-03)	(8.35E-03)	(1.61E-03)	<8.52E-02	(1.86E-03)	<8.52E-02	<8.52E-02	(6.52E-04)	<8.52E-02	(6.52E-04)	(9.07E-03)	(4.75E-03)	<8.52E-02	(9.95E-04)	<8.52E-02	(2.37E-03)	<8.52E-02	<8.52E-02				
Pb	mM	<6.03E-02	<6.03E-02	<6.03E-02	<6.03E-02	<6.03E-02	<6.03E-02	<6.03E-02	<6.03E-02	<6.03E-02	<6.03E-02	<6.03E-02	<6.03E-02	<6.03E-02	<6.03E-02	<6.03E-02	<6.03E-02	<6.03E-02	<6.03E-02	<6.03E-02	<6.03E-02	<6.03E-02	<6.03E-02					
S	mM	<3.12E+00	(6.77E-02)	(1.13E-01)	<3.12E+00	(1.60E-01)	<3.12E+00	<3.12E+00	(6.77E-02)	(1.13E-01)	(8.79E-02)	<3.12E+00	<3.12E+00	<3.12E+00	<3.12E+00	(2.93E-02)	(8.55E-02)	(7.17E-02)	<3.12E+00	(1.01E-01)	<3.12E+00	<3.12E+00	<3.12E+00					
Se	mM	(2.63E-02)	(8.90E-03)	(1.97E-02)	<3.17E-01	(3.70E-02)	<3.17E-01	(2.63E-02)	(8.90E-03)	(1.97E-02)	(5.66E-03)	(2.75E-02)	<3.17E-01	(8.08E-02)	(1.95E-02)	(6.89E-02)	(1.55E-02)	(2.10E-02)	(2.83E-02)	(2.24E-02)	(2.68E-02)	(1.09E-02)	(3.56E-02)	(2.64E-02)	(3.62E-02)			
Si	mM	<8.90E+00	<8.90E+00	<8.90E+00	<8.90E+00	<8.90E+00	<8.90E+00	<8.90E+00	<8.90E+00	<8.90E+00	<8.90E+00	<8.90E+00	<8.90E+00	<8.90E+00	<8.90E+00	<8.90E+00	<8.90E+00	<8.90E+00	<8.90E+00	<8.90E+00	<8.90E+00	<8.90E+00	<8.90E+00					
Sr	mM	(1.01E-03)	(2.52E-03)	(1.69E-03)	(2.39E-04)	(1.54E-03)	(7.85E-04)	(1.01E-03)	(2.52E-03)	(1.69E-03)	(1.01E-03)	(3.90E-03)	(5.22E-03)	(5.22E-03)	(4.57E-03)	(9.37E-03)	(4.57E-03)	(8.84E-03)	(7.22E-03)	(9.30E-03)	(5.22E-03)	(8.99E-03)	(7.00E-03)	(6.06E-03)	(1.06E-02)			

Table F.3. (contd)

Tank C-106 (404) CaCO₃ Results

Parameter	Units	Single Contact				Periodic Replenishment Tests											
		1 day	1 day (dup)	1 month	1 month (dup)	Stage 1	Stage 1 (dup)	Stage 2	Stage 2 (dup)	Stage 3	Stage 3 (dup)	Stage 4	Stage 4 (dup)	Stage 5	Stage 5 (dup)	Stage 6	Stage 6 (dup)
pH	std units																
Alkalinity	mM as CaCO ₃	40.2	40.2	36.6	29.3	40.2	40.2	40.2	40.2	40.2	58.5	40.2	40.2	25.6	40.2	40.2	40.2
Radionuclides																	
⁹⁰ Sr	mM	9.354E-05	1.817E-04			9.354E-05	1.817E-04	1.145E-04	1.130E-04	3.395E-05	1.472E-05	8.711E-05	5.555E-05	2.779E-05	5.398E-05		
⁹⁹ Tc	mM	(5.56E-07)	(4.04E-07)	(3.43E-06)	(3.91E-06)	(5.56E-07)	(4.04E-07)	(5.05E-07)	(6.06E-07)	(4.04E-07)	(3.03E-07)	(7.07E-07)	(5.05E-07)	(5.05E-07)	(5.05E-07)	(3.08E-06)	(2.63E-06)
²³⁸ U	mM	2.80E-06	(1.97E-06)	2.19E-04	1.97E-04	2.80E-06	(1.97E-06)	3.15E-06	3.57E-06	4.24E-06	(2.06E-06)	3.91E-06	3.95E-06	(1.85E-06)	3.61E-06	3.74E-06	4.03E-06
¹²⁹ I	mM	(6.78E-07)	(5.05E-07)	0.00E+00	0.00E+00	(6.78E-07)	(5.05E-07)									(1.47E-06)	
²³⁹ Pu	mM	(1.26E-06)	(1.67E-06)	(2.93E-06)	(2.09E-06)	(1.26E-06)	(1.67E-06)	(2.09E-06)	(1.26E-06)	(1.26E-06)	(1.67E-06)	(1.67E-06)	(1.26E-06)	(2.93E-06)	(1.26E-06)	(2.51E-06)	(1.67E-06)
²³⁷ Np	mM	(1.69E-07)	(1.27E-07)	(3.80E-07)	(3.38E-07)	(1.69E-07)	(1.27E-07)	(1.69E-07)	(1.69E-07)	(8.44E-08)	(1.27E-07)	(8.44E-08)	(8.44E-08)	(1.27E-07)	(1.27E-07)	(4.22E-08)	(4.22E-08)
²⁴¹ Am	mM	(1.12E-06)	(8.30E-07)	(1.33E-06)	(7.47E-07)	(1.12E-06)	(8.30E-07)	(1.04E-06)	(9.13E-07)	(1.16E-06)	(1.29E-06)	(1.24E-06)	(1.12E-06)	(1.08E-06)	(1.08E-06)	<2.07E-06	<2.07E-06
Metals																	
Al	mM	9.07E-01	6.96E-01	(3.07E-01)	(3.72E-01)	9.07E-01	6.96E-01	1.38E+00	1.69E+00	1.86E+00	9.77E-01	1.57E+00	1.63E+00	6.95E-01	1.37E+00	1.63E+00	1.28E+00
As	mM	(1.40E-02)	(3.42E-02)	(9.72E-03)	<3.34E-01	(1.40E-02)	(3.42E-02)	(3.35E-02)	<3.34E-01	(4.29E-02)	(4.79E-02)	(3.34E-02)	(3.05E-03)	(4.02E-02)	(9.62E-03)	(4.11E-03)	(9.48E-04)
B	mM	<2.31E+01	<2.31E+01	<2.31E+01	<2.31E+01	<2.31E+01	<2.31E+01	<2.31E+01	<2.31E+01	<2.31E+01	<2.31E+01	<2.31E+01	<2.31E+01	(2.21E-01)	<2.31E+01	(1.37E-01)	(1.26E-01)
Ba	mM	(1.29E-03)	(1.33E-03)	(8.09E-04)	(9.51E-04)	(1.29E-03)	(1.33E-03)	(6.68E-04)	(7.19E-04)	(6.78E-04)	(8.09E-04)	(8.55E-04)	(8.36E-04)	(1.19E-03)	(8.76E-04)	(4.85E-04)	(3.73E-04)
Be	mM	(4.70E-03)	(3.32E-03)	(5.67E-03)	(5.47E-03)	(4.70E-03)	(3.32E-03)	(3.81E-03)	(4.42E-03)	(3.11E-03)	(4.79E-03)	(2.55E-03)	(2.84E-03)	(1.42E-02)	(8.92E-03)	(1.15E-03)	(9.14E-04)
Bi	mM	<5.98E-02	(3.55E-03)	<5.98E-02	<5.98E-02	<5.98E-02	(3.55E-03)	(1.51E-03)	(8.16E-03)	<5.98E-02	<5.98E-02	<5.98E-02	(2.53E-03)	<5.98E-02	(1.75E-03)	<5.98E-03	(6.54E-05)
Ca	mM	1.97E+00	1.67E+00	3.22E+00	3.15E+00	1.97E+00	1.67E+00	2.66E+00	3.01E+00	3.32E+00	1.73E+00	2.81E+00	2.78E+00	1.32E+00	2.32E+00	2.80E+00	2.31E+00
Cd	mM	<2.22E-02	<2.22E-02	<2.22E-02	(2.01E-04)	<2.22E-02	<2.22E-02	(7.84E-04)	<2.22E-02	<2.22E-02	<2.22E-02	<2.22E-02	<2.22E-02	(5.62E-04)	(5.49E-04)	<2.22E-03	<2.22E-03
Co	mM	<4.24E-02	<4.24E-02	<4.24E-02	<4.24E-02	<4.24E-02	<4.24E-02	<4.24E-02	<4.24E-02	(2.71E-04)	<4.24E-02	<4.24E-02	<4.24E-02	(1.68E-03)	<4.24E-02	(1.03E-03)	(7.56E-04)
Cr	mM	(3.44E-03)	(1.86E-03)	(5.00E-03)	(5.89E-03)	(3.44E-03)	(1.86E-03)	(4.36E-03)	(2.32E-03)	(3.32E-03)	(1.23E-03)	(1.43E-03)	(3.80E-03)	(4.51E-03)	(1.07E-03)	(2.49E-03)	(2.19E-03)
Cu	mM	<1.97E-01	<1.97E-01	<1.97E-01	<1.97E-01	<1.97E-01	<1.97E-01	<1.97E-01	<1.97E-01	<1.97E-01	<1.97E-01	<1.97E-01	<1.97E-01	<1.97E-01	<1.97E-01	(3.02E-03)	(2.68E-03)
Fe	mM	(1.26E-03)	(1.71E-03)	(3.46E-03)	(2.11E-03)	(1.26E-03)	(1.71E-03)	<4.48E-02	(4.14E-03)	(8.69E-04)	(4.37E-04)	(1.20E-03)	(9.31E-04)	(5.01E-03)	(2.50E-03)	(3.87E-03)	(3.40E-03)
K	mM	<1.60E+01	<1.60E+01	<1.60E+01	<1.60E+01	<1.60E+01	<1.60E+01	<1.60E+01	<1.60E+01	<1.60E+01	<1.60E+01	<1.60E+01	<1.60E+01	<1.60E+01	<1.60E+01	<1.60E+01	<1.60E+01
Li	mM	<3.60E+00	<3.60E+00	<3.60E+00	<3.60E+00	<3.60E+00	<3.60E+00	<3.60E+00	<3.60E+00	<3.60E+00	<3.60E+00	<3.60E+00	<3.60E+00	<3.60E+00	<3.60E+00	(5.13E-03)	(6.57E-03)
Mg	mM	(1.55E-02)	(1.67E-02)	(2.11E-02)	(1.40E-02)	(1.55E-02)	(1.67E-02)	(1.51E-02)	(1.59E-02)	(1.26E-02)	(1.75E-02)	(1.39E-02)	(1.32E-02)	(1.66E-02)	(1.65E-02)	(1.39E-02)	(9.13E-03)
Mn	mM	<4.55E-02	<4.55E-02	<4.55E-02	<4.55E-02	<4.55E-02	<4.55E-02	<4.55E-02	<4.55E-02	<4.55E-02	<4.55E-02	<4.55E-02	<4.55E-02	(2.40E-04)	<4.55E-02	(9.13E-05)	<2.28E-03
Mo	mM	(2.58E-03)	(3.10E-03)	(1.26E-03)	<5.21E-02	(2.58E-03)	(3.10E-03)	<5.21E-02	<5.21E-02	(2.32E-03)	<5.21E-02	(1.90E-03)	<5.21E-02	(4.70E-03)	(4.86E-03)	(6.28E-04)	(1.12E-04)
Na	mM	(2.03E-01)	(5.72E-02)	2.33E+00	2.38E+00	(2.03E-01)	(5.72E-02)	(1.32E-01)	(8.42E-02)	(3.20E-02)	<1.09E-01	(1.39E-01)	(2.30E-01)	(4.84E-02)	(1.02E-01)	(1.64E-01)	(1.33E-01)
Ni	mM	(5.00E-03)	(2.41E-03)	(1.04E-03)	<8.52E-02	(5.00E-03)	(2.41E-03)	<8.52E-02	<8.52E-02	(1.36E-03)	(5.20E-04)	<8.52E-02	<8.52E-02	(1.52E-02)	(6.03E-03)	(1.73E-03)	(1.32E-03)
Pb	mM	<6.03E-02	<6.03E-02	<6.03E-02	<6.03E-02	<6.03E-02	<6.03E-02	<6.03E-02	<6.03E-02	<6.03E-02	<6.03E-02	<6.03E-02	<6.03E-02	<6.03E-02	<6.03E-02	<6.03E-03	(3.33E-05)
S	mM	<3.12E+00	(6.74E-02)	<3.12E+00	<3.12E+00	<3.12E+00	(6.74E-02)	(3.14E-03)	<3.12E+00	<3.12E+00	<3.12E+00	<3.12E+00	(9.35E-02)	<3.12E+00	(1.19E-01)	(3.93E-03)	<1.56E-01
Se	mM	(2.16E-02)	<3.17E-01	(2.66E-02)	(4.24E-02)	(2.16E-02)	<3.17E-01	(1.46E-02)	(4.21E-02)	(4.72E-02)	<3.17E-01	(3.93E-02)	(1.08E-02)	(4.01E-02)	<3.17E-01	(3.84E-03)	(4.19E-03)
Si	mM	<8.90E+00	<8.90E+00	<8.90E+00	<8.90E+00	<8.90E+00	<8.90E+00	<8.90E+00	<8.90E+00	<8.90E+00	<8.90E+00	<8.90E+00	<8.90E+00	<8.90E+00	<8.90E+00	(2.01E-02)	(2.08E-02)
Sr	mM	(1.41E-03)	(1.42E-03)	(4.70E-04)	(4.94E-04)	(1.41E-03)	(1.42E-03)	(1.70E-03)	(1.31E-03)	(1.41E-03)	(5.20E-04)	(9.43E-04)	(1.01E-03)	(1.83E-03)	(1.28E-03)	(1.20E-03)	(7.78E-04)
Ti	mM	(2.32E-04)	<5.22E-02	(5.78E-04)	(3.33E-04)	(2.32E-04)	<5.22E-02	<5.22E-02	<5.22E-02	<5.22E-02	<5.22E-02	<5.22E-02	<5.22E-02	(1.55E-03)	(5.99E-04)	<5.22E-03	(1.15E-04)
Tl	mM	(1.12E-02)	(6.50E-03)	(7.18E-04)	<6.12E-02	(1.12E-02)	(6.50E-03)	(5.86E-03)	(3.11E-03)	<6.12E-02	(2.67E-03)	(1.01E-02)	(3.91E-03)	(2.30E-03)	<6.12E-02		
V	mM	<2.45E-01	<2.45E-01	<2.45E-01	<2.45E-01	<2.45E-01	<2.45E-01	<2.45E-01	<2.45E-01	<2.45E-01	<2.45E-01	<2.45E-01	<2.45E-01	<2.45E-01	<2.45E-01	<2.45E-01	<2.45E-01
Zn	mM	(5.67E-03)	(7.74E-03)	(6.20E-03)	(5.96E-03)	(5.67E-03)	(7.74E-03)	(2.54E-03)	(2.44E-04)	(2.41E-03)	(1.61E-03)	(7.68E-03)	(7.43E-03)	(4.25E-03)	(3.81E-03)	6.61E-03	5.73E-03
Zr	mM	<2.74E-02	<2.74E-02	(4.36E-03)	(1.08E-03)	<2.74E-02	<2.74E-02	(4.14E-04)	<2.74E-02	<2.74E-02	<2.74E-02	(9.31E-05)	<2.74E-02	(3.45E-04)	<2.74E-02	<1.57E-04	(2.98E-04)
Anions																	
NO ₂ ⁻ as NO ₂ ⁻	mM	<9.80E-02	<9.80E-02	<9.80E-02	<9.80E-02	<9.80E-02	<9.80E-02	<9.80E-02	<9.80E-02	<9.80E-02	<9.80E-02	<9.80E-02	<9.80E-02	<9.80E-02	<9.80E-02	<9.80E-02	<9.80E-02
NO ₃ ⁻ as NO ₃ ⁻	mM	<6.98E-02	<6.98E-02	<6.98E-02	<6.98E-02	<6.98E-02	<6.98E-02	<6.98E-02	<6.98E-02	<6.98E-02	<6.98E-02	<6.98E-02	<6.98E-02	<6.98E-02	<6.98E-02	<6.98E-02	<6.98E-02
CO ₃ ²⁻	mM	<8.33E+00	<8.33E+00	<8.33E+00	<8.33E+00	<8.33E+00	<8.33E+00	<8.33E+00	<8.33E+00	<8.33E+00	<8.33E+00	<8.33E+00	<8.33E+00	<8.33E+00	<8.33E+00	<8.33E+00	<8.33E+00
SO ₄ ²⁻	mM	<4.26E-02	<4.26E-02	1.72E-01		<4.26E-02	<4.26E-02	<4.26E-02	<4.26E-02	<4.26E-02	<4.26E-02	<4.26E-02	<4.26E-02	<4.26E-02	<4.26E-02	<4.26E-02	<4.26E-02
PO ₄ ³⁻ as PO ₄ ³⁻	mM	<5.32E-02	<5.32E-02	<5.32E-02	<5.32E-02	<5.32E-02	<5.32E-02	<5.32E-02	<5.32E-02	<5.32E-02	<5.32E-02	<5.32E-02	<5.32E-02	<5.32E-02	<5.32E-02	<5.32E-02	<5.32E-02
Cl	mM	<6.66E-02	<6.66E-02	<6.65E-02	<6.65E-02	<6.66E-02	<6.66E-02	<6.66E-02	<6.66E-02	<6.66E-02	<6.66E-02	<6.66E-02	<6.66E-02	<6.66E-02	<6.66E-02	<6.66E-02	<6.66E-02
F	mM	<6.16E-02	<6.16E-02	<6.16E-02	<6.16E-02	<6.16E-02	<6.16E-02	<6.16E-02	<6.16E-02	<6.16E-02	<6.16E-02	<6.16E-02	<6.16E-02	<6.16E-02	<6.16E-02	<6.16E-02	<6.16E-02
Oxalate	mM	<3.92E-02	<3.92E-02	<3.92E-02	<3.92E-02	<3.92E-02	<3.92E-02	<3.92E-02	<3.92E-02	<3.92E-02	<3.92E-02	<3.92E-02	<3.92E-02	<3.92E-02	<3.92E-02	<3.92E-02	<3.92E-02

Table F.4. (contd)

Tank C-106 (405) CaCO₃ Results

Parameter	Units	Single Contact				Periodic Replenishment Tests											
		1 day	1 day (dup)	1 month	1 month (dup)	Stage 1	Stage 1 (dup)	Stage 2	Stage 2 (dup)	Stage 3	Stage 3 (dup)	Stage 4	Stage 4 (dup)	Stage 5	Stage 5 (dup)	Stage 6	Stage 6 (dup)
pH	std units																
Alkalinity	mM as CaCO ₃	40.2	40.2	32.9	36.6	40.2	40.2	54.9	40.2	62.2	40.2	47.5	40.2	40.2	40.2	40.2	43.9
Radionuclides																	
⁹⁰ Sr	mM	2.137E-04	2.744E-04			2.137E-04	2.744E-04	1.088E-04	7.534E-05	8.109E-05	5.061E-05	1.309E-04	5.541E-05	4.551E-05	3.078E-05		
⁹⁹ Tc	mM	(9.09E-07)	(7.07E-07)	(2.63E-06)	(2.42E-06)	(9.09E-07)	(7.07E-07)	(2.02E-07)	(2.02E-07)	(1.01E-07)	(3.03E-07)	(5.05E-07)	(4.04E-07)	(4.04E-07)	(4.04E-07)	(3.23E-06)	(1.92E-06)
²³⁸ U	mM	4.08E-06	(3.77E-06)	2.69E-04	3.21E-04	4.08E-06	(3.77E-06)	4.12E-06	2.39E-06	4.25E-06	(4.37E-06)	5.08E-06	4.79E-06	(5.21E-06)	4.92E-06	5.00E-06	4.37E-06
¹²⁹ I	mM	(1.08E-06)	(6.95E-07)	0.00E+00	0.00E+00	(1.08E-06)	(6.95E-07)										(9.33E-07)
²³⁹ Pu	mM	(2.09E-06)	(1.26E-06)	(2.51E-06)	(1.67E-06)	(2.09E-06)	(1.26E-06)	(1.67E-06)	(1.67E-06)	(8.37E-07)	(1.26E-06)	(1.26E-06)	(1.26E-06)	(2.09E-06)	(2.09E-06)	(8.37E-07)	(1.26E-06)
²³⁷ Np	mM	(8.44E-08)	(8.44E-08)	(2.95E-07)	(2.85E-07)	(8.44E-08)	(8.44E-08)	(8.44E-08)	(1.69E-07)	(1.27E-07)	(1.27E-07)	(8.44E-08)	(8.44E-08)	(4.22E-07)	(1.27E-07)	(2.11E-06)	(4.22E-08)
²⁴¹ Am	mM	(1.08E-06)	(9.96E-07)	(7.88E-07)	(9.13E-07)	(1.08E-06)	(9.96E-07)	(1.16E-06)	(1.20E-06)	(1.08E-06)	(1.08E-06)	(6.22E-07)	(1.04E-06)	(9.96E-07)	(7.47E-07)	<4.15E-08	<4.15E-08
Metals																	
Al	mM	1.07E+00	1.21E+00	(2.42E-01)	(3.15E-01)	1.07E+00	1.21E+00	1.50E+00	8.44E-01	1.65E+00	1.71E+00	1.62E+00	1.66E+00	1.57E+00	1.53E+00	1.58E+00	1.48E+00
As	mM	(1.76E-02)	(3.75E-02)	(7.12E-03)	<1.13E-02	(1.76E-02)	(3.75E-02)	(1.56E-02)	<1.36E-02	(8.37E-03)	(2.32E-02)	(4.27E-02)	(3.67E-02)	(3.08E-02)	(3.80E-02)	(1.77E-03)	(8.70E-04)
B	mM	<2.31E+01	<2.31E+01	<2.31E+01	<2.31E+01	<2.31E+01	<2.31E+01	<2.31E+01	<2.31E+01	<2.31E+01	<2.31E+01	<2.31E+01	<2.31E+01	(1.93E-01)	<2.31E+01	(1.19E-01)	(1.13E-01)
Ba	mM	(1.39E-03)	(1.09E-03)	(8.33E-04)	(5.16E-04)	(1.39E-03)	(1.09E-03)	(1.09E-03)	(8.73E-04)	(4.32E-04)	(1.07E-03)	(8.45E-04)	(5.68E-04)	(6.08E-04)	(6.67E-04)	(5.67E-04)	(6.26E-04)
Be	mM	(6.83E-03)	(4.43E-03)	(2.69E-03)	(3.95E-03)	(6.83E-03)	(4.43E-03)	(4.32E-03)	(3.54E-03)	(3.25E-03)	(3.07E-03)	(2.57E-03)	(2.53E-03)	(1.27E-02)	(7.19E-03)	(8.85E-04)	(8.03E-04)
Bi	mM	<5.98E-02	(7.14E-03)	<1.02E-03	<5.98E-02	<5.98E-02	(7.14E-03)	(2.43E-03)	(3.12E-03)	<5.98E-02	<5.98E-02	<5.98E-02	(1.33E-03)	<7.82E-04	(2.92E-03)	<1.57E-04	(2.67E-04)
Ca	mM	2.96E+00	1.65E+00	1.92E-01	1.81E-01	2.96E+00	1.65E+00	2.93E+00	2.99E+00	2.91E+00	2.98E+00	2.62E+00	2.46E+00	1.38E+01	1.08E-01	2.53E+00	2.64E+00
Cd	mM	<3.30E-04	<2.22E-02	<2.22E-02	(2.22E-02)	<3.30E-04	<2.22E-02	(2.22E-02)	<2.22E-02	<2.22E-02	<2.22E-02	<5.78E-04	<4.74E-05	(2.22E-02)	(2.22E-02)	<2.22E-03	<2.22E-03
Co	mM	<4.24E-02	<4.24E-02	<4.24E-02	<4.24E-02	<4.24E-02	<4.24E-02	<4.24E-02	<4.24E-02	(4.24E-02)	<4.24E-02	<4.24E-02	<4.24E-02	(9.51E-04)	<4.70E-04	(1.13E-03)	(8.59E-04)
Cr	mM	(6.16E-03)	(2.04E-03)	(4.03E-03)	(5.74E-03)	(6.16E-03)	(2.04E-03)	(4.38E-03)	(3.22E-03)	(4.23E-03)	(1.84E-03)	(3.22E-03)	(4.56E-03)	(6.41E-03)	(3.08E-03)	(3.00E-03)	(2.41E-03)
Cu	mM	<1.97E-01	<1.97E-01	<1.97E-01	<1.97E-01	<1.97E-01	<1.97E-01	<1.97E-01	<1.97E-01	<1.97E-01	<1.97E-01	<1.97E-01	<1.97E-01	<1.97E-01	<1.97E-01	(2.44E-03)	(2.22E-03)
Fe	mM	(2.56E-03)	(1.70E-03)	(1.99E-03)	(1.00E-03)	(2.56E-03)	(1.70E-03)	<1.46E-03	(2.14E-03)	(9.90E-04)	(4.48E-02)	(9.55E-04)	(4.48E-02)	(3.89E-03)	(1.92E-03)	(3.86E-03)	(3.25E-03)
K	mM	<1.60E+01	<1.60E+01	<1.60E+01	<1.60E+01	<1.60E+01	<1.60E+01	<1.60E+01	<1.60E+01	<1.60E+01	<1.60E+01	<1.60E+01	<1.60E+01	<1.60E+01	<1.60E+01	(3.20E+00)	<3.65E-02
Li	mM	<3.60E+00	<3.60E+00	<3.60E+00	<3.60E+00	<3.60E+00	<3.60E+00	<3.60E+00	<3.60E+00	<3.60E+00	<3.60E+00	<3.60E+00	<3.60E+00	<3.60E+00	<3.60E+00	(3.39E-03)	(5.31E-03)
Mg	mM	(1.44E-02)	(1.34E-02)	(1.15E-02)	(1.51E-02)	(1.44E-02)	(1.34E-02)	(1.64E-02)	(2.15E-02)	(1.39E-02)	(1.32E-02)	(1.28E-02)	(1.21E-02)	(1.94E-02)	(1.42E-02)	(8.87E-03)	(8.45E-03)
Mn	mM	<4.55E-02	<4.55E-02	<4.55E-02	<4.55E-02	<4.55E-02	<4.55E-02	<4.55E-02	<4.55E-02	<4.55E-02	<4.55E-02	<4.55E-02	<4.55E-02	(4.55E-02)	<4.55E-02	(2.28E-03)	<2.28E-03
Mo	mM	(2.73E-03)	(5.21E-02)	(5.21E-02)	<5.21E-02	(2.73E-03)	(5.21E-02)	<5.21E-02	<5.21E-02	(8.26E-04)	<4.04E-03	(3.60E-03)	<1.98E-03	(4.37E-03)	(5.21E-02)	(5.96E-04)	(4.51E-04)
Na	mM	(2.96E-01)	(2.17E-01)	1.71E+00	1.80E+00	(2.96E-01)	(2.17E-01)	(7.28E-02)	(1.19E-01)	(1.63E-01)	<7.23E-02	(1.39E-01)	(1.42E-01)	(1.04E-01)	(4.26E-02)	(2.81E-01)	(2.12E-01)
Ni	mM	(6.97E-04)	(4.76E-04)	(8.52E-02)	<8.52E-02	(6.97E-04)	(4.76E-04)	<8.52E-02	<8.52E-02	(1.35E-03)	(8.52E-02)	<3.52E-04	<8.52E-02	(1.06E-02)	(5.37E-03)	(1.18E-03)	(8.18E-04)
Pb	mM	<6.03E-02	<6.03E-02	<6.03E-02	<6.03E-02	<6.03E-02	<6.03E-02	<6.03E-02	<6.03E-02	<6.03E-02	<6.03E-02	<6.03E-02	<6.03E-02	<6.03E-02	<6.03E-02	<6.03E-02	(6.50E-05)
S	mM	<1.62E-01	(3.12E+00)	<3.12E+00	<7.38E-02	<1.62E-01	(3.12E+00)	(3.12E+00)	<3.12E+00	<3.12E+00	<3.12E+00	<3.12E+00	(1.14E-01)	<3.12E+00	(3.12E+00)	(1.94E-02)	<1.15E-02
Se	mM	(3.17E-01)	<3.17E-01	(2.49E-02)	(5.58E-02)	(3.17E-01)	<3.17E-01	(4.03E-03)	(3.56E-02)	(3.57E-02)	<2.23E-02	(6.20E-02)	(3.06E-02)	(1.72E-02)	<4.84E-02	(4.29E-03)	(5.21E-03)
Si	mM	<8.90E+00	<8.90E+00	<8.90E+00	<8.90E+00	<8.90E+00	<8.90E+00	<8.90E+00	<8.90E+00	<8.90E+00	<8.90E+00	<8.90E+00	<8.90E+00	<8.90E+00	<8.90E+00	(1.62E-02)	(1.52E-02)
Sr	mM	(2.81E-03)	(2.29E-03)	(6.16E-04)	(4.43E-04)	(2.81E-03)	(2.29E-03)	(1.54E-03)	(6.99E-04)	(1.20E-03)	(7.88E-04)	(7.88E-04)	(7.59E-04)	(1.98E-03)	(9.54E-04)	(1.01E-03)	(7.79E-04)
Ti	mM	(5.22E-02)	<5.22E-02	(6.11E-04)	(5.22E-02)	(5.22E-02)	<5.22E-02	<5.22E-02	<5.22E-02	<5.22E-02	<5.22E-02	<5.22E-02	<1.73E-04	(1.28E-03)	(7.70E-04)	<5.22E-03	(5.22E-03)
Tl	mM	(6.12E-02)	(6.12E-02)	(2.66E-03)	<9.70E-03	(6.12E-02)	(6.12E-02)	(2.50E-03)	(6.12E-02)	<7.30E-03	(7.37E-04)	(4.89E-03)	(1.05E-02)	(6.12E-02)	<5.97E-03		
V	mM	<2.45E-01	<2.45E-01	<2.45E-01	<2.45E-01	<2.45E-01	<2.45E-01	<2.45E-01	<2.45E-01	<2.45E-01	<2.45E-01	<2.45E-01	<2.45E-01	<2.45E-01	<2.45E-01	<4.91E-03	<1.00E-04
Zn	mM	(5.02E-03)	(3.76E-03)	(5.10E-03)	(5.04E-03)	(5.02E-03)	(3.76E-03)	(6.70E-03)	(2.83E-03)	(4.64E-03)	(5.21E-03)	(1.88E-03)	(3.77E-03)	(3.74E-03)	(3.20E-03)	5.08E-03	6.57E-03
Zr	mM	<1.07E-03	<2.74E-02	(2.74E-02)	(7.33E-05)	<1.07E-03	<2.74E-02	(2.74E-02)	<5.33E-04	<2.74E-02	<2.74E-02	(2.74E-02)	<5.82E-04	(6.32E-04)	<2.74E-02	<2.78E-04	(3.09E-04)
Anions																	
NO ₂ ⁻ as NO ₂ ⁻	mM	<9.80E-02	<9.80E-02	<9.80E-02	<9.80E-02	<9.80E-02	<9.80E-02	<9.80E-02	<9.80E-02	<9.80E-02	<9.80E-02	<9.80E-02	<9.80E-02	<9.80E-02	<9.80E-02	<9.80E-02	<9.80E-02
NO ₃ ⁻ as NO ₃ ⁻	mM	<6.98E-02	<6.98E-02	<6.98E-02	<6.98E-02	<6.98E-02	<6.98E-02	<6.98E-02	<6.98E-02	<6.98E-02	<6.98E-02	<6.98E-02	<6.98E-02	<6.98E-02	<6.98E-02	<6.98E-02	<6.98E-02
CO ₃ ²⁻	mM	<8.33E+00	<8.33E+00	<8.33E+00	<8.33E+00	<8.33E+00	<8.33E+00	<8.33E+00	<8.33E+00	<8.33E+00	<8.33E+00	<8.33E+00	<8.33E+00	<8.33E+00	<8.33E+00	<8.33E+00	<8.33E+00
SO ₄ ²⁻	mM	<4.26E-02	<4.26E-02	1.07E-01		<4.26E-02	<4.26E-02	<4.26E-02	<4.26E-02	<4.26E-02	<7.58E-02	<4.26E-02	<4.26E-02	<4.26E-02	<4.26E-02	<4.26E-02	<4.26E-02
PO ₄ ³⁻ as PO ₄ ³⁻	mM	<5.32E-02	<5.32E-02	<5.32E-02	<5.32E-02	<5.32E-02	<5.32E-02	<5.32E-02	<5.32E-02	<5.32E-02	<5.32E-02	<5.32E-02	<5.32E-02	<5.32E-02	<5.32E-02	<5.32E-02	<5.32E-02
Cl	mM	<6.66E-02	<6.66E-02	<6.65E-02	<6.65E-02	<6.66E-02	<6.66E-02	<6.66E-02	<6.66E-02	<6.66E-02	<5.38E-01	<8.03E-02	<6.66E-02	<6.66E-02	<6.66E-02	<6.66E-02	<6.66E-02
F	mM	<6.16E-02	<6.16E-02	<6.16E-02	<6.16E-02	<6.16E-02	<6.16E-02	<6.16E-02	<6.16E-02	<6.16E-02	<6.16E-02	<6.16E-02	<6.16E-02	<6.16E-02	<6.16E-02	<6.16E-02	<6.16E-02
Oxalate	mM	<3.92E-02	<3.92E-02	<3.92E-02	<3.92E-02	<3.92E-02	<3.92E-02	<3.92E-02	<3.92E-02	<3.92E-02	<5.39E-02	<3.92E-02	<3.92E-02	<3.92E-02	<3.92E-02	<3.92E-02	<3.92E-02

Distribution

No. of Copies

OFFSITE

Steve Airhart
Freestone Environmental Services
1933 Jadwin Avenue
Richland, WA 99354

Dr. Harry Babad
2540 Cordoba Court
Richland, WA 99352-1609

Pat Brady
Geochemistry Department, 6118
Sandia National Laboratories
P.O. Box 5800
Albuquerque, NM 87185-0750

Charles R. Bryan
Sandia National Laboratories
4100 National Parks Highway
Carlsbad, NM 88220

Susan Carroll
Lawrence Livermore National Laboratory
MS L-219
Livermore, CA 94550

Jon Chorover
Associate Professor – Environmental
Chemistry
Department of Soil, Water, and
Environmental Science
Shantz 429, Building #38
University of Arizona
Tucson, AZ 85721-0038

Dave G. Coles
Coles Environmental Consulting
750 South Rosemont Road
West Linn, OR 97068

No. of Copies

Mark Conrad
Department of Earth and Planetary Sciences
University of California, Berkeley
Berkeley, CA 94720

Dr. James A. Davis
U.S. Geological Survey
MS 465
345 Middlefield Road
Menlo Park, CA 94025

Donald J. DePaolo
Geology & Geophysics Dept. MC4767
University of California
Berkeley, CA 94720-4767

Dirk A. Dunning
Oregon Office of Energy
625 Marion Street, N.E.
Salem, OR 97301-3742

Mark Ewanic
MSE Technology Applications, Inc.
200 Technology Way
Butte, MT 59701

Markus Flury
Department of Crop and Soil Sciences
Washington State University
Pullman, WA 99164

Amy P. Gamerdinger
2122 E. Hawthorne
Tucson, AZ 85719

Jim Harsh
Department of Crop & Soil Sciences
Washington State University
Johnson Hall, Room 249
Pullman, WA 99164-6420

**No. of
Copies**

Dr. Cliff Johnston
Soil Chemistry and Mineralogy
1150 Lily Hall
Purdue University
West Lafayette, IN 47907-1150

Dr. Daniel I. Kaplan
Westinghouse Savannah River Company
Building 774-43A, Room 215
Aiken, SC 29808

Dr. David Kosson
Vanderbilt University
VU Station B #351831
2301 Vanderbilt Place
Nashville, TN 37235-1831

Dr. Jim Krumhansl
Sandia National Laboratory
P.O. Box 5800
Albuquerque, NM 87185-0750

Dr. Christine Langston
Westinghouse Savannah River Co.
Building 774-43A
Aiken, SC 29808

Dr. Peter C. Lichtner
Los Alamos National Laboratory
P.O. Box 1663
Los Alamos, NM 87545

Sandra Lilligren
Nez Perce
P.O. Box 365
Lapwai, ID 83540

Kate Maher
The Center for Isotope Geochemistry
301 McCone Hall
University of California, Berkeley
Berkeley, CA 94702-4746

**No. of
Copies**

Melaine A. Mayes
Environmental Sciences Division
Oak Ridge National Laboratory
P.O. Box 2008
Oak Ridge, TN 37831-6038

Dr. Kathryn L. Nagy
Department of Earth and Environmental
Sciences
University of Illinois at Chicago (MC-186)
845 West Taylor Street
Chicago, IL 60607-7059

Heino Nitsche
Director, Center for Advanced
Environmental and Nuclear Studies
Lawrence Berkeley National Laboratory
1 Cyclotron Road
MS 70A-1150
Berkeley, CA 94720

Phil Reed
U.S. Nuclear Regulatory Commission
Office of Nuclear Regulatory Research
Division of Systems Analysis and
Regulatory Effectiveness
Radiation Protection, Env. Risk and Waste
Management Branch
MS T9-F31
Washington, D.C. 20555-0001

Richard J. Reeder
Department of Geosciences
State University of New York at Stony
Brook
Stony Brook, NY 11794-2100

Al Robinson
68705, E 715 PRNE
Richland, WA 99352

**No. of
Copies**

Phil Rogers
13 Mountain Oak
Littleton, CO 80127

Dr. Sherry Samson
Department EES
University of Illinois at Chicago (MC-186)
845 West Taylor Street
Chicago, IL 60607-7059

David Shafer
Desert Research Institute
University of Nevada
P.O. Box 19040
Las Vegas, NV 89132-0040

Dawn A. Shaughnessy
Glen T. Seaborg Center
Lawrence Berkeley National Laboratory
1 Cyclotron Road
MS 70A-1150
Berkeley, CA 94720

Doug Sherwood
Rivers Edge Environmental
1616 Riverside Drive
West Richland, WA 99353

David K. Shuh
Lawrence Berkeley National Laboratory
1 Cyclotron Road
MS 70A-1150
Berkeley, CA 94720

James "Buck" Sisson
Idaho National Engineering and
Environmental Laboratory
P.O. Box 1625, MS 2107
Idaho Falls, ID 83415-2107

**No. of
Copies**

Carl I. Steefel
Lawrence Livermore National Laboratory
Earth & Environmental Sciences Directorate
MS L-204
P.O. Box 808
Livermore, CA 94551-9900

Dr. Samuel J. Traina, Director
Sierra Nevada Research Institute
University of California, Merced
P.O. Box 2039
Merced, CA 95344

Dan Tyler
Freestone Environmental Services
1933 Jadwin Avenue
Richland, WA 99354

Dr. T. T. Chuck Vandergraaf
Atomic Energy of Canada, Limited
Whiteshell Nuclear Research Establishment
Pinawa, Manitoba ROE 1LO
Canada

Dr. Jiamin Wan
Lawrence Berkeley National Laboratory
1 Cyclotron Road, MS 70-0127A
Berkeley, CA 94720

Mr. Ronald G. Wilhelm
Office of Radiation and Indoor Air
401 M Street, S.W.
Mail Code 6603J
Washington, D.C. 20460

W. Alexander Williams
U.S. Department of Energy
Office of Environmental Restoration
EM-33
19901 Germantown Road
Germantown, MD 20874-1290

<u>No. of Copies</u>		<u>No. of Copies</u>	
ONSITE		3 Environmental Protection Agency	
4 DOE Office of River Protection		N. Ceto	B5-01
P. E. LaMont	H6-60	D. A. Faulk	B5-01
R. W. Lober	H6-60	M. L. Goldstein	B5-01
R. A. Quinterro	H6-60	2 Fluor Federal Services	
S. A. Wiegman	H6-60	R. Khaleel	E6-17
8 DOE Richland Operations Office		R. J. Puigh	E6-17
B. L. Foley	A6-38	4 Fluor Hanford, Inc.	
J. P. Hanson	A5-13	T. W. Fogwell	E6-35
R. D. Hildebrand	A6-38	B. H. Ford	E6-35
K. A. Kapsi	A5-13	J. G. Hogan	H1-11
J. G. Morse	A6-38	M. I. Wood	H8-44
K. M. Thompson	A6-38	Stoller	
DOE Public Reading Room (2)	H2-53	R. G. McCain	B2-62
14 CH2M HILL Hanford Group, Inc.		5 Washington State Department of Ecology	
M. P. Connelly (5)	H6-03	J. A. Caggiano	H0-57
T. E. Jones	H6-03	S. Dahl	H0-57
F. J. Anderson	H6-03	J. J. Lyon	H0-57
F. M. Mann	H6-03	E. A. Rochette	H0-57
J. G. Kristofzski	H6-03	J. Yokel	H0-57
D. Parker	H6-03	49 Pacific Northwest National Laboratory	
J. A. Voogd	H6-03	B. W. Arey	K8-93
W. J. McMahon	H6-03	D. H. Bacon	K9-33
D. A. Myers	H6-03	S. R. Baum	P7-22
D. M. Nguyen	R2-12	B. N. Bjornstad	K6-81
3 Duratek Federal Services, Inc., Northwest Operations		C. F. Brown	P7-22
M. G. Gardner	H1-11	R. W. Bryce	E6-35
K. D. Reynolds	H1-11	K. J. Cantrell	K6-81
D. E. Skoglie	H1-11	R. E. Clayton	K6-75

**No. of
Copies**

W. J. Deutsch (5)
 P. E. Dresel
 K. M. Geisler
 M. J. Fayer
 A. R. Felmy
 M. D. Freshley
 J. S. Fruchter
 N. J. Hess
 D. G. Horton
 J. P. Icenhower
 C. T. Kincaid
 K. M. Krupka (3)
 I. V. Kutnyakov
 G. V. Last
 M. J. Lindberg
 W. J. Martin
 S. V. Mattigod

K6-81
 K6-96
 P7-22
 K9-33
 K8-96
 K9-33
 K6-96
 P7-50
 K6-81
 K6-81
 E6-35
 K6-81
 P7-22
 K6-81
 P7-22
 K6-81
 K6-81

**No. of
Copies**

B. P. McGrail
 P. D. Meyer
 C. J. Murray
 S. M. Narbutovskih
 R. D. Orr
 E. M. Pierce
 N. Qafoku
 S. P. Reidel
 R. G. Riley
 R. J. Serne
 H. T. Schaef
 W. Um
 M. Valenta
 B. A. Williams
 S. B. Yabusaki
 J. M. Zachara
 Hanford Technical Library (2)

K6-81
 BPO
 K6-81
 K6-96
 K6-81
 K3-62
 K3-61
 K6-81
 K2-21
 P7-22
 K6-81
 P7-22
 P7-22
 K6-81
 K9-36
 K8-96
 P8-55